REDUCING THE RISK IN DRILLING PRODUCTION WELLS: A MULTIDISCIPLINARY APPROACH

CENTRE FOR NEWFOUNDLAND STUDIES

TOTAL OF 10 PAGES ONLY MAY BE XEROXED

(Without Author's Permission)

ASHLEY PAUL WILLCOTT

Reducing the Risk in Drilling Production Wells: A Multidisciplinary Approach

by

©Ashley Paul Willcott

A thesis submitted to the
School of Graduate Studies
in partial fulfillment of the
requirements for the degree of
Master of Engineering

Faculty of Engineering and Applied Science
Memorial University of Newfoundland
October 2005

St. John's Newfoundland Canada

Abstract

Numerical predictive tools are frequently used in the oil and gas industry as a means to determine the optimal procedure to maximize the profitability of a project in a nondestructive and cost effective manner. The present work provides a link between geostatistics and risk engineering to address geological uncertainty in reservoir formations. The geological properties of a reservoir influence the potential productivity of a well. Unfortunately the reservoir properties are never fully known with complete certainty. By quantifying the uncertainty in the reservoir geology a risk factor can be associated with the well path. This risk factor can be improved by adding measurements while drilling to the geostatistical simulations. The demonstration of how to quantify the risk and then apply measurements while drilling to reduce the risk is the key focus of this research. This methodology is demonstrated through the use of two case studies.

Acknowledgments

I would like to acknowledge the contributions of the following individuals to this thesis. First and foremost to my supervisors Dr. Thormod Johansen and Dr. Faisal Khan; members of the Faculty of Engineering and Applied Science at Memorial University of Newfoundland. It was with their guidance and motivation that sparked my interest in their respective fields and their enthusiasm that helped me to complete the work, the top notch working environment and my relationship with them that made my experience here as a masters student so enjoyable.

Secondly, I would like to thank my girlfriend and companion, Jeanette Edge, for opening my eyes to the possibilities available at Memorial University. Without her I would not have realized how much I could learn, and how much opportunity there is at the university. She also has been there for me when I needed her the most and reminded me that enjoying life is just as important as my research (which was definitely needed). I could not have done this without you and for that Jeanette, I thank you.

I would also like acknowledge the continued support from my parents, who have stood by me in every path in life I have chosen to follow. You have taught me so much about the importance of education and it is your guidance that helps me see that I am able to be successful at whatever I desire to do.

Finally I would like to take this opportunity to acknowledge the following for their monetary support. The Natural Sciences and Engineering Research Council (NSERC) for its recognition of this research for being considered and awarded a Canada Graduate Scholarship (CGS-M). It is truly an honor to receive such an award. I would also

like to thank the Pan-Atlantic Petroleum Systems Consortium (PPSC) and funding from the Canada Research Chair operating grant for helping this research become a reality. I am also grateful for being awarded the Dean's Excellence award from the School of Graduate Studies for some additional funding. Finally I would like to thank the Faculty of Engineering and Applied Sciences for giving me the opportunity to supplement my income with numerous teaching assistantships.

Contents

List of Tables

List of Figures

Nomenclature

a	=	variogram range
C, c	=	covariance
C_o	=	variogram sill
C_1	=	variogram sill contribution for a variogram in combination model
E	=	expected value
F	=	function for lagrange multiplier method
f_w	=	fractional flow function
g	=	gravity
HW	=	cross sectional area of shale channel
K	=	absolute permeability
k_i	=	phase specific permeability
k_{ri}	=	relative permeability
$\vec{L}$	=	lag distance
$\vec{L}_u$	=	distance vector component in the direction of maximum continuity
$\vec{L}_{u'}$	=	distance vector component with the original sample data axes
$\vec{L}_v$	=	distance vector component in the direction of minimum continuity
$\vec{L}_{v'}$	=	distance vector component $\perp$ to u'
$\vec{L}_D$	=	dimensionless scaled lag distance
m	=	local mean at $\vec{u}_o$
m_x, m_y	=	mean of variable x,y
M_{Ea}	=	exponential variogram model with range a
M_{Ga}	=	gaussian variogram model with range a
M_{Sa}	=	spherical variogram model with range a
n	=	number of variable pairs
p	=	pressure
P_{base}	=	baseline production for case 1
P_{base2}	=	baseline production for case 2
P_{95}	=	95^{th} percentile of random production
$P_{statei95}$	=	95^{th} percentile of state i production
$Risk$	=	Risk factor
S_w	=	water saturation
$slope$	=	slope of the tangent of the fractional flow function
$ttbt$	=	time to breakthrough for a single channel
u_w	=	water flux
u_T	=	total flux
$\vec{U}_i, \vec{u}_i$	=	variable position vector at the i^{th} location
$\vec{u}_o$	=	variable position vector at the predicted variable location
v	=	darcy velocity

VAR	=	variance
X, x	=	random variable
$X(\vec{u_i})$	=	sampled data
$X^*(\vec{u_o})$	=	parameter estimate
X_o	=	parameter estimation constant
Y, y	=	random variable

Greek Symbols

α	=	angle of inclination counterclockwise from horizontal
γ	=	variogram
λ	=	kriging weight
μ	=	lagrange parameter
μ_i	=	phase viscosity for phase i
ρ	=	density
ρ_c	=	correlation coefficient
ϕ	=	porosity
σ	=	frontal velocity
σ_x, σ_y	=	standard deviation of variable x,y
σ_E	=	error variance
θ	=	direction of maximum continuity

Subscripts

i, j	=	variable counters
$1, 2$	=	unique random variable identifier
o, w	=	oil and water when referring to permeabilities
u, v	=	direction of maximum and minimum continuity respectively
u', v'	=	orthogonal vector directions based on original sample data

Chapter 1

Introduction

The oil and gas industry depends on many numerical tools to predict, manage, and optimize major exploration and production (E&P) project parameters such as reserve capacity, reservoir management procedures, and completions schemes. Due to the inherent uncertainty involved in the different aspects of exploration and production processes in oil and gas projects, there is a need to use these tools to determine the scenarios that offer the most profitable benefits. These tools help quantify the uncertainty in the project parameters and allow the decision makers to make educated choices.

During drilling is one area where a tool to quantify geological uncertainty would be useful. Data collected during the drilling process can have a sizable impact on the uncertainty and thus the risk involved with the drilling of production wells. This is the concept explored in the first part of this research; the methodology of how to incorporate these "real-time" measurements in a way that quantifies the risk associated with this uncertainty. Subsequently, applications of the methodology are demonstrated through two case studies.

The use of geostatistics became popular in the 1980s and at that time it was considered a new approach to describe and quantify spatial dependence of reservoir attributes (Kelkar & Perez, 2002). The methodology is still used today in many industrial applications, one area being to populate grid blocks in reservoir simulation software packages. This particular area has research potential in the field of risk engineering and is currently being investigated as a means to determine and, in essence, lower the risk (and the cost) involved with the drilling of production wells in reservoirs.

Risk assessment is a technique for quantifying the hazard involved with a particular activity along with its probability of its occurrence. The risk methodology is a stochastic tool to help guide decisions in a scientific and mathematical manner in common and understandable terms. Though seldom applied in geostatistical applications, risk assessment offers an alternate approach to determining locations and paths of well bores in reservoir formations. Geostatistics offers a method to quantify the spatial relationship a variable has in a geographic location. The purpose of this research is to present an original methodology of how to integrate the fields of risk engineering and geostatistics together with reservoir simulation and to demonstrate the concepts through the use of two case studies. The approach involves quantifying the risk involved with drilling a specified well path with geostatistical uncertainty. This quantification can then be made more precise by the addition of measurements acquired while drilling (MWD - measurements while drilling).

1.1 Motivation

Decision making tools are very important in today's petroleum industry. Historically, the oil industry is known for being very traditional in how wells are drilled and how

reservoirs are managed. This is because the tools were not previously available to help or guide the engineer in such areas. More recently, through the advancement of technology and the development of faster computers and more efficient algorithms, there has been an evolution of these types of tools. In petroleum production well planning, the wells are often mapped before the drilling commences. These trajectories and the choice of project details such as kickoff location (where the drilling begins) and the type of completions in the well, are often based on the available information from the reservoir. Pre-drill information may come from seismic data, core samples or well-logging techniques. Even though the information is useful and it allows for an "educated guess" for the best choice of project details, it fails to fully characterize the reservoir with a high degree of certainty. This is why it is necessary to use information gathered while drilling to help in the trajectory planning and modification in the case of unforeseen circumstances (in the scenario where the original chosen well path is not the optimal choice). The first step in developing a tool to help in this respect is to first quantify the risk involved in the process. When the risk is quantified it can then be compared to different scenarios to find the optimal solution. The motivation behind this research is to take the first step in the development of the methodology for such a tool that can be used in real-time while drilling. The first step is to quantify the risk and outline the methodology in a clear and understandable way. Methodologies that have the ability to quantify the impact of uncertainties in petroleum field development are still not well established due to the amount of variables that have to be considered (Schiozer, Ligero & Santos, 2004). Using geostatistics, many variables may be considered and this impact can be calculated based on the change in the flow simulations generated by a reservoir simulator.

The use of geostatistics in reservoir engineering is not new. It has been used as a tool

to help in a number of different stages of development in reservoir fields. Risk analyses have also been used to help manage reservoirs as well. The two concepts, however, have not been used together in conjunction with real-time measurements while drilling to improve the mathematical field model. An improvement of the mathematical field model with new information while drilling would give the reservoir engineer more quantitative information about the attributes of the reservoir which would allow for more informed decision making. During drilling, information about the formation can be relayed to the surface and can be used to tune a geostatistical simulator to be more representative of the actual reservoir. The more certain a reservoir engineer is about the reservoir parameters, the less risk is involved in drilling the well or changing the trajectory while drilling.

The complexity of exploration and production projects is increasing. They are becoming more ambitious and exploring more uncharted territory because technological advancements make it possible to do so. Traditionally, oil companies have a compartmentalized structure that lacks efficiency and cross-disciplinary information exchange (Cayeux et al., 2001). The proposed multidisciplinary approach suggests that combining geostatistics with reservoir engineering would improve and reduce the risk involved with the drilling of production wells.

1.2 Methodology

The methodology proposed can best be explained through the use of a flow chart. The flow chart shown in Figure 1.1 gives the steps needed to go through the geostatistical analysis and the risk assessment of a reservoir. The following section briefly describes these steps. Each step is discussed in detail in the body of the report.

Figure 1.1 shows the process involved with using geostatistics to predict the desired variable at the unsampled location. It begins with obtaining geostatistical inputs from various sources. These sources may include core samples, seismic data, outcrop information, well logs or any number of other information sources. This information (raw data) needs to be studied to determine if a transformation is necessary.

A transformation is useful if more information can be obtained from transformed data. It may also be necessary to convert qualitative data into quantitative data. One example of where a transformation would be useful is for some permeability data. When most of the data lies at an extreme end of the data population but some data exists over a number of other magnitudes, then the data may appear to be log normal. A log transformation would allow for more information to be seen in the data. Once the information is in its usable format it is then necessary to determine the directions of maximum and minimum continuity. This is necessary for anisotropic reservoirs (where parameters vary in distance and direction - not isotropic or homogeneous).

Figure 1.2 shows the process in determining the directions of maximum and minimum continuity. Where an adequate amount of information exists a variogram map may be created. This means that the variogram (a mathematical expression that signifies a variable's spatial relationship) is estimated at various incremented angles (with an angular tolerance) until 180 degrees is reached (since the variogram is symmetric) while varying the lag distance. The variogram at each angle is compared to the variance of the entire original sample. In the comparison, the lag distance should be recorded where the variogram and the sample variance are equal. The angle exhibiting the maximum lag is considered the direction of maximum continuity. Similarly, the direction of minimum continuity is the angle which shows the minimum lag distance.

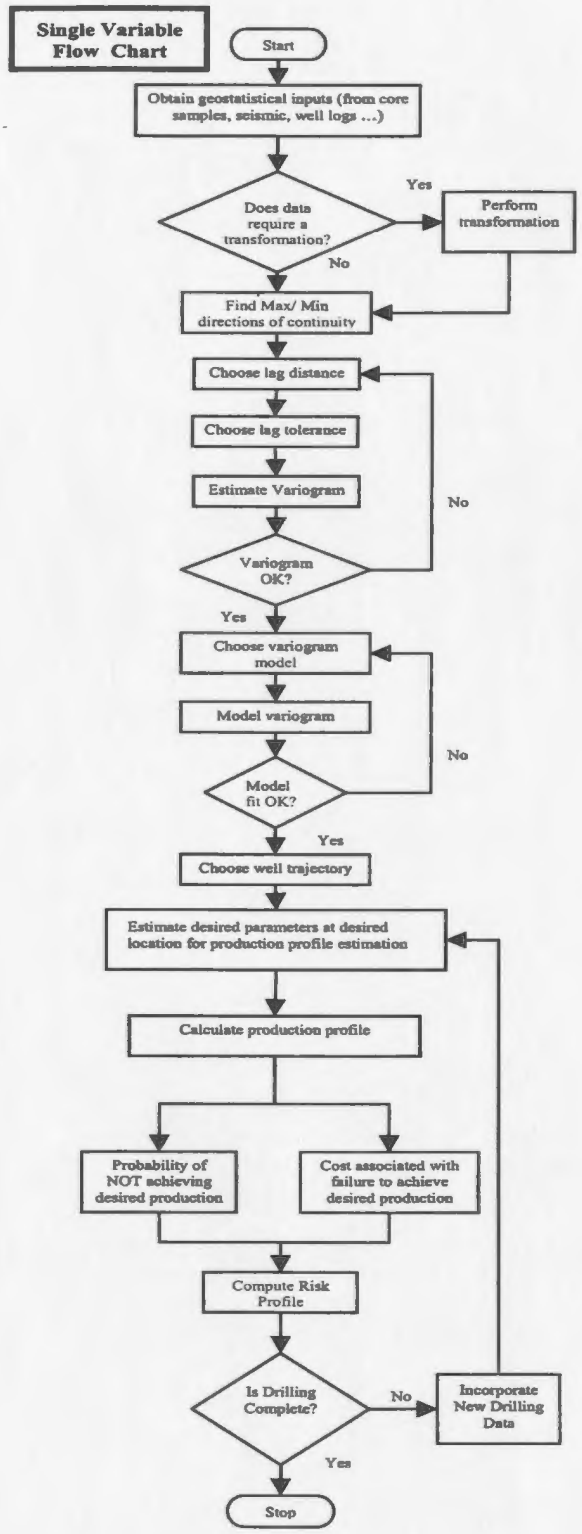

Figure 1.1: Geostatistics/Risk Methodology

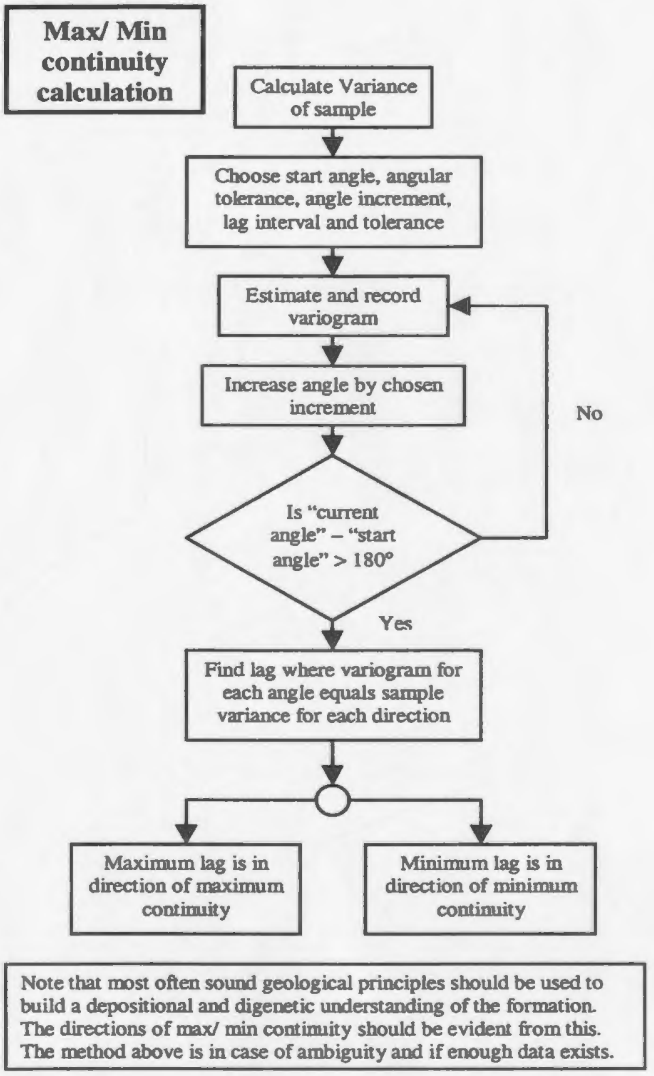

Figure 1.2: Continuity Direction Calculation

These directions are usually perpendicular to each other. It should be noted that sometimes there is a lack of information so a realistic variogram estimation is not possible. In this case sound geological theory should be used to determine these directions based on the information known about the facies in the location of interest (Deutsch, 2002).

After the directions of maximum and minimum continuity are determined the variogram must be estimated in those directions. In this way the variogram parameters (angle, lag, and respective tolerances) can be optimized in order to reduce the fluctuation of the variogram while retaining its shape and trend. From the variogram estimation, the variogram modeling can be initiated. The variogram model attempts to fit the variogram estimate with known models with certain mathematical properties.

Now the well path must be stated. If different well trajectories are being explored then this is the step where that linkage must be made. For now it is sufficient to say that the well path is known at this step. Using the variogram models and geostatistical simulation methods, the reservoir can be populated with estimated data. The geostatistical simulator has the ability to create equiprobable images of the reservoir known as realizations on which a geostatistical analysis can be performed. Once the reservoir grid has been populated the reservoir simulation can take place.

The reservoir simulator will calculate the production rates based on each realization. Once the simulation has been run a desired number of times on the different realizations the risk analysis can be completed. For this there are two parts. First the probability of not achieving the desired production and second, the consequences associated with not achieving the desired production. Multiplying these together yields

a risk factor. Since the production rates have been calculated for a number of realizations the risk factor has a distribution which may be analyzed to see if the risk is acceptable. The next procedure is introduction of the measurements while drilling to the methodology. Using measurements along the well bore, the geostatistical realizations can be recalculated and the risk factors can be re-evaluated. Now the reservoir parameters are known with a little more certainty and the project can move forward with more information. If this process is completed for a number of different drilling states, then each state should realize a reduction in risk, making the decisions that are made more informed. This is the main concept being proposed and developed in this research.

1.3 Thesis Outline

The present section gives a brief introduction to the thesis and it gives the reader insight into the motivation behind the research. Chapter 2 shows the results of a literature search in the particular areas of geostatistics, risk engineering, and reservoir engineering to show the work that has been done so far. Chapter 3 deals with the basic methodology of how to apply geostatistical concepts to determine information about variables at unsampled locations. It represents an introduction into the basic concepts of applied geostatistics so that the methodology may be fully understood. Chapter 4 concentrates on risk engineering concepts and demonstrates how risk engineering can be a useful tool for decision making and how it can be implemented. Chapter 5 introduces all of the major geostatistical and risk concepts through the use of a simplified case study. This case study is very useful in that it shows valuable insight into how to apply the concepts of geostatistics to estimate unsampled values. It then proceeds to combine these values with the concept of risk assessment

to estimate the risk involved with production along a specified well path without using measurements while drilling. Chapter 6 contains a more detailed case study to further demonstrate the concepts and it also presents an original methodology on how to incorporate measurements while drilling into the development of the risk profiles. The final sections conclude the study with observations while making certain recommendations for future research.

Chapter 2

Literature Review

2.1 General Review

The application of geostatistics in reservoir characterization has been limited whereas it has been used extensively in mining. The transition of the application of geostatistics from mining to reservoir characterization is indeed a difficult task as stated by Chopra, Severson and Carhart (1990). The use of geostatistics in reservoir characterization to properly define a reservoir can greatly enhance the profitability of the petroleum host formation and thus should be given due consideration. The power of geostatistics is that it can produce equiprobable images of the reservoir that incorporates data uncertainty. This creates a probable bandwidth of performance based on the physical formation rather than implementing a best guess approach. These images honor all available data which is another important advantage of using geotatistics, data integration. Geostatistics has the ability to integrate many different types of data (Qassab et al., 2000) such that different sources of information with different levels of resolution can be used together. It also provides a methodology which has more potential to capture spatial correlations than conventional techniques such as

triangulation and the piecewise linear squares method (Chopra et al., 1990).

A full scale geostatistical modeling study can be performed in a relatively short period of time (1-3 months if the input data is available). Once this initial model is determined, updates can be performed extremely quickly (Damsleth et al., 1997). This means it can be used effectively and quickly when new information becomes available such as during the drilling process. Geostatistics is a very powerful tool for quantifying geological uncertainty. One way in which this quantifiable uncertainty can be used is in a risk analysis. This would provide information on where the geological uncertainty causes the most monetary risk and allow for decisions to be made based on the monetary impact of the geological uncertainty.

Risk analysis has been used in the past for many different applications in the oil and gas industry. It has been used in the planning of underbalanced drilling projects (Arild et al., 2004), and in scale management in deep water (Mackay et al., 2004). It has also been used for calculating well performance taking into account reservoir and completion uncertainties (Wehunt, 2003). Other applications noted in the literature explore the use of risk analysis to help prevent blowouts as well as explosions, fire, and cargo tank explosions on FPSOs (Overfield et al., 2000; Khan et al., 2004; Khan et al., 2002). The literature search revealed that risk analysis has not been used in reservoir characterization while drilling so far. This thesis provides a framework for the application of risk analysis to reservoir characterization during drilling at a preproduction stage. Subsequent sections of this chapter provide further detail on the subject topic.

2.2 Geostatistics and Reservoir Engineering

Geostatistics uses stochastic imaging. Essentially this means that once the known data is fixed in a simulation the other unsampled points are allowed to vary. Each variation provides a new still image of the reservoir which has an equal likelihood of occurring. The collective set of stochastic images can be referred to as a probability distribution that accounts for space dependencies through the use of spatial models of the unknown variable. With more available information, the spread of the posterior distribution decreases and the images have less variation (Journel, 1990). This is due to the fact that the uncertainty of the distribution decreases with an increasing amount of information about the formation.

Another recent study (Galli et al., 2004) involves stochastic modeling with Bayesian updating. The researchers used geostatistics to honor field data with the framework to measure the effect of additional information. The major dilemma was the high level of uncertainty raised doubt to the feasibility of a certain project. Through the use of the development of three probable cases, the project could be evaluated and studied. A Bayesian approach was used to incorporate the different scenarios that were optimistic and pessimistic. This study provided clear evidence that geostatistics has an important place in reservoir engineering as a method to quantify reservoir uncertainties.

Geostatistics has also been used to improve reservoir characterization by coupling seismic data and simulated annealing. Simulated annealing is a procedure which uses geostatistics and an analogy to physical metallurgy (metal annealing) to create random realizations based on static data and simulation. In the cooling of molten metal, the quality of the metal depends on the temperature and the rate of cooling of the

metal. In essence it is based on thermodynamic principles and on obtaining an energy equilibrium by allowing the molecules of the metals to find the lowest energy state. Because simulated annealing is based on the physical analogy, knowledge of three analogous system components are needed; energy, temperature and interactions of a molecular system (Kelkar et al., 2002). By defining an objective function representing the energy of the process, it can then be perturbed by the interchange mechanism (the molecular interaction) and ultimately minimized. In the study, it was recognized that a strong relationship existed between seismic impedance and rock porosity (z= ρ v), so the inter-well spatial relationships in the lateral direction could be characterized with more accuracy using 3-D seismic attributes and transforms (Abdassah et al., 1996).

A study conducted in 1996 regarding a reservoir in the North Sea concluded that there is a need to improve an existing simple layer model to better represent the production data. This could best be achieved using geostatistics. It was found that through the use of geostatistics, a higher level of heterogeneity was captured and the model resembled the production data much more closely (Sweet et al., 1996).

There are many helpful and useful texts which fully describe the methods of geostatistics in both mining applications as well as in applied reservoir characterization. A complete listing of references cited in the compilation of this study is presented in the last chapter called References.

2.3 Risk Analysis in Geostatistics

This section reviews some of the literature available regarding work that has been completed to date in the area of risk analysis and geostatistics with an emphasis on

oil and gas related projects.

Srivastava (1990) presents an early study on the combination of risk analysis and geostatistical methods. The presented work presents a case study that demonstrates a methodology that calculates the optimal volume of that gas should be injected into a gas injector well when the connected pore volume is uncertain. Using geostatistics, the uncertainty in the pore volume was estimated and the risk factor was computed based on the cost of the solvent vs. the price of oil produced (Srivastava, 1990). This paper does not include a real-time analysis, however, the risk approach discussed is valuable.

Another work by Pathak, Ogbe et al. (2000) uses geostatistics to evaluate well placements. It reviews 15 potential well locations at 3 realizations (high, medium and low permeability values). The reservoir development strategy focuses on maximum recovery, accelerating production and mitigating risk. The approach does not use risk analysis or a real-time use of geostatistics but it does provide insight on what factors to focus on when choosing an optimal well path as well as a good methodology for a basis for risk analysis. Similar studies include those by Yeten et al. (2003), and Manceau et al. (2001).

Thayer et al. (2003) also completed a study outlining the combination of geostatistics and risk assessment however it was not related to oil and gas. It does provide an alternate source of application to geostatistics that is refreshing in that it involves the use of geostatistics to quantify human and ecological risk assessment at a contamination site. Other important studies with similar objectives were completed by Khan and Husain (2002 and 2003).

2.4 Risk Analysis in Reservoir Engineering

"Management scientists use a wide variety of tools and techniques to model, analyze, and solve complex decision problems." (Evans et al., 2002). This process becomes increasingly complex when dealing with parameters that have uncertainty in their determination scheme. For example, in reservoir characterization the parameters of interest include those which are determined from intrusive tests such as well logging, coring and data available from other non-intrusive tests such as seismic imaging. Porosity and permeability are the most important parameters since they have such a large impact on oil in place predictions and flow simulations. In order to integrate a large set of inputs together, a methodology must be in place. Tools in the past have been so cumbersome, inefficient and difficult to use that project managers would avoid using them even if the potential results outweighs the time commitments involved with such an analysis.

One example of where many different aspects of a project were combined into a full-scale risk analysis was documented by Solis et al.(2004). They investigated the application of risk to a case study with uncertain rock parameters, different development schedules, and capital expenditure uncertainties (such as price inflation and discount factors). The methodology presented concentrated on an interest in optimizing the field development scenario by balancing the risk and uncertainty to maximize asset profitability. Although this method is a powerful tool, it is different than the methodology presented in this thesis, since it fails to include detailed reservoir characterization models in the stochastic simulation analysis.

Part of the evaluation of risk involves the calculation of uncertainty. Geostatistics achieves this through the generation of multiple realizations, however, it is not the

only way to evaluate the uncertainty. In an effort to reduce the number of input parameters, reduce the computation time and still have reasonable uncertainty predictions, a number alternative procedures have been proposed.

- Scaling Analysis: This involves developing dimensionless groups which allow for scales that are geometrically similar, to have comparable results. The use of scaling results in fewer parameters than the dimensional counterpart.

- Variable Sensitivity Analysis: This involves analyzing the problem to determine the effect of the inputs on the uncertainty of the problem. Techniques for completing this task include Monte Carlo simulation, first-order analysis, second order analysis, response surface methods, and experimental design methods including Box-Behnken design and Taguchis' approach. The Box-Behnken design and Taguchi's method are approaches to experimental design with deliberate testing of factors (or variables) at deliberate factor levels (high, medium and low levels, for example) to determine the relationships between all variables involved. The approaches are part of a larger field called Design of Experiments and more information can be found on these topics by referring to Mason et al. (2003) and Taguchi (1987).

One study found that the combination of scaling and experimental design and response surface modeling offered the most potential to reduce computational time and effort (Chewaroungroaj et al., 2000).

During the development phase of a petroleum reservoir there are many managerial decisions to be made. These decisions are always related to the risk involved because of the uncertainties involved in the process. A risk analysis is made even more critical

by the fact that most of these important decisions are made during the initial field development stages when the uncertainty is at its highest levels. The most common uncertainties that exist that effect the success of a project occur in the geological model (volume in place, faults, continuity, porosity and permeability distribution etc.). Development can be influenced not only by geological, economic, and technological risks but also by production strategies, schedules and management decisions. To obtain a level of precision necessary to fully understand the risk, numerical simulation techniques are necessary (Schoizer & Ligero & Santos, 2004).

A risk assessment was performed on a reservoir in Saskatchewan, Canada to investigate the economic feasibility of using a carbon dioxide miscible flood to improve recovery from the reservoir. The risk analysis included factors such as organizational performance, market prices, service factors, competing projects and productivity. This proves that a risk analysis is capable of incorporating many different types of information to yield a comprehensible result. The risk analysis provided an essential evaluation tool for the development of a clear understanding of the project, and it also provided a source of information to help reduce project exposure to critical risks (Barnart & Coulthard, 2000). A similar study used a risk analysis approach to optimize a water injection strategy on a field in Brazil (Manceau et al., 2005).

2.5 Model Updating

There are many different ways to update numerical reservoir models throughout the life of a project. The following section explores some methods in which numerical models have been updated using data retrieved after the project has begun. This type of updating improves the reservoir accuracy by decreasing uncertainty in the

formation.

The integration of dynamic data into petroleum reservoir characterization has been an active area of research in recent years. Integration of multiphase production history is particularly important since it is the most widely prevalent dynamic data (Xue et al., 1997). Traditional inversion methods involve perturbing reservoir parameters at all locations until the production data is matched. Such methods are computationally demanding and do not always yield realistic reservoir models. For this reason a two-stage approach was proposed where the original static data is used to generate stochastic realizations. Then specific pilot points are chosen to preserve the structure of the stochastic models. These points are perturbed and the perturbation is transfered to the structure through geostatistics. The methodology has decreased the amount of time it takes to complete an inversion problem through the use of pilot points. It also provides a platform for integrating dynamic and static data. In this case the dynamic data refers to production data. A similar study was conducted by Lamy et al. (1998).

The development phase of a reservoir is dynamic with different information becoming available at different times. One should base decisions on all available data (Özdoğan et al., 2004). Well placement has a very significant impact on future recovery so care needs to be taken when choosing the well locations and trajectory. The study by Özdoğan et al.(2004) suggests an iterative process whereby the well is chosen, the production is estimated and recorded, a new well is chosen and the process continues until a desired number of wells are estimated. The optimal well is the one which shows the best production. To incorporate dynamic data the paper suggests using history matching. A similar study was completed by Fenwick et al. (2003). By dynamic data however, the paper refers to information gathered after wells have been

completed and have some production history and the results can only be used before drilling secondary wells. This is helpful, but the information can also be used during the drilling process to tune the primary wells while drilling.

Another study used a history matching process to update reservoir models. The numerical model was updated such that it predicted the present and past behavior of the reservoir. The Kalman filter was used to implement the history matching and is well discussed in Brouwer et al. (2004). Similar studies have also been completed by Nævdal et al. (2003) and Gu et al. (2004). The reservoir management with the Kalman filter updates the model as information becomes available but it uses history matching with controlling values. The Kalman filter is represented by a set of mathematical equations. These equations use a recursive algorithm to estimate the state of a process in a way that minimizes the mean of the squared error. The filter supports estimations of past, present, and even future states, and it can do so even when the nature of the modeled system is not known (Welch et al., 2004). History matching can also be done for geostatistical realizations as well. As shown by Rossini et al. (1994), a methodology exists that preserves the reservoir heterogeneity, maintains the static models initially created and still matches the production history. Their belief was that only past production can provide a guide to the most realistic reservoir realization. This particular procedure contributes to making the fluid flow model a more reliable tool for reservoir management without increasing the time for execution. Another study on history matching involved matching production data to the geostatistical data simultaneously with the upscaling of grid blocks (Fenwick et al., 2003). This study does not concentrate on real-time data, however, it does provide some interesting insight on possible ways to improve the history matching process.

Another study focuses on assessing the uncertainty while focusing on well placement optimization. It is stated that "decision analysis tools are used during exploration and initial development stages but not in later stages because of the complexity of decision trees" (Güyagüler et al., 2001). It defines three types of risk: risk-adverse (avoidance of risk), risk-prone (takes risk for financial gain), and risk-neutral (balance of risk and financial gain). The optimization will be based on the risk attitude of the experimenter. The optimization of well placement through the use of the least squares method to reduce the number of realizations in conjunction with geostatistics is suggested in another study (Pan et al., 1998). The optimization is concerned with the field development schedule on not a real-time optimization of a single well path. A net present value objective function is used in the optimization.

Literature about utilizing information while drilling to update numerical reservoir models is limited. One study proposed the use of nuclear magnetic resonance technology to evaluate reservoir quality in shaly sand reservoirs. The information gathered while drilling was used to aid in the geosteering of the production drill string to drill within thin target layers (Oguntona et al., 2004). Real-time data use is also discussed in a recent study by Saputelli et al. (2003).

The literature cited in this section demonstrates that work has been done linking geostatistics, reservoir engineering and risk engineering. All highlight advancements in technology and methodologies to improve the way reservoirs are characterized. The current study proposes a further advancement and a new methodology for combining the three areas of geostatistics, reservoir engineering and risk engineering along with measurements while drilling to reduce the risk involved with the drilling of production wells.

Chapter 3

Geostatistical Background

There are many tools available for the statistical analysis of natural phenomena. Though these studies may be useful to gain valuable qualitative insight, most classical statistical investigations fail to incorporate the spatial relationships in geological data sets (Isaaks, 1989). Geostatistics is the form of statistics that takes advantage of the spatial continuity of a geological data set while providing adapted classical regression techniques.

It is necessary to have an estimation method for reservoir properties not only to carry out feasibility studies on the profitability of a reservoir but also to estimate the life of the reservoir, expected time to production, life of the well, along with many other useful pieces of information. This estimation is made more accurate by maximizing the use of all the available information or raw data available to help tune the estimation. Using raw data such as data from well logs, well-test data, 2-D and 3-D seismic information, outcrop information and cored data, reservoir heterogeneities can be accounted for and the mathematical model of the reservoir can be made to closely resemble the actual formation. The mathematical model must honor both form (geological environment, rock types, etc.) and function (petrophysical properties that

effect performance) which is inherent in the geostatistical method of point estimation.

Approximately 90% of geostatistical reservoir characterization studies make use of the concept of variograms and variogram modeling methods (Gringarten et al., 1999). Variograms are a mathematical representation of the spatial relationship of a variable based on sample data. Once the relationship is estimated a simple model is fitted to the estimation. Then the desired parameters are determined using a technique known as kriging which may be extended to include simulation by incorporating uncertainties into the procedure. In order to fully understand these concepts it is necessary to be familiar with basic statistics, the common variogram models and common kriging techniques. This chapter outlines these concepts.

3.1 Spatial Relationships

3.1.1 Spatial Data Sets

The basic assumption in spatial data sets is that two pieces of data located geographically close to each other are more likely to have similarities than two pieces of data that are further apart. These data sets have a number of differences from random data sets. In the case of reservoir spatial data sets, there is no random sampling. This is because all drilled wells are not drilled simultaneously and each new well's location is chosen based on the information gathered from previously drilled wells. A second difference is that spatial data sets have biased sampling. This is because wells are drilled based on the location that shows the most potential for favorable profitability. This determination of potential may be based from available information from seismic tests, outcrop information and any other available source. A final difference in spatial data sets is the fact that local variability exists. This means that a

reservoir may intersect a number of different lithofacieses each of which show its own characteristics. This behavior must be understood so that the estimation will take it into account. In analyzing such data sets it is imperative to remove intrinsic biases. Methods exist to remove such biases. One method is denoted sample declustering. This method subdivides all the data into equally spaced regions whereby each data point in the region is assigned a weight based on the number of sample points in that region. The result is that regions where many sample points are available no longer skew the overall analysis of the data. There are methods to estimate the size of the sub regions however different sizes should be tried in order to find minimum reservoir properties. This will maximize the effect sample declustering may achieve (Kelkar & Perez, 2002).

3.1.2 Concept of Lag Distance

To describe spatial relationships the concept of lag distance is employed. The strength of the relationship between a variable and its relative location is based on the covariance between the variable of interest (the sampled property such as porosity or permeability) and lag distance. The key to maximizing the use of lag distance as a secondary variable is choosing the appropriate lag interval where the number of sample points within the lag tolerance is minimized while maintaining an acceptable level of accuracy in the reservoir characteristic under study (too many points leads to data smearing and excessive computer time and too few points leads to high fluctuation). This optimization takes experience and experimentation.

Definition of Covariance:

Geostatistics employs bivariate statistics very liberally. This is intuitive in the fact that the relationship between petrophysical properties and their relative spatial location is a primary concern. The predominant bivariate concept is covariance:

$$C(X,Y) = E(XY) - E(X)E(Y) \tag{3.1}$$

Where:

- E is the expected value of the random variable or variable pair

Which can also be written as:

$$c(x,y) = \frac{1}{n}\sum_{i=1}^{n} x_i y_i - \frac{1}{n}\sum_{i=1}^{n} x_i \; \frac{1}{n}\sum_{i=1}^{n} y_i \tag{3.2}$$

Where:

- x and y are random variables
- n is the number of variable pairs

Note that this is a measure of the strength of relationship between two variables. If covariance is positive then the variables are positively proportional, if it is negative they are inversely proportional, and if it is near zero then the variables are considered unrelated.

This equation can be written in this form to incorporate lag distance to be used in computation:

$$c\left(\vec{L}\right) = \frac{1}{n\left(\vec{L}\right)} \sum_{i=1}^{n\left(\vec{L}\right)} x\left(\vec{U}_i\right) x\left(\vec{U}_i + \vec{L}\right) - \left[\frac{1}{n\left(\vec{L}\right)} \sum_{i=1}^{n\left(\vec{L}\right)} x\left(\vec{U}_i\right)\right]^2 \tag{3.3}$$

Where:

- $\vec{U}_i$ is the variable position vector at the i^{th} location

To determine the number of pairs in a lag interval it is necessary to use a lag tolerance and a search radius equal to the lag distance +/- the lag tolerance. Figure 3.1 shows one lag distance and the lag tolerances associated with it. The sample point of interest is in the center of the figure. The number of pairs available at this lag distance is 9 (each point is paired to the point of interest). If the chosen lag distance or tolerance is too short then the model will experience high fluctuations, if the lag distance or tolerance chosen is too long then the model will lose important information about the property being studied. When estimating the variogram we use all value pairs within the search neighborhood using each sampled point as a reference (one at a time through the complete data set). Keep in mind that the search neighborhood is not always a radial region but it may be confined to an angular tolerance as well. This will be discussed in more detail later.

3.1.3 Assumption of Stationarity

The primary assumption in the application of the geostatistical procedure is the assumption of stationarity. This assumption means that the proposed model based on the sampled data can adequately describe the behavior of the population. This assumption has been mathematically verified in the geostatistical procedure and it provides a basis for the estimating methodology. This assumption is broken into two

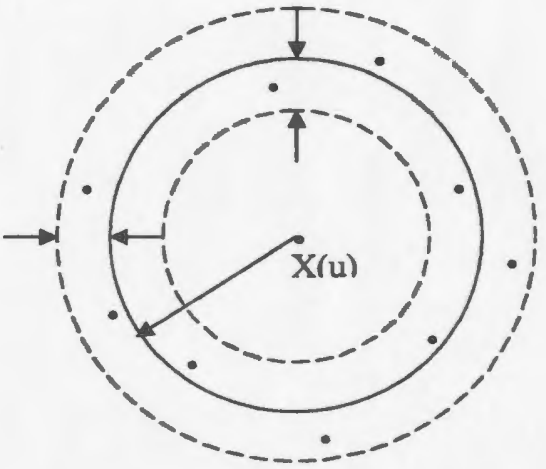

Figure 3.1: Lag Distance Visualization

parts which can be expressed mathematically:

First Order of Stationarity:

$$E\left[X\left(\vec{U}\right)\right] = E\left[X\left(\vec{U}+\vec{L}\right)\right] \tag{3.4}$$

The first order of stationarity requires local means be approximately constant. It is sometimes necessary to modify regions or spatial relationships in order to obtain satisfactory compliance with this order of stationarity.

Second Order of Stationarity:

$$C\left[X\left(\vec{U}_1\right), X\left(\vec{U}_1+\vec{L}\right)\right] = C\left[X\left(\vec{U}_2\right), X\left(\vec{U}_2+\vec{L}\right)\right] \tag{3.5}$$

The second order of stationarity implies that random variables are independent of location and are only a function of the relative vectors between desired and sampled locations. This means that the variance of the population is constant and is equal to

the covariance at a lag distance of zero.

$$VAR\left[X(\vec{U})\right] = VAR\left[X(\vec{U}+\vec{L})\right] = C(0) \tag{3.6}$$

This can be derived from the definition of covariance when the lag distance is zero. In this case Equation 3.1 reduces to variance of the single variable:

$$C\left(X\left(\vec{u}\right), X\left(\vec{u}+0\right)\right) = E\left(X^2\right) - \left[E\left(X\right)\right]^2 = VAR\left(X\right) \tag{3.7}$$

3.2 Variograms

3.2.1 Variogram Estimation

"The variogram is the most commonly used geostatistical technique for describing the spatial relationship" (Kelkar & Perez, 2002). Mathematically it is defined as:

$$\gamma(\vec{L}) = \frac{1}{2}VAR\left[X\left(\vec{U}\right) - X\left(\vec{U}+\vec{L}\right)\right] \tag{3.8}$$

In words this means that the variogram is half the variance of the difference between a sampled value and its pair some lag distance away. In practice the equation can be written in this form (Isaaks et al., 1988):

$$\gamma(\vec{L}) = \frac{1}{2n\left(\vec{L}\right)} \sum_{i=1}^{n(\vec{L})} \left[x\left(\vec{u_i}\right) - x\left(\vec{u_i}+\vec{L}\right)\right]^2 \tag{3.9}$$

The variogram estimation is the first step to simulating variables at unknown locations and it should be carried out in order to determine the type of variogram model to

use. Using the preceding equations the variogram is available for estimation however some problems may occur where some data transformation may be necessary.

There are four basic possible problems in estimating variograms. These include:

- *Lack of sufficient pairs* - More pairs mean more precision however it also means more computation time as well. A good starting point is to make the maximum lag distance half the maximum distance between sample points in the region of interest. The lag tolerance may also play a role in avoiding a lack of sufficient pairs. If not enough pairs exist then the lag tolerance should be increased.

- *Instability* - Small differences in values lead to large fluctuations since the variogram estimate involves the squared difference of the variable pair. Removing anomalies and using a greater lag tolerance may help to avoid this problem.

- *Influence of Outliers* - Points that fall well outside the range of the rest of the data are known as outliers. These points tend to skew the overall variogram results. To avoid this problem a data transformation may be necessary (such as a log transform) or if a physical reason exists that discounts the existence of such a point then the point may be removed.

- *Biased Sampling* - In the case where clustering occurs (this is very common in spatial data sets) then variogram transforms may be employed. The general-relative transform and the pairwise-relative transform are two of the most common (Kelkar and Perez, 2002).

3.2.2 Variogram Modeling

Once the variogram is estimated a model can then be created to fit the estimation. The variogram estimation is needed in order to create the model but the estimation itself is not sufficient for point estimation. The estimation is based on a discrete set of data points whereas the model is continuous.

There are two requirements for the modeling of variograms. One requirement is to use the minimum number of parameters to model the variogram. This is to increase the simplicity of the model thereby reducing computational requirements in the estimation procedure. If a simple model is a good representation of the variogram estimate then more complicated models should not be explored. The second requirement is that the condition of positive definiteness should be satisfied. The positive definite requirement is a system condition. The system of interest in this case is the matrix developed by the variogram model used in the kriging process (see Section 3.3 on kriging). In order for a variogram model to satisfy the condition of positive definiteness the following must be true:

$$\sum_{i=1}^{n}\sum_{j=1}^{n}\lambda_i\lambda_j \cdot c(\vec{u_i},\vec{u_j}) \;\geq\; 0 \tag{3.10}$$

Where:

- λ_i, λ_j *are kriging weights*
- $c(\vec{u_i},\vec{u_j})$ *is the covariance of two sample points located at* $\vec{u_i},\vec{u_j}$ *from the sample point of interest*

Note that the kriging weights are derived in part by the evaluation of the variogram

models (this is demonstrated in the kriging section). The positive definite requirement can also be stated in terms of the variogram model instead of the form of covariance. This variogram form is equally sufficient. It is stated:

$$\begin{aligned} -\sum_{i=1}^{n}\sum_{j=1}^{n}\lambda_i\lambda_j \cdot \gamma(\vec{u_i},\vec{u_j}) &\geq 0 \quad \textit{and} \\ \sum_{i=1}^{n}\lambda_i &= 0 \end{aligned} \tag{3.11}$$

Where:

- $\gamma(\vec{u}_i,\vec{u}_j)$ *is the variogram of two sample points located at* $\vec{u}_i,\vec{u}_j$ *from the sample point of interest*

All of the common variogram models have already been tested for positive definiteness. Combinations of the common variogram models have been tested as well.

The following is a summary of some of the common variogram models.

Models with a Sill

A sill is a constant value that the variogram reaches as the lag distance increases. Note that the parameter a is the range of the variogram (the lag distance where the sill is reached), the parameter L is the lag distance, and the variable C_o is the sill value.

Nugget-Effect Model: This model indicates a total lack of information with respect to spatial relationships. It is defined in the following manner:

$$\begin{aligned} \gamma(\vec{L}) &= 0 \quad if \ \vec{L}=0 \quad and \\ \gamma(\vec{L}) &= C_o \quad if \ \vec{L}\geq 0 \end{aligned} \tag{3.12}$$

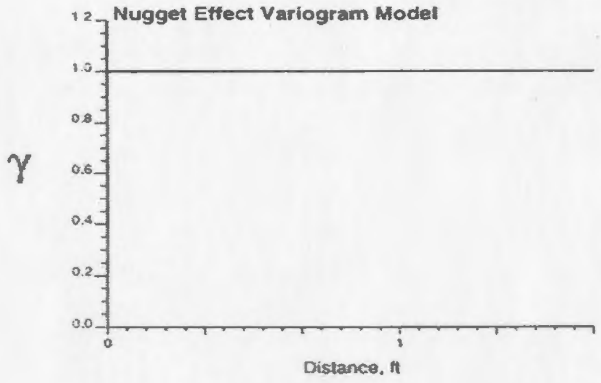

Figure 3.2: Nugget Variogram Model

Spherical Model: This is the most common variogram model with sill. It has its highest slope at the origin. It is mathematically defined in the following manner:

$$\begin{aligned} M_{Sa}(\vec{L}) &= C_o\left[\tfrac{3}{2}\left(\tfrac{L}{a}\right)-\tfrac{1}{2}\left(\tfrac{L}{a}\right)^2\right] \quad if \ \vec{L}\geq a \\ M_{Sa}(\vec{L}) &= C_o \qquad\qquad\qquad\qquad\qquad if \ \vec{L}\leq a \end{aligned} \tag{3.13}$$

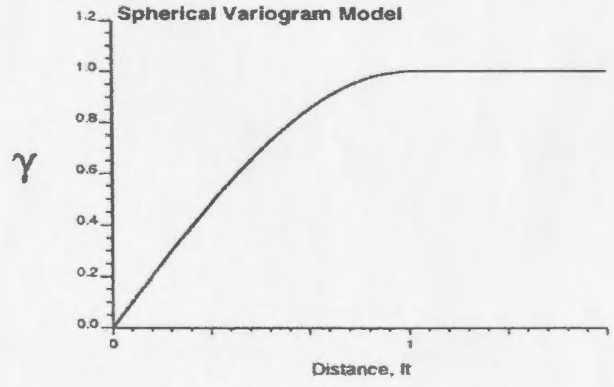

Figure 3.3: Spherical Variogram Model

Exponential Model: This model shows a more gradual change in the initial slope than the spherical model. It is defined mathematically as:

$$M_{Ea}(\vec{L}) = C_o \left[1 - exp\left(-3\frac{L}{a}\right)\right] \quad if \quad \vec{L} \geq 0 \tag{3.14}$$

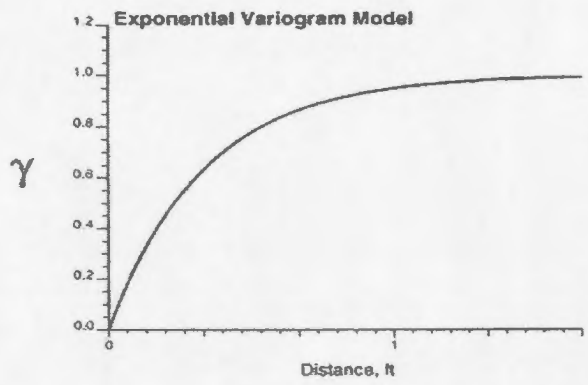

Figure 3.4: Exponential Variogram Model

Gaussian Model: This model has a slope of zero at the origin and it reaches 95% the sill value.

$$M_{Ga}(\vec{L}) = C_o \left[1 - exp\left(-3\frac{L^2}{a^2}\right)\right] \quad if \quad \vec{L} \geq 0 \tag{3.15}$$

Combination Models: Any linear combination of these models can be used. The following is an example:

$$\gamma(\vec{L}) = C_o + C_1 M_{Sa}(\vec{L}) \tag{3.16}$$

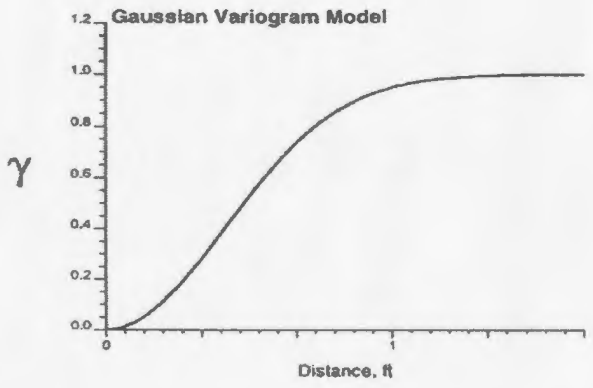

Figure 3.5: Gaussian Variogram Model

Models Without a Sill

Variogram estimates that exhibit trends and do not approach sill values will need a model without a sill to represent it. There are a number of variograms that can handle this behavior. Some examples of this type of variogram model include the fractional gaussian noise model, the fractional brownian motion model and the logarithmic model. The fractional gaussian noise and fractional brownian motion models are based on empirical parameters available in various literature sources. The details of these models are located in Appendix A. One common variogram without sill is the hole-effect model. This model is described next.

Hole-Effect Models: Sometimes an estimated variogram exhibits a cyclic behavior. There are certain natural phenomena where hole effect variograms are expected to be applicable. If there are discrete regions where the property of interest exists in certain thresholds (different thresholds in different regions) then there may be natural cyclic behavior. This is often apparent for vertical variograms since it is common to have facies change in the vertical direction due to the natural formation of rock layers through sedimentary deposit. If this behavior is apparent in an areal data set then it

is useful to check maps of the data to see if the cyclic behavior is obvious. If there is no evident explanation for the hole effect then it may be reasonable to conclude that the apparent hole effect is actually undesirable noise (Isaaks, 1989).

Sine Model:

$$\gamma(\vec{L}) = C_o \left[1 - \frac{\sin(aL)}{L}\right] \tag{3.17}$$

Where:

- $a = \frac{max(\gamma(\vec{L})) - C_o}{C_o} < 0.212$ *where a is the range of the variogram*

Cosine Model:

$$\gamma(\vec{L}) = C_o[1 - \cos(aL)] \tag{3.18}$$

For all a.

This cosine model is applicable over a wider range of amplitudes but only in one dimension.

3.2.3 Variogram - Covariance Relationship

The relationship between the variogram and the covariance between two sample points is fundamental to the solution of the kriging problem. To fully understand this relationship we start with the definition of variance, Equation 3.7. Next we can define a second random variable and include this in the variance equation in the following manner:

$$VAR(X - Y) = E\left[(X - Y)^2\right] - \left[E(X - Y)\right]^2 \tag{3.19}$$

Expanding this equation we get:

$$VAR(X-Y) = E(X)^2 + E(Y)^2 - 2E(XY) - [E(X)]^2 - [E(Y)]^2 + 2[E(X)][E(Y)] \tag{3.20}$$

Now realizing Equation 3.7 can also be written for the new random variable

$$VAR(Y) = E(Y)^2 - [E(Y)]^2 \tag{3.21}$$

and acknowledging also that covariance can be written in the form of expectation:

$$C(X,Y) = E(XY) - E(X)E(Y) \tag{3.22}$$

we can substitute into Equation 3.20 to obtain:

$$VAR(X-Y) = VAR(X) + VAR(Y) - 2C(X,Y) \tag{3.23}$$

If we now assume that the variable $X = X(\vec{u})$ and variable $Y = X(\vec{u}+\vec{L})$ then we get:

$$VAR\left[X(\vec{u}) - X(\vec{u}+\vec{L})\right] = VAR[X(\vec{u})] + VAR\left[X(\vec{u}+\vec{L})\right] - 2C\left[X(\vec{u}), X(\vec{u}+\vec{L})\right] \tag{3.24}$$

Now if we write the covariance of the lag distance in the following way:

$$C\left[X(\vec{u}), X(\vec{u}+\vec{L})\right] = C\left(\vec{L}\right) \tag{3.25}$$

and use the second order of stationarity (Equation 3.6) and the equation of the variogram (Equation 3.8) then Equation 3.24 can be rewritten:

$$\gamma\left(\vec{L}\right) = C(0) - C\left(\vec{L}\right) \tag{3.26}$$

This relationship is used in the kriging process.

3.2.4 Anisotropic Models

A variogram is rarely is isotropic. Anisotropy is when the variogram estimate varies with lag distance and direction. Both geological and variogram continuity are direction dependent. In regions where structures are prominently sedimentary, continuity is noticeably less in the vertical direction than in the horizontal direction. The horizontal continuity depends further on the direction of deposition and diagenesis alteration (Deutch, 2002). The directions exhibiting the most continuity can most often be found by studying the geological interpretation of the initial data existing for the region. If not enough information is present for conclusive evidence of the directions of continuity then the variogram may be calculated in many different directions to search for the primary anisotropy axis. There are two basic types of anisotropic models; geometric and zonal. The major difference between the anisotropic models and the non-anisotropic models is the definition of the lag search neighborhood in the variogram estimation and in the kriging procedure. When modeling a structure where anisotropy exists, angular restrictions are necessary. In non-anisotropic models the lag neighborhood is a circular in that it searches a radius completely around the sample point of interest. In an anisotropic estimation the variogram can have an angular tolerance as well as a lag tolerance so the search neighborhood is more like a search light than a target. Once the maximum and minimum directions of continuity are determined (they are generally perpendicular) same procedures are followed as noted in the estimation section. Only the pairs that exist within both the radial lag tolerance and the angular tolerance will be considered.

Geometric Anisotropy

If a variogram shows similar shape and equal sill in the maximum and minimum directions of continuity then a geometric anisotropic model is apparent. This means the structure of the variogram in the two directions is the same but the range at which the sill is reached is different for each variogram. Once the variograms in both directions have been determined it is necessary to normalize them to be used in the kriging process since only one variogram is used during kriging. To do this we define a coordinate transformation. In two dimensions it occurs in the following manner.

$$\vec{L}_u = \vec{L}_{\acute{u}} \cos\theta + \vec{L}_{\acute{v}} \sin\theta \tag{3.27}$$

$$\vec{L}_v = -\vec{L}_{\acute{u}} \sin\theta + \vec{L}_{\acute{v}} \cos\theta \tag{3.28}$$

$$L_D = \sqrt{\left(\frac{\vec{L}_u}{a_u}\right)^2 + \left(\frac{\vec{L}_v}{a_v}\right)^2} \tag{3.29}$$

Where:

- *θ is the maximum direction of continuity*
- *u and v are orthogonal directions*
- *a is the sill value in the given direction*

This operation actually converts the anisotropic ellipse (with the maximum direction of continuity being the primary axis) into an isotropic model. This is done through the use of a rotation matrix: $\begin{pmatrix} \cos\theta & \sin\theta \\ -\sin\theta & \cos\theta \end{pmatrix}$ and a rescaling parameter L_D (Goovaerts, 1997).

Zonal Anisotropy

When the variogram exhibits different shapes and sills in each of the maximum and minimum directions of continuity then the model to employ is the zonal anisotropic model. Zonal anisotropy is considered by some sources (Deutch, 2002) to be a limit case of geometric anisotropy where the range in one direction is greater than the field size so the variogram does not appear to reach the sill value (but the sill values are the same). Other sources (Goovaerts, 1997) state that this model requires that the models in both directions to be the same linear combination of variogram models but the sill value may change. Regardless, the coordinate transformation is similar to that of geometric transformation where only a different normalized lag must be calculated for each model such that the overall variogram is the sum of the two (Perez, 2002). In this case it is only important to realize that zonal anisotropy is typical in the vertical direction.

3.3 Kriging

Kriging is a linear estimating technique that estimates a variable value at an unsampled location. The technique involves estimating through weighting neighboring points to predict the value of a variable at a desired location. The primary goal of the technique is to calculate the weights that should be assigned to each neighboring sampled point such that the prediction uses the most applicable sampled data. The weights depend on the spatial relationship between the location of interest and the adjacent sampled points as well as the relationships among the sampled points themselves. Kriging works on the premise that the optimal solution is obtained using an a minimum-variance-unbiased-estimation (MVUE) technique. This means firstly

that the estimate is near or equal to the true parameter and secondly that the best prediction of the parameter is obtained when the variance of the local neighborhood is minimized. One important consideration when utilizing a kriging technique is that a search neighborhood must be defined around the location where the estimation is to be made. This search neighborhood should be chosen keeping in mind the fact that a large search neighborhood will result in a large number of sample points being generated which in turn leads to an increase in computational time to estimate the point.

3.3.1 Linear Kriging Techniques

There are a few linear kriging techniques that can be used to predict parameters at unsampled locations. One technique is simple kriging. Simple kriging is the easiest kriging technique to apply but it may not be the most practical. The primary drawback with the procedure is that it requires the knowledge of a global mean. This global mean is seldom known with any certainty. Another problem is that the first order of stationarity must be strictly valid (local means do not vary). Other forms of kriging relax this restriction. Another type of kriging is universal kriging. Universal kriging is a technique that estimates a variable in the presence of a trend. When there is a trend simple kriging does not produce accurate estimates so universal kriging must be used (first order of stationarity does not hold in the presence of a trend). To account for this, the universal kriging technique makes use of a residual parameter added to the estimate equation. More information regarding these techniques can be found in Appendix A. A final type of kriging to be noted here is ordinary kriging. It is described next.

Ordinary Kriging

Ordinary kriging is similar to simple kriging only instead of assuming a global mean a local mean is used (which is different for each search neighborhood).

The equation for estimating a desired parameter is:

$$X^*(\vec{u_o}) = X_o + \sum_{i=1}^{n} \lambda_i X(\vec{u_i}) \tag{3.30}$$

Where:

- $X^*(\vec{u_o})$ *is the estimate*
- $X(\vec{u_i})$ *is the sampled data*
- X_o *is a calculated constant*
- λ_i *is a calculated weight*

Using the MVUE technique there is an unbiased condition that must be satisfied:

$$E\left[X^*(\vec{u_o}) - X(\vec{u_o})\right] = 0 \tag{3.31}$$

From this a further assumption can be made such that the following is true:

$$E\left[X^*(\vec{u_o})\right] = E\left[X(\vec{u_i})\right] = m\left(\vec{u_o}\right) \tag{3.32}$$

Where:

- $m(\vec{u_o})$ *is a local mean at* $\vec{u_o}$

The constant X_o is defined in the following way:

$$X_o = m(\vec{u_o})\left(1 - \sum_{i=1}^{n} \lambda_i\right) \tag{3.33}$$

To eliminate the local means from the equation the following restriction is imposed:

$$\sum_{i=1}^{n} \lambda_i = 1 \tag{3.34}$$

With these assumptions Equation 3.30 becomes:

$$X^*(\vec{u_o}) = \sum_{i=1}^{n} \lambda_i X(\vec{u_i}) \tag{3.35}$$

Now the minimum variance condition is imposed. The minimum variance condition starts with a mathematical definition of error variance:

$$\hat{\sigma}_E^2 = VAR[X(\vec{u_o}) - X^*(\vec{u_o})] = VAR\left[X(\vec{u_o}) - \sum_{i=1}^{n} \lambda_i X(\vec{u_i})\right] \tag{3.36}$$

Expanding this into a form with covariance using Equation 3.23 the following equation is obtained:

$$\begin{aligned} \hat{\sigma}_E^2 &= VAR[X(\vec{u_o})] + VAR\left[\sum_{i=1}^{n} \lambda_i X(\vec{u_i})\right] - 2C\left[X(\vec{u_o}), \sum_{i=1}^{n} \lambda_i X(\vec{u_i})\right] \\ &= C(\vec{u_o}, \vec{u_o}) + \sum_{i=1}^{n}\sum_{j=1}^{n} \lambda_i \lambda_j C(\vec{u_i}, \vec{u_j}) - 2\sum_{i=1}^{n} \lambda_i C(\vec{u_i}, \vec{u_o}) \end{aligned} \tag{3.37}$$

To minimize this error variance the Lagrange multiplier method is used. For this a function F is defined:

$$F = \hat{\sigma}_E^2 + \left(\sum_{i=1}^{n} \lambda_i - 1\right) \tag{3.38}$$

$$= C(\vec{u_o}, \vec{u_o}) + \sum_{i=1}^{n}\sum_{j=1}^{n} \lambda_i \lambda_j C(\vec{u_i}, \vec{u_j}) - 2\sum_{i=1}^{n} \lambda_i C(\vec{u_i}, \vec{u_o}) + 2\mu\left(\sum_{i=1}^{n} \lambda_i - 1\right)$$

Where μ is the Lagrange parameter and is multiplied by the constraint. To minimize the error variance partial derivatives for $i = 1, ..., n$ are calculated and set to zero and the derivative with respect to the Lagrange parameter is also calculated:

$$\begin{aligned} \frac{\partial F}{\partial \lambda_i} &= 0 \\ &= 2\sum_{j=1}^{n} \lambda_j C(\vec{u_i}, \vec{u_j}) + 2\mu - 2C(\vec{u_i}, \vec{u_0}) \\ \frac{\partial F}{\partial \mu} &= 0 \\ &= \sum_{i=1}^{n} \lambda_i - 1 \end{aligned} \tag{3.39}$$

Solving these equations simultaneously is equivalent to solving the following matrix equation:

$$\begin{bmatrix} C(\vec{u}_1, \vec{u}_1) & \cdots & C(\vec{u}_1, \vec{u}_n) & 1 \\ \vdots & & \vdots & \vdots \\ C(\vec{u}_n, \vec{u}_1) & \cdots & C(\vec{u}_n, \vec{u}_n) & 1 \\ 1 & \cdots & 1 & 0 \end{bmatrix} \begin{bmatrix} \lambda_1 \\ \vdots \\ \lambda_n \\ \mu \end{bmatrix} = \begin{bmatrix} C(\vec{u}_1, \vec{u}_0) \\ \vdots \\ C(\vec{u}_n, \vec{u}_0) \\ 1 \end{bmatrix} \tag{3.40}$$

In this matrix equation the left covariance matrix is based on sampled data so it is known. It is based on the current search neighborhood at the location where the desired parameter is to be predicted. The covariance column matrix on the right can be calculated by using Equation 3.26 and the variogram model developed (since the experimental sill is also known - $C(0)$). The weights (λ_i's) are calculated by inverting the left covariance matrix equation and multiplying by the column matrix on the right. By calculating the weights in this manner the error variance is at a minimum. Finally to calculate the desired parameter estimate use Equation 3.35.

A Simple Example

Consider the following information:

Field information:

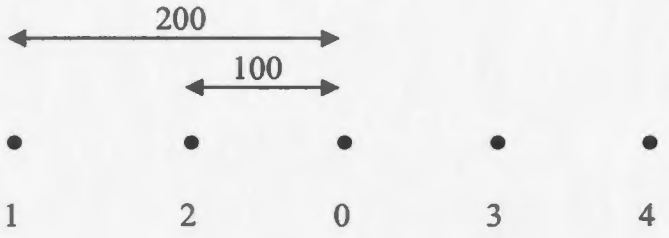

Figure 3.6: Kriging Example Field Configuration

With a variogram with the following structure:

$$\gamma(\vec{L}) = 100 M_{S_{500}}(\vec{L}) \quad east/west\ direction$$

$$\gamma(\vec{L}) = 100 M_{S_{250}}(\vec{L}) \quad north/south\ direction$$

The maximum direction of continuity is zero degrees (east/west direction)

Table 3.1: Ordinary Kriging Example

X(m)	Y(m)	Sampled Data
-200	0	30
-100	0	20
100	0	100
200	0	50

The object of this exercise is to estimate the value of the parameter are location zero. The first task is to deal with the anisotropy. To do this the lag parameter must be rotated and scaled. Looking at the first two points, the parameter L_D from Equations 3.27 and 3.28 is calculated first by calculating $L_{\acute{u}}$ and $L_{\acute{v}}$. These are just the difference between the coordinate points ($\acute{u}$ in the x direction and $\acute{v}$ in the y direction), so 100

and 0 respectively:

$$\vec{L_u} = -100 - (-200) = 100$$
$$\vec{L_v} = 0 - 0 = 0$$

Then calculating the parameters L_u and L_v using the rotation matrix given in Equations 3.27 to 3.29 and rescaling according to L_D it is found that the parameter L_D becomes 0.2:

$$L_D = \sqrt{\left(\frac{100}{500}\right)^2 + \left(\frac{0}{250}\right)^2} = 0.2 \tag{3.41}$$

Now the variogram is calculated for this pair of points.

$$\gamma(0.2) = 100\left[\frac{3}{2}\left(\frac{0.2}{1}\right) - \frac{1}{2}\left(\frac{0.2}{1}\right)^3\right] = 29.6 \tag{3.42}$$

To compute the covariance between these two points we can use Equation 3.26 and solve for $C(\vec{L})$. The sill of the sample is equal to 100 (it is the sum of the coefficients in the variogram model plus the nugget - in this case there is only one coefficient and no nugget). Solving the equation for the covariance at the given lag results in a value of 70.4. This process is repeated for each pair until the covariance matrices are complete in Equation 3.40. The left covariance matrix involves only the points in that are sampled where the right column matrix involves a lag distance between each sampled point and the desired point. The matrix equation becomes:

$$\begin{bmatrix} 100.0 & 70.4 & 20.8 & 5.6 & 1 \\ 70.4 & 100.0 & 43.2 & 20.8 & 1 \\ 20.8 & 43.2 & 100.0 & 70.4 & 1 \\ 5.6 & 20.8 & 70.4 & 100.0 & 1 \\ 1 & 1 & 1 & 1 & 0 \end{bmatrix} \begin{bmatrix} \lambda_1 \\ \lambda_2 \\ \lambda_3 \\ \lambda_4 \\ \mu \end{bmatrix} = \begin{bmatrix} 43.2 \\ 70.4 \\ 70.4 \\ 43.2 \\ 1 \end{bmatrix} \tag{3.43}$$

Solving the matrix equation by inverting the left covariance matrix and multiplying by the right covariance matrix the following result can be obtained: $\lambda_1 = -0.0181, \lambda_2 =$

$0.518, \lambda_3 = 0.518, \lambda_4 = -0.0181, \mu = -2.14$. Using this result a prediction can be made for the parameter from Equation 3.35. It becomes:

$$X^*(\vec{u_o}) = -0.0181 * 30 + 0.518 * 20 + 0.581 * 100 - 0.0181 * 50 = 39.227 \quad (3.44)$$

3.3.2 Non-Linear Kriging Techniques

There are forms of kriging which incorporate some non-linearities into them however the solving process is still linear. The non-linearization comes from a transformation of the variables involved. This technique has a number of advantages over comparable linear methods. Firstly it can generate a more stable spatial relationship. It can also estimate uncertainty better. Finally it has the flexibility to use different types of data. The common types of non-linear kriging are (Perez,2002):

- *Log – Normal Kriging*
- *Multi – Gaussian Kriging*
- *Indicator Kriging*
- *Probability Kriging*

This type of kriging has not been used in this research but it does lend itself to further research possibilities.

3.4 Geostatistical Simulation Techniques

In using kriging to estimate values of a variable at an unsampled location, the MVUE technique was used. This means that a single solution is created based on the sta-

tistical properties of the data in the sample population. This implies that the best solution occurs when the variance of the population is minimized by the prediction. The solution, however, is only one probable case out of multiple equiprobable solutions. The other solutions exists due to the uncertainty in the predicted data. Not only is there uncertainty but there is also the fact that natural phenomena does not always follow statistical laws of probabilities. Geostatistical simulation allows for the calculation of many probable solutions.

The simulation technique used in this research is a conditional simulation technique. It is a part of a larger class of simulation types called Monte Carlo simulations (see section on Risk Analysis). The conditional term refers to the fact that some information about the sample population is assumed to be known (or the spatial relationships in data pairs are honored). The conditional simulation methodology is optimized when as much information as possible is used and the computation time that is required to complete the simulation is minimized. It is for this reason that different simulation methods have been developed which prioritizes different types of information depending on which information is considered more important.

So where is the degree of freedom which sets simulation apart from kriging? The answer to this question is in the behavior of the search neighborhood and which sampled points are included in the prediction. In kriging only the raw data is used to create the realization. In simulation, previously estimated points are used in the prediction.

Where do the multiple equiprobable realizations come from? They come from the randomization of the order in which the desired locations are visited during the estimation. Consider a grid which is only sparsely populated with sampled data points.

Each empty grid block is assigned a number from one to the total number of empty grid blocks. Take this list of numbers and randomize the order in which they occur. Follow the order of this list to carry out the estimation of the entire grid. The estimation at each grid block would use raw data as well as any previously estimated values within the search neighborhood. This is one realization. For extra realizations, randomize the order and estimate all the points for the desired number of realizations.

There are a number of features which set simulation techniques apart from kriging.

1. Kriging uses a weighting system to compute the value of a variable at an unsampled location. This means that extreme values are dampened and are difficult to reproduce. Simulation offers the flexibility, through the use of random variates, to honor initial distributions while allowing for extreme values to be possible outcomes.

2. A final feature which makes simulation uniquely different from conventional estimation techniques is the ability to quantify uncertainty. Although conventional techniques do allow for the calculation of error variance (which gives indications about surrounding sample configurations) it may not give a good representation of local uncertainty. Simulation creates local variability through the development of equiprobable images.

Chapter 4

Risk Analysis

This section is designed to inform about risk analysis, an essential topic for the understanding of the quantification of uncertainty. The following sections will describe the general methodology of risk assessment while outlining how it is employed in the analysis presented in this thesis.

4.1 What is Risk Analysis?

Perhaps a better starting point would be to define what risk is. Risk is simply the probability that an event or scenario will occur causing harm to someone or something. A risk analysis is the systematic determination of risk for a number of different scenarios so that problematic events may be identified or at the very least quantified. The comparison of the different scenarios to obtain desired information about the effect of uncertain parameters on an outcome can be referred to as a risk analysis. In other words, the risk analysis examines the impact that uncertain variables, and their interaction with each other, have on an output variable. This type of analysis can be applied in virtually any field where uncertainty exists. Some examples of typical

fields where this type of analysis is currently being used are in operations management (machine reliability and maintenance, project management, etc.), finance (rate of return analysis, retirement planning, etc.), marketing (sales projection, analysis of distribution strategies, etc.) and engineering (reliability of a spring, toxic waste, population risk, etc.) (Evans & Olsen, 2002). Typical examples of risks involved with industrial projects include uncertainties associated with new designs, manufacturing risks, transportation and installation risks, market risks, contractual risks and delayed permits (Bernasconi, 2004).

4.1.1 The Process of Risk Analysis

A typical Risk Analysis can be described in six steps (Torhaug, 1990):

1. System Definition: The scope of the problem must be defined prior to the risk assessment to ensure that all parameters effecting the problem are properly addressed.

2. Hazard Identification: Events which have a negative effect on the situation under consideration should be fully explored and identified in this stage. Some well-known techniques that may be used for this are HAZOP studies (hazard and operability studies), Failure mode and effect analysis and the use of checklists to identify sources of danger.

3. Cause-Consequence Analysis: This step is based on the hazards identified. The result of a consequence analysis is the development of all relevant accident scenarios and the probability of occurrence associated with them. There are models which may be used to help determine this information. Typical models include

the use of failure and accident statistics, fault tree analysis and probabilistic methods.

4. Risk Estimation and Evaluation: The risk assessment is based on the combined results from the cause and consequence analysis.

5. Analysis of Results: The results of a risk analysis are probability distributions that negative events will occur or accident scenarios will be realized.

4.2 What is Simulation?

The most common method of quantifying risk is through stochastic simulation. Simulation has been used for analyzing systems and aiding decision making (Evans & Olsen, 2002). Before modern computing capabilities arrived this simulation was very time consuming and labor intensive. In more recent times these possible outcomes can be modeled in a computer program allowing for many iterations of a simulation to take place in a matter of seconds. This opens up the window of opportunity for completely analyzing complex situations while incorporating uncertainty into the model. Simulation is now widely accepted in the business world as well as in many other industrial applications and in various stages of petroleum exploration and production businesses.

4.2.1 Types of Simulation

In order to use simulation as a tool, it is necessary to first create a model. The model is a representation of the behavior of the reality of the event or events of interest. A means to numerically mimic actual events in virtual space. The accuracy of the

risk analysis is directly related to how close this representation can come to reality so proper care and caution should be used in creating the model. There are many different types of models which may be used to represent a real system. They can be prescriptive or descriptive; deterministic or probabilistic; or, discrete or continuous. A prescriptive model is one which leads directly to the conclusion of an optimal solution and it suggests this conclusion. A descriptive model presents the results of the simulation to give a better idea on how the the system behaves while giving measures of system performance. In a deterministic model all parameters are known with certainty (which is rarely the case in reality). In this manner the outcome of the system is known with certainty. A probabilistic model, on the other hand, have certain parameters known only within a certain range or distribution. These models resemble reality much more closely than the deterministic models. Discrete models are models which have variables which change at a discontinuous rate. This may mean that the distribution of this variable is set at fixed points under certain conditions or it changes at fixed times. A continuous model is a model that changes smoothly over time. Many situations occur as a combination of discrete and continuous events and this should be taken into account during the development of the model. A good way to create a simulation is to create a deterministic model first (in a spreadsheet for example) and then give the uncertain variables realistic distributions that will change during each iteration of the simulation.

4.2.2 Types of Simulation Models

This section outlines two common simulation models, Monte-Carlo simulation models and systems simulation models. Monte-Carlo simulation is a type of simulation where the final goal is to determine the distribution of an output variable based on the

probabilistic properties of input variables. In this manner Monte-Carlo simulation can be used to determine the amount of risk involved with certain decisions. Another type of simulation model is systems simulation. These models handle sequences of events that occur over time. The major difference between the two is that Monte-Carlo simulation is often referred to as a static model and a systems simulation is regarded as a dynamic model.

4.2.3 The Simulation Process

A simulation process comprises five essential steps (Evans & Olsen, 2002):

1. Develop a conceptual model of the problem: The problem must be properly understood in this stage. It is very important that the relationships the variables have with each other be understood so that the model can accurately depict the reality of the scenario. It is also important to establish goals and objectives of the study as well. The best way to begin this stage is to develop a simple conceptual model first and add details later.

2. Build the simulation model: This stage of the simulation process involves gathering all the equations, formulas and necessary data along with the probability distributions of the uncertain variables. The accuracy of the distributions are reflected in the accuracy of the results. This may involve using a spreadsheet linking all the variables together.

3. Verify and validate the model: At this stage it is important to ensure that there are no logical errors in the model (verification). It is also vital to show that the results of the situation is a representation of reality. This creates the credibility

the model will need and guarantee that the results that are obtained may be analyzed legitimately.

4. Design experiments using the model: This is where the user determines which values of the controlled variables will be used in the simulations.

5. Perform the experiments and analyze the results: Finally the simulation may be run and results obtained for analysis.

4.2.4 Advantages and Disadvantages of Simulation

The advantages of simulation are numerous. Firstly, simulation allows a decision maker to develop scenarios with possible outcomes and analyze these outcomes before making a decision (or the impact of a decision may be the variable under scrutiny). These outcomes can be simulated very quickly once the simulation model has been developed and the distribution of the uncertain variables chosen. In essence it is a non-destructive manner of exploring and experimenting with many different possible decisions. The second advantage is the simplicity of the method. Simulation is a quantification method that provides otherwise complex situations with real numbers to analyze. Systems that are generally hard to analyze can be easily understood with a simulation method. A third and non-exhaustive advantage for simulation is the capability to model any assumption, especially when analytical methods are inappropriate or do not exist (Evan & Olsen, 2002).

Any method with so many advantages is sure to have disadvantages as well. One such disadvantage is the amount of time that is required to obtain input information, to develop the simulation model, and run the simulation to analyze the results. The substantial time and effort is a disadvantage when decisions are needed within a

relatively short amount of time. The simulation may take a lot of time to run, and the results may require time for analysis. The increase of computing speed in modern computers offsets this disadvantage however the analysis of the results may still be time consuming. The second disadvantage is the lack of precision. Simulation may have sampling errors. This is where results may not appear practical yet are inside the bounds of available solutions based on the uncertainty of the input variables. Analytical solutions usually do not have this sort of uncertainty.

When analyzing a system where parameters are uncertain the outcome cannot be uniquely defined. The probability distribution of the parameters will produce a probability distribution of the outcome. This is concept is intuitive but how can this be accomplished in practice? The answer lies in the generation of random numbers. The use of a random number generator removes any biases from the analysis. In assigning distributions to input parameters and randomly drawing values from the distributions for the outcome calculation, a sense of variability and uncertainty can be developed (Voit & Schwacke, 2000). The following section gives the details on how random number generators work.

4.3 Random Number Generation

Simulation uses the generation of pseudo-random numbers to randomize different simulation iterations. The reason the words "pseudo-random" are used is because computer applications use an algorithm to generate these random numbers. This means that the generation of the random numbers is deterministic and that the same sequence of random numbers can be regenerated if desired. The sequence of numbers, however, does appear to be random. For a sequence to appear random is must have

the following properties:

- All numbers are uniformly distributed between 0 and 1. The means that when the amount of numbers generated is large each value is equally likely to occur (the histogram should be relatively flat).
- Numbers in the stream have no serial correlation. Serial correlation is the relationship between any random number in the stream and the following random numbers. In other words there should be no patterns existing in the randomly generated data set.
- The random number stream has a long cycle. This means that when the initially generated random number occurs only after many simulation iterations have occurred (and this point may never be reached).

4.3.1 Random Number Generation Techniques

There are many algorithms for generating random numbers. Two common types of algorithms are the midsquare technique and congruential random number generators.

The midsquare technique takes an initial four digit number called the random number seed, squares it and takes the set of middle four digits as the next number in the sequence. This method takes advantage of the fact that the square of any 4 digit number has no more than 8 digits. The sequence of random numbers can be reproduced by remembering the random number seed. This was one of the first numerical methods to generate reproducible random numbers. It's limitation is that for certain random number seeds the stream of random numbers can converge to a single value of zero, and do so rather quickly. This yields the stream useless as a random number

generator.

The congruential random number generator uses the mathematical concept of the modulus. If the modulus (m) is a positive integer then $x \ mod \ m$ is simply the remainder after dividing $x \ by \ m$ as many times as possible. For example, $9 \ mod \ 4 = 1$ and $6 \ mod \ 3 = 0$. The generators have the form $z_{i+1} = f(z_i) \ mod \ m$ where the f is some function (typically multiplicative or linear) of the initial seed. The modulus computation takes advantage of the fact that the solution will always yield integers between 0 and m - 1. Dividing this value by m will results in values between 0 and 1, which will be random numbers. It has been found that the the best generators (those with the largest cycles) occur when the modulus is as high as possible (as high as the operating system allows) (Evans & Olsen, 2002).

Once a technique has been identified it is important to test this algorithm for uniformity. A number of statistical tests may be used for this task including the Chi-Square test or the Kolmogorov-Smirnov test. In testing for serial correlation it is possible to apply the Chi-Square test to pairs of numbers a certain distance apart (Evans & Olsen, 2002). These tests will not be discussed any further since it is not the purpose of this paper to prove the algorithms of the random number generators are sufficient, however, some extra information on them can be found in Appendix A. The purpose of this section is to give general background information to bridge the knowledge gap to give a little more insight on how numerous simulation iterations may be realized. A number of computer languages and mathematical applications have the capability of generating random numbers with internal algorithms (not seen by the user). Fortran and C++ for example have the RAND(x) and RANDOMIZE command respectively. Other applications such as MATLAB and Excel also have built in random functions available to the user with algorithms similar to those used above. These

are the random number generators used in the development of the methodology in this paper.

When the distribution of the parameter of interest is not uniform then it is necessary to transform the set of random numbers generated to fit the desired distribution. If the distribution of the parameter is similar to a simple distribution (such as exponential or triangular) then a simple inversion of the uniform variates will create the desired distribution. What this means is that the probability density function of the desired distribution is explicitly inverted. For more complicated distributions with no closed form solution of inversion problem a numerical method is necessary. A number of methods exist for each distribution such as the Marsaglia and Bray model for normal distributions (Devroye, 1986) and the Wallace model (Wallace, 1996). These generators have been included in built-in functions in computer programs such as MATLAB and Excel for users to use at their discretion.

4.4 Risk Calculation

Risk calculation is based two things. First it is based on the probability that an event will occur that will cause harm or have a negative effect on a person or thing. The second factor in the risk calculation is the consequence if such an event occurs. Multiplying both factors together yields a risk factor. If both factors are discrete in nature then both will have corresponding parts multiplying together and added in the end. If both factors are continuous then the functions are multiplied together.

$$risk = probability \;\; X \;\; consequences \tag{4.1}$$

Chapter 5

Case Study 1

This section presents the first of two oil based production case studies. Both case studies demonstrate different aspects of the methodology shown in this thesis. This case study shows how to employ geostatistics to estimate point locations along a well path. These estimates are then used to estimate productivity from a field example. The concept of risk is then used to quantify the degree of uncertainty in the project in terms of monetary risk.

5.1 Reservoir Definition

The first task is to initialize some of the needed reservoir parameters such as the dimensions of the reservoir and the estimated total flow velocity for both oil and water phases together. The total flow will be constant throughout the reservoir but the water saturation will change as the water front moves through.

5.1.1 Geometry

It is useful to note at this point that the reservoir is based on a field example (Kelkar et al., 2002) which is given in two dimensions and in field units. The calculations performed were all completed in SI units and the appropriate conversions were implemented where necessary. The length, width and height of the reservoir are assumed to be 2438.4 m (8000 ft), 243.8 m (800 ft) and 50 m respectively.

5.1.2 Reservoir Attributes

The total flow velocity is calculated using these dimensions and an expected flow rate of 2500 m^3/day (this is the water and oil mixed velocity). The viscosities of oil and water are assumed to be 0.3 centipoise (cp) and 10 cp respectively.

The variable of interest in this study is porosity. The porosity is distributed throughout the reservoir in a manner given in Appendix B and is taken from the field example.

5.1.3 Well Trajectory

The well trajectory in this case study was chosen based on the porosity distribution and attempts to optimize production based on favorable porosity values. The choice in well trajectory in this case study is arbitrary in that the purpose of the case study is to demonstrate the methodology of how to quantify the risk associated with the geostatistical realization of a reservoir. The trajectory is noted here for completeness. The well follows the straight line between the two points.

Table 5.1: Well Trajectory: Case 1

X(m)	Y(m)
-500	8000
14975	212.58

5.1.4 Assumptions

The object of the production calculation in this study is to use the porosity data and a constant reservoir pressure to estimate the volume of oil produced. To do this a number of assumptions are used to simplify the calculation. The assumptions are used because the complexity of the problem is unnecessary in describing the methodology. The first assumption is that each porosity value calculated (one for every 25 feet along the x-direction) it is independent from other porosity values. In other words each porosity value exists in a channel or between shale layers. See Figure 5.1 for a representation of the 2-D reservoir.

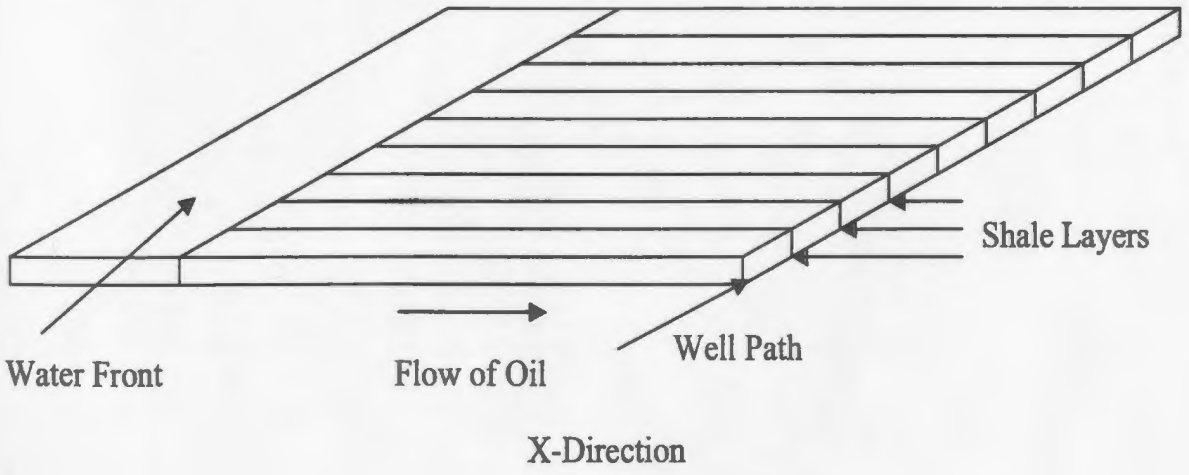

Figure 5.1: Reservoir Description

This type of model is a transformation of a stream tube model. A stream tube model is a model where flow can be visualized to go from one location to another

in a group of parallel pipes. It follows that the flow through each pipe is unaffected by neighboring flows. Such an assumption allows the calculation of the production to be performed without solving complex fluid dynamics equations which may only be solved numerically. This model is used in many different situations to simplify problems in practice. It is applicable when the end point mobility ratio is near one (the ratio of the water mobility to oil mobility in a oil-water reservoir, where mobility refers to the ability of the fluid to permeate) and the fluid is incompressible. These assumptions are adopted for this case study as well. The traditional stream tube model is depicted in Figure 5.2.

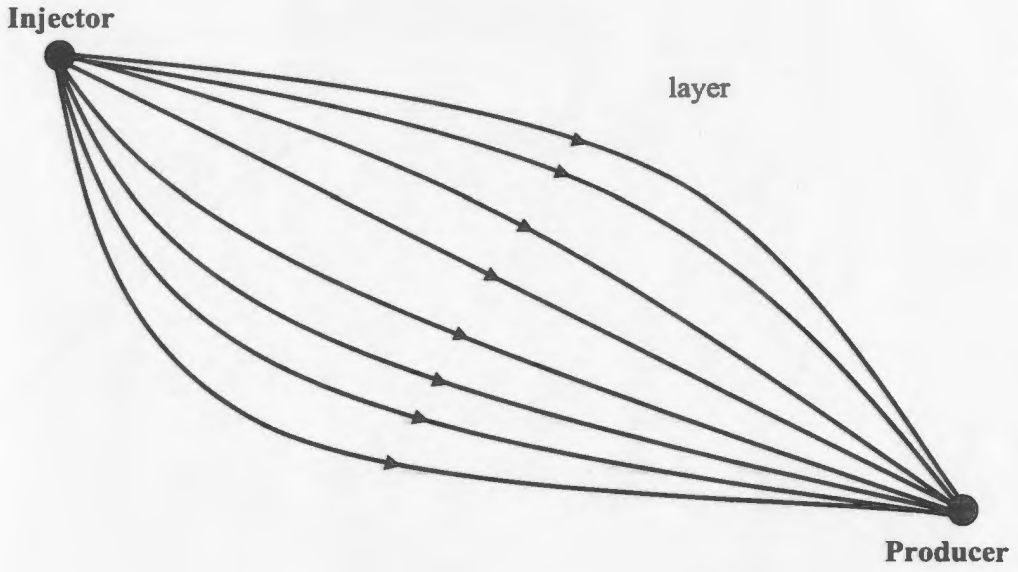

Figure 5.2: Stream Tube Model

A further assumption is in reference to the reservoir saturations. It is assumed that the reservoir is initially completely saturated with oil and the stream tube model is 100% efficient (there is no residual oil). This is for the sake of simplicity.

5.2 Reservoir Engineering Background

In order to completely understand the problem some reservoir engineering concepts must be mentioned briefly.

5.2.1 Darcy's Law

A fundamental law in reservoir engineering is Darcy's law. The following equation relates flow velocity to pressure, permeability and water saturation. Note that the i can be any fluid or phase.

$$\vec{v_i} = -\frac{K k_{ri}(S_w)}{\mu_i}\left(\frac{\partial p_i}{\partial x} + \rho_i g \sin(\alpha)\right) \tag{5.1}$$

Where:

- $\vec{v_i}$: *volumetric flux (Darcy Velocity)*
- K : *absolute permeability (the rock property that allows a liquid or gas to move through it)*
- k_{ri} : *relative permeability (described in the following section)*
- S_w : *the water saturation (the percentage of pore space in a formation occupied by water)*
- μ_i : *the phase viscosity (the property of a fluid's resistance to flow)*
- $\frac{\partial p_i}{\partial x}$: *the phase pressure gradient*
- ρ : *density*

- g : *acceleration due to gravity*
- α : *the angle of inclination counterclockwise from the horizontal*

5.2.2 Relative Permeability

In Darcy's law the permeability represents a rock property at a point. In the presence of numerous phases there may be different fluid fronts moving through the formation at different flow velocities. To account for this the concept of relative permeability is used. In an oil/water reservoir the relative permeabilities are:

$$k_{ro} = \frac{k_o}{K} \qquad \textit{and} \qquad k_{rw} = \frac{k_w}{K} \tag{5.2}$$

Where:

- k_{ri} : *phase permeability relative to overall permeability*
- k_i : *phase specific permeability relative to overall permeability*
- K : *absolute permeability*

These relative permeabilities are a function of water saturation only as can be seen in the following section.

5.2.3 Fractional Flow

Fractional flow is a means to simplify the reservoir simulation method by removing one unknown from the set of equations. It is defined as:

$$f_w = \frac{u_w}{u_T} \tag{5.3}$$

Where:

- $u_w : water\ flux$
- $u_T : total\ flux$

Using Equation 5.3 in conjunction with Darcy's Law (Equation 5.1) the fractional flow reduces to:

$$f_w = \frac{\frac{k_{rw}}{\mu_w}}{\frac{k_{rw}}{\mu_o} + \frac{k_{ro}}{\mu_o}} \tag{5.4}$$

The relative permeabilities can be assumed to be the following functions of water saturation (Ahmed, 2001).

$$k_{rw} = (S_w)^2 \tag{5.5}$$

$$k_{ro} = (1 - S_w)^2 \tag{5.6}$$

Substituting this into the fractional function yields the following:

$$f_w = \frac{\frac{(S_w)^2}{\mu_w}}{\frac{(S_w)^2}{\mu_w} + \frac{(1-S_w)^2}{\mu_o}} \tag{5.7}$$

Noting that the viscosities are constants the fractional flow function as a function of water saturation will appear similar to Figure 5.3:

5.2.4 Frontal Velocity

As immiscible fluids flow through a reservoir the bulk velocity of the fluid is known as the frontal velocity. If, for example, water is injected into a well on one side of a reservoir to enhance the productivity on another side, then the velocity of this water toward the producer well is known as the velocity of the water front (frontal

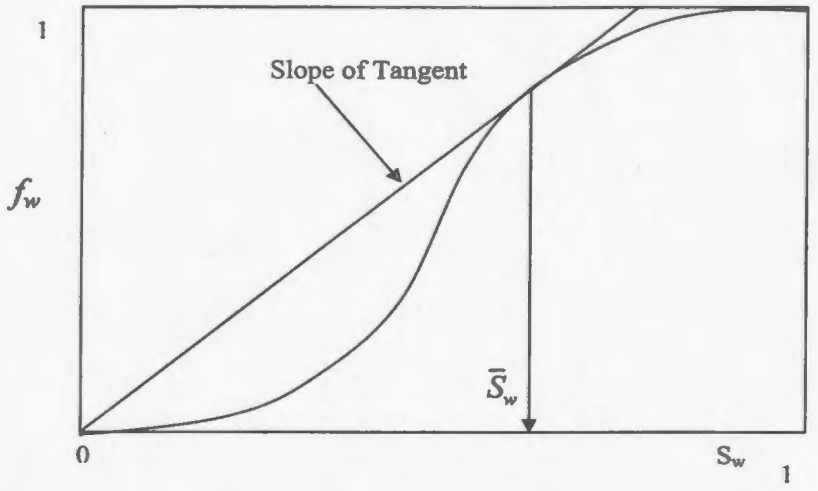

Figure 5.3: Fractional Flow Function

velocity). At any instant in time the fractional flow function can be plotted versus water saturation. The figure would resemble Figure 5.3. The frontal velocity can be determined in the following way:

The frontal velocity is mathematically defined as:

$$\sigma = \frac{u_T}{\phi} slope \tag{5.8}$$

Where:

- u_T : *the total flux of the fluid through the formation*
- ϕ : *the porosity of the formation*
- *slope* : *the slope of the tangent of the fractional flow function*

5.3 Solution

In order to solve this problem, the geostatistical methods and the risk implementation is done through the use of MATLAB. A copy of the code is given in Appendix C.

5.3.1 Geostatistical Analysis

The first step for estimating the porosity along the well path is to first use the field data to estimate the variograms. The first assumption made is that the reservoir is anisotropic (as is normally the case). This means that the variogram will vary in distance and direction (not homogeneous or isotropic). In an anisotropic variogram calculation it is necessary to determine the direction of maximum continuity. Since no extra information exists that would allow the directions of continuity to be conclusively determined, it is necessary to calculate a variogram map. This requires that a number of variograms be calculated in a number of different directions to see which direction exhibits the most and least amount of continuity. The direction with most continuity reaches the experimental sill (variance of the sample population) at the largest lag distance. Consult Figure 5.4 to observe this behavior. It shows the result of the variogram estimate at each corresponding angular direction.

From the figure the maximum directions of continuity are in the 0° direction (indicated with a "□" in the figure) and the 22.5° direction (indicated with a "◇" in the figure. Upon closer inspection of the data there are more pairs for the 0° direction. Not only are there more pairs for that direction but there are so few for short lag distances at the 22.5° that it is unrepresentative of the population (there are zero pairs at the first lag distance and only three pairs for the second lag distance compared to five and thirty pairs at the same lag distances in the zero direction). For this reason,

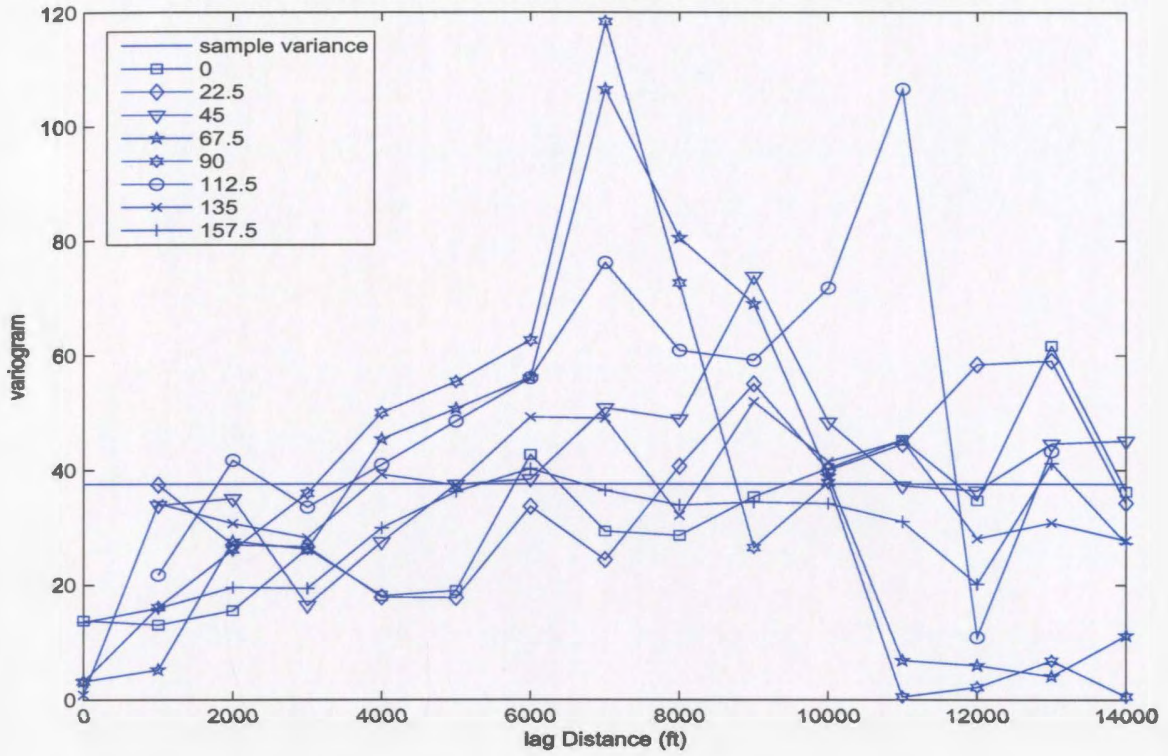

Figure 5.4: Direction of Maximum Continuity

the 0°, or east-west direction, is chosen as the direction of maximum continuity (the principal direction). The minor direction is taken perpendicular to the direction of maximum continuity for modeling purposes (Goovaerts, 1997). This direction is 90° from the horizontal or in the north-south direction.

To estimate the variogram from the sample data, the distance between each point and every other point in the data set must be calculated. In this case study there are 68 sample points in the sample population. For this problem the two dimensional Cartesian distance equation is used to create a matrix of 68 elements by 68 elements. Each element represents the distance between that point and another point in the data set (the diagonal is zero since that is the distance between each point and itself). The variogram estimate can be tuned by altering the lag, lag tolerance, search

angle, and angular tolerance to optimize accuracy and decrease fluctuation. Here it is important to keep the essential structure of the variogram intact while minimizing the fluctuation. The configuration chosen was a lag of 1000 ft, a lag tolerance of 450 ft, search angles in the direction of maximum and minimum continuity (one estimate for each) and an angular tolerance of 20 degrees.

Using Equation 3.9 and searching the data methodically, the variogram can be estimated at each lag distance. The estimation yields the Figure 5.5.

The Figure 5.5 demonstrates the result of the variogram estimation as well as the comparable models (which will be discussed later). As can be seen there is still some fluctuation in the estimates. It can also be noted that the direction does have an effect on the result of the variogram so the assumption that the reservoir is anisotropic is correct. The anisotropic model is necessary to capture the spatial variation with respect to the direction. One anomaly that should be noted is where the largest lag distances in the north-south estimate show near zero results. Upon closer inspection into the number of pairs existing at each lag distance it can be found that this is based on only one or two data pairs. These points may be neglected in the modeling process since they are only representative of a few points and not of the entire population. Another anomaly is the peak for the north model. In geostatistics there are often times where the variogram estimate will be difficult to model. In this case there does not seem to be an explanation for the peak so the modeling will attempt to achieve the best fit based on this estimation.

Once the variogram is estimated the variogram model must then be chosen. Different models must be selected and matched to the estimation by varying the parameters of the model. There are two models, one for each direction. The chosen variogram

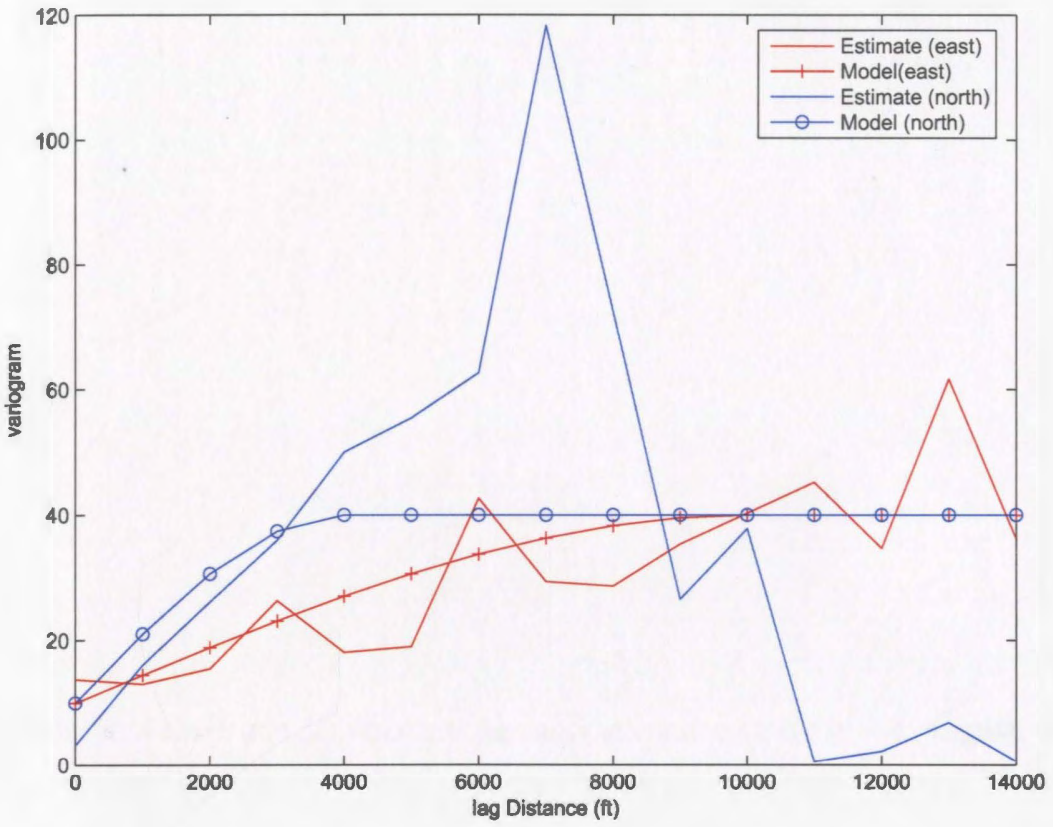

Figure 5.5: Variogram Estimation Vs Variogram Model

models are linear combinations of a model with a sill. Both models are spherical (Equation 3.13) with a nugget (Equation 3.12). This type of structure is used since it is very simple in nature. When major spatial features can be captured with simple models then more complicated models should not be explored. More complicated models, even if they have a better fit, do not always lead to more accurate estimates (Goovaerts, 1997). Both variogram models tend toward the same sill yet at different rates. This is known as geometric anisotropy which is common in horizontal sample populations in two dimensions.

For the East-West direction: (Principal Direction)

$$\gamma\left(\vec{L}\right) = 10 + 30M_{S(4000)}\left(\vec{L}\right) \tag{5.9}$$

For the North-South direction: (Minor Direction)

$$\gamma\left(\vec{L}\right) = 10 + 30M_{S(10000)}\left(\vec{L}\right) \tag{5.10}$$

Figure 5.5 compares the variogram estimate to the model. As can be seen the fit captures the trend and removes fluctuations.

We can allow for the degree of fit to be relaxed because of the lack of data pairs at certain lag distances. Geometric anisotropy is common in horizontal variograms (where the directional variograms advance to the same sill but over different ranges). For this reason the sill for this model is the same in both directions. Zonal anisotropy for this two dimensional case is unlikely since the reservoir exists in a horizontal layer. Typical zonal anisotropic behavior occurs when comparing horizontal to vertical variograms (Kelkar & Perez, 2002).

Now that the variogram model has been verified against the estimate the kriging procedure can take place. In this case the interest lies in determining the porosity along a given path noted earlier.

For the kriging, ordinary kriging was chosen since there is no global mean information and there is an absence of a trend in the variogram estimates. If a global mean was known then simple kriging could be used. In the presence of a trend universal kriging would be necessary. The first step in completing the kriging procedure is to decide on both the nature of search neighborhood for the prediction location and on how many sample points to use for the estimation. For simplicity the search neighborhood

chosen is an omni-directional one on the well path (and circular in nature). For computational reasons, four of the closest sample points were used to estimate the porosity at any point on the well path. A MATLAB procedure called *risk.m* (see Appendix C) is used to sort the data into the four closest points to each estimation location (at 25 ft intervals along the x-direction on the well path).

Next covariance for the left and right hand side of the matrix equation (Equation 3.40) need to be calculated. This is done by using the variogram models and Equation 3.26. Once all the covariance elements have been calculated the weighting parameters can be calculated by inverting the covariance matrix on the left-hand side of the equation and multiplying it by the covariance matrix on the right-hand side. Using Equation 3.35 the estimate can then be made. This is similar to the example given in the chapter on Geostatistics.

This procedure has to be repeated for each point on the well path where an estimate is desired. In this problem a new estimate is required every 25 feet in the x direction. This results in 620 estimates. For validation purposes the resulting array of estimated porosity values is given with the well path data and the nearest four porosity sample points in Appendix B. It can be seen from this data that the estimates fall within the range of the nearest sample points for each location. The geostatistics calculations are also a part of the MATLAB file *risk.m*. This marks the end of the use of geostatistics for this case study.

5.3.2 Production Calculation

The basic outline for estimating the total production of this particular reservoir involves the calculation of the time to breakthrough of the water front into the well

bore. Since the formation is assumed to be completely saturated with a single phase oil initially, the time of water breakthrough marks the point in time that a molecule of water travels the entire distance of the reservoir and enters the well bore. Once the water breaks through into the production well, the production is assumed to end at that shale layer. This means that once water breaks through in a shale channel then oil is no longer produced locally from that channel. Of course the calculation of time to breakthrough for each shale layer is computed independently so there will be a different time to breakthrough for each shale layer. Summing up the production of all the shale layers at any given time will result in the total production of the reservoir at that time.

The production calculations are completed in the MATLAB file *pro.m*. The frontal velocity is based on the fractional flow function. More specifically the velocity of the water front is equal to the slope of the tangent of the fractional flow function which given by the Equation 5.7. In order to calculate the maximum slope of this function a MATLAB numerical subroutine was created called *Swbar.m* and can be found in Appendix C. This routine calculates the value of S_w at the place of maximum slope. This value came to be 0.986 and the function itself can be seen in Figure 5.6. Then the slope can be calculated by simply dividing the value of the fractional flow function at the location of maximum slope by the saturation at the same location (since it passes through the origin). This slope is constant throughout this particular reservoir since it is assumed that the relative permeabilities (which are rock/ fluid properties) are consistent throughout the formation.

Once the velocity of the front is determined for each shale layer, the time to breakthrough can be estimated simply by dividing the distance (length of the reservoir) by the velocity of the front. Once this is reached no more oil is produced. Using the

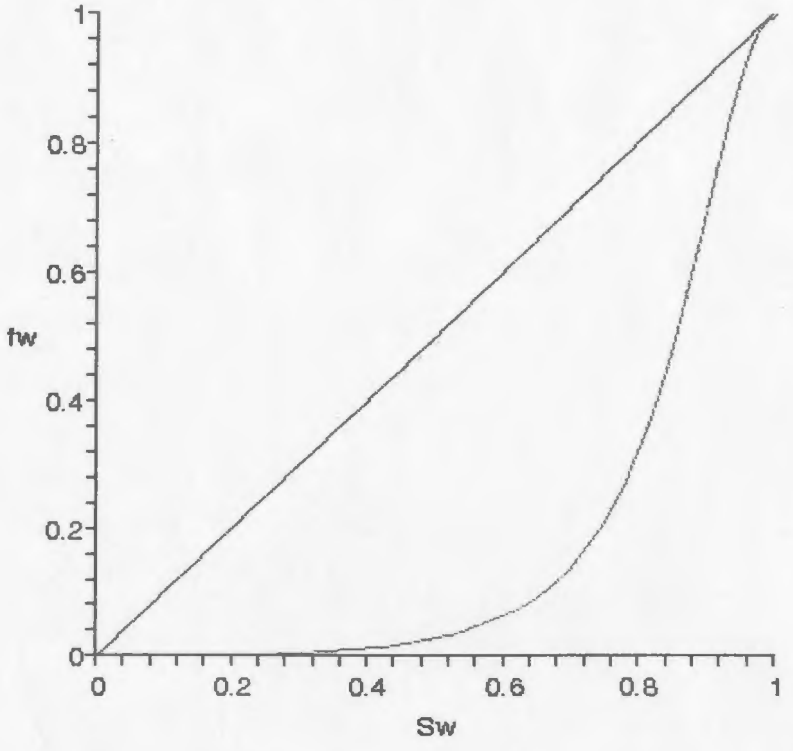

Figure 5.6: Fractional Flow Function

cross-sectional area of the shale layer the total production of each layer can then be determined and finally a production profile can be generated. This profile is considered the baseline profile and all other profiles will be compared to it to determine the consequences of not achieving this baseline production. It was developed using geostatistics. The computation of the production volume for each channel is done in the following manner:

$$Production_i = (HW)(\sigma\phi)\, ttbt_i \tag{5.11}$$

Where

- HW : $cross - sectional\ area$

- σ : *frontal velocity*
- ϕ : *channel porosity*
- $ttbt_i$: *time to break through for a single shale layer*

5.3.3 Risk Calculation

In order to carry out the risk calculation it is necessary to quantify both the consequence of the hazardous event as well as its probability of occurring. The consequence for this case study is the cost associated with not achieving the desired production, in other words, the cost of the deviation from the baseline. The porosity distribution results in the production's deviation from the baseline. The total production based on a number of different porosity distributions was calculated. The porosity distributions were generated through the use of a random number generator with a normal distribution. The normal distribution was chosen because it most closely resembles the sample data set and the central limit theorem suggests that if the sample size is large enough the distribution of the mean can be approximated by a normal distribution regardless of the shape of the population distribution (Evans et al., 2002). This allows for a realistic analysis to be carried out. A number of porosity sets (500 sets) have been used to create 500 production profiles. The porosity was chosen in a manner to mimic the available sample data as much a possible with a normal distribution. The mean of the sample set of porosity is 24.17% and the standard deviation is 4.84% which is the same as the baseline.

Figure 5.7 demonstrates the degree of fit between the distribution of the porosity data set associated with the geostatistical analysis and 3 arbitrary randomized normal porosity data sets from the 500 available. This shows how well the geostatistical

realization fits the normal distribution realizations. It is also evident that the porosities developed from the normal random generation represent the geostatistical porosity distribution. The mean and standard deviation of all cases are the same. The fit is reasonable given the fact that randomized models do not intend to fit realistic models but only represent the statistical properties of the original data. The goal is to estimate the uncertainty and risk involved with a realistic model.

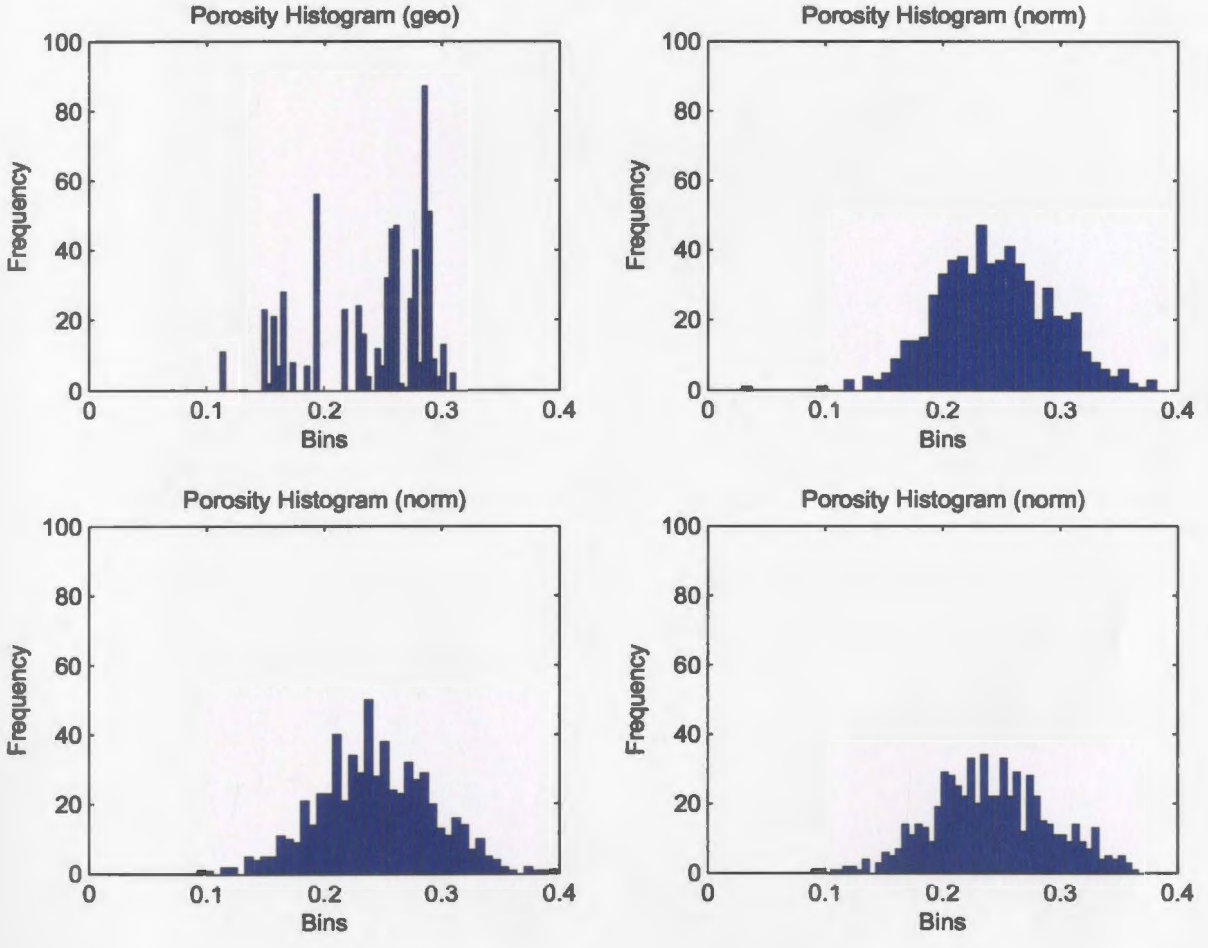

Figure 5.7: Porosity Distribution Comparison

Using the porosity distributions shown in Figure 5.7, the production profiles generated are shown in Figure 5.8.

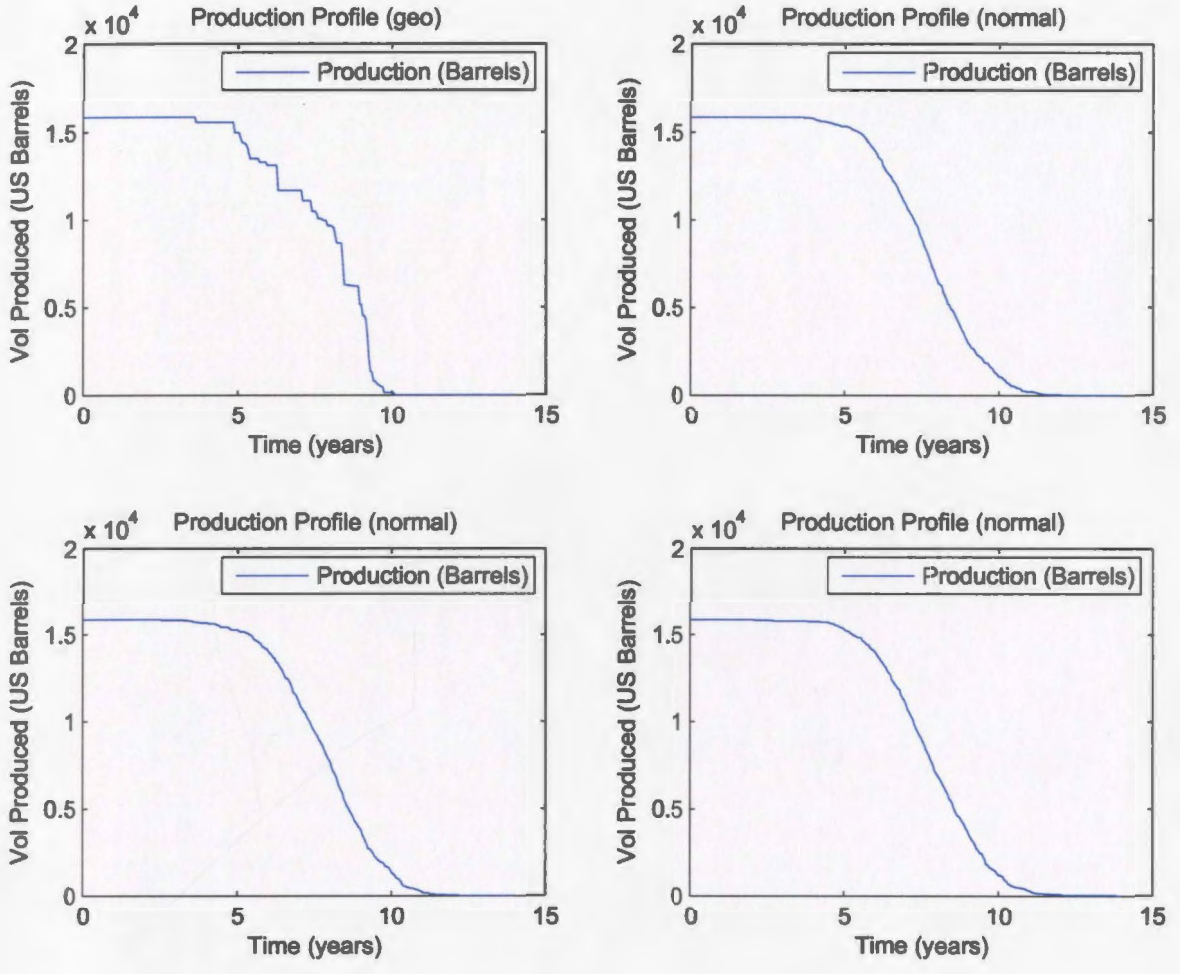

Figure 5.8: Production Distribution Comparison

The profiles show a very close relationship with each other. Each of these profiles represents one possible image of the reservoir and the collective distribution represents a bandwidth of probable solutions to the predicted production. By taking the total production volume for the baseline case and the total production from each normal randomized production image a group of possible production volumes are formed. In this case study a 95% confidence level is acceptable for the risk analysis. In practice, a management team would have to decide on what degree of confidence is necesary for any given study to be accepted. To adhere to the 95% confidence level, the 95th

percentile is taken from the distribution of the production calculated from the normal randomized reservoir images. This is the value used to determine the consequences of not achieveing the baseline production. The 95th percentile is the production volume below which 95% of all the production from the normal random reservoir images fall. To determine the consequences, the difference is take between the percentile and the baseline production and multiplied by the price of oil. In this case, since a probabilistic analysis is not being undertaken, the price of oil is take as a constant value of $50 per US barrel. The uncertainty in the calculation of risk factor is 5% since the confidence level is 95%. The calculation of risk factor is summarized in the following equation:

$$Risk = (P_{95} - P_{base})\,(\$Oil)\,(0.05) \tag{5.12}$$

Where

- P_{95} : *95th percentile of random production*
- P_{base} : *baseline production*
- $\$Oil$: *Price of oil per US Barrel*
- 0.05 : *uncertainty*

The preceding equation calculates one risk factor for the 500 reservoir images. In order to determine a distribution of risk factors to better understand the risk, the process of generating the random images and calculating the risk factors was repeated 500 times. The results are given next.

5.4 Results

When discussing risk it is noteworthy to mention that risk is only present when there is a hazard or negative event occurring. This means when the calculated deviation between production and baseline is positive there is no inherent risk. For the sake of argument, this occurrence of risk that is positive will be considered advantageous or positive risk and will be discussed as a risk factor even though there is no risk involved.

Figure 5.9 represents the cumulative distribution of risk factors for this case study. It can be seen from the plot that the negative risk is small at only 5%. This means that from the images studied only 5% of them incurred a negative risk. The remaining 95% either had no deviation or demonstrated a profit.

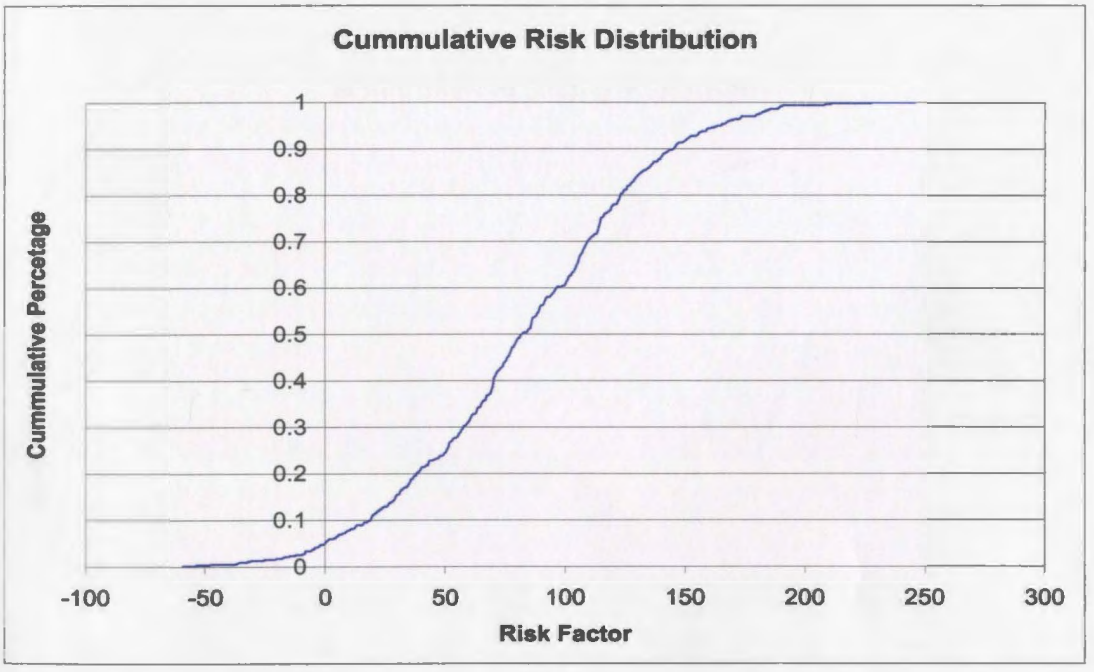

Figure 5.9: Cumulative Risk Distribution

The mean risk factor is given as 82.34. This risk factor represents the deviation of the production volume in thousands of barrels of oil, multiplied by the price of oil per barrel and then multiplied by 5%. It is in thousands of dollars with the uncertainty taken into account.

5.5 Summary

The objective of this chapter was to demonstrate a methodology for calculating the risk factor associated with a geological uncertainty. This methodology incorporates the use of geostatistics to generate a baseline porosity image and a random number generator to develop alternative porosity images (images are the predicted porosity values along the well path). Production volumes from the groupings of 500 images were compared to the production volume of the baseline image where the 95th percentile of production for each grouping was considered to have an acceptable confidence level. There were 500 total groupings considered for this case study. The comparison was completed by multiplying the difference between the 95th percentile of each grouping and the baseline production by the price of oil and the uncertainty in the 95th percentile (5%). This calculation yields a distribution of risk factors which was illustrated in Figure 5.9. This case is a building block for determining the risk involved during well planning. The concepts shown serve as a base for the the next case study which provides a more detailed example of how to quantify the risk involved when there is an uncertain geology. The next case will also shows how this risk can be improved by using measurements while drilling.

Chapter 6

Case Study 2

This case study presents an in depth account of how the concepts of risk and geostatistics can be used together to help in the management of risk while drilling production wells in petroleum reservoirs. Compared to case study one, this case study takes a more complex reservoir model, analyzes the reservoir realizations more rigorously and computes the production profiles using a reservoir simulator instead of assuming existence of shale layers (a stream tube model). It also demonstrates the use of measurements while drilling to show what effect the inclusion of this type of data can have on the risk factor of not predicting the actual production. All the simulations of interest in this chapter deal with forecasting. The reservoir is updated with measurements while drilling throughout the drilling process before any actual production takes place. Comparisons can be made since the baseline reservoir realization is assumed to be the fully characterized realization and the reservoir simulation associated with the baseline represents actual production. This chapter also shows how commercially available software can be used to apply this methodology in a realistic manner. Before introducing the problem statement however, it is appropriate to identify the software used in the case.

6.1 Applications Utilized

A number of commercially available computer applications have been used to apply the methodology in this case study. It was necessary to make use of such software since it is time consuming, difficult and redundant to develop such applications and software development is not the key component of this research. The software utilized is currently being used by major companies in each application's specific area of focus. The first package is Eclipse (Schlumberger), the second application is GSLIB (Statios) and the third is NETool. Other educational tools used include Excel (Microsoft) and MATLAB (MathWorks Inc.).

6.1.1 Eclipse

Eclipse is a comprehensive reservoir simulation package widely used by major oil companies to mathematically model reservoirs. This program was used because of its industry familiarity and its integration into the other software utilized in this research. The dataset used for the analysis was initially in an Eclipse format. Eclipse office is the application which manages all the different subprograms needed to prime the data for input into the Eclipse simulator. It is also used to view the results of the simulation as well as generate reports. It was used to export the data from the dataset applicable to the geostatistical analysis (this was the primary use of Eclipse for this research). Eclipse is a very complex and detailed reservoir simulator which requires a great amount of background information in reservoir engineering for it to be utilized to its full potential and since the objective of this research does not concentrate on comprehensive reservoir simulation it will only be commented on where utilized in the analysis.

6.1.2 GSLIB

GSLIB (Geostatistical Software Library) is a piece of software developed to aid the the modeling of variograms and to simulate numerous realizations of a field comprised of spatial variables. It was developed by Statios as a platform to be used with other programs (as the source code is provided upon purchase) or as an educational tool. Statios also provides other geostatistical software and consultation to major mining companies. This program was used to take the spatial data acquired from Eclipse and to model it. Once modeled, the simulation was performed by GSLIB to develop as many realizations as desired. The realizations were then imported into NETool where the near well simulations took place.

6.1.3 NETool

NETool is a reservoir simulator focusing on simulations near the well bore. In contrast with Eclipse, NETool runs much faster because of its concentration on information near the well bore. It was for this reason that NETool was used to perform the reservoir simulations (since the number of realizations would cause the computation time to be incredibly high). Working with information before there is a production history (during drilling) there is a lot of uncertainty. Because of this a near well simulator is much more efficient as it can provide information about the production rates much faster than a comprehensive reservoir simulator. After initial flow rates decline during production a more comprehensive reservoir simulator should be used (such as Eclipse).

6.1.4 MATLAB

In order for all the commercially available software to be used together in the same project, there was a need for some processing of the data so that it could be read properly. To do this, software routines were created using MATLAB because it was readily available and simple and easy to use. All the routines created for this research are noted where they are used and can be found in Appendix C.

6.2 Reservoir Definition

The reservoir for this case is based on an actual reservoir. The data was obtained in the form of Eclipse files which is an industry standard for certain oil companies (other companies may use their own reservoir simulators). The information obtained was tuned to suit the purposes of demonstrating the methodology of this research. This means that the complexity of the actual formation is not fully represented in this case study. The reasons for this is because the main goal of this research is to demonstrate the methodology in a realistic and understandable way. Having unnecessary complexity makes the demonstration more difficult to understand.

6.2.1 Variables Selection

The first task is to determine the variables to work with for the case study. Similar to the first case study the objective of this case study is to quantify the risk in the production capacity of the reservoir. The permeability of the field has a significant effect on the production of a field. A favorable permeability would allow the oil to flow very well throughout the duration of production. Favorable permeability does not

always lead to optimal production. In the case where there is water or gas injection, a water aquifer present or a gas cap drive mechanism, it is possible to have a water or gas breakthrough while there is still oil remaining in the reservoir. This would cause oil to be left behind in the reservoir as residual oil due to the adverse mobility ratio of oil to water or oil to gas. This means one phase would flow better than the other and leave the less mobile phase behind. Porosity also has an effect on production. This was the primary variable in the first case study however this property is a static property and one which reservoir engineers usually have a better idea about compared to permeability since more tools exist to measure porosity. Permeability normally requires some sort of estimation technique like geostatistics to determine its value at certain locations. It is possible to use a correlation between porosity and permeability as well but only if there is some relationship evident between the two properties. Such a correlation will be explored further in later sections.

6.2.2 Geometry

The geometry of the reservoir in this case study is a regular grid of 1400 m by 3250 m by 150 m in depth. This regular grid was used due to the constraints in the geostatistical realization procedure. The original reservoir grid was more complex but it was redefined for easy integration into the geostatistical simulator. NETool can accept irregular grids from Eclipse but the geostatistical simulator grid must match it. For this reason the grids were standardized as a 28 by 65 unit grid in 50 m square grid blocks that are 150m in height. Figure 6.1 shows the plan view of the grid.

From the figure it can be seen that there are some gaps or holes in the formation. In these locations the porosity and permeability values are near zero or equal to zero.

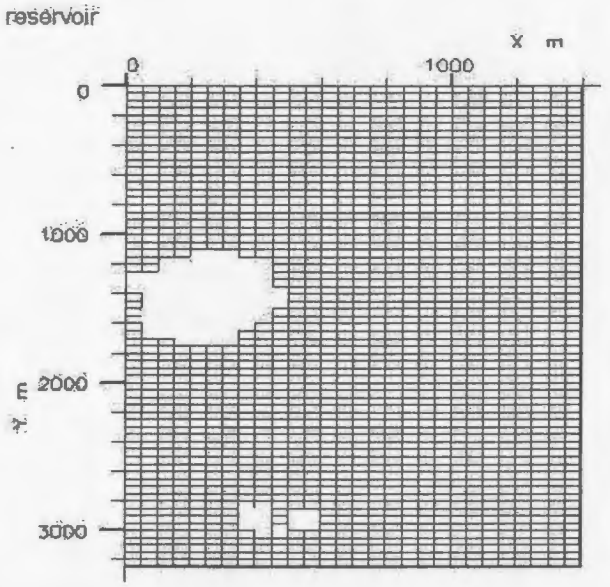

Figure 6.1: Reservoir Geometry - Plan View

This may mean that there is shale or calcite present or some other tight formation where oil may not flow and cannot exist. The following figures (6.2 and 6.3) give three dimensional representations of the permeability and porosity distributions. Another feature may also be seen, their layered structure. The distribution of the permeability in the top layer (the layer that is visible) is the same as any other layer. This is due to the fact that in the geostatistical modeling, three dimensional modeling is much more complex than two dimensional modeling. To demonstrate the methodology for this case study the extra complexity involved with three dimensional modeling is unecessary and the two dimensional case is sufficient. The thickness of the reservoir is small compared to the length and width of the model so it is expected to behave as a two dimensional model. Also the vertical variability of a formation is generally based on the events that occur in geological time to form the reservoir. Different geological layers form during different periods of geological time. By assuming that this reservoir occupies only a single geological layer then the apparent similarities can

be accounted for.

6.2.3 Reservoir attributes

The reservoir attributes (such as oil and water saturations) do not effect the methodology of the case study. The oil, gas and water saturations have simple distributions allowing permeability to be the most sensitive parameter of the reservoir. This allows the well trajectory (which is also independent from the methodology) to be chosen based on the permeability of the reservoir.

6.2.4 Well Trajectory

Based on the reservoir conditions stated earlier the well trajectory can be chosen based on the permeability distribution. The well provides the pathway of the oil from the reservoir to the production location. The trajectory chosen based on the permeability distribution of the base case shown in the Figure 6.4 and is summarized in Table 6.1.

Table 6.1: Well Trajectory: Case 2

X(m)	Y(m)	Z(m)
831.25	14.19	3050.0
905.63	478.98	3050.0
1019.38	730.9	3050.0
1141.88	1071.51	3050.0
1120.0	1287.94	3050.0
805.0	2114.63	3050.0
730.63	2739.08	3050.0
761.25	3168.4	3050.0
761.25	3242.9	3050.0

Basically, the well trajectory was chosen along a path where the permeability was

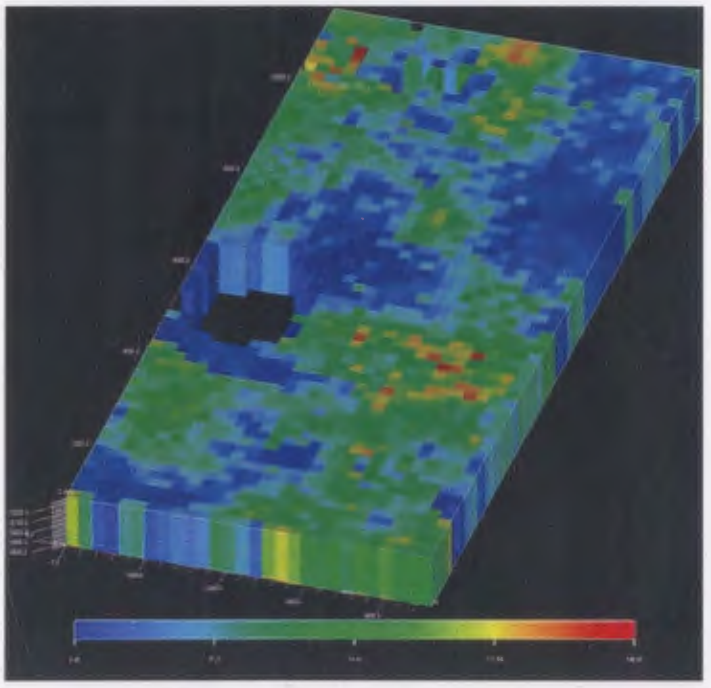

Figure 6.2: Permeability Distribution

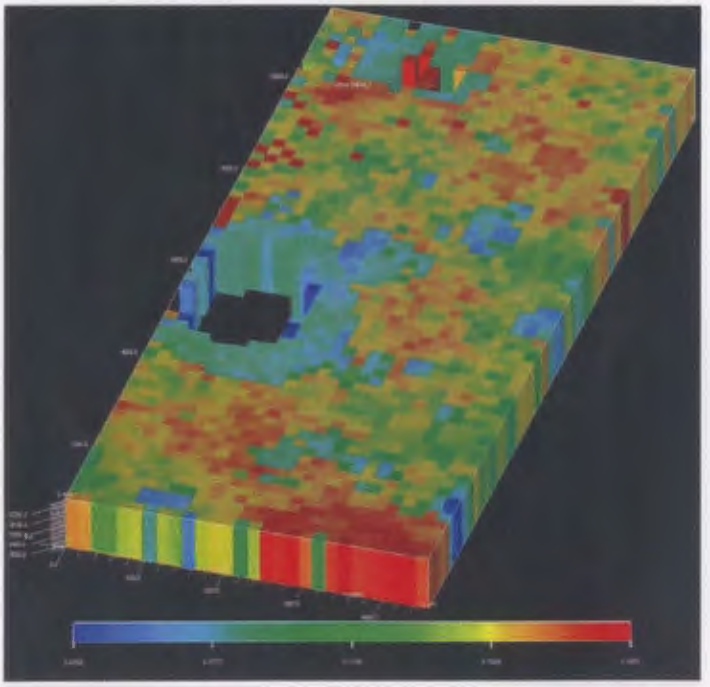

Figure 6.3: Porosity Distribution

the highest. This is to maximize the production levels from the formation since permeability is a measure of how easily the oil can move through the formation. The well trajectory is approximately 3.3 km.

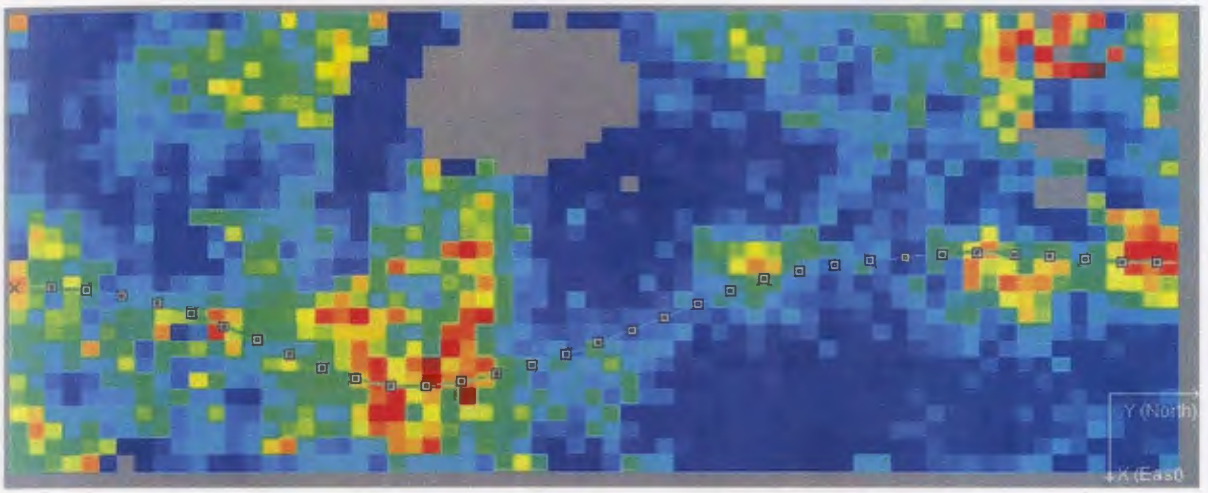

Figure 6.4: Well Trajectory: Case 2

6.3 Data Analysis

Before beginning the geostatistical analysis it is important to first analyze the data to determine if there is a need for any data transformation or declustering of the data. This data set has some qualities which set it apart from data sets normally used when developing a reservoir model. Not only does this data set inherit the properties of a spatial data set but it is also exhaustive. This means that the reservoir grid data obtained is completely filled (no empty cells). In practice this will not be the case since the reservoir engineer will only have data from certain locations in the reservoir (from an exploratory analysis, seismic, and/or outcrop information). One of the steps in initializing a reservoir simulator such as Eclipse is the population of the grid with an initial distribution. This can be done with geostatistics or some other estimation procedure. The data obtained for this case study had this grid already populated so it

will be used as the exhaustive data set. Certain data points will be removed from the exhaustive data set so that all that remains is a sample. This sample will represent what the reservoir engineer has to work with. The geostatistical realizations will be developed from this data set and compared to the exhaustive data set (which will be considered the actual reservoir properties for demonstration purposes).

6.3.1 The Exhaustive Data Set

The data analysis section is broken into two parts. The first part deals with the exhaustive data set and the second part deals with the sample data set.

Univariate Calculation

The calculation of the univariate statistical parameters will give information on how the parameters of permeability and porosity are distributed independently. From this analysis it should be evident if any transformation should take place. It should also show the distribution, range and maximum and minimum values of the parameters. The best way to do this is to view the frequency histograms of each parameter.

Figure 6.5 shows the frequency histogram of the permeability data. The upper right hand side of the figure displays the summary data for the histogram as well as some of the univariate properties of the permeability data set. The values of median and mean (35.2215 mD and 40.5255 mD respectively) show that the data is skewed to the right with a coefficient of variation of 0.780. This means that the maximum values of the permeability are having an effect on the mean which is not completely representative of the data, however, this skewness is not a concern since the degree of skewness is not high enough to warrant it.

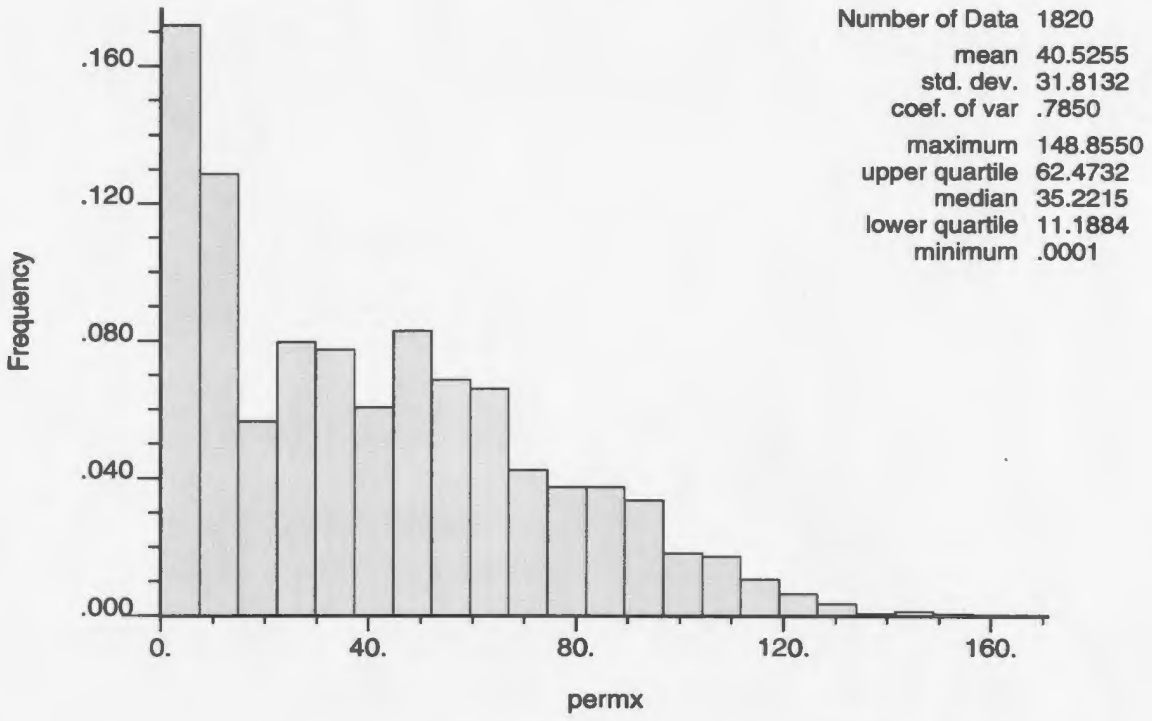

Figure 6.5: Permeability Histogram

One aspect of the distribution which should be checked is the log normality of the data. Often in permeability data sets log normality exists since there is often variability over many magnitudes. This data set does not appear to be log normal from the histogram of the non-transformed data but it does seem skewed toward the low end of the spectrum.

From the log plot in Figure 6.6 it can be seen that the variability of the data set does not occur over many different magnitudes so the histogram is very steep. Compared to Figure 6.5, Figure 6.6 does not show as much information about the distribution of the data set. Another feature to note is the spike at the left side of the histogram. This is due to the fact that the location where zero or near zero permeability exists in the data set the permeability was set to a minimum value so that it could be

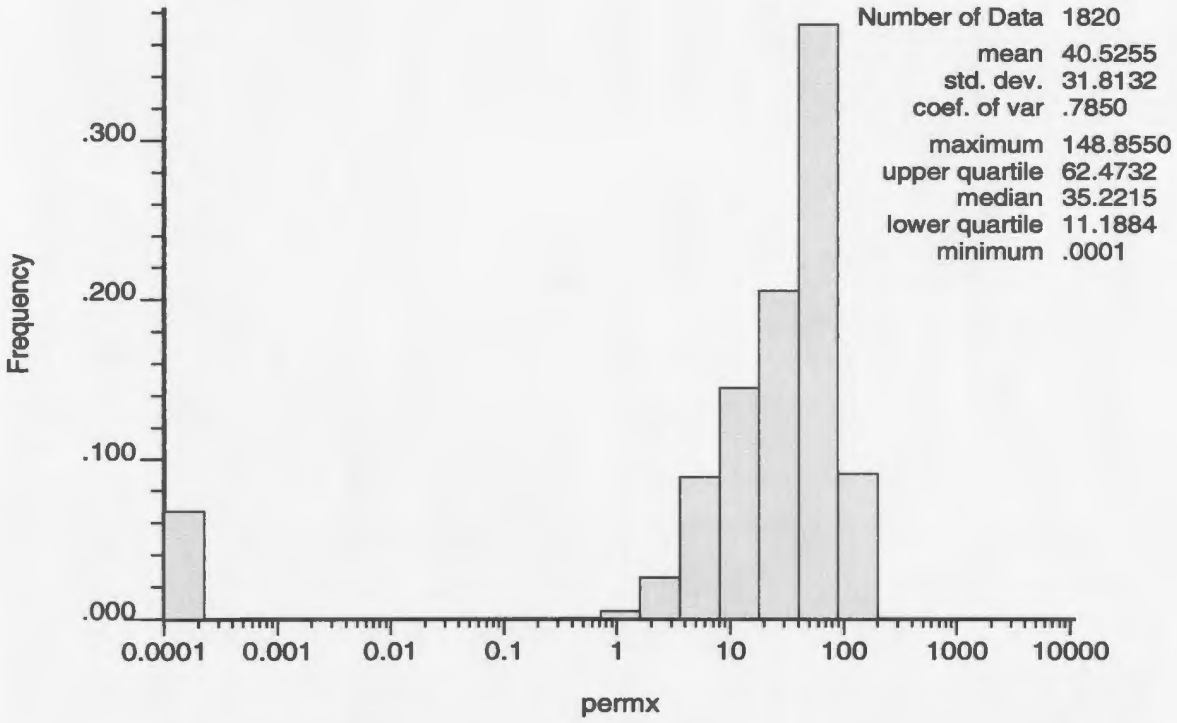

Figure 6.6: Log of Permeability Histogram

transformed into a log domain. The failure of this data set to be log normal can also be seen from the log normality plot in Figure 6.7.

Figure 6.7 shows the cumulative probability plot for the data. Along the y-axis is the probability in normal probability increments and along the x-axis is the permeability of the data in log increments. This proves that the data is not log normal. If the data was log normal then it would plot as a straight line. The normal probability plot of the non-transformed data shows that the data is not strictly normal either. It plots the cumulative probability versus the untransformed data. Figure 6.8 shows that the data is near normal past a certain threshold, however, there is curvature in the normal probability plot.

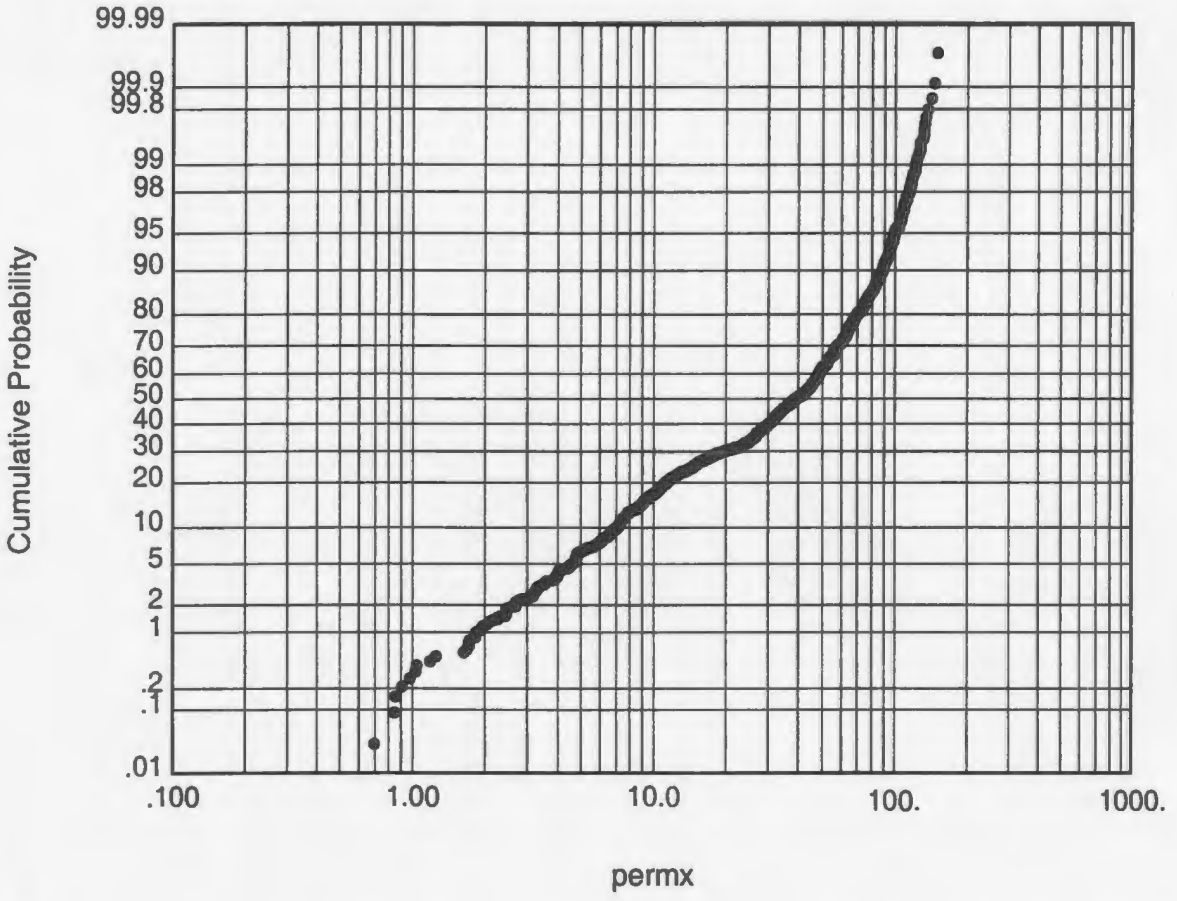

Figure 6.7: Log Normal Permeability Probability Plot

The distribution of the source data is only important if the estimation technique used incorporates the distribution as an assumption. Some estimation tools built on the assumption of normality may still even be useful when the data is not normally distributed. This section discusses the distribution of the data to give the reader an awareness of where some sources of error may occur.

The other property, porosity, usually has less variability compared to permeability. This is because it only varies as a percentage rather than a physical measurable value (like permeability). This can be seen from the histogram in Figure 6.9 and the

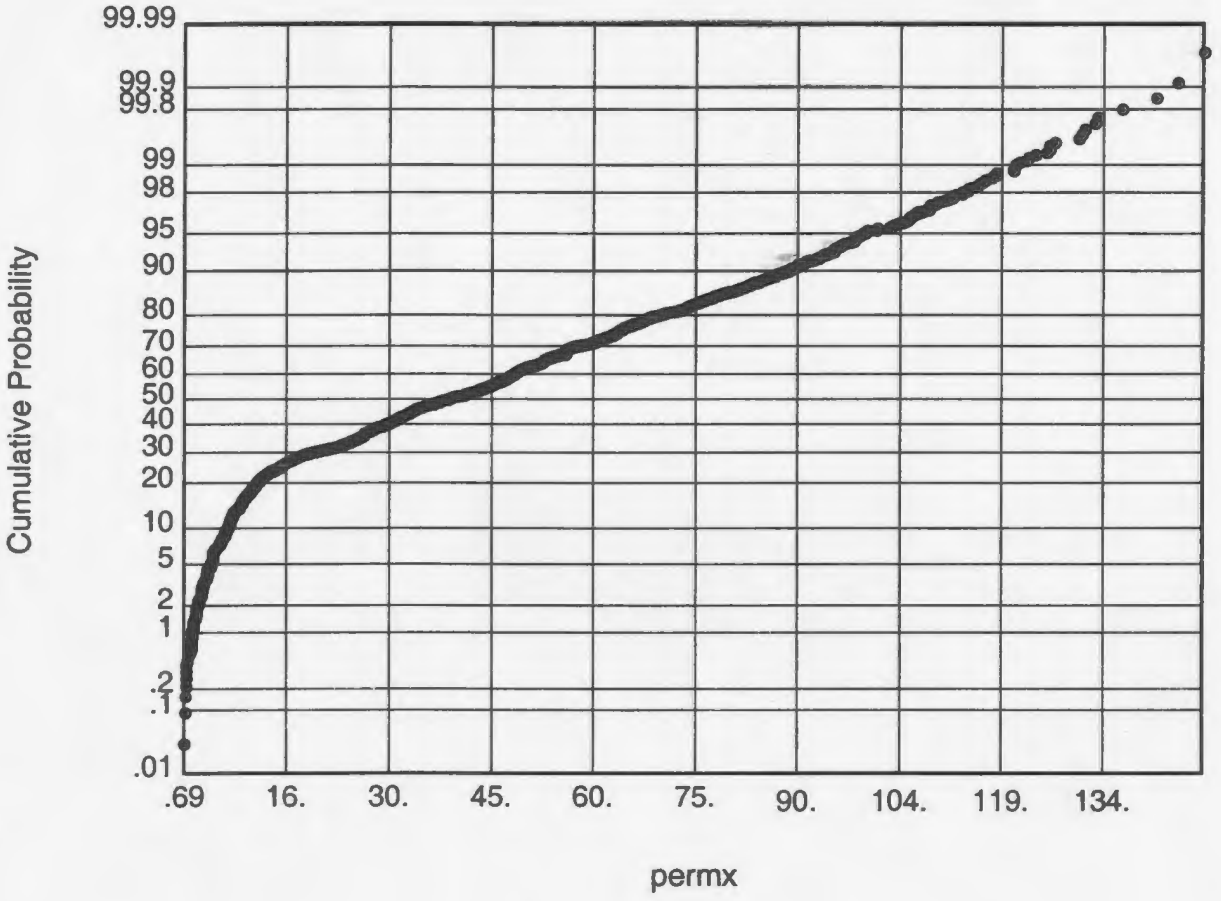

Figure 6.8: Normal Permeability Probability Plot

summary statistics related to the porosity values. The histogram is a figure showing the probability frequency of the porosity values corresponding with the porosity value on the x-axis.

The plot indicates that the porosity basically exists around two thresholds, one at 7.5% and one at 15.5%. The variability is much less as can be seen from the standard deviation compared to the permeability data. The mean and median do not match each other but this is due to the existence of what seems to be two populations. This information may be useful in the geostatistical simulation process.

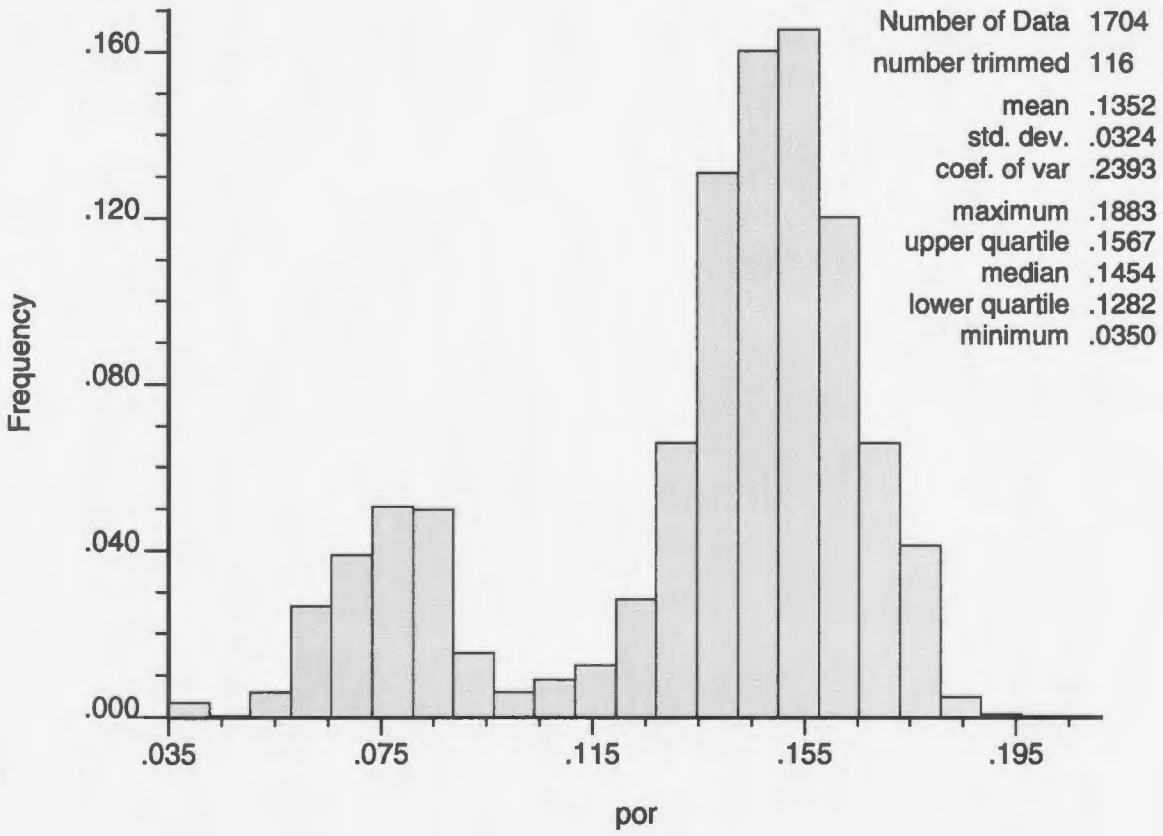

Figure 6.9: Porosity Histogram

Bivariate Calculation

Through a univariate analysis, information describing distributions of each variable independently is produced. It is interesting to consider these variables together to see if there is a physical relationship or a correlation between them. There are a number of different ways to analyze the multivariate data. One way to examine the data is by using a q-q plot. A q-q plot is a plot which displays the quantiles from each distribution versus each other.

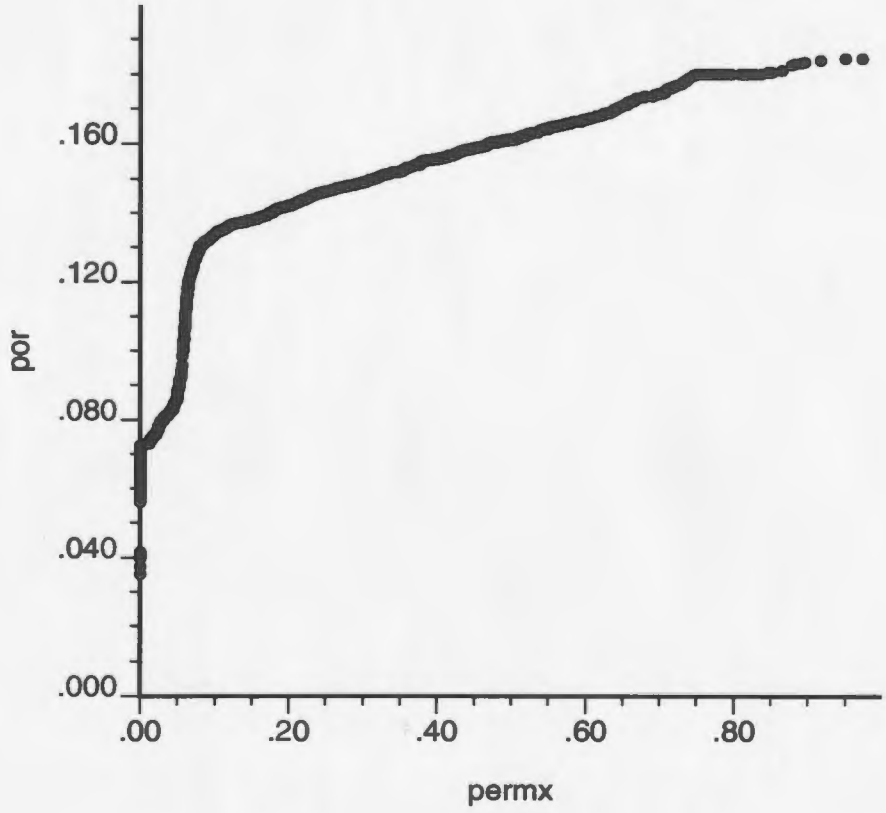

Figure 6.10: q-q Plot

In this case, because we are comparing two different units (porosity as a percentage and permeability in mD) it is necessary to normalize the permeability into a percentage. After normalizing permeability using the maximum permeability the q-q plot becomes the Figure 6.10. This figure plots the porosity quantile values (on the y-axis) against the permeability quantile values (on the x-axis). Note that the normalized permeability is not log-transformed in any of the bivariate plots. A q-q plot of identical distributions will display a straight line along x = y. The visual comparison presented here obviously shows that the distributions are different and the curvature

in the line observed proves that the relationship between porosity and permeability in this reservoir is weak.

The most common way to display bivariate data is the scatter plot. This plot creates a cloud of data. If there is a relationship in the data then the cloud will present a shape and the relationship can be quantified by fitting a line of best fit through the cloud of data. Figure 6.11 reiterates that the relationship between the two variables is weak.

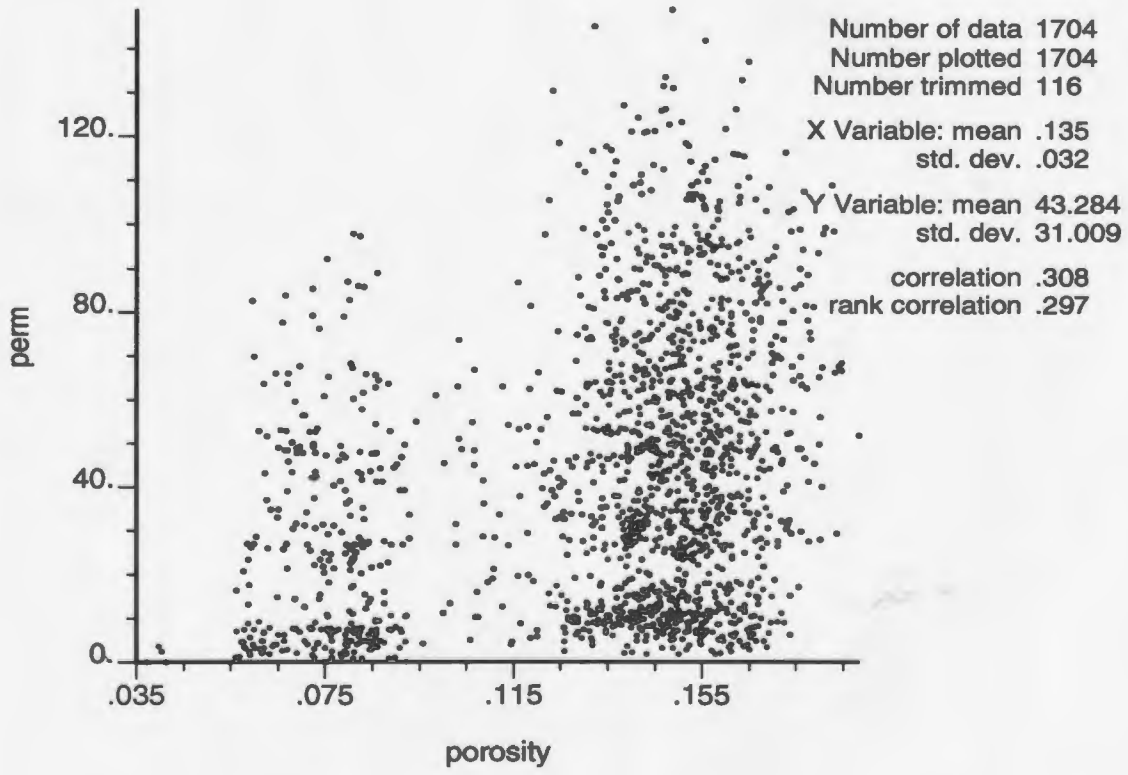

Figure 6.11: q-q Plot

The scatter plot can serve a number of purposes. First it gives a qualitative view of how the variables are related. It is also useful for identifying data that may be

erroneous. An erratic piece of data may have a major impact on the estimation procedures later on so at this stage it is necessary to address any data point that appears to be an anomaly. A data point such as this would appear out of place on a scatter plot. Finally, the scatter plot can also be used to validate initial data and help in the understanding of the results later. The scatter plot here does not show any obvious errors nor does is show any obvious relationship in the data. If there was a third parameter, such as an indicator marking geological formations, perhaps these two porosity distributions could be separated and a conditional dependency could be implemented, but such data does not exist in this case.

Correlation Coefficient:

The correlation coefficient between porosity and permeability is calculated using:

$$\rho_c = \frac{\frac{1}{n}\sum_{i=1}^{n}(x_i - m_x)(y_i - m_y)}{\sigma_x \sigma_y} \tag{6.1}$$

The correlation coefficient is computed as 0.308. This deterministically shows that there is little relationship between permeability or porosity. The estimation procedure will be completed without the conditional estimation of permeability based on porosity. Another note to make is that from this point onwards, permeability will be of interest and not porosity. In the estimation and risk procedures for this case study, porosity is considered a known quantity with a distribution shown in Figure 6.3. This is to reduce unnecessary complexity. Porosity is generally a better defined variable since information about porosity can come from many more sources than permeability (eg. cores, logs and 3-D seismic).

6.3.2 The Sample Data Set

The sample data set is extracted from the exhaustive data set in a random way so that no biases due to data selection are incurred. A simple program was developed in MATLAB to extract ninety percent of the data points leaving ten percent for the geostatistical analysis. The details of the programs responsible for this task can be found in Appendix C with the names *samplepop.m* and *myrandint.m*. The following few sections will show the data analysis for this sample population. Figure 6.12 shows the locations where random sampled variables exist in the data set. It is a scatter plot showing where all the data points for the sample population are (filled circles) and the exhaustive data set includes both the filled circles and the hollow circles. Out of 1820 data points in the exhaustive data set, the sample consists of 182 points.

Univariate Calculation

The histogram shown in Figure 6.13 demonstrates that the sample population is in good agreement with the exhaustive data set (in comparison with Figure 6.5). The plot gives the frequency probability versus the permeability for the sample data. The good agreement is most likely due to the fact that the sampling is unbiased and random. In practice this would most likely not be the case since sampling occurs in locations where the most favorable reservoir properties are believed to exist. The univariate summary statistics of the permeability distributions show similarity. The mean of the exhaustive data set (40.5255 mD) is very similar to the mean of the sample data set (41.5865 mD). The variability of the data, measured by the standard deviation, also shows good agreement. The maximum of the sample is a little lower than the exhaustive data set since the extreme permeability values were not sampled

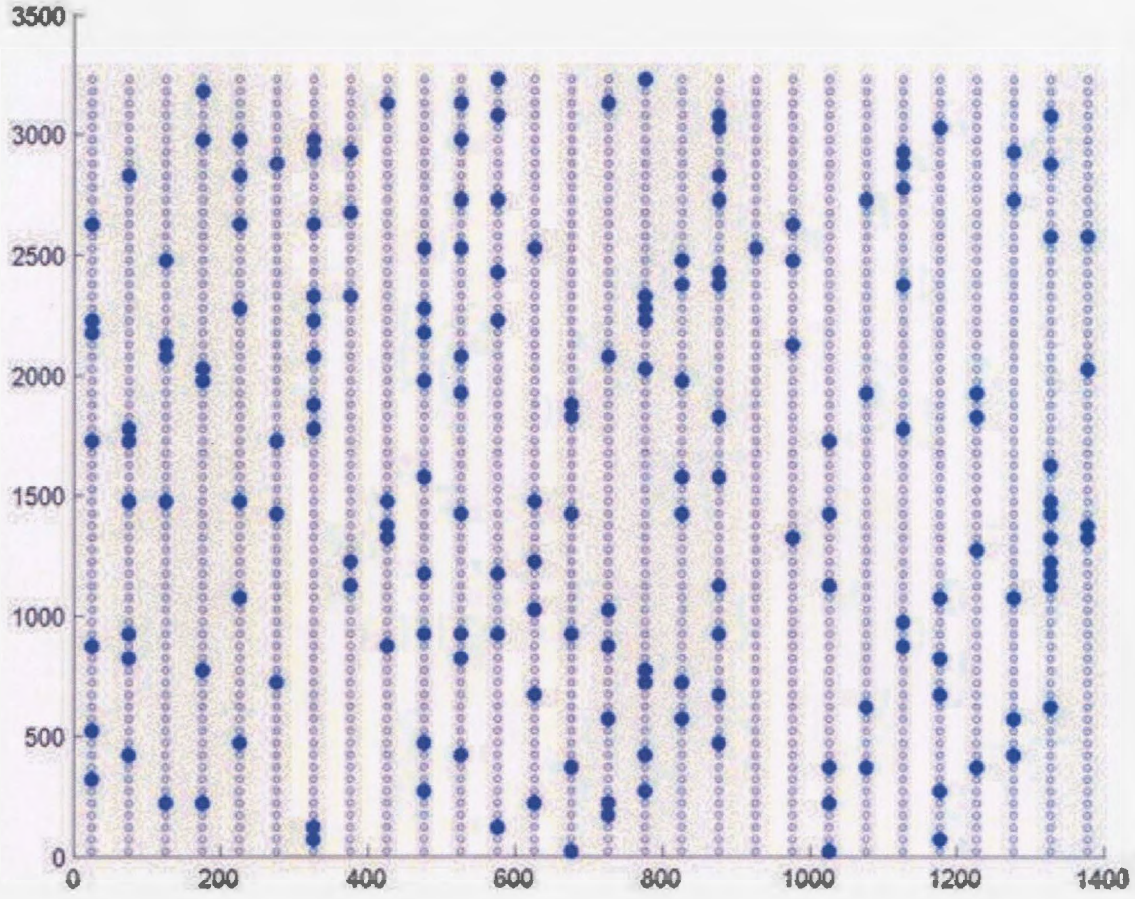

Figure 6.12: Sample Location in the Sample Population Scatter Plot

in the sample data set. The other univariate plot of interest is the probability plot (Figure 6.14). This plot shows good agreement with the exhaustive data set. It shows that the sample data set is near a normal distribution past a certain threshold. By comparison with Figure 6.8 it can be seen that both the exhaustive data set and the sample population exhibit the same normal probability behavior. What this means is that the sample set is no more or less normal than the exhaustive data set. The sample is a good representation of the entire population.

There is no need to analyze bivariate distributions here since the second variable of

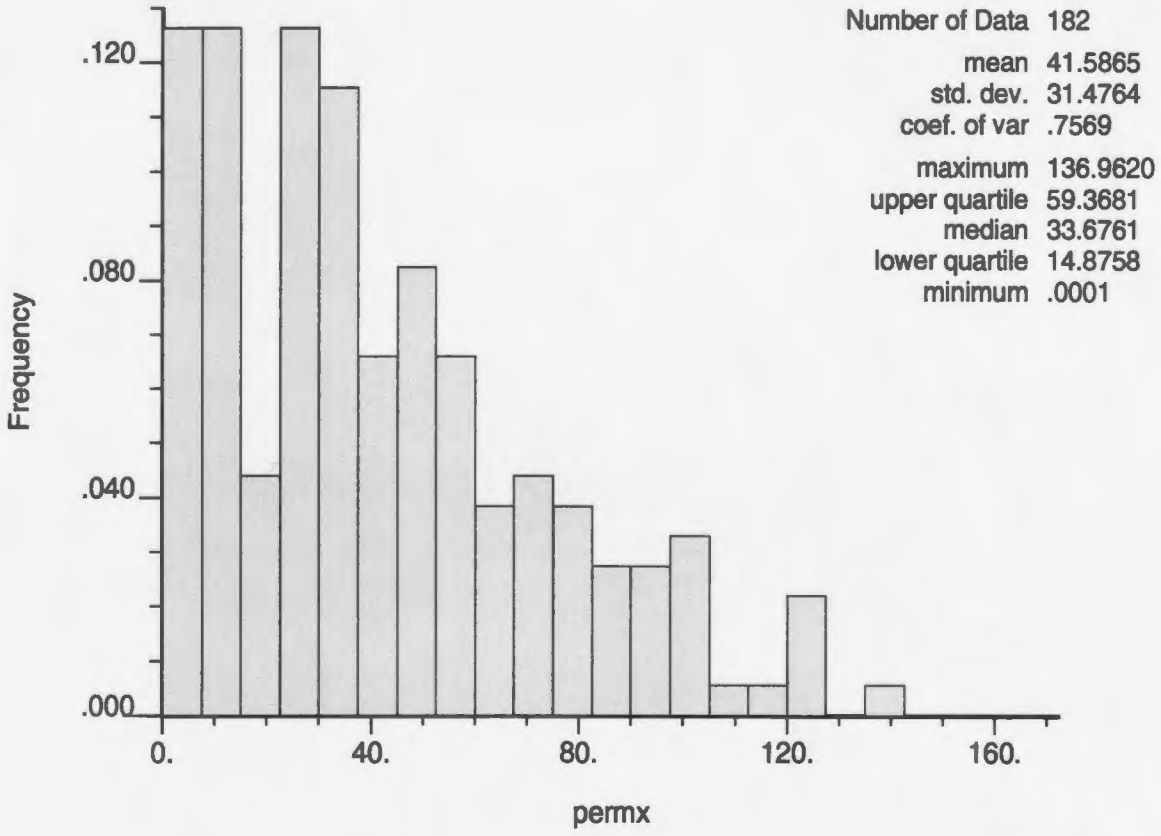

Figure 6.13: Sample Population Histogram

porosity is not being used in the estimation.

6.4 Spatial Description

At this point it is important to quantify how the permeability is distributed in space. This distribution of the permeability can be seen in the contour plot in Figure 6.15. In this plot the contours are set up in 5 equally spaced thresholds (6 classes) of permeability. This means there is a new contour line approximately every 29 mD. It

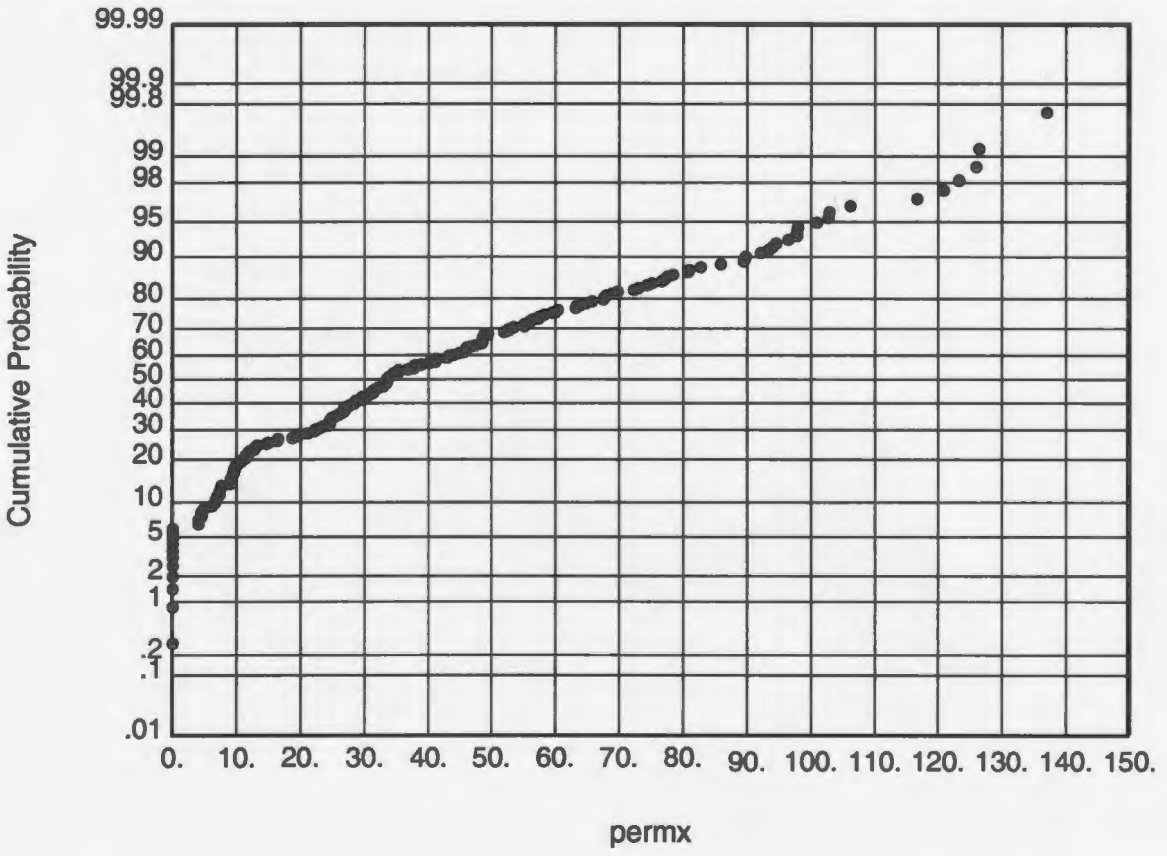

Figure 6.14: Normal Probability Plot of Sample Population

should be noted that the data missing (from Figure 6.2) has been replaced by data in the lowest threshold (where the permeability is near zero).

To examine the spatial characteristics of this data set there are a number of different techniques. The most common technique, and the technique that will be used here, uses variograms.

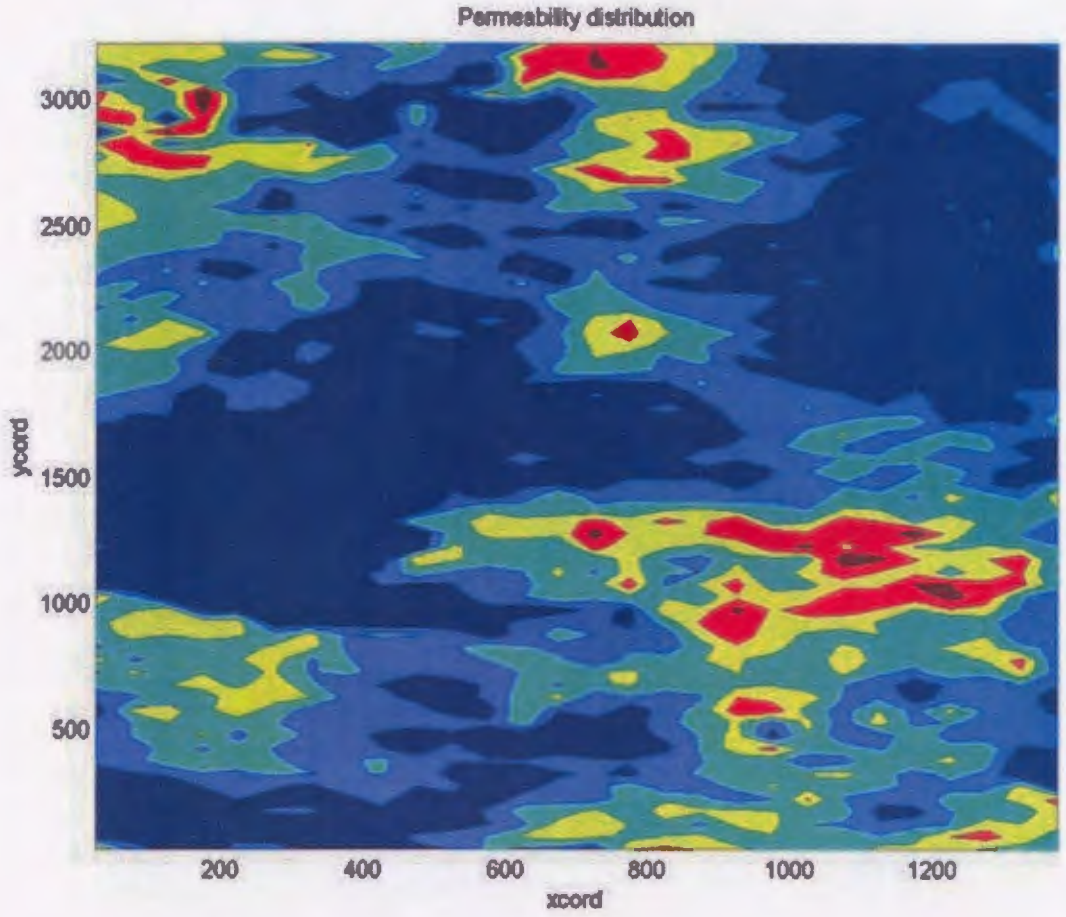

Figure 6.15: Permeability Contour Plot

6.4.1 Choosing the Variogram Parameters

Before investigating the influence of direction on the permeability it is a good idea to analyze the impact of distance. This involves the calculation of what is called an omnidirectional variogram. An omnidirectional variogram is a variogram that has a directional tolerance of plus or minus 90 degrees (recall that when invoking a search neighborhood when estimating the variogram, only 180 degrees of direction needs to be addressed due to symmetry). In the omnidirectional variogram there is

no directional influence. This type of variogram is a good way to determine a good starting point for the parameters for the variogram estimate such as the lag interval, tolerance and number of lags (discussed in Chapter 3). Through some trial and error it was found that with the following parameters the variogram demonstrates relatively good continuity with minimal fluctuation.

Table 6.2: Variogram Parameters

Lag	100
Tolerance	50
Number of Lags	30

Figure 6.16 shows the omnidirectional variogram for both the sample data set (in red) and the exhaustive data set (in blue). It reiterates that the sample data set is a good representation of the total population. The parameters used in the generation of this plot are given in Table 6.2.

The next step in the variogram estimation procedure is to determine the angle of continuity if the formation is anisotropic (which is the assumption unless the conclusion can be made that the reservoir is isotropic or homogeneous). To do this a variogram map is calculated. The standardized variogram is estimated at a number of different directions (0 to 180 degrees in 22.5 degree increments for a total of 8 estimations in this case study). Since the variogram is standardized the sample population variance is equal to one (this is the sample sill). The lag distance where each variogram reaches the sample sill is recorded. The direction at which the variogram estimate reaches the sill with the largest lag is the direction of maximum continuity. Note that the information regarding the exhaustive data set is also included in Table 6.3 and is identified by (e).

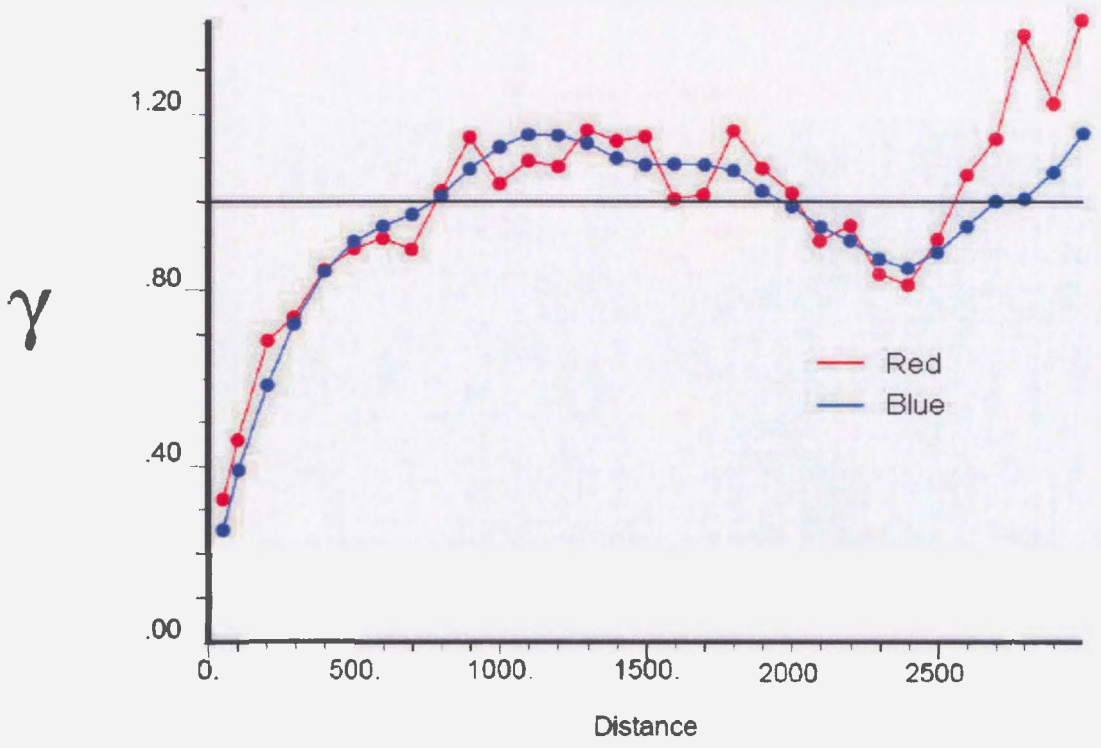

Figure 6.16: Omnidirectional Variogram Estimates

Table 6.3 shows the lag distance were the variogram reaches the population sill for 8 different angles. The second row indicates the lags for the sample variograms reaching the sample sill and the third row indicates the variograms for the exhaustive population reaching the exhaustive sill (for comparison). The directions of maximum and minimum continuity can be conclusively stated from this table. In both cases there is maximum continuity in the direction of 45 degrees counter clockwise from the positive x-axis (45 degrees north of east). By convention the minimum direction of continuity is taken perpendicular to this direction. The sample population demonstrates this explicitly with a minimum lag at 135 degrees. The table indicates that for the exhaustive data the minimum direction of continuity is 157.5 degrees counter clockwise from the positive x-axis. It is generally accepted that the maximum and minimum

Table 6.3: Maximum Lag Computation

Angle	0°	22.5°	45°	67.5°	90°	112.5°	135°	157.5°
Lag (s)	808.51	875.21	1461.73	1310.19	697.87	584.48	570.30	576.57
Lag (e)	812.79	963.90	1823.49	987.78	745.67	601.32	512.94	473.36

directions are perpendicular (Goovaerts, 1997) and that the maximum direction be located first. For this reason the maximum and minimum directions of continuity are taken as 45 degrees and 135 degrees respectively. The sample variogram plots for all directions can be found in Appendix D.

Once the anisotropy axis has been determined the next task is to determine the angular tolerance to use for the estimate. The angular tolerance should be chosen such that the number of pairs is minimized and that the behavior of the data is not masked. It is also important however, to have enough pairs to reduce the amount of fluctuation since an erratic variogram is difficult to model. The optimal tolerance balances both of these effects. Table 6.4 summarizes the number of pairs in each variogram estimation in the directions of maximum and minimum of continuity with angular tolerances from $\pm 10°$ to $\pm 40°$.

Based on Table 6.4 it can be seen that by increasing the tolerance the number of pairs is also increasing. The maximum number of pairs occurs when the tolerance is at a maximum. The $\pm 40°$ column exhibits the largest number of pairs for this reason. If the variograms are examined for each of these tolerance levels it can be seen that for the first three levels, the fluctuation of the variogram is higher than in the fourth level. The fourth level does not mask any of the behavior of the population due to the inclusion of the data pairs from the tolerance and therefore this tolerance level is chosen for the modeling procedure. This is because the variograms calculated based on this tolerance level exhibit the minimum amount of fluctuation while producing a

Table 6.4: Angular Tolerance Comparison

±10°		±20°		±30°		±40°	
$N45°E$	$N45°W$	$N45°E$	$N45°W$	$N45°E$	$N45°W$	$N45°E$	$N45°W$
16	18	16	18	16	18	16	18
16	18	57	44	57	44	57	44
7	15	7	15	50	44	50	44
13	14	75	78	75	78	108	103
39	32	68	62	106	86	142	116
43	49	67	83	90	112	113	143
41	43	109	101	150	125	185	149
38	46	66	71	109	129	164	181
77	68	135	103	181	156	230	216
30	56	115	109	196	179	252	225
52	56	113	139	192	220	239	257
70	47	128	117	173	157	222	208
89	86	154	146	233	235	268	299
47	53	107	106	160	166	231	238
77	76	159	160	196	208	284	281
77	67	147	139	205	189	284	246
49	57	113	123	179	187	251	258
49	61	112	137	159	186	236	258
54	52	132	128	188	160	256	236
76	69	131	114	179	164	256	239
40	43	101	107	161	178	230	242
41	58	105	118	167	188	228	246
37	36	84	96	139	155	208	207
49	42	116	111	148	165	210	219
56	54	108	101	156	165	209	222
35	55	74	109	136	180	188	237
31	49	69	107	115	158	170	213
38	38	64	75	104	130	154	189
30	43	66	86	99	140	150	195

manageable amount of pairs to work with.

In summary, the parameters chosen for the variogram estimate for which the model will be based on is as follows:

- Lag Distance Increment = 100 m
- Lag Tolerance = ± 50
- Angular Tolerance = $\pm 40°$
- Direction of Maximum Continuity = $45°$
- Direction of Minimum Continuity = $135°$

Looking ahead, the simulation method that will be used will be sequential Gaussian simulation (SGS). For this the sample variogram must be based on the normal score transformed data. This does not change the variogram estimate parameters noted previously, instead it makes the structure of the variograms more interpretable. Figure 6.17 shows the normal score variogram estimates for the minimum (yellow) and maximum (red) continuity directions versus lag distance. From this figure it can be seen that the fluctuation is greatly reduced. This decrease will help in the variogram modeling process.

6.4.2 Modeling the Sample Variogram

The estimation procedure for spatial variables using geostatistics requires the modeling of variograms. By choosing a model that is positive definite to match the estimate, the kriging solution will necessarily exist. Using the models discussed earlier, the following variograms were developed to model the variogram estimates. The procedure

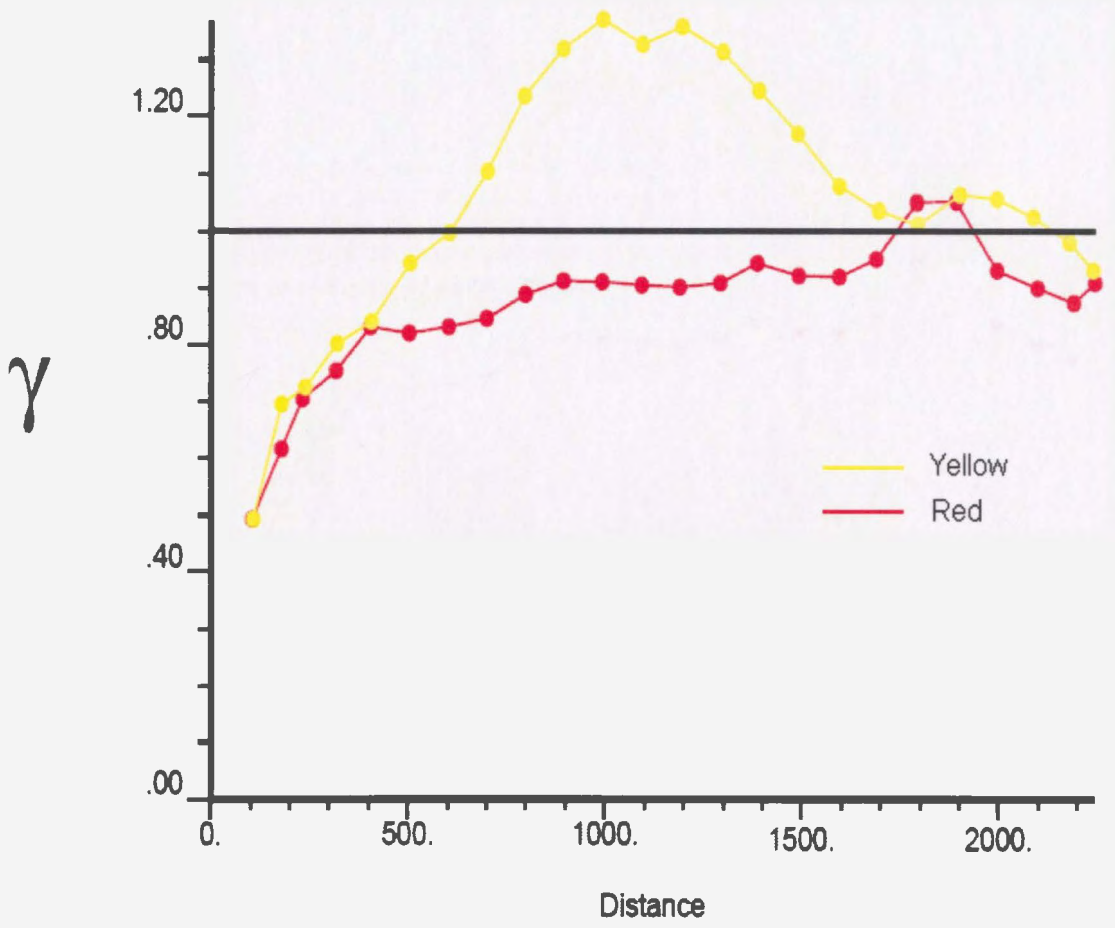

Figure 6.17: Normal Score Variogram Estimates

in determining the optimal variogram parameters was through trial and error. Other acceptable models which adequately model the spatial relationships within the data may exist.

Variogram which represents the spatial data in the 45° direction (maximum continuity):

$$\gamma(L) = 0.49 + 0.33\left[\frac{3}{2}\left(\frac{L}{1800}\right) - \frac{1}{2}\left(\frac{L}{1800}\right)^3\right] + 0.2\left[1 - exp\left(\frac{-3L}{1000}\right)\right] \qquad (6.2)$$

Variogram which represents the spatial data in the 135° direction (minimum conti-

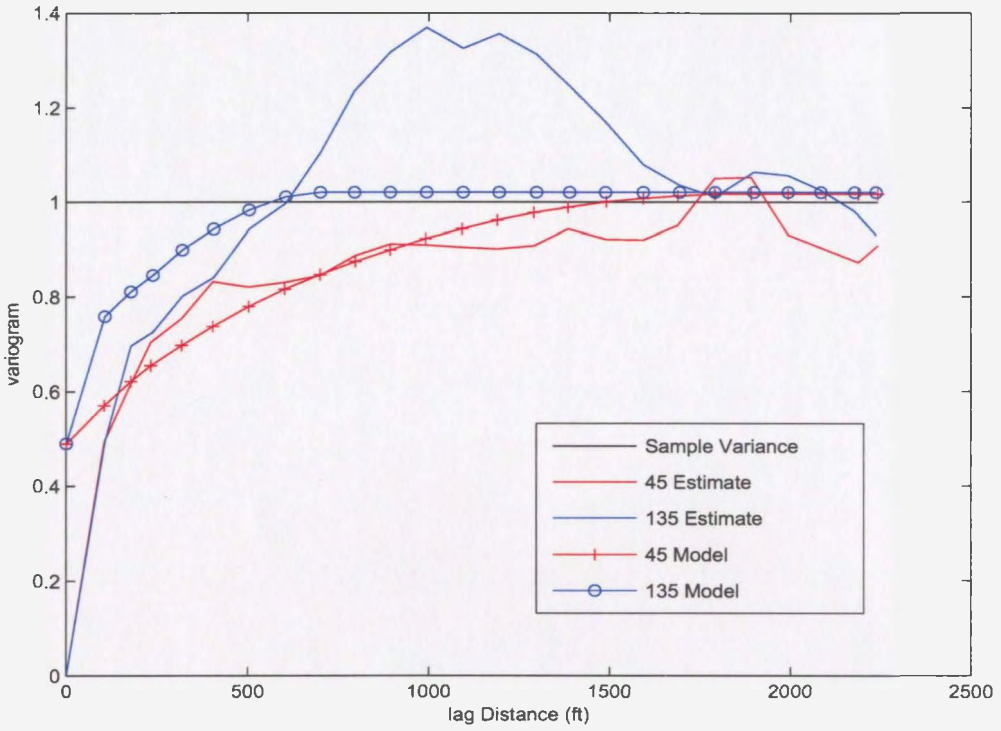

Figure 6.18: Sample Variogram Models

nuity):

$$\gamma(L) = 0.49 + 0.33\left[\frac{3}{2}\left(\frac{L}{700}\right) - \frac{1}{2}\left(\frac{L}{700}\right)^3\right] + 0.2\left[1 - exp\left(\frac{-3L}{700}\right)\right] \qquad (6.3)$$

The variograms were found through experimentation with the different modeling parameters (the range and sill values). There were also some modeling assumptions made here as well. The models were chosen to reach the same sill (of 1.02). In most cases where only horizontal variograms are being modeled, geometric anisotropy is present and not zonal anisotropy. Typical zonal anisotropy exists primarily in vertically layered formations (Kelkar & Perez, 2002). In this case there is not enough information to conclusively say that this formation has zonal anisotropy in the horizontal layer so geometric anisotropy is assumed (since it is most common and the

data fit is reasonable). Since the direction of minimum continuity has a fluctuation vertically before nearing the sill, the modeled sill was taken as slightly higher then the sample variance (1.02 instead of 1.0) to attempt to account for this behavior. The direction of maximum continuity reaches the sill at approximately 1800 m (this is the range for the spherical contribution of the variogram). The model variogram under predicts the estimate in the 45° and 135° orientations so the exponential model was added to it to compensate for this. The effect of this part of the model has a range of 1000 m in the 45° orientation and 700m in the 135° orientation. The nugget was chosen as the variogram value where the first data pairs in the estimate yield a value. The variogram estimate plot shows a value of zero at a lag of zero because there are no data pairs. Now that the variogram models have been fitted to the data set the simulation can be performed. The variogram models will produce the permeability realizations during the simulation and the spatial distribution can be compared with the baseline realizations to ensure the model predicts a reasonable fit. In practice a more rigorous validation procedure should be applied however for the demonstration of this methodology, this is sufficient.

6.5 Solution

In order to carry out the simulation and calculation of the risk estimate for the production rates, the following steps will be followed.

1. Generation of the permeability skeleton for each state.
2. Generation of geostatistical realizations for each state (Sequential Gaussian Simulation).

3. Use of reservoir simulator to develop production rates for each realization.

4. Complete the risk factor calculation.

6.5.1 Permeability Skeleton

The permeability skeleton is based on the sample data set. Figure 6.12 shows the locations of the sample points that are considered to be known before any measurements while drilling are considered. Specific locations in a field are known through core samples and outcrop information and this is what the sample field data set is representing, the information which is known. This state is denoted as state zero in the analysis.

The development of the permeabilities for the other five states is completed through the use of a MATLAB procedure ($MWD.m$) designed to sample data near the well bore from the exhaustive data set and input the data into the permeability skeleton. Each state is composed of the permeability from state zero plus a number of extra sample points along the well path. The distance along the well path where the extra sample points are added depends on the state being considered. For the first state, measurements are inserted from the initial well bore point to 650 meters along the well path. Each state thereafter adds permeability values another 650 meters per state. Since the length of the well bore is slightly larger than five times the 650 meter segment length the final state, state 5, is slightly larger than the other states (by 95.1 meters). Figure 6.19 shows the permeability for state one. Similarly the other states were developed. The file details can be found in Appendix C for further consultation.

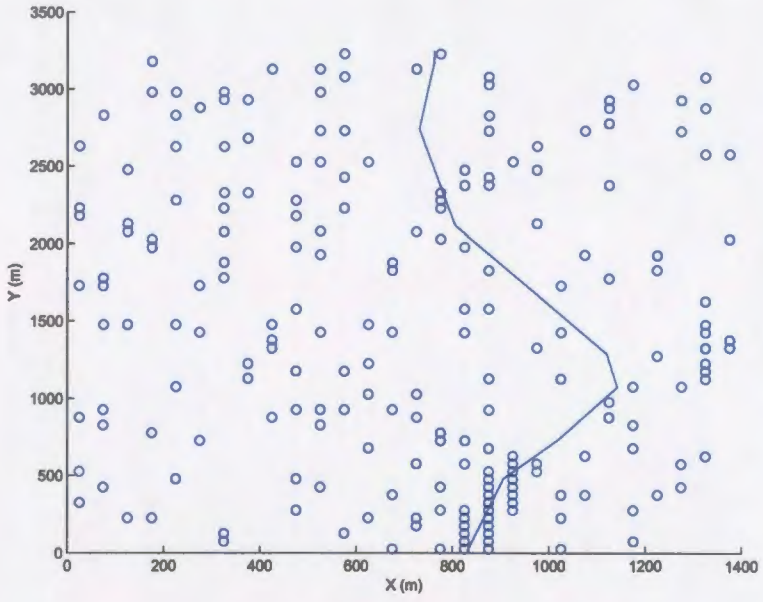

Figure 6.19: Permeability Skeleton - State 1

6.5.2 Geostatistical Realizations

Then next task is to develop the geostatistical realizations to fill the remaining grid blocks in the permeability skeletons for each state. The process of running GSLIB to develop the realizations was set up as a batch script and is shown in the top right side of the GSLIB screenshot depicted in Figure 6.20. The first three action items are mathematical processes and the last two are for the generation of the display for the user. The first process is the normal score transform. This takes the permeability skeleton for the given state and it transforms the data such that the mean becomes zero and the standard deviation becomes one. This is done to satisfy a requirement of the sequential Gaussian simulation technique (SGS) used here. SGS was chosen over other methods because it has analytical simplicity, it is a well known and respected technique, the transform retains the original structure of the population along with extreme values, and it also ensures that the uncertainty at the unsampled location

that the estimate is near or equal to the true parameter and secondly that the best prediction of the parameter is obtained when the variance of the local neighborhood is minimized. One important consideration when utilizing a kriging technique is that a search neighborhood must be defined around the location where the estimation is to be made. This search neighborhood should be chosen keeping in mind the fact that a large search neighborhood will result in a large number of sample points being generated which in turn leads to an increase in computational time to estimate the point.

3.3.1 Linear Kriging Techniques

There are a few linear kriging techniques that can be used to predict parameters at unsampled locations. One technique is simple kriging. Simple kriging is the easiest kriging technique to apply but it may not be the most practical. The primary drawback with the procedure is that it requires the knowledge of a global mean. This global mean is seldom known with any certainty. Another problem is that the first order of stationarity must be strictly valid (local means do not vary). Other forms of kriging relax this restriction. Another type of kriging is universal kriging. Universal kriging is a technique that estimates a variable in the presence of a trend. When there is a trend simple kriging does not produce accurate estimates so universal kriging must be used (first order of stationarity does not hold in the presence of a trend). To account for this, the universal kriging technique makes use of a residual parameter added to the estimate equation. More information regarding these techniques can be found in Appendix A. A final type of kriging to be noted here is ordinary kriging. It is described next.

visitation influences the final configuration. A new random path is created for each realization. The random path is chosen based on an algorithm internal to the program GSLIB. The next step involves the estimation of the parameter at the unsampled location. This estimation procedure is called kriging and was demonstrated in the first case study. The kriging will occur in the same way as set out in the chapter on Geostatistics once the random path has been selected. Once the kriging has been completed the back transform occurs to obtain data back into the original domain. This is done in preparation for input into the reservoir simulator.

It should be noted that in practice, when new information is introduced in the form of measurements while drilling, the spatial characteristics of the new sample population should be checked. In other words, the variogram models should be verified with new variogram estimates based on the updated sample population. In this case study however, since the base realization is known, the variogram models for each state are known to follow the baseline realization so a check is not necessary.

Figure 6.21 shows a number of realizations compared with the base realization. In the figure the first realization in the top left is the base realization. To the right are arbitrary realizations from state one and state two. Below on the bottom row going from left to right is state three, four and five respectively. From this figure the similarities can be seen and the model is shown to be visually appropriate. The finer details of each state can only be evident by studying the statistics of the states or quantifying them in terms of risk. One way to do this is to use a numerical reservoir simulator and study the variation in production rates.

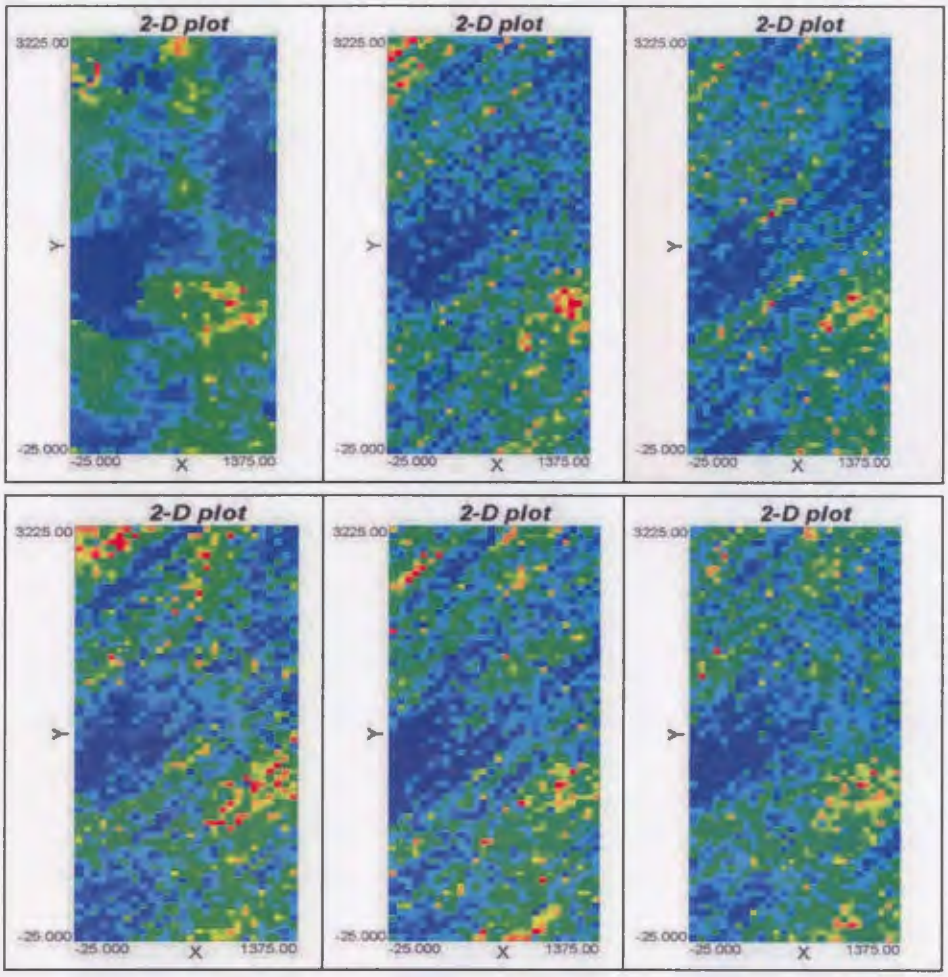

Figure 6.21: GSLIB Realizations for a Base Case Compared to Each State

6.5.3 Reservoir Simulation

The reservoir simulation allows for the quantification of the uncertainty in the permeability in terms of oil production rates based on geostatistics. Geostatistics is extremely useful because it allows for multiple variables to be studied with a single response. In this case only one variable is being studied to show the methodology of how to incorporate the measurements while drilling into the risk calculation. This is

done through the development of geostatistical realizations and a reservoir simulator called NETool.

Currently NETool is capable of running batches of simulations. The limitation is that the output is opened into spreadsheet format which draws computer memory. This means that only eight realizations can be run at a single time with a limited amount of output before the accessible memory of the computer is exhuasted. The output from GSLIB is in the form of a single text file with 500 realizations. This means there is a need for some pre-processing before the simulation takes place so that only eight realizations are run at any given time.

A MATLAB file (*split.m*) was created to perform the conversion of the single file with 500 realizations, into 62 separate files each with eight realizations in each file and a final file with the balance of the realizations. In practice this procedure would need to be customized depending on the number of realizations used, the capability of the user's computer and the numerical simulator used. Details of this procedure can be found in Appendix C.

NETool requires the importation of a grid with saturations, pressures, and all other relative information about the formation. This comes directly from the Eclipse files with no need for any data processing. Once this is completed the well path should be set in NETool. Figure 6.22 shows where the input of the trajectory can be modified and/or typed into NETool. The other parameters used in NETool that are necessary (including type of completions, global parameters , etc) are included in Appendix D.

The output from the reservoir simulation includes the upscaled permeability along the well path, and the total production rates for all realizations for each state. This is what is being used for the risk analysis. In total there were 500 realizations for

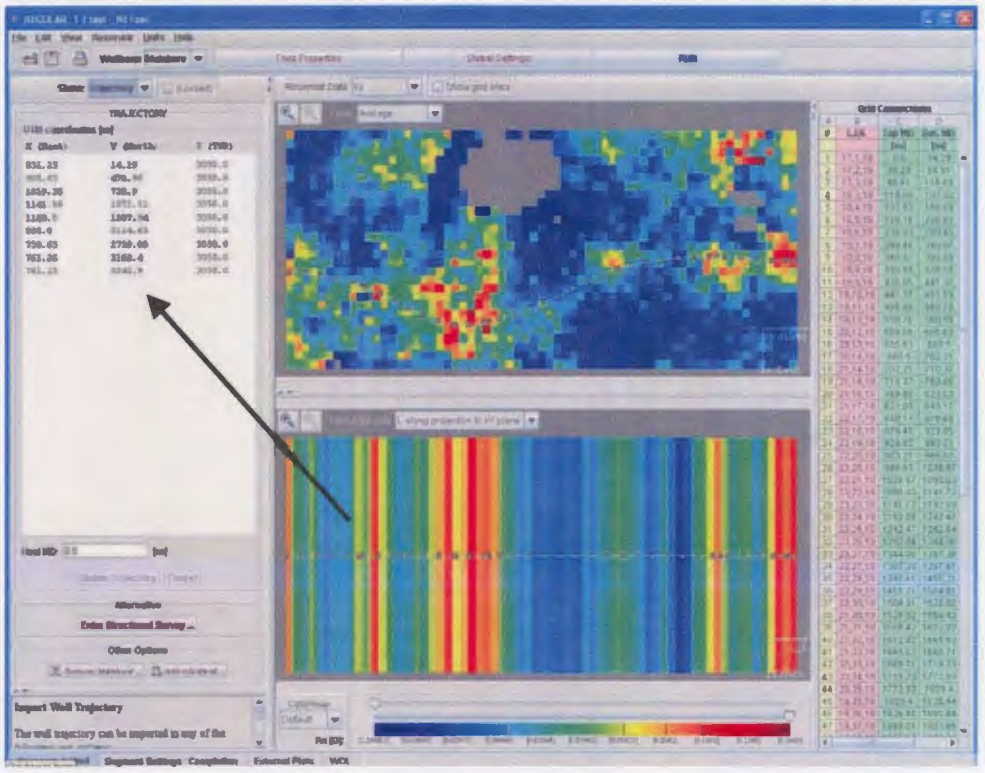

Figure 6.22: NETool Well Trajectory Input

each of the six states (one state before MWD and five states throughout the drilling process).

Once the simulations were completed, some post processing was necessary to prepare for the risk analysis. The production rates were calculated and input into separate output locations. In order for the data analysis to take place the information from each realization was copied and pasted into Microsoft Excel. This data can be seen in Appendix D.

6.5.4 Risk Calculation

This section describes the procedure for calculating the risk for this case study. The information used in the risk analysis is based on data collected from the reservoir simulations from the NETool output. The calculation of risk is described in the chapter on risk analysis. Specifically, Equation 4.1 is used to calculate the risk. The consequence is defined as the deviation of the production rate of the 95th percentile of the 500 realizations of the state, from the base case production rate, multiplied by the price of oil. The price of oil is taken as a constant value of $50 per barrel. Thus, each state has a single quantifiable consequence. Since the 95th percentile of the production is taken as the acceptable probability with an acceptable confidence level, the uncertainty involved with each calculation is 5%. Multiplying the consequence by the uncertainty yields the risk value. The next question is how do we analyze the risk. Since each state has a quantifiable risk value associated with it, the risk at each state can be compared. The following equation fully explains the risk calculation.

$$Risk = (P_{statei95} - P_{base2})(\$50)(0.05)) \tag{6.4}$$

Where

- $P_{statei95}$: *is the 95th percentile production value of the* i^{th} *state in barrels of oil*
- P_{base2} : *is the production of the baseline case in barrels of oil*
- $50 : *is the price of oil per barrel*
- 0.05 : *is the uncertainty in the state production*

6.6 Results

The calculated risk values associated with each state is summarized in Table 6.5

Table 6.5: Summary of Risk Factors

State	0	1	2	3	4	5
Risk Factor	-1239.15	-606.93	-476.90	-470.23	-240.32	-36.93
Risk Improvement(%)	N/A	51.02	21.42	1.40	48.89	84.64

To put these numbers into perspective, they represent the deviation between the state production and the actual production, in terms of dollars, multiplied by the uncertainty in the state production. Each state presents some degree of risk since all the risk factors given in the table are negative. This means that the state production prediction consistently makes conservative predictions. This can be thought of as a safety factor.

From the table it is evident that the risk factor is decreasing with each progressing state calculation. The second largest improvement is from state zero to state one. The reason for this may be that the decrease in variability due to the added information permeates through the reservoir grid. Thus the greatest improvement in risk factor occurs when the first measurements while drilling are incorporated since they influence the grid when it is populated with the least amount of data. The concept is that adding conclusive data where there is little certainty improves the risk more than adding the same amount of conclusive data where there is already a level of confidence existing.

In theory, in the final state, the risk factor should near zero since the permeability around the well trajectory is known. In this case the predicted production should equal the expected production causing the deviation to be small in comparison to

other states. The final state in this analysis demonstrates the biggest improvement in reduction of risk because of the decrease in variation of permeability values along the well path. The reduction in variation means that the production simulation is more certain however the risk factor does not become zero. In this state the risk factor is close to -37. It is believed that the variogram models chosen, under predict the permeability values for the geostatistical realizations. This is because difficulties in modeling the variograms cause the variogram chosen to be unable to fully represent the peak in the direction of minor continuity. This reiterates that care and caution needs to be take when developing a geostatistical model and the process is not always straightforward.

6.7 Summary

This case study presents an example of how risk can be quantified in the presence of geological uncertainty. It then continues to demonstrate how measurements while drilling can improve this risk factor.

Geostatistics was used to create equiprobable realizations of the reservoir creating a bandwidth of probable permeability distributions throughout the reservoir formation. The spatial relationship of permeability was modeled by using variograms and then sequential Gaussian simulation was used to create the realizations. A total of 500 realizations were generated for each state in the drilling process where each state represents a time block where measurements while drilling are gathered and received.

A baseline realization exists from the exhaustive data set and the risk involved is based on the deviation between this baseline and the simulated realizations. Each state provides a distribution of production rates. The 95th percentile was deemed an

acceptable confidence level for this case study so the 95th percentile of the production rates for each state was used in the risk calculation. The risk is a function of two parameters, the consequence of the hazard and the uncertainty that this negative event will occur. The hazard is not achieving the baseline production (the difference in the production rates between the baseline and the 95th percentile of the state) and the consequence is this difference multiplied by the price of oil. The uncertainty for this occurrence is five percent based on the use of the 95th percentile value for the simulated production values.

The utilization of measurements while drilling occurs at 5 states throughout the drilling process. Each state provides more information about the reservoir. The gathered information is used to reduce the risk involved with drilling a production well. The measurements while drilling were used as extra information in the geostatistical simulator and it served to tune the realizations. Each state reduces the risk by reducing the variability in the distribution of the permeability and bringing it closer to the actual baseline.

The results demonstrate a marked improvement of risk factor for each state. The more information utilized in the drilling process the more the risk is reduced. For this reason this methodology can serve as a guide on how to incorporate measurements while drilling to help reduce the risk in drilling production wells in petroleum reservoirs.

Chapter 7

Observations and Discussion

This research proves that there is a place in the field of geostatistics, reservoir engineering and risk engineering where improvements can be made to reduce the risk in drilling production wells. In many cases the literature suggests that only experience may offer the best advice on how to deal with risk in field situations. Often a full-scale geological model requires professionals from different disciplines that have years of experience in their field to develop acceptable reservoir models based on the available information. This research shows the methodology of how measurements while drilling can be incorporated into the risk calculation in real-time.

The chapters leading up to the case studies give the necessary background in the fields of risk engineering and geostatistics to understand the proposed methodology. The literature review provides a history of the work that has been done in related areas and with similar ambitions. The literature review demonstrated that even though work has been done in risk engineering and geostatistics in the oil and gas industry, no methodology exists to utilize measurements while drilling in real-time. The chapter covering geostatistical background highlights all the major concepts used in both case studies. It gives information about modeling spatial relationships and

how to estimate points at unsampled locations which is essential to understanding the case studies. The risk engineering chapter gives information about how to calculate risk. By highlighting simulation it gives insight into how risk can be calculated when there is uncertainty in a data set.

7.1 Case Study 1

The first case study demonstrated the basic concepts of geostatistics. The porosity field data set was used to estimate porosity at unsampled locations along the path of the well. Once the porosity along the well path was completely defined (kriged at all desired locations) the production volume for the life of the project was fully defined by using a stream tube model and several reservoir engineering concepts. This production volume image was considered the baseline image and represented the expected production from the formation. Other porosity images were generated based on a random number generator with an algorithm capable of creating a data set with the same mean and standard deviation of the kriged porosity data. 500 images were generated for each grouping and this was repeated 500 times. The production volume for all images was computed using the same stream tube model and this information was compared to the baseline production by using a risk calculation. The risk factor calculation was calculated according to the following equation:

$$Risk = (P_{95} - P_{base})\,(\$Oil)\,(0.05) \tag{7.1}$$

From all the risk factors calculated there is a resulting risk distribution. The resulting risk profile is shown in Figure 5.9. From this figure it can be seen that there was only a 5% chance of risk (meaning that there was only a 5% chance of not achieveing the

expected production). This is shown where the distribution line crosses the y-axis on the figure. For the other 95% there was no risk since the deviation in production favored the randomized images and there is no hazard. The main purpose of this case study was to demonstrate a methodology for quantifying the risk in a project when there is uncertainty in the geology. It also demonstrates major geostatistical concepts used in the second case study.

7.2 Case Study 2

The second case study approaches the uncertainty in the geology with much more rigor than the first case study. In this case study there is a baseline permeability realization from a numerical reservoir model. For the study, 90% of the permeability values were removed randomly to represent a sample population. A geostatistical analysis of this sample population revealed an anisotropic variogram which represented the spatial relationship of the data. This relationship was used to create 500 realizations using sequential Gaussian simulation. This is the initial state of the case. Specific information from the baseline realization was then added into the sample population along the well path. This represents measurements aquired while drilling. The entire well path was split into 5 sections and each section represents a new state. After the information from the baseline realization was added to the sample population for a given state, the geostatistical simulation generates 500 realizations for a risk calculation.

It was found that the risk for each state continuously decreased as more information was used in the geostatistical simulation. This is demonstrated in the following table.

Each state experienced a marked improvement in risk over the previous state. This

Table 7.1: Summary of Risk Factors

State	0	1	2	3	4	5
Risk Factor	-1239.15	-606.93	-476.90	-470.23	-240.32	-36.93
Risk Improvement(%)	N/A	51.02	21.42	1.40	48.89	84.64

result is encouraging. It also showed that the risk reduction was most pronounced in the early states. The purpose of this case study was mainly to demonstrate a methodology of how to incorporate measurements while drilling into a risk calculation while drilling. It shows that by using such information the risk was significantly reduced. It demonstrates how the disciplines of risk engineering, geostatistics and reservoir engineering can be used together in a multidisciplinary way to reduce the risk in drilling production wells.

Chapter 8

Conclusions and Recommendations

This research has explored the concept of using measurements while drilling in real-time to update geostatistical reservoir models. The main focus was to present a methodology on how to integrate the concepts of geostatistics, reservoir engineering and risk analysis and to utilize these concepts in a practical way. Through the use of two case studies the methodology was demonstrated in a rigorous fashion in a useful way. The proposed methodology is original in that it integrates a number of different disciplines allowing for the utilization of "real-time" data obtained throughout the drilling process. Such a methodology was not previously available and it provides a novel approach to improving decision making during the drilling of production wells. By utilizing information from MWD, decisions can be made based on the statistical and spatial characteristics of the petroleum host formation. As drilling progresses, the uncertainty decreases as a result of the additional information, thereby decreasing the risk.

The results of the case studies indicate how the proposed methodology can provide a great advantage when used in real-time to reduce risk. It also demonstrates that geostatistics can provide a pathway to utilize the measurements while drilling to

decrease the uncertainty in the geology of the reservoir.

There are a number of areas in this research where care and caution must be used to implement the methodology. One area where there is uncertainty in geostatistical methodology is in the determination of the directions of maximum and minimum continuity. The mathematical way to calculate these directions is through the use of a variogram map. This method is only suggested as a last resort; if the information is not available to allow for the conclusive designation of the directions. One way to show conclusive evidence is to have an experienced geologist who knows the location and geographical particulars, offer that evidence. Experience is integral. Another area where experience is needed is in variogram modeling. Variogram modeling is easy if the variogram estimate is well-behaved. In nature, however, there are often inexplicable fluctuations. In these cases it is up to the geoscientist to determine which parts of the variogram estimation are important to model and which ones represent some sort of removable trend or which fluctuations can be ignored.

The validation procedures for geostatistical models are not obvious. Without a baseline comparison (since the reservoir is usually largely uncertain) it is sometimes difficult to validate the models. One method involves removing one point at a time from the sample data set and kriging to see if the model can predict it correctly. The limitation of this method is that the estimation at the sampled location is often not representative of estimation at all unsampled locations. In this research a qualitative validation technique was used to see if the model predictions were appropriate however in practice this procedure should be more rigorous.

The following are areas where further research may be applicable:

Up to now the geostatistics in reservoir characterization has primarily been used to

make decisions before the drilling of production wells. This means that the information that is gained while drilling (from measurements while drilling) is not being used to tune the geostatistical models. If the measurements while drilling were used in the geostatistical models then the information could be used to make better decisions and optimize well paths while in the drilling process through the use of risk analysis. This may be necessary if unexpected formations appear while drilling and a change in drilling trajectory is needed. Some work has been completed to date regarding how geostatistics can be used to optimize well trajectories and manage reservoirs however its use in real-time has not been explored.

Another area for future research would be to include many different types of data with different measurements while drilling to form a more comprehensive case study of how the risk factor would behave with the addition of multiple variables in the geostatistical and reservoir simulation and in three dimensions.

Work should also be done to integrate the three fields of reservoir engineering, risk engineering and applied geostatistics into software that can import measurements while drilling. This would allow the concept of using measurements while drilling to update the field model in real-time more accessible.

References

1. *@Risk: Advanced Risk Analysis for Spreadsheets, A Guide to Using @Risk Version 4.5.* (2002). Newfield, New York: Palisade Corporation

2. Abdassah, D., Mucharam, L., Soengkowo, I., Trikoranto, H., & Sumantri, R., (1996). "Coupling Seismic Data With Simulated Annealing Method Improves Reservoir Characterization," *Society of Petroleum Engineers,* SPE 36968, SPE Asia Pacific Oil and Gas Conference, 28-31 October, Adelaide, Australia.

3. Al Qassab, H. M., Fitzmaurice, J., Al-Ali, Z. A., Al-Khalifa, M. A., Aktas, G. A., & Glover, P. W., (2000). "Cross-Discipline Integration in Reservoir Modeling: The Impact on Fluid Flow Simulation and Reservoir Management," *Society of Petroleum Engineers,* SPE 62902, SPE Annual Technical Conference and Exhibition, 1-4 October, Dallas, Texas.

4. Amed, T., (2001). *Reservoir Engineering Handbook, 2nd ed.* Boston: Gulf Publishing Professional.

5. Arild, ø., Nilsen T., & Sandy M., (2004). "Risk-based Decision Support for Planning of an Underbalanced Drilling Operation," *Society of Petroleum Engineers,* SPE 91242, SPE/IADC Underbalanced Technology Conference and Exhibition, 11-12 October, Houston, Texas.

6. Aylor, W. K., (1997). "Precision and Scale of Seismic Data for Geostatistical Reservoir Modeling," *Journal of Petroleum Technology,* Vol. 49, January, pp. 35-36.

7. Barnhart, W., & Coulthard, C., (2000). "Weyburn CO_2 Miscible Flood Conceptual Design and Risk Assessment," *Journal of Canadian Petroleum Technology,* Vol. 39, No. 9, pp. 25-33.

8. Bernasconi, J., (2004). "Part III: Risk Analysis in Practice," *ABB Review,* Vol. 4, pp 71-74.

9. Brouwer, D. R., Nævdal, G., Jansen, J. D., Vefring, E. H., & van Kruijsdijk, C. P. J. W., (2004). "Improved Reservoir Management Through Optimal Control and Continuous Model Updating," *Society of Petroleum Engineers Inc.,* SPE 90149, SPE Annual Technical Conference and Exhibition, 26-29 September, Houston, Texas.

10. Cayeaux, E., Genevois, J.M., Crepin, S., & Thibeau, S., (2001). "Well Planning Quality Improved Using Cooperation between Drilling and Geosciences," *Society of Petroleum Engineers Inc.,* SPE 71331, SPE Annual Technical Conference and Exhibition, 30 September-3 October, New Orleans, Louisiana.

11. Chewaroungroaj, J., Varela, O. J., & Lake, L. W., (2000). "An Evaluation of Procedures to Estimate Uncertainty in Hydrocarbon Recovery Predictions," *Society of Petroleum Engineers,* SPE 59449, SPE Asia Pacific Conference on Integrated Modelling for Asset Management, 25-26 April, Yokohama, Japan.

12. Chopra, A. K., Severson, C. D., & Carhart, S. R., (1990). "Evaluation of Geostatistical Techniques for Reservoir Characterization," *Society of Petroleum Engineers,* SPE 20734, SPE Annual Technical Conference and Exhibition, 23-26 September, New Orleans, Louisiana.

13. Damsleth, E. & Omre, H., (1997). "Geostatistical Approaches in Reservoir Evaluation," *Journal of Petroleum Technology,* Vol. 49, No. 5, pp. 498-501.

14. Deutsch, C. V., (2002). *Geostatistical Reservoir Modeling.* New York: Oxford University Press.

15. Devroye, L., (1986). *Non-Uniform Random Variate Generation.* New York: Springer-Verlag.

16. Evans, J. R., & Olson, D. L., (2002). *Introduction to Simulation and Risk Analysis, 2nd ed.* Upper Saddle River, New Jersey: Prentice Hall.

17. Fenwick, D.H., & Roggero, F., (2003). "Updating Stochastic Reservoir Models With New Production Data ," *Society of Petroleum Engineers,* SPE 84467, SPE Annual Technical Conference and Exhibition, 5-8 October, Denver, Colorado.

18. Galli, A., Armstrong, M., Portella, R. C. M., de Souza Jr, O. G., & Yokota, H. K., (2004). "Stochastic-Aided Design and Bayesian Updating: New Tools to Use Expert Knowledge in Quantitative Models that Incorporate Uncertainty," *Society of Petroleum Engineers Inc.,* SPE 90414, SPE Annual Technical Conference and Exhibition, 26-29 September, Houston, Texas.

19. Goovaerts, P., (1997). *Geostatistics for Natural Resources Evaluation.* New York: Oxford University Press.

20. Gringarten, E., & Deutsch, C. V., (1999). "Methodology for Variogram Interpretation and Modeling for Improved Reservoir Characterization," *Society of Petroleum Engineers Inc.,* SPE 56654, SPE Annual Technical Conference and Exhibition, 3-6 October, Houston, Texas.

21. Gu, T., & Oliver, D.S., (2004). "History Matching of the PUNQ-S3 Reservoir Model Using the Ensemble Kalman Filter ," *Society of Petroleum Engineers Inc.,* SPE 89942, SPE Annual Technical Conference and Exhibition, 26-29 September, Houston, Texas.

22. Güyagüler, B., & Horne, R. N., (2001). "Uncertainty Assessment of Well Placement Optimization," *Society of Petroleum Engineers Inc.,* SPE 71625, SPE Annual Technical Conference and Exhibition, 30 September-3 October, New Orleans, Louisiana.

23. Isaaks, E. H., & Srivastava, R. M., (1989). *Applied Geostatistics.* New York : Oxford University Press.

24. Isaaks, E. H., & Srivastava, R.M., (1988). "Spatial Continuity Measures for Probabilistic and Deterministic Geostatistics," *Mathematical Geology,* Vol. 20, No. 4, pp. 313 - 341 .

25. Journel, A. G., (1990). "Geostatistics for Reservoir Characterization," *Society of Petroleum Engineers Inc.,* SPE 20750, SPE Annual Technical Conference and Exhibition, 23-26 September, New Orleans, Louisiana.

26. Kelkar, M., & Perez, G., (2002). *Applied Geostatistics for Reservoir Characterization.* Richardson, Texas: Society of Petroleum Engineers Inc.

27. Khan, F. I., Amyotte, P., & Veitch, B., (2004). "Evaluation of inherent safety potential in Offshore Oil and gas activities", *OMAE 2004,* paper number 51528, June 20-25, Vancouver, Canada.

28. Khan, F. I., & Husain, T., (2003). "Evaluation of a Petroleum Hydrocarbon Contaminated Site for Natural Attenuation using RBMNA Methodology", *Environmental Modeling and Software,* Vol. 18, pp. 179-194.

29. Khan, F. I., & Husain, T., (2002). "Evaluation of Contaminated Sites Using Risk Based Monitored Natural Attenuation", *Chemical Engineering Progress-AIChE,* USA, January, pp. 34-44.

30. Khan, F. I., Sadiq, R., & Husain, T., (2002). "Risk based process safety assessment and control measures design for offshore process facilities", *Journal of Hazardous Materials,* Vol. 94, No. 1, pp. 1-36.

31. Lamy, P., Swaby, P.A., Rowbotham, P.S., Dubrule, O., & Haas, A., (1998). "From Seismic to Reservoir Properties Using Geostatistical Inversion," *Society of Petroleum Engineers Inc.,* SPE 49147, SPE Annual Technical Conference and Exhibition, 27-30 September, New Orleans, Louisiana.

32. Mackay, E.J., Jordan, M.M., Feasey, N.D.,Shah D., & Kumar, P., (2004). "Integrated Risk Analysis for Scale Management in Deepwater Developments," *Society of Petroleum Engineers Inc.,* SPE 87459, SPE International Symposium on Oilfield Scale, 26-27 May, Aberdeen, United Kingdom.

33. Manceau, E., Mezghani, M., Zabalza-Mezghani, & I.,Roggero F., (2001). "Combination of Experimental Design and Joint Modeling Methods for Quantifying the Risk Associated With Deterministic and Stochastic Uncertainties - An Integrated Test Study," *Society of Petroleum Engineers Inc.,* SPE 71620, SPE Annual Technical Conference and Exhibition, 30 September-3 October, New Orleans, Louisiana.

34. Manceau, E., Feraille, M., Zabalza-Mezghani, I., Portella, R.C.M, & Reis, L.C., (2005). "Advanced Risk Analysis Approach for Optimization of a Water Injection Program - Illustration on a Brazilian Field Case," *Society of Petroleum Engineers Inc.,* SPE 94845, SPE Latin American and Caribbean Petroleum Engineering Conference, 20-23 June, Rio de Janeiro, Brazil.

35. Mason, R.L., Gunst, R.F., & Hess, J.L., (2003). *Statistical Design & Analysis of Experiments, 2^{nd} Edition.* Hoboken, New York: John Wiley & Sons Inc.

36. Nævdal, G., Johnsen, L.M., Aanonsen, S.I., & Vefring, E.H., (2003). "Reservoir Monitoring and Continuous Model Updating using Ensemble Kalman Filter," *Society of Petroleum Engineers Inc.,* SPE 87459, 2003 Annual Technical Conference and Exhibition, Denver, Colorodo, October 5-8.

37. Oguntona, J.A., Kelsch, K., Osman, K., Ingebrigtsen, E., Butt, P., & Saha, S., (2004). "Thin Sand Development Made Possible through Enhanced Geosteering and Reservoir Planning with While-drilling Resistivity and NMR Logs: Example from Niger Delta," Society of Petroleum Engineers Inc., SPE 88889, Nigeria Annual International Conference and Exhibition, 2-4 August, Abuja, Nigeria.

38. Overfield, R.E., Collins, J.F. (2000). "Quantitative Risk Assessment as a Design Tool – Recent FPSO Experience," *Society of Petroleum Engineers Inc.,* SPE 61255, SPE International Conference on Health, Safety and Environment in Oil and Gas Exploration and Production, 26-28 June, Stavanger, Norway.

39. Özdoğan, U., & Horne, R. N., (2004). "Optimization of Well Placement with a History Matching Approach," *Society of Petroleum Engineers Inc.,* SPE 90091, SPE Annual Technical Conference and Exhibition, 26-29 September, Houston, Texas.

40. Pan, Y., & Horne, R. N., (1998). "Improved Methods for Multivariate Optimization of Field Development Scheduling and Well Placement Design," *Society of Petroleum Engineers Inc.,* SPE 49055, SPE Annual Technical Conference and Exhibition, 27-30 September, New Orleans, Louisiana.

41. Pathnak, R., Ogbe, D. O., & Jensen, J. L., (2000). "Application of Geostatistical and Fluid Flow Simulations to Evaluate Options for Well Placement," *Society of Petroleum Engineers Inc.,* SPE 62554.

42. Roald, T.H., (2000). "New Risk Assessment Approach Shows Significant Reduction in Oil Blowout Risk," *Society of Petroleum Engineers Inc.,* SPE 61469, SPE International Conference on Health, Safety and Environment in Oil and Gas Exploration and Production, 26-28 June, Stavanger, Norway.

43. Rossini, C., Brega, F., Piro, L., Rovellini, M., & Spotti, G., (1994). "Combined Geostatistical and Dynamic Simulations for Developing a Reservoir Management Strategy: A Case History," *Journal of Petroleum Technology,* November, pp. 979-985.

44. Saputelli, L., Economides, M., Nikolaou, M., & Kelessidis, V., (2003). "Real-time Decision-making for Value Creation while Drilling ," *Society of Petroleum Engineers Inc.,* SPE 85314, SPE/IADC Middle East Drilling Technology Conference and Exhibition, 20-22 October, Abu Dhabi, United Arab Emirates.

45. Schiozer, D. J., Ligero, E. L., & Santos, J. A. M., (2004). "Risk Assessment for Reservoir Development Under Uncertainty," *Journal of the Brazilian Society of Mechanical Sciences and Engineering,* Vol. 26, No. 2, pp. 213-217.

46. Solis, R. Rojas, S., Ramirez, G. B., Sputelli, L., & Narayanan, K., (2004). "Risk, Uncertainty and Optimization for Offshore Gas Asset Planning in Litoral Tabasco," *Society of Petroleum Engineers Inc.,* SPE 90177, SPE Annual Technical Conference and Exhibition, 26-29 September, Houston, Texas.

47. Srivastava, R. M., (1990). "An Application of Geostatistical Methods for Risk Analysis in Reservoir Management," *Journal of Petroleum Technology,* Vol. 49, No. 5, pp. 498-501.

48. Sweet, M. L., Blewden, C. J., Carter, A. M., & Mills, C. A., (1996). "Modeling Heterogeneity in a Low-Permeability Gas Reservoir Using Geostatistical Techniques, Hyde Field, Southern North Sea," *AAPG Bulletin,* Vol. 80, No. 11, pp. 1719-1735.

49. Taguchi, G., (1987). *System of Experimental Design, Vol.1-2.* White Plains, New York: Unipub/ Kraus International Publications.

50. Thayer, W. C., Griffith, D. A., Goodrum, P. E., Diamond, G. L., & Hasset, J. M., (2003). "Application of Geostatistics to Risk Assessment," *Risk Analysis,* Vol. 2, No. 5, pp. 945-959.

51. Torhaug, M., (1990). "Use of Risk Analysis in the Offshore Industry," *Proceedings of the Ninth International Conference on Offshore Mechanics and Arctic Engineering,* Vol. 2, pp 277-281.

52. Voit, E. O., & Schwacke, L. H., (2000). "Random Number Generation from Right-Skewed, Symmetric, and Left-Skewed Distributions," *Risk Analysis,* Vol. 20, No.1, pp 59.

53. Wallace, C. S., (1996). "Fast Pseudorandom Generators for Normal and Exponential Variates," *ACM Transactions on Mathematical Software,* Vol. 22, No. 1, pp 119-127.

54. Wehunt, C.D., (2003). "Well Performance with Operating Limits under Reservoir and Completion Uncertainties," *Society of Petroleum Engineers,* SPE 84501, SPE Annual Technical Conference and Exhibition, 5-8 October, Denver, Colorado.

55. Welch, G., & Bishop, G., (2004). "An Introduction to the Kalman Filter," *http : //www.cs.unc.edu/ welch/media/pdf/kalman_intro.pdf*

56. Xue, G., & Datta-Gupta, A., (1997). "Structure Preserving Inversion: An Efficient Approach to Conditioning Stochastic Reservoir Models to Dynamic Data," *Society of Petroleum Engineers,* SPE 38727, SPE Annual Technical Conference and Exhibition, 5-8 October, San Antonio, Texas.

57. Yeten, B., Brouwer, D.R., Durlofsky, L.J., & Aziz, K.,(2004). "Decision Analysis under Uncertainty for Smart Well Deployment," *Journal of Petroleum Science,* Vol. 43, pp. 183-199.

Appendix A

Extra Geostatistical Information

Models Without a Sill

Fractional Gaussian Noise, $f_{GN}Model$:

This model uses a number of empirical parameters (available in the literature) to account for trends occurring in variogram estimates. Mathematically it is defined as:

$$\gamma(\vec{L}) = \tfrac{1}{2}C_S\delta^{2H-2}\left[2 - \left(\tfrac{|L|}{\delta}+1\right)^{2H} + 2\left(\tfrac{|L|}{|\delta|}\right)^{2}H - \left(\tfrac{|L|}{\delta}-1\right)^{2H}\right] \tag{8.1}$$

Where:

- C_s – *Scaling Parameter*
- H – *Intermittency Exponent* $(0,1)$
- δ – *Averaging Parameter*

Fractional Brownian Motion, $f_{BM}Model$:

The applicability of this model is still a topic of debate. It does however; seem to predict a variogram with some degree of accuracy. Mathematically it is defined as the following:

$$\gamma(\vec{L}) = C_S L^{2H} \tag{8.2}$$

Logarithmic Model:

This model is used in mining however its use in reservoir engineering is very limited.

$$\gamma(\vec{L}) = C_o log(L) \tag{8.3}$$

Cross Variograms

Cross variograms represent the spatial relationship between two parameters located at a certain lag distance from each other. This is especially applicable when there are two parameters to consider (e.g.: porosity, and permeability) and relative spatial distance (lag). The equation for the cross variogram is:

$$\gamma_c(\vec{L}) = \frac{1}{2}E\left\{\left[X\left(\vec{U}\right) - X\left(\vec{U}+\vec{L}\right)\right]\left[Y\left(\vec{U}\right) - Y\left(\vec{U}+\vec{L}\right)\right]\right\} \tag{8.4}$$

However in practice it is more convenient to use the concept in the following form:

$$\gamma_c(\vec{L}) = \frac{1}{2n(\vec{L})}\sum_{i=1}^{n(\vec{L})}\left[x\left(\vec{u_i}\right) - x\left(\vec{u_i}+\vec{L}\right)\right]\left[y\left(\vec{u_i}\right) - y\left(\vec{u_i}+\vec{L}\right)\right] \tag{8.5}$$

With these equations it should be noted that the cross-variogram is symmetric but the cross-covariance is not always symmetric. In most cases it can be assumed that the cross-covariance is symmetric and this will allow for the calculation of the cross-covariance at an unsampled location by rearranging the following equation:

$$\gamma_c(\vec{L}) = C_c(0) - C_c(\vec{L}) \tag{8.6}$$

Note that this equation also holds for regular variograms and will be used in the following section.

Other Types of Kriging

Simple Kriging

This procedure is the easiest kriging technique to apply but it may not be the most practical. It begins with the assumption that the value at the estimated location may be estimated by a linear combination:

$$X^*(\vec{u}) = \lambda_o + \sum_{i=1}^{n}\lambda_i X(\vec{u_o}) \tag{8.7}$$

Using the unbiased condition (the fact that the difference between the expected value of the sample and the expected value of the estimate is zero) and the first order of stationarity a matrix involving the covariance between two sample points, the weights and the covariance between the sample point and the estimate can be derived (Kelkar and Perez, 103). In matrix form this is:

$$\begin{bmatrix} C(\vec{u}_1,\vec{u}_1) & \cdots & C(\vec{u}_1,\vec{u}_n) \\ \vdots & & \vdots \\ C(\vec{u}_n,\vec{u}_1) & \cdots & C(\vec{u}_n,\vec{u}_n) \end{bmatrix} \begin{bmatrix} \lambda_1 \\ \vdots \\ \lambda_n \end{bmatrix} = \begin{bmatrix} C(\vec{u}_1,\vec{u}_0) \\ \vdots \\ C(\vec{u}_n,\vec{u}_0) \end{bmatrix} \tag{8.8}$$

The covariance matrix on the left-hand side of the equation is known since it is developed completely from sample point data. The covariance matrix on the right-hand side of the equation can be estimated by using the variogram model and variogram-covariance relationship. Knowing these parameters, the matrix of weighting parameters can be calculated. Using the unbiased condition and using the first order of stationarity we can estimate the constant λ_o in the linear kriging equation using the following equation (Kelkar & Perez, 103):

$$\lambda_0 = m\left(1 - \sum_{i=1}^{n} \lambda_i\right) \tag{8.9}$$

Where:

- m – *Global Mean*

Now all the parameters in the matrix are known except the estimate, so the estimate can now be carried out.

Universal Kriging

$$X^*(\vec{u_o}) = m(\vec{u}) + R(\vec{u}) \tag{8.10}$$

Where $m(\vec{u})$ represents the trend (it can have any form - linear, quadratic, etc.).

For this formulation the following matrix can be derived (See Kelkar & Perez, page 125):

$$\begin{bmatrix} C(\vec{u}_1,\vec{u}_1) & \cdots & C(\vec{u}_1,\vec{u}_n) & f_0(\vec{u_0}) & \cdots & f_0(\vec{u_n}) \\ \vdots & & \vdots & \vdots & & \vdots \\ C(\vec{u}_n,\vec{u}_1) & \cdots & C(\vec{u}_n,\vec{u}_n) & f_L(\vec{u_0}) & \cdots & f_L(\vec{u_n}) \\ f_0(\vec{u_0}) & \cdots & f_0(\vec{u_n}) & 0 & \cdots & 0 \\ \vdots & & \vdots & \vdots & & \vdots \\ f_L(\vec{u_0}) & \cdots & f_L(\vec{u_n} & 0 & \cdots & 0 \end{bmatrix} \begin{bmatrix} \lambda_1 \\ \vdots \\ \lambda_n \\ \mu_o \\ \vdots \\ \mu_L \end{bmatrix} = \begin{bmatrix} C(\vec{u}_1,\vec{u}_0) \\ \vdots \\ C(\vec{u}_n,\vec{u}_0) \\ f_0(\vec{u_0}) \\ \vdots \\ f_L(\vec{u_0} \end{bmatrix} \tag{8.11}$$

The f function is known as the trend function and lies in the function for $m(\vec{u})$ in the following manner:

$$m(\vec{u}) = \sum_{i=1}^{n} a_i f_i(\vec{u_i}) \tag{8.12}$$

where the a_i parameters are coefficient of the function f_i. Note that $f_o(\vec{u})$ is defined to be equal to one. Universal kriging is a linear form of kriging however this is a misnomer since the local mean may drift according to a non-linear trend.

Fitness Tests

@Risk has a powerful tool that allows a user to fit a set of sample data to a distribution. It calculates the parameters for each distribution (shape and/or scale parameters, mean, standard deviation depending on the distribution) that would best represent the data for a number of different probability distributions. Then it ranks the different distributions based on a number of different goodness-of-fit statistics such as the Chi-Squared Statistic and the Kolmogorov-Smirninov Statistic. Since it is up to the user to choose which statistic to use, the more prominent ones will be briefly discussed.

The chi-squared statistic is the best known technique for calculating the goodness-of-fit statistic (Palisade Corporation, 2002). After splitting the parameter into 'bins' the chi-squared statistic can be calculated in the following manner:

$$X^2 = \sum_{i=1}^{\kappa} \frac{(N_i - E_i)^2}{E_i} \tag{8.13}$$

Where:

- κ : *the number of bins*
- N_i : *the observed number of samples in the* i^{th} *bin*
- E_i : *the expected number of samples in the* i^{th} *bin*

This statistic has the disadvantage of not having any guidelines of how to divide the sample data into bins. In some cases the statistic will change based on the selection of the bins. One way to help in this respect is to adjust the bin sizes such that all bins have an equal amount of probability

The Kolmogorov-Smirnov Statistic is another technique which may be used. It is defined in the following way:

$$D_n = max\left(|F_n(x) - \hat{F}(x)|\right) \tag{8.14}$$

Where:

- n : *the total number of data points*
- $\hat{F}(x)$: *the fitted cumulative distribution function*
- $F_n(x) = \frac{N_x}{n}$
- N_x : *the number of* $X_i's$ *less than* x

This statistic does not require binning but it does not detect tail discrepancies.

Other techniques include the Anderson-Darling Statistic which is similar to the Kolmogorov-Smirinov and the Root-Mean Squared Error technique which is used only for density and cumulative curve data. The concept for each technique is the same; each is a measure of difference between a value expected based on the chosen distribution and the actual value. The lower the statistic the better the fit. In this manner different distributions can be tested; the parameters needed for the distribution (such as shape and scale parameters) can be optimized and the different distributions can be ranked accordingly.

In this research the chi-squared technique was used with equiprobable bin sizes. Note that α_1 and α_2 vary in meaning depending on the distribution. In the case of Beta distribution they represent shape parameters, in the Weibull distribution they represent the shape and scale parameters respectively and for the Normal distribution they represent the mean and standard distribution respectively.

Appendix B

Case Study 1 Field Data

Field Data

	X	Y	ϕ
1	21450	5180	11.78
2	-2280	10200	27.58
3	-800	8320	26.63
4	-4300	330	23.22
5	-3630	-4950	25.59
6	8615	4505	23.78
7	2310	-330	27.06
8	-3630	6260	26.57
9	-3630	6930	24.99
10	1925	10140	18.09
11	9165	10140	5.94
12	11955	10140	8.01
13	14445	10140	17.43
14	16405	10140	16.18
15	18405	10140	18.54
16	1005	6170	30.36
17	565	7500	21.90
18	8395	6150	28.99
19	8320	6170	21.75
20	9770	6170	24.32
21	12836	7150	23.02
22	11200	6170	22.25
23	12825	5580	27.26
24	10807	5633	26.63
25	13765	6170	13.86
26	15125	6170	15.38
27	3205	3530	28.60
28	3255	4860	28.77
29	5845	3500	27.83
30	7205	3530	29.02
31	6029	4860	27.08
32	8485	3530	30.40
33	9845	3530	30.63
34	9770	3530	23.20

	X	Y	ϕ
35	8485	4605	25.06
36	8559	3952	27.89
37	10985	3477	24.83
38	10995	4860	24.03
39	12432	4944	25.14
40	11128	3477	26.40
41	12535	3455	26.52
42	15275	3530	26.03
43	13765	4860	22.87
44	16960	3585	15.33
45	2565	2200	25.16
46	4565	2220	26.53
47	5845	2220	31.89
48	7205	2316	19.49
49	9920	2220	22.04
50	9633	247	16.89
51	11880	890	14.86
52	12560	890	18.56
53	11125	2220	29.18
54	11126	1750	9.59
55	12510	890	15.61
56	11050	2220	24.83
57	12295	300	16.60
58	14337	2318	25.77
59	15170	890	29.00
60	13765	2220	32.00
61	15050	2195	23.19
62	13736	856	16.21
63	15535	225	12.54
64	16405	2220	16.23
65	20740	400	17.31
66	23100	3960	15.44
67	-4620	-1980	24.70
68	11225	8547	13.82

Wall Trajectory

X	Y
15000	200
-500	8000

Case Study 1 Validation Data

Total Estimated

Well Path X	Well Path Y	Estimated Porosity	Distance from well path	Flow Unit Index	Flow unit Porosity	Mat Index
-500	8000	27.528	438.63	3	26.63	1
			1176.53	17	21.90	1
			2369.37	16	30.36	1
			2829.91	2	27.58	1
-475	7987.4	27.528	465.01	3	26.63	2
			1148.55	17	21.90	2
			2343.80	16	30.36	2
			2855.44	2	27.58	2
-450	7974.8	27.528	491.57	3	26.63	3
			1120.58	17	21.90	3
			2318.29	16	30.36	3
			2881.01	2	27.58	3
-425	7962.3	27.528	518.27	3	26.63	4
			1092.60	17	21.90	4
			2292.83	16	30.36	4
			2906.63	2	27.58	4
-400	7949.7	27.528	545.10	3	26.63	5
			1064.63	17	21.90	5
			2267.44	16	30.36	5
			2932.29	2	27.58	5
-375	7937.1	27.528	572.05	3	26.63	6
			1036.66	17	21.90	6
			2242.10	16	30.36	6
			2958.00	2	27.58	6
-350	7924.5	27.528	599.09	3	26.63	7
			1008.68	17	21.90	7
			2216.83	16	30.36	7
			2983.74	2	27.58	7
-325	7911.9	27.528	626.21	3	26.63	8
			980.71	17	21.90	8
			2191.63	16	30.36	8
			3009.53	2	27.58	8
-300	7899.4	27.528	653.41	3	26.63	9
			952.74	17	21.90	9
			2166.49	16	30.36	9
			3035.35	2	27.58	9
-275	7886.8	27.528	680.67	3	26.63	10
			924.77	17	21.90	10
			2141.43	16	30.36	10
			3061.22	2	27.58	10
-250	7874.2	27.528	707.99	3	26.63	11
			896.80	17	21.90	11
			2116.44	16	30.36	11
			3087.11	2	27.58	11
-225	7861.6	27.528	735.35	3	26.63	12
			868.83	17	21.90	12
			2091.52	16	30.36	12
			3113.05	2	27.58	12
-200	7849	19.411	762.77	3	26.63	13
			840.86	17	21.90	13
			2066.68	16	30.36	13
			3124.77	10	18.09	13
-175	7836.5	19.411	790.22	3	26.63	14
			812.90	17	21.90	14
			2041.93	16	30.36	14
			3117.10	10	18.09	14
-150	7823.9	19.411	784.93	17	21.90	15
			817.71	3	26.63	15
			2017.25	16	30.36	15
			3109.68	10	18.09	15
-125	7811.3	19.411	756.97	17	21.90	16
			845.23	3	26.63	16
			1992.67	16	30.36	16
			3102.48	10	18.09	16
-100	7798.7	19.411	729.01	17	21.90	17
			872.78	3	26.63	17
			1968.18	16	30.36	17
			3095.52	10	18.09	17
-75	7786.1	19.411	701.05	17	21.90	18
			900.36	3	26.63	18
			1943.78	16	30.36	18
			3088.80	10	18.09	18
-50	7773.5	19.411	673.09	17	21.90	19
			927.96	3	26.63	19
			1919.48	16	30.36	19
			3082.32	10	18.09	19
-25	7761	19.411	645.14	17	21.90	20
			955.58	3	26.63	20
			1895.28	16	30.36	20
			3076.08	10	18.09	20
0	7748.4	19.411	617.19	17	21.90	21
			983.23	3	26.63	21
			1871.18	16	30.36	21
			3070.09	10	18.09	21
25	7735.8	19.411	589.24	17	21.90	22
			1010.89	3	26.63	22
			1847.20	16	30.36	22
			3064.33	10	18.09	22
50	7723.2	19.411	561.30	17	21.90	23
			1038.58	3	26.63	23
			1823.33	16	30.36	23
			3058.83	10	18.09	23
75	7710.6	19.411	533.36	17	21.90	24
			1066.27	3	26.63	24
			1799.58	16	30.36	24
			3053.57	10	18.09	24
100	7698.1	19.411	505.43	17	21.90	25
			1093.99	3	26.63	25
			1775.95	16	30.36	25
			3048.55	10	18.09	25
125	7685.5	19.411	477.50	17	21.90	26
			1121.71	3	26.63	26
			1752.45	16	30.36	26
			3043.79	10	18.09	26
150	7672.9	19.411	449.58	17	21.90	27
			1149.45	3	26.63	27

Well Path X	Well Path Y	Estimated Porosity	Distance from well path	Flow Unit Index	Flow unit Porosity	Mat Index
7575	3936.5	26.083	549.64	30	29.02	324
			984.12	36	27.89	324
			996.85	32	30.40	324
			1129.18	35	25.06	324
7600	3923.9	26.083	557.82	30	29.02	325
			959.41	36	27.89	325
			968.69	32	30.40	325
			1116.76	35	25.06	325
7625	3911.3	26.083	567.28	30	29.02	326
			934.89	36	27.89	326
			940.73	32	30.40	326
			1104.91	35	25.06	326
7650	3898.7	26.083	577.90	30	29.02	327
			910.56	36	27.89	327
			912.78	32	30.40	327
			1093.65	35	25.06	327
7675	3886.1	26.083	589.68	30	29.02	328
			884.83	32	30.40	328
			886.45	36	27.89	328
			1082.99	35	25.06	328
7700	3873.5	26.083	602.54	30	29.02	329
			856.88	32	30.40	329
			862.58	36	27.89	329
			1072.96	35	25.06	329
7725	3861	26.083	616.39	30	29.02	330
			828.94	32	30.40	330
			838.95	36	27.89	330
			1063.57	35	25.06	330
7750	3848.4	26.083	631.19	30	29.02	331
			801.00	32	30.40	331
			815.61	36	27.89	331
			1054.84	35	25.06	331
7775	3835.8	26.083	646.85	30	29.02	332
			773.06	32	30.40	332
			792.56	36	27.89	332
			1046.78	35	25.06	332
7800	3823.2	26.083	663.33	30	29.02	333
			745.12	32	30.40	333
			769.85	36	27.89	333
			1039.42	35	25.06	333
7825	3810.6	26.083	680.56	30	29.02	334
			717.19	32	30.40	334
			747.49	36	27.89	334
			1032.76	35	25.06	334
7850	3798.1	26.083	689.26	32	30.40	335
			698.49	30	29.02	335
			725.52	36	27.89	335
			1026.83	35	25.06	335
7875	3785.5	26.083	661.34	32	30.40	336
			703.98	36	27.89	336
			717.06	30	29.02	336
			1021.62	35	25.06	336
7900	3772.9	26.083	633.42	32	30.40	337
			682.90	36	27.89	337
			736.22	30	29.02	337
			1017.16	35	25.06	337
7925	3760.3	26.083	605.52	32	30.40	338
			662.34	36	27.89	338
			755.94	30	29.02	338
			1013.45	35	25.06	338
7950	3747.7	25.287	577.61	32	30.40	339
			642.34	36	27.89	339
			776.17	30	29.02	339
			1007.80	6	23.78	339
7975	3735.2	25.287	549.72	32	30.40	340
			622.96	36	27.89	340
			796.86	30	29.02	340
			1001.13	6	23.78	340
8000	3722.6	25.287	521.84	32	30.40	341
			604.25	36	27.89	341
			817.99	30	29.02	341
			995.19	6	23.78	341
8025	3710	25.287	493.96	32	30.40	342
			586.28	36	27.89	342
			839.52	30	29.02	342
			990.01	6	23.78	342
8050	3697.4	25.287	466.11	32	30.40	343
			569.12	36	27.89	343
			861.43	30	29.02	343
			985.60	6	23.78	343
8075	3684.8	25.287	438.26	32	30.40	344
			552.84	36	27.89	344
			883.67	30	29.02	344
			981.97	6	23.78	344
8100	3672.3	25.287	410.44	32	30.40	345
			537.53	36	27.89	345
			906.24	30	29.02	345
			979.12	6	23.78	345
8125	3659.7	25.287	382.64	32	30.40	346
			523.27	36	27.89	346
			929.09	30	29.02	346
			977.07	6	23.78	346
8150	3647.1	25.287	354.88	32	30.40	347
			510.14	36	27.89	347
			952.23	30	29.02	347
			975.82	6	23.78	347
8175	3634.5	28.818	327.14	32	30.40	348
			498.25	36	27.89	348
			975.37	6	23.78	348
			975.61	30	29.02	348
8200	3621.9	28.818	299.46	32	30.40	349
			487.67	36	27.89	349
			975.72	6	23.78	349
			999.24	30	29.02	349
8225	3609.4	28.818	271.84	32	30.40	350
			478.50	36	27.89	350

			1729.09	16	30.36	27
			3039.27	10	18.09	27
175	7660.3	19.411	421.67	17	21.90	28
			1177.20	3	26.63	28
			1705.86	16	30.36	28
			3035.01	10	18.09	28
200	7647.7	19.411	393.77	17	21.90	29
			1204.96	3	26.63	29
			1682.78	16	30.36	29
			3031.00	10	18.09	29
225	7635.2	19.411	365.88	17	21.90	30
			1232.73	3	26.63	30
			1659.85	16	30.36	30
			3027.25	10	18.09	30
250	7622.6	19.411	338.01	17	21.90	31
			1260.51	3	26.63	31
			1637.08	16	30.36	31
			3023.74	10	18.09	31
275	7610	19.411	310.16	17	21.90	32
			1288.30	3	26.63	32
			1614.47	16	30.36	32
			3020.50	10	18.09	32
300	7597.4	19.411	282.34	17	21.90	33
			1316.10	3	26.63	33
			1592.03	16	30.36	33
			3017.51	10	18.09	33
325	7584.8	19.411	254.55	17	21.90	34
			1343.91	3	26.63	34
			1569.77	16	30.36	34
			3014.77	10	18.09	34
350	7572.3	19.411	226.82	17	21.90	35
			1371.72	3	26.63	35
			1547.69	16	30.36	35
			3012.30	10	18.09	35
375	7559.7	19.411	199.15	17	21.90	36
			1399.54	3	26.63	36
			1525.81	16	30.36	36
			3010.08	10	18.09	36
400	7547.1	19.411	171.59	17	21.90	37
			1427.37	3	26.63	37
			1504.13	16	30.36	37
			3008.12	10	18.09	37
425	7534.5	19.411	144.19	17	21.90	38
			1455.20	3	26.63	38
			1482.67	16	30.36	38
			3006.42	10	18.09	38
450	7521.9	19.411	117.07	17	21.90	39
			1461.42	16	30.36	39
			1483.04	3	26.63	39
			3004.98	10	18.09	39
475	7509.4	19.411	90.48	17	21.90	40
			1440.41	16	30.36	40
			1510.88	3	26.63	40
			3003.80	10	18.09	40
500	7496.8	19.411	65.08	17	21.90	41
			1419.63	16	30.36	41
			1538.73	3	26.63	41
			3002.88	10	18.09	41
525	7484.2	19.411	43.01	17	21.90	42
			1399.11	16	30.36	42
			1566.59	3	26.63	42
			3002.22	10	18.09	42
550	7471.6	19.411	32.11	17	21.90	43
			1378.85	16	30.36	43
			1594.45	3	26.63	43
			3001.82	10	18.09	43
575	7459	19.411	42.17	17	21.90	44
			1358.86	16	30.36	44
			1622.31	3	26.63	44
			3001.68	10	18.09	44
600	7446.5	19.411	63.97	17	21.90	45
			1339.16	16	30.36	45
			1650.18	3	26.63	45
			3001.80	10	18.09	45
625	7433.9	19.411	89.29	17	21.90	46
			1319.76	16	30.36	46
			1678.05	3	26.63	46
			3002.19	10	18.09	46
650	7421.3	19.411	115.85	17	21.90	47
			1300.67	16	30.36	47
			1705.92	3	26.63	47
			3002.83	10	18.09	47
675	7408.7	19.411	142.95	17	21.90	48
			1281.91	16	30.36	48
			1733.80	3	26.63	48
			3003.74	10	18.09	48
700	7396.1	19.411	170.34	17	21.90	49
			1263.49	16	30.36	49
			1761.69	3	26.63	49
			3004.90	10	18.09	49
725	7383.5	19.411	197.89	17	21.90	50
			1245.43	16	30.36	50
			1789.57	3	26.63	50
			3006.33	10	18.09	50
750	7371	19.411	225.55	17	21.90	51
			1227.74	16	30.36	51
			1817.46	3	26.63	51
			3008.02	10	18.09	51
775	7358.4	19.411	253.29	17	21.90	52
			1210.44	16	30.36	52
			1845.35	3	26.63	52
			3009.96	10	18.09	52
800	7345.8	19.411	281.07	17	21.90	53
			1193.54	16	30.36	53
			1873.25	3	26.63	53
			3012.17	10	18.09	53
825	7333.2	19.411	308.89	17	21.90	54
			1177.07	16	30.36	54
			1901.14	3	26.63	54
			3014.63	10	18.09	54
850	7320.6	19.411	336.74	17	21.90	55
			1161.04	16	30.36	55
			1929.04	3	26.63	55

			976.87	6	23.78	350
			1023.08	30	29.02	350
8250	3596.8	25.175	244.30	32	30.40	351
			470.81	36	27.89	351
			978.83	6	23.78	351
			1035.25	35	25.06	351
8275	3584.2	25.175	216.88	32	30.40	352
			464.69	36	27.89	352
			981.57	6	23.78	352
			1042.18	35	25.06	352
8300	3571.6	25.175	189.62	32	30.40	353
			460.19	36	27.89	353
			985.11	6	23.78	353
			1049.82	35	25.06	353
8325	3559	25.175	162.61	32	30.40	354
			457.36	36	27.89	354
			989.42	6	23.78	354
			1058.13	35	25.06	354
8350	3546.5	25.175	136.00	32	30.40	355
			456.24	36	27.89	355
			994.50	6	23.78	355
			1067.12	35	25.06	355
8375	3533.9	25.175	110.07	32	30.40	356
			456.82	36	27.89	356
			1000.35	6	23.78	356
			1076.76	35	25.06	356
8400	3521.3	25.175	85.45	32	30.40	357
			459.12	36	27.89	357
			1006.93	6	23.78	357
			1087.04	35	25.06	357
8425	3508.7	25.175	63.67	32	30.40	358
			463.10	36	27.89	358
			1014.25	6	23.78	358
			1097.93	35	25.06	358
8450	3496.1	25.175	48.71	32	30.40	359
			468.72	36	27.89	359
			1022.27	6	23.78	359
			1109.42	35	25.06	359
8475	3483.5	25.175	47.52	32	30.40	360
			475.92	36	27.89	360
			1031.00	6	23.78	360
			1121.50	35	25.06	360
8500	3471	25.175	60.91	32	30.40	361
			484.64	36	27.89	361
			1040.41	6	23.78	361
			1134.13	35	25.06	361
8525	3458.4	25.175	82.03	32	30.40	362
			494.78	36	27.89	362
			1050.48	6	23.78	362
			1147.31	35	25.06	362
8550	3445.8	25.175	106.37	32	30.40	363
			506.27	36	27.89	363
			1061.19	6	23.78	363
			1161.01	35	25.06	363
8575	3433.2	25.175	132.16	32	30.40	364
			519.02	36	27.89	364
			1072.52	6	23.78	364
			1175.23	35	25.06	364
8600	3420.6	25.06	158.69	32	30.40	365
			532.93	36	27.89	365
			1084.46	6	23.78	365
			1175.10	34	23.20	365
8625	3408.1	25.06	185.66	32	30.40	366
			547.93	36	27.89	366
			1098.98	6	23.78	366
			1151.47	34	23.20	366
8650	3395.5	25.06	212.88	32	30.40	367
			563.91	36	27.89	367
			1110.07	6	23.78	367
			1128.05	34	23.20	367
8675	3382.9	24.898	240.29	32	30.40	368
			580.80	36	27.89	368
			1104.84	34	23.20	368
			1123.70	6	23.78	368
8700	3370.3	24.898	267.81	32	30.40	369
			598.52	36	27.89	369
			1081.85	34	23.20	369
			1137.86	6	23.78	369
8725	3357.7	27.572	295.42	32	30.40	370
			617.01	36	27.89	370
			1059.10	34	23.20	370
			1133.17	33	30.63	370
8750	3345.2	27.572	323.09	32	30.40	371
			636.19	36	27.89	371
			1036.61	34	23.20	371
			1110.49	33	30.63	371
8775	3332.8	27.572	350.82	32	30.40	372
			656.00	36	27.89	372
			1014.40	34	23.20	372
			1088.06	33	30.63	372
8800	3320	27.572	378.58	32	30.40	373
			676.39	36	27.89	373
			992.47	34	23.20	373
			1065.89	33	30.63	373
8825	3307.4	27.572	406.38	32	30.40	374
			697.31	36	27.89	374
			970.86	34	23.20	374
			1044.00	33	30.63	374
8850	3294.8	27.572	434.20	32	30.40	375
			718.71	36	27.89	375
			949.58	34	23.20	375
			1022.41	33	30.63	375
8875	3282.3	27.572	462.03	32	30.40	376
			740.55	36	27.89	376
			928.66	34	23.20	376
			1001.14	33	30.63	376
8900	3269.7	27.572	489.89	32	30.40	377
			762.79	36	27.89	377
			908.11	34	23.20	377
			980.20	33	30.63	377
8925	3257.1	27.572	517.76	32	30.40	378
			785.40	36	27.89	378
			887.98	34	23.20	378

			3017.35	10	18.09	55
875	7308.1	19.411	364.61	17	21.90	56
			1145.47	16	30.36	56
			1956.95	3	26.63	56
			3020.32	10	18.09	56
900	7295.5	19.411	392.49	17	21.90	57
			1130.37	16	30.36	57
			1984.85	3	26.63	57
			3023.56	10	18.09	57
925	7282.9	19.411	420.39	17	21.90	58
			1115.77	16	30.36	58
			2012.76	3	26.63	58
			3027.05	10	18.09	58
950	7270.3	19.411	448.30	17	21.90	59
			1101.70	16	30.36	59
			2040.67	3	26.63	59
			3030.79	10	18.09	59
975	7257.7	19.411	476.22	17	21.90	60
			1088.16	16	30.36	60
			2068.58	3	26.63	60
			3034.78	10	18.09	60
1000	7245.2	19.411	504.15	17	21.90	61
			1075.17	16	30.36	61
			2096.49	3	26.63	61
			3039.03	10	18.09	61
1025	7232.6	19.411	532.08	17	21.90	62
			1062.77	16	30.36	62
			2124.41	3	26.63	62
			3043.53	10	18.09	62
1050	7220	19.411	560.02	17	21.90	63
			1050.96	16	30.36	63
			2152.32	3	26.63	63
			3048.28	10	18.09	63
1075	7207.4	19.411	587.97	17	21.90	64
			1039.78	16	30.36	64
			2180.24	3	26.63	64
			3053.28	10	18.09	64
1100	7194.8	19.411	615.91	17	21.90	65
			1029.23	16	30.36	65
			2208.16	3	26.63	65
			3058.53	10	18.09	65
1125	7182.3	19.411	643.86	17	21.90	66
			1019.35	16	30.36	66
			2236.09	3	26.63	66
			3064.02	10	18.09	66
1150	7169.7	19.411	671.82	17	21.90	67
			1010.14	16	30.36	67
			2264.01	3	26.63	67
			3069.76	10	18.09	67
1175	7157.1	19.411	699.77	17	21.90	68
			1001.63	16	30.36	68
			2291.94	3	26.63	68
			3075.75	10	18.09	68
1200	7144.5	28.745	727.73	17	21.90	69
			993.83	16	30.36	69
			2319.86	3	26.63	69
			3072.79	28	28.77	69
1225	7131.9	28.745	755.69	17	21.90	70
			986.77	16	30.36	70
			2347.79	3	26.63	70
			3046.73	28	28.77	70
1250	7119.4	28.745	783.66	17	21.90	71
			980.46	16	30.36	71
			2375.72	3	26.63	71
			3020.71	28	28.77	71
1275	7106.8	28.745	811.62	17	21.90	72
			974.91	16	30.36	72
			2403.65	3	26.63	72
			2994.73	28	28.77	72
1300	7094.2	28.745	839.59	17	21.90	73
			970.13	16	30.36	73
			2431.58	3	26.63	73
			2968.78	28	28.77	73
1325	7081.6	28.745	867.55	17	21.90	74
			966.15	16	30.36	74
			2459.52	3	26.63	74
			2942.87	28	28.77	74
1350	7069	28.745	895.52	17	21.90	75
			962.96	16	30.36	75
			2487.45	3	26.63	75
			2916.99	28	28.77	75
1375	7056.5	28.745	923.49	17	21.90	76
			960.57	16	30.36	76
			2515.39	3	26.63	76
			2891.16	28	28.77	76
1400	7043.9	28.745	951.46	17	21.90	77
			959.00	16	30.36	77
			2543.33	3	26.63	77
			2865.37	28	28.77	77
1425	7031.3	28.745	958.24	16	30.36	78
			979.43	17	21.90	78
			2571.26	3	26.63	78
			2839.61	28	28.77	78
1450	7018.7	28.745	958.30	16	30.36	79
			1007.41	17	21.90	79
			2599.20	3	26.63	79
			2813.90	28	28.77	79
1475	7006.1	28.745	959.17	16	30.36	80
			1035.38	17	21.90	80
			2627.14	3	26.63	80
			2788.24	28	28.77	80
1500	6993.5	28.745	960.86	16	30.36	81
			1063.35	17	21.90	81
			2655.08	3	26.63	81
			2762.62	28	28.77	81
1525	6981	28.745	963.36	16	30.36	82
			1091.33	17	21.90	82
			2683.03	3	26.63	82
			2737.04	28	28.77	82
1550	6968.4	28.745	966.67	16	30.36	83
			1119.30	17	21.90	83
			2710.97	3	26.63	83
			2711.52	28	28.77	83

			959.62	33	30.63	378
8950	3244.5	27.572	545.64	32	30.40	379
			808.34	36	27.89	379
			868.27	34	23.20	379
			939.43	33	30.63	379
8975	3231.9	27.572	573.54	32	30.40	380
			831.59	36	27.89	380
			849.04	34	23.20	380
			919.64	33	30.63	380
9000	3219.4	27.572	601.44	32	30.40	381
			830.30	34	23.20	381
			855.13	36	27.89	381
			900.29	33	30.63	381
9025	3206.8	27.572	629.34	32	30.40	382
			812.10	34	23.20	382
			878.93	36	27.89	382
			881.41	33	30.63	382
9050	3194.2	28.208	657.26	32	30.40	383
			794.46	34	23.20	383
			863.01	33	30.63	383
			902.97	36	27.89	383
9075	3181.6	28.208	685.18	32	30.40	384
			777.43	34	23.20	384
			845.15	33	30.63	384
			927.23	36	27.89	384
9100	3169	28.208	713.11	32	30.40	385
			761.05	34	23.20	385
			827.84	33	30.63	385
			951.69	36	27.89	385
9125	3156.5	28.208	741.04	32	30.40	386
			745.36	34	23.20	386
			811.13	33	30.63	386
			976.35	36	27.89	386
9150	3143.9	28.208	730.41	34	23.20	387
			768.97	32	30.40	387
			795.06	33	30.63	387
			1001.18	36	27.89	387
9175	3131.3	28.208	716.24	34	23.20	388
			779.66	33	30.63	388
			796.91	32	30.40	388
			1026.17	36	27.89	388
9200	3118.7	28.208	702.89	34	23.20	389
			764.97	33	30.63	389
			824.85	32	30.40	389
			1051.31	36	27.89	389
9225	3106.1	28.208	690.43	34	23.20	390
			751.04	33	30.63	390
			852.80	32	30.40	390
			1076.59	36	27.89	390
9250	3093.5	23.314	678.89	34	23.20	391
			737.91	33	30.63	391
			880.75	32	30.40	391
			1100.90	49	22.04	391
9275	3081	23.314	668.32	34	23.20	392
			725.62	33	30.63	392
			908.70	32	30.40	392
			1075.77	49	22.04	392
9300	3068.4	23.314	658.78	34	23.20	393
			714.22	33	30.63	393
			936.65	32	30.40	393
			1050.79	49	22.04	393
9325	3055.8	23.314	650.30	34	23.20	394
			703.75	33	30.63	394
			964.60	32	30.40	394
			1025.96	49	22.04	394
9350	3043.2	23.314	642.92	34	23.20	395
			694.24	33	30.63	395
			992.56	32	30.40	395
			1001.30	49	22.04	395
9375	3030.6	28.745	636.69	34	23.20	396
			685.75	33	30.63	396
			976.82	49	22.04	396
			1020.52	32	30.40	396
9400	3018.1	28.745	631.65	34	23.20	397
			678.31	33	30.63	397
			952.53	49	22.04	397
			1048.48	32	30.40	397
9425	3005.5	28.745	627.81	34	23.20	398
			671.95	33	30.63	398
			928.44	49	22.04	398
			1076.44	32	30.40	398
9450	2992.9	28.745	625.20	34	23.20	399
			666.71	33	30.63	399
			904.59	49	22.04	399
			1104.40	32	30.40	399
9475	2980.3	28.745	623.84	34	23.20	400
			662.60	33	30.63	400
			880.97	49	22.04	400
			1132.36	32	30.40	400
9500	2967.7	28.745	623.73	34	23.20	401
			659.67	33	30.63	401
			857.62	49	22.04	401
			1160.33	32	30.40	401
9525	2955.2	28.745	624.87	34	23.20	402
			657.91	33	30.63	402
			834.56	49	22.04	402
			1188.29	32	30.40	402
9550	2942.6	28.745	627.27	34	23.20	403
			657.33	33	30.63	403
			811.80	49	22.04	403
			1216.26	32	30.40	403
9575	2930	28.745	630.89	34	23.20	404
			657.95	33	30.63	404
			789.38	49	22.04	404
			1244.23	32	30.40	404
9600	2917.4	28.745	635.73	34	23.20	405
			659.76	33	30.63	405
			767.33	49	22.04	405
			1272.20	32	30.40	405
9625	2904.8	28.745	641.76	34	23.20	406
			662.74	33	30.63	406
			745.67	49	22.04	406
			1300.16	32	30.40	406

1575	6955.8	26.027	970.77	16	30.36	84
			1147.28	17	21.90	84
			2686.04	28	28.77	84
			2738.91	3	26.63	84
1600	6943.2	26.027	975.66	16	30.36	85
			1175.25	17	21.90	85
			2660.61	28	28.77	85
			2766.86	3	26.63	85
1625	6930.6	26.027	981.32	16	30.36	86
			1203.23	17	21.90	86
			2635.24	28	28.77	86
			2794.80	3	26.63	86
1650	6918.1	26.027	987.74	16	30.36	87
			1231.21	17	21.90	87
			2609.91	28	28.77	87
			2822.75	3	26.63	87
1675	6905.5	26.027	994.91	16	30.36	88
			1259.19	17	21.90	88
			2584.65	28	28.77	88
			2850.70	3	26.63	88
1700	6892.9	26.027	1002.80	16	30.36	89
			1287.16	17	21.90	89
			2559.44	28	28.77	89
			2878.65	3	26.63	89
1725	6880.3	26.027	1011.41	16	30.36	90
			1315.14	17	21.90	90
			2534.29	28	28.77	90
			2906.60	3	26.63	90
1750	6867.7	26.027	1020.72	16	30.36	91
			1343.12	17	21.90	91
			2509.19	28	28.77	91
			2934.54	3	26.63	91
1775	6855.2	26.027	1030.70	16	30.36	92
			1371.10	17	21.90	92
			2484.16	28	28.77	92
			2962.50	3	26.63	92
1800	6842.6	26.027	1041.34	16	30.36	93
			1399.08	17	21.90	93
			2459.20	28	28.77	93
			2990.45	3	26.63	93
1825	6830	26.027	1052.82	16	30.36	94
			1427.06	17	21.90	94
			2434.30	28	28.77	94
			3018.40	3	26.63	94
1850	6817.4	26.027	1064.51	16	30.36	95
			1455.04	17	21.90	95
			2409.46	28	28.77	95
			3046.35	3	26.63	95
1875	6804.8	26.027	1077.00	16	30.36	96
			1483.02	17	21.90	96
			2384.70	28	28.77	96
			3074.30	3	26.63	96
1900	6792.3	26.027	1090.06	16	30.36	97
			1511.00	17	21.90	97
			2360.01	28	28.77	97
			3102.26	3	26.63	97
1925	6779.7	26.027	1103.66	16	30.36	98
			1538.98	17	21.90	98
			2335.39	28	28.77	98
			3130.21	3	26.63	98
1950	6767.1	26.027	1117.83	16	30.36	99
			1566.96	17	21.90	99
			2310.85	28	28.77	99
			3158.17	3	26.63	99
1975	6754.5	26.027	1132.50	16	30.36	100
			1594.94	17	21.90	100
			2286.39	28	28.77	100
			3186.12	3	26.63	100
2000	6741.9	26.027	1147.67	16	30.36	101
			1622.93	17	21.90	101
			2262.01	28	28.77	101
			3214.08	3	26.63	101
2025	6729.4	26.027	1163.30	16	30.36	102
			1650.91	17	21.90	102
			2237.72	28	28.77	102
			3242.03	3	26.63	102
2050	6716.8	26.027	1179.40	16	30.36	103
			1678.89	17	21.90	103
			2213.51	28	28.77	103
			3269.99	3	26.63	103
2075	6704.2	26.027	1195.94	16	30.36	104
			1706.87	17	21.90	104
			2189.39	28	28.77	104
			3297.95	3	26.63	104
2100	6691.6	26.027	1212.89	16	30.36	105
			1734.85	17	21.90	105
			2165.37	28	28.77	105
			3325.91	3	26.63	105
2125	6679	28.363	1230.25	16	30.36	106
			1762.84	17	21.90	106
			2141.44	28	28.77	106
			3329.08	27	28.60	106
2150	6666.5	28.363	1247.99	16	30.36	107
			1790.82	17	21.90	107
			2117.61	28	28.77	107
			3309.13	27	28.60	107
2175	6653.9	28.363	1266.11	16	30.36	108
			1818.80	17	21.90	108
			2093.89	28	28.77	108
			3289.30	27	28.60	108
2200	6641.3	28.363	1284.58	16	30.36	109
			1846.78	17	21.90	109
			2070.27	28	28.77	109
			3269.58	27	28.60	109
2225	6628.7	28.363	1303.39	16	30.36	110
			1874.77	17	21.90	110
			2046.76	28	28.77	110
			3249.98	27	28.60	110
2250	6616.1	28.363	1322.52	16	30.36	111
			1902.75	17	21.90	111
			2023.37	28	28.77	111
			3230.51	27	28.60	111
2275	6603.5	28.363	1341.96	16	30.36	112

9650	2892.3	28.745	648.93	34	23.20	407
			666.89	33	30.63	407
			724.45	49	22.04	407
			1328.13	32	30.40	407
9675	2879.7	28.745	657.22	34	23.20	408
			672.18	33	30.63	408
			703.70	49	22.04	408
			1356.10	32	30.40	408
9700	2867.1	28.745	666.59	34	23.20	409
			678.58	33	30.63	409
			683.47	49	22.04	409
			1384.08	32	30.40	409
9725	2854.5	25.272	663.80	49	22.04	410
			676.98	34	23.20	410
			686.06	33	30.63	410
			1405.38	37	24.83	410
9750	2841.9	25.272	644.75	49	22.04	411
			688.36	34	23.20	411
			694.59	33	30.63	411
			1388.72	37	24.83	411
9775	2829.4	25.272	626.37	49	22.04	412
			700.66	34	23.20	412
			704.13	33	30.63	412
			1372.42	37	24.83	412
9800	2816.8	25.272	608.72	49	22.04	413
			713.86	34	23.20	413
			714.64	33	30.63	413
			1356.51	37	24.83	413
9825	2804.2	25.272	591.87	49	22.04	414
			726.08	33	30.63	414
			727.89	34	23.20	414
			1341.00	37	24.83	414
9850	2791.6	25.272	575.88	49	22.04	415
			738.40	33	30.63	415
			742.71	34	23.20	415
			1325.89	37	24.83	415
9875	2779	24.379	560.84	49	22.04	416
			751.57	33	30.63	416
			758.27	34	23.20	416
			1301.21	56	24.83	416
9900	2766.5	24.379	546.82	49	22.04	417
			765.53	33	30.63	417
			774.54	34	23.20	417
			1273.23	56	24.83	417
9925	2753.9	24.379	533.89	49	22.04	418
			780.24	33	30.63	418
			791.46	34	23.20	418
			1245.25	56	24.83	418
9950	2741.3	24.379	522.15	49	22.04	419
			795.67	33	30.63	419
			808.99	34	23.20	419
			1217.27	56	24.83	419
9975	2728.7	24.379	511.67	49	22.04	420
			811.77	33	30.63	420
			827.10	34	23.20	420
			1189.29	56	24.83	420
10000	2716.1	24.379	502.54	49	22.04	421
			828.50	33	30.63	421
			845.75	34	23.20	421
			1161.31	56	24.83	421
10025	2703.5	24.379	494.82	49	22.04	422
			845.83	33	30.63	422
			864.90	34	23.20	422
			1133.33	56	24.83	422
10050	2691	24.379	488.58	49	22.04	423
			863.71	33	30.63	423
			884.52	34	23.20	423
			1105.36	56	24.83	423
10075	2678.4	24.379	483.88	49	22.04	424
			882.13	33	30.63	424
			904.58	34	23.20	424
			1077.38	56	24.83	424
10100	2665.8	24.379	480.77	49	22.04	425
			901.03	33	30.63	425
			925.06	34	23.20	425
			1049.40	56	24.83	425
10125	2653.2	24.379	479.28	49	22.04	426
			920.40	33	30.63	426
			945.92	34	23.20	426
			1021.43	56	24.83	426
10150	2640.6	24.379	479.42	49	22.04	427
			940.20	33	30.63	427
			967.14	34	23.20	427
			993.45	56	24.83	427
10175	2628.1	26.356	481.19	49	22.04	428
			960.41	33	30.63	428
			965.47	56	24.83	428
			988.69	34	23.20	428
10200	2615.5	26.616	484.57	49	22.04	429
			937.50	56	24.83	429
			981.00	33	30.63	429
			1006.00	53	29.18	429
10225	2602.9	29.442	489.53	49	22.04	430
			909.53	56	24.83	430
			978.07	53	29.18	430
			1001.95	33	30.63	430
10250	2590.3	29.442	496.02	49	22.04	431
			881.55	56	24.83	431
			950.14	53	29.18	431
			1023.24	33	30.63	431
10275	2577.7	29.442	503.99	49	22.04	432
			853.58	56	24.83	432
			922.21	53	29.18	432
			1044.84	33	30.63	432
10300	2565.2	29.442	513.36	49	22.04	433
			825.61	56	24.83	433
			894.29	53	29.18	433
			1066.74	33	30.63	433
10325	2552.6	29.442	524.06	49	22.04	434
			797.64	56	24.83	434
			866.38	53	29.18	434
			1088.92	33	30.63	434
10350	2540	15.682	536.00	49	22.04	435

			1930.73	17	21.90	112
			2000.09	28	28.77	112
			3211.17	27	28.60	112
2300	6591	28.363	1361.70	16	30.36	113
			1958.72	17	21.90	113
			1976.94	28	28.77	113
			3191.95	27	28.60	113
2325	6578.4	28.363	1381.73	16	30.36	114
			1953.91	28	28.77	114
			1986.70	17	21.90	114
			3172.86	27	28.60	114
2350	6565.8	28.363	1402.03	16	30.36	115
			1931.01	28	28.77	115
			2014.68	17	21.90	115
			3153.91	27	28.60	115
2375	6553.2	28.363	1422.59	16	30.36	116
			1908.25	28	28.77	116
			2042.67	17	21.90	116
			3135.09	27	28.60	116
2400	6540.6	28.363	1443.40	16	30.36	117
			1885.63	28	28.77	117
			2070.65	17	21.90	117
			3116.41	27	28.60	117
2425	6528.1	28.363	1464.45	16	30.36	118
			1863.15	28	28.77	118
			2098.63	17	21.90	118
			3097.87	27	28.60	118
2450	6515.5	28.363	1485.73	16	30.36	119
			1840.83	28	28.77	119
			2126.62	17	21.90	119
			3079.47	27	28.60	119
2475	6502.9	28.363	1507.22	16	30.36	120
			1818.66	28	28.77	120
			2154.60	17	21.90	120
			3061.22	27	28.60	120
2500	6490.3	28.363	1528.93	16	30.36	121
			1796.66	28	28.77	121
			2182.58	17	21.90	121
			3043.11	27	28.60	121
2525	6477.7	28.363	1550.84	16	30.36	122
			1774.82	28	28.77	122
			2210.57	17	21.90	122
			3025.16	27	28.60	122
2550	6465.2	28.363	1572.94	16	30.36	123
			1753.16	28	28.77	123
			2238.55	17	21.90	123
			3007.36	27	28.60	123
2575	6452.6	28.363	1595.23	16	30.36	124
			1731.68	28	28.77	124
			2266.54	17	21.90	124
			2989.71	27	28.60	124
2600	6440	28.363	1617.69	16	30.36	125
			1710.39	28	28.77	125
			2294.52	17	21.90	125
			2972.23	27	28.60	125
2625	6427.4	28.363	1640.32	16	30.36	126
			1689.29	28	28.77	126
			2322.50	17	21.90	126
			2954.90	27	28.60	126
2650	6414.8	28.363	1663.12	16	30.36	127
			1668.40	28	28.77	127
			2350.49	17	21.90	127
			2937.74	27	28.60	127
2675	6402.3	28.363	1647.71	28	28.77	128
			1686.07	16	30.36	128
			2378.47	17	21.90	128
			2920.75	27	28.60	128
2700	6389.7	28.363	1627.25	28	28.77	129
			1709.18	16	30.36	129
			2406.46	17	21.90	129
			2903.92	27	28.60	129
2725	6377.1	28.363	1607.01	28	28.77	130
			1732.42	16	30.36	130
			2434.44	17	21.90	130
			2887.28	27	28.60	130
2750	6364.5	28.363	1587.01	28	28.77	131
			1755.81	16	30.36	131
			2462.43	17	21.90	131
			2870.80	27	28.60	131
2775	6351.9	28.363	1567.25	28	28.77	132
			1779.33	16	30.36	132
			2490.41	17	21.90	132
			2854.51	27	28.60	132
2800	6339.4	28.363	1547.75	28	28.77	133
			1802.97	16	30.36	133
			2518.40	17	21.90	133
			2838.40	27	28.60	133
2825	6326.8	28.363	1528.50	28	28.77	134
			1826.74	16	30.36	134
			2546.38	17	21.90	134
			2822.47	27	28.60	134
2850	6314.2	28.363	1509.54	28	28.77	135
			1850.63	16	30.36	135
			2574.37	17	21.90	135
			2806.73	27	28.60	135
2875	6301.6	28.363	1490.85	28	28.77	136
			1874.63	16	30.36	136
			2602.35	17	21.90	136
			2791.19	27	28.60	136
2900	6289	28.363	1472.47	28	28.77	137
			1898.73	16	30.36	137
			2630.34	17	21.90	137
			2775.84	27	28.60	137
2925	6276.5	28.363	1454.38	28	28.77	138
			1922.95	16	30.36	138
			2658.32	17	21.90	138
			2760.69	27	28.60	138
2950	6263.9	28.363	1436.62	28	28.77	139
			1947.26	16	30.36	139
			2686.31	17	21.90	139
			2745.74	27	28.60	139
2975	6251.3	28.363	1419.19	28	28.77	140
			1971.68	16	30.36	140

			769.68	56	24.83	435
			838.47	53	29.18	435
			1107.37	54	9.59	435
10375	2527.4	15.682	549.12	49	22.04	436
			741.71	56	24.83	436
			810.56	53	29.18	436
			1080.92	54	9.59	436
10400	2514.8	15.682	563.32	49	22.04	437
			713.74	56	24.83	437
			782.66	53	29.18	437
			1054.54	54	9.59	437
10425	2502.3	15.682	578.53	49	22.04	438
			685.78	56	24.83	438
			754.76	53	29.18	438
			1028.25	54	9.59	438
10450	2489.7	15.682	594.66	49	22.04	439
			657.82	56	24.83	439
			726.88	53	29.18	439
			1002.05	54	9.59	439
10475	2477.1	15.682	611.66	49	22.04	440
			629.86	56	24.83	440
			699.00	53	29.18	440
			975.95	54	9.59	440
10500	2464.5	15.682	601.90	56	24.83	441
			629.43	49	22.04	441
			671.13	53	29.18	441
			949.95	54	9.59	441
10525	2451.9	15.682	573.95	56	24.83	442
			643.27	53	29.18	442
			647.93	49	22.04	442
			924.07	54	9.59	442
10550	2439.4	15.682	546.00	56	24.83	443
			615.42	53	29.18	443
			667.10	49	22.04	443
			898.32	54	9.59	443
10575	2426.8	15.682	518.05	56	24.83	444
			587.58	53	29.18	444
			686.86	49	22.04	444
			872.71	54	9.59	444
10600	2414.2	15.682	490.11	56	24.83	445
			559.76	53	29.18	445
			707.19	49	22.04	445
			847.25	54	9.59	445
10625	2401.6	15.682	462.18	56	24.83	446
			531.96	53	29.18	446
			728.02	49	22.04	446
			821.95	54	9.59	446
10650	2389	15.682	434.25	56	24.83	447
			504.18	53	29.18	447
			749.31	49	22.04	447
			796.83	54	9.59	447
10675	2376.5	15.682	406.33	56	24.83	448
			476.42	53	29.18	448
			771.04	49	22.04	448
			771.91	54	9.59	448
10700	2363.9	21.877	378.42	56	24.83	449
			448.69	53	29.18	449
			747.20	54	9.59	449
			793.16	49	22.04	449
10725	2351.3	21.877	350.52	56	24.83	450
			421.00	53	29.18	450
			722.74	54	9.59	450
			815.64	49	22.04	450
10750	2338.7	21.877	322.63	56	24.83	451
			393.34	53	29.18	451
			698.54	54	9.59	451
			838.45	49	22.04	451
10775	2326.1	21.877	294.77	56	24.83	452
			365.74	53	29.18	452
			674.63	54	9.59	452
			861.56	49	22.04	452
10800	2313.5	21.877	266.93	56	24.83	453
			338.20	53	29.18	453
			651.05	54	9.59	453
			884.96	49	22.04	453
10825	2301	21.877	239.13	56	24.83	454
			310.73	53	29.18	454
			627.83	54	9.59	454
			908.61	49	22.04	454
10850	2288.4	21.877	211.37	56	24.83	455
			283.38	53	29.18	455
			605.01	54	9.59	455
			932.51	49	22.04	455
10875	2275.8	21.877	183.68	56	24.83	456
			256.15	53	29.18	456
			582.64	54	9.59	456
			956.63	49	22.04	456
10900	2263.2	21.877	156.10	56	24.83	457
			229.11	53	29.18	457
			560.78	54	9.59	457
			980.95	49	22.04	457
10925	2250.6	21.877	128.70	56	24.83	458
			202.33	53	29.18	458
			539.49	54	9.59	458
			1005.47	49	22.04	458
10950	2238.1	21.877	101.62	56	24.83	459
			175.93	53	29.18	459
			518.83	54	9.59	459
			1030.16	49	22.04	459
10975	2225.5	21.877	75.20	56	24.83	460
			150.10	53	29.18	460
			498.88	54	9.59	460
			1055.01	49	22.04	460
11000	2212.9	21.877	50.50	56	24.83	461
			125.20	53	29.18	461
			479.75	54	9.59	461
			1080.02	49	22.04	461
11025	2200.3	21.877	31.82	56	24.83	462
			101.92	53	29.18	462
			461.51	54	9.59	462
			1105.18	49	22.04	462
11050	2187.7	21.877	32.26	56	24.83	463
			81.64	53	29.18	463

			2714.29	17	21.90	140
			2730.99	27	28.60	140
3000	6238.7	23.429	1402.09	28	28.77	141
			1996.18	16	30.36	141
			2716.46	27	28.60	141
			2742.28	17	21.90	141
3025	6226.1	23.429	1385.36	28	28.77	142
			2020.78	16	30.36	142
			2702.13	27	28.60	142
			2770.26	17	21.90	142
3050	6213.5	23.429	1368.98	28	28.77	143
			2045.46	16	30.36	143
			2688.02	27	28.60	143
			2798.25	17	21.90	143
3075	6201	23.429	1352.99	28	28.77	144
			2070.23	16	30.36	144
			2674.13	27	28.60	144
			2826.23	17	21.90	144
3100	6188.4	23.429	1337.40	28	28.77	145
			2095.08	16	30.36	145
			2660.46	27	28.60	145
			2854.22	17	21.90	145
3125	6175.8	23.429	1322.21	28	28.77	146
			2120.01	16	30.36	146
			2647.02	27	28.60	146
			2882.20	17	21.90	146
3150	6163.2	23.429	1307.45	28	28.77	147
			2145.01	16	30.36	147
			2633.80	27	28.60	147
			2910.19	17	21.90	147
3175	6150.6	23.429	1293.12	28	28.77	148
			2170.09	16	30.36	148
			2620.82	27	28.60	148
			2938.17	17	21.90	148
3200	6138.1	23.429	1279.25	28	28.77	149
			2195.23	16	30.36	149
			2608.07	27	28.60	149
			2966.16	17	21.90	149
3225	6125.5	23.429	1265.84	28	28.77	150
			2220.45	16	30.36	150
			2595.56	27	28.60	150
			2994.14	17	21.90	150
3250	6112.9	23.429	1252.91	28	28.77	151
			2245.73	16	30.36	151
			2583.30	27	28.60	151
			3022.13	17	21.90	151
3275	6100.3	27.53	1240.48	28	28.77	152
			2271.07	16	30.36	152
			2571.28	27	28.60	152
			3020.42	31	27.08	152
3300	6087.7	27.53	1228.57	28	28.77	153
			2296.47	16	30.36	153
			2559.51	27	28.60	153
			2992.46	31	27.08	153
3325	6075.2	27.53	1217.18	28	28.77	154
			2321.94	16	30.36	154
			2547.99	27	28.60	154
			2964.50	31	27.08	154
3350	6062.6	27.53	1206.33	28	28.77	155
			2347.46	16	30.36	155
			2536.73	27	28.60	155
			2936.54	31	27.08	155
3375	6050	27.53	1196.04	28	28.77	156
			2373.04	16	30.36	156
			2525.73	27	28.60	156
			2908.58	31	27.08	156
3400	6037.4	27.53	1186.31	28	28.77	157
			2398.67	16	30.36	157
			2514.99	27	28.60	157
			2880.62	31	27.08	157
3425	6024.8	27.53	1177.18	28	28.77	158
			2424.35	16	30.36	158
			2504.52	27	28.60	158
			2852.66	31	27.08	158
3450	6012.3	27.53	1168.64	28	28.77	159
			2450.08	16	30.36	159
			2494.32	27	28.60	159
			2824.70	31	27.08	159
3475	5999.7	27.53	1160.72	28	28.77	160
			2475.87	16	30.36	160
			2484.39	27	28.60	160
			2796.74	31	27.08	160
3500	5987.1	27.53	1153.42	28	28.77	161
			2474.74	27	28.60	161
			2501.70	16	30.36	161
			2768.79	31	27.08	161
3525	5974.5	27.53	1146.75	28	28.77	162
			2465.37	27	28.60	162
			2527.57	16	30.36	162
			2740.83	31	27.08	162
3550	5961.9	27.53	1140.74	28	28.77	163
			2456.28	27	28.60	163
			2553.49	16	30.36	163
			2712.88	31	27.08	163
3575	5949.4	27.53	1135.38	28	28.77	164
			2447.48	27	28.60	164
			2579.45	16	30.36	164
			2684.92	31	27.08	164
3600	5936.8	27.53	1130.69	28	28.77	165
			2438.97	27	28.60	165
			2605.46	16	30.36	165
			2656.97	31	27.08	165
3625	5924.2	30.005	1126.68	28	28.77	166
			2430.75	27	28.60	166
			2629.02	31	27.08	166
			2631.51	16	30.36	166
3650	5911.6	30.005	1123.35	28	28.77	167
			2422.83	27	28.60	167
			2601.06	31	27.08	167
			2657.59	16	30.36	167
3675	5899	30.005	1120.71	28	28.77	168
			2415.20	27	28.60	168
			2573.11	31	27.08	168

			444.29	54	9.59	463
			1130.46	49	22.04	463
11075	2175.2	21.877	51.34	56	24.83	464
			67.16	53	29.18	464
			428.21	54	9.59	464
			1155.87	49	22.04	464
11100	2162.6	21.877	62.63	53	29.18	465
			76.14	56	24.83	465
			413.40	54	9.59	465
			1181.40	49	22.04	465
11125	2150	21.877	70.00	53	29.18	466
			102.59	56	24.83	466
			400.00	54	9.59	466
			1207.03	49	22.04	466
11150	2137.4	21.877	86.28	53	29.18	467
			129.69	56	24.83	467
			388.16	54	9.59	467
			1232.77	49	22.04	467
11175	2124.8	21.877	107.50	53	29.18	468
			157.10	56	24.83	468
			378.03	54	9.59	468
			1258.60	49	22.04	468
11200	2112.3	21.877	131.28	53	29.18	469
			184.68	56	24.83	469
			369.74	54	9.59	469
			1284.53	49	22.04	469
11225	2099.7	21.877	156.45	53	29.18	470
			212.37	56	24.83	470
			363.42	54	9.59	470
			1310.54	49	22.04	470
11250	2087.1	21.877	182.45	53	29.18	471
			240.13	56	24.83	471
			359.18	54	9.59	471
			1336.62	49	22.04	471
11275	2074.5	15.149	208.96	53	29.18	472
			267.94	56	24.83	472
			357.09	54	9.59	472
			1330.08	51	14.86	472
11300	2061.9	15.149	235.82	53	29.18	473
			295.78	56	24.83	473
			357.18	54	9.59	473
			1307.61	51	14.86	473
11325	2049.4	15.149	262.91	53	29.18	474
			323.64	56	24.83	474
			359.46	54	9.59	474
			1285.35	51	14.86	474
11350	2036.8	15.149	290.17	53	29.18	475
			351.53	56	24.83	475
			363.89	54	9.59	475
			1263.33	51	14.86	475
11375	2024.2	15.149	317.55	53	29.18	476
			370.38	54	9.59	476
			379.43	56	24.83	476
			1241.54	51	14.86	476
11400	2011.6	15.149	345.04	53	29.18	477
			378.84	54	9.59	477
			407.34	56	24.83	477
			1220.01	51	14.86	477
11425	1999	15.149	372.59	53	29.18	478
			389.12	54	9.59	478
			435.26	56	24.83	478
			1198.74	51	14.86	478
11450	1986.5	15.149	400.21	53	29.18	479
			401.11	54	9.59	479
			463.19	56	24.83	479
			1177.75	51	14.86	479
11475	1973.9	15.149	414.63	54	9.59	480
			427.88	53	29.18	480
			491.13	56	24.83	480
			1157.07	51	14.86	480
11500	1961.3	15.149	429.56	54	9.59	481
			455.58	53	29.18	481
			519.07	56	24.83	481
			1136.69	51	14.86	481
11525	1948.7	15.149	445.74	54	9.59	482
			483.32	53	29.18	482
			547.01	56	24.83	482
			1116.64	51	14.86	482
11550	1936.1	15.149	463.06	54	9.59	483
			511.08	53	29.18	483
			574.96	56	24.83	483
			1096.94	51	14.86	483
11575	1923.5	15.149	481.37	54	9.59	484
			538.87	53	29.18	484
			602.92	56	24.83	484
			1077.61	51	14.86	484
11600	1911	15.149	500.59	54	9.59	485
			566.68	53	29.18	485
			630.87	56	24.83	485
			1058.67	51	14.86	485
11625	1898.4	15.149	520.60	54	9.59	486
			594.50	53	29.18	486
			658.83	56	24.83	486
			1040.13	51	14.86	486
11650	1885.8	15.149	541.31	54	9.59	487
			622.34	53	29.18	487
			686.79	56	24.83	487
			1022.02	51	14.86	487
11675	1873.2	15.149	562.66	54	9.59	488
			650.19	53	29.18	488
			714.76	56	24.83	488
			1004.37	51	14.86	488
11700	1860.6	15.149	584.57	54	9.59	489
			678.06	53	29.18	489
			742.72	56	24.83	489
			987.19	51	14.86	489
11725	1848.1	15.149	606.97	54	9.59	490
			705.93	53	29.18	490
			770.69	56	24.83	490
			970.52	51	14.86	490
11750	1835.5	15.149	629.83	54	9.59	491
			733.81	53	29.18	491
			798.66	56	24.83	491

			2683.71	16	30.36	168
3700	5886.5	30.005	1118.76	28	28.77	169
			2407.88	27	28.60	169
			2545.16	31	27.08	169
			2709.88	16	30.36	169
3725	5873.9	30.005	1117.51	28	28.77	170
			2400.86	27	28.60	170
			2517.21	31	27.08	170
			2736.07	16	30.36	170
3750	5861.3	30.005	1116.96	28	28.77	171
			2394.15	27	28.60	171
			2489.26	31	27.08	171
			2762.30	16	30.36	171
3775	5848.7	30.005	1117.12	28	28.77	172
			2387.74	27	28.60	172
			2461.31	31	27.08	172
			2788.57	16	30.36	172
3800	5836.1	30.005	1117.97	28	28.77	173
			2381.65	27	28.60	173
			2433.37	31	27.08	173
			2814.87	16	30.36	173
3825	5823.5	30.005	1119.52	28	28.77	174
			2375.87	27	28.60	174
			2405.42	31	27.08	174
			2841.20	16	30.36	174
3850	5811	30.005	1121.77	28	28.77	175
			2370.41	27	28.60	175
			2377.47	31	27.08	175
			2867.57	16	30.36	175
3875	5798.4	30.005	1124.71	28	28.77	176
			2349.53	31	27.08	176
			2365.27	27	28.60	176
			2893.96	16	30.36	176
3900	5785.8	30.005	1128.34	28	28.77	177
			2321.59	31	27.08	177
			2360.44	27	28.60	177
			2920.38	16	30.36	177
3925	5773.2	30.005	1132.64	28	28.77	178
			2293.64	31	27.08	178
			2355.94	27	28.60	178
			2946.83	16	30.36	178
3950	5760.6	27.886	1137.62	28	28.77	179
			2265.70	31	27.08	179
			2351.77	27	28.60	179
			2949.84	29	27.83	179
3975	5748.1	27.886	1143.27	28	28.77	180
			2237.76	31	27.08	180
			2347.92	27	28.60	180
			2924.16	29	27.83	180
4000	5735.5	27.886	1149.56	28	28.77	181
			2209.82	31	27.08	181
			2344.39	27	28.60	181
			2898.52	29	27.83	181
4025	5722.9	27.886	1156.50	28	28.77	182
			2181.38	31	27.08	182
			2341.20	27	28.60	182
			2872.92	29	27.83	182
4050	5710.3	27.886	1164.08	28	28.77	183
			2153.95	31	27.08	183
			2338.34	27	28.60	183
			2847.38	29	27.83	183
4075	5697.7	27.886	1172.27	28	28.77	184
			2126.01	31	27.08	184
			2335.81	27	28.60	184
			2821.87	29	27.83	184
4100	5685.2	27.886	1181.07	28	28.77	185
			2098.08	31	27.08	185
			2333.61	27	28.60	185
			2796.42	29	27.83	185
4125	5672.6	27.886	1190.46	28	28.77	186
			2070.15	31	27.08	186
			2331.75	27	28.60	186
			2771.01	29	27.83	186
4150	5660	27.886	1200.43	28	28.77	187
			2042.21	31	27.08	187
			2330.22	27	28.60	187
			2745.66	29	27.83	187
4175	5647.4	27.886	1210.96	28	28.77	188
			2014.29	31	27.08	188
			2329.03	27	28.60	188
			2720.35	29	27.83	188
4200	5634.8	27.886	1222.05	28	28.77	189
			1986.36	31	27.08	189
			2328.17	27	28.60	189
			2695.10	29	27.83	189
4225	5622.3	27.886	1233.67	28	28.77	190
			1958.43	31	27.08	190
			2327.65	27	28.60	190
			2669.90	29	27.83	190
4250	5609.7	27.886	1245.81	28	28.77	191
			1930.51	31	27.08	191
			2327.46	27	28.60	191
			2644.76	29	27.83	191
4275	5597.1	27.886	1258.46	28	28.77	192
			1902.58	31	27.08	192
			2327.61	27	28.60	192
			2619.68	29	27.83	192
4300	5584.5	27.886	1271.59	28	28.77	193
			1874.66	31	27.08	193
			2328.10	27	28.60	193
			2594.65	29	27.83	193
4325	5571.9	27.886	1285.21	28	28.77	194
			1846.75	31	27.08	194
			2328.93	27	28.60	194
			2569.69	29	27.83	194
4350	5559.4	27.886	1299.28	28	28.77	195
			1818.83	31	27.08	195
			2330.09	27	28.60	195
			2544.79	29	27.83	195
4375	5546.8	27.886	1313.80	28	28.77	196
			1790.91	31	27.08	196
			2331.58	27	28.60	196
			2519.96	29	27.83	196

			954.38	51	14.86	491
11775	1822.9	15.149	653.08	54	9.59	492
			761.70	53	29.18	492
			826.63	56	24.83	492
			938.79	51	14.86	492
11800	1810.3	15.149	676.69	54	9.59	493
			789.60	53	29.18	493
			854.60	56	24.83	493
			923.79	51	14.86	493
11825	1797.7	15.149	700.63	54	9.59	494
			817.50	53	29.18	494
			882.57	56	24.83	494
			909.41	51	14.86	494
11850	1785.2	23.841	724.85	54	9.59	495
			845.41	53	29.18	495
			895.66	51	14.86	495
			910.54	56	24.83	495
11875	1772.6	23.841	749.34	54	9.59	496
			873.32	53	29.18	496
			882.59	51	14.86	496
			938.51	56	24.83	496
11900	1760	23.841	774.06	54	9.59	497
			870.23	51	14.86	497
			901.24	53	29.18	497
			966.49	56	24.83	497
11925	1747.4	23.841	799.00	54	9.59	498
			858.60	51	14.86	498
			929.16	53	29.18	498
			994.46	56	24.83	498
11950	1734.8	15.544	824.14	54	9.59	499
			847.73	51	14.86	499
			957.08	53	29.18	499
			1013.58	55	15.61	499
11975	1722.3	15.544	837.66	51	14.86	500
			849.45	54	9.59	500
			985.01	53	29.18	500
			989.38	55	15.61	500
12000	1709.7	16.228	828.41	51	14.86	501
			874.93	54	9.59	501
			965.39	55	15.61	501
			992.71	52	18.56	501
12025	1697.1	16.228	820.02	51	14.86	502
			900.56	54	9.59	502
			941.61	55	15.61	502
			968.31	52	18.56	502
12050	1684.5	16.228	812.50	51	14.86	503
			918.07	55	15.61	503
			926.32	54	9.59	503
			944.12	52	18.56	503
12075	1671.9	11.198	805.88	51	14.86	504
			894.79	55	15.61	504
			920.13	52	18.56	504
			952.21	54	9.59	504
12100	1659.4	11.198	800.19	51	14.86	505
			871.78	55	15.61	505
			896.39	52	18.56	505
			978.21	54	9.59	505
12125	1646.8	11.198	795.44	51	14.86	506
			849.08	55	15.61	506
			872.89	52	18.56	506
			1004.32	54	9.59	506
12150	1634.2	11.198	791.66	51	14.86	507
			826.69	55	15.61	507
			849.66	52	18.56	507
			1030.53	54	9.59	507
12175	1621.6	11.198	788.85	51	14.86	508
			804.66	55	15.61	508
			826.73	52	18.56	508
			1056.83	54	9.59	508
12200	1609	11.198	783.01	55	15.61	509
			787.02	51	14.86	509
			804.12	52	18.56	509
			1083.21	54	9.59	509
12225	1596.5	11.198	761.77	55	15.61	510
			781.86	52	18.56	510
			786.19	51	14.86	510
			1109.67	54	9.59	510
12250	1583.9	11.198	740.98	55	15.61	511
			759.97	52	18.56	511
			786.36	51	14.86	511
			1136.21	54	9.59	511
12275	1571.3	11.198	720.68	55	15.61	512
			738.50	52	18.56	512
			787.52	51	14.86	512
			1162.81	54	9.59	512
12300	1558.7	11.198	700.91	55	15.61	513
			717.48	52	18.56	513
			789.67	51	14.86	513
			1189.48	54	9.59	513
12325	1546.1	11.198	681.71	55	15.61	514
			696.94	52	18.56	514
			792.80	51	14.86	514
			1216.21	54	9.59	514
12350	1533.5	16.483	663.14	55	15.61	515
			676.95	52	18.56	515
			796.90	51	14.86	515
			1234.77	57	16.60	515
12375	1521	16.483	645.25	55	15.61	516
			657.53	52	18.56	516
			801.96	51	14.86	516
			1223.59	57	16.60	516
12400	1508.4	16.483	628.09	55	15.61	517
			638.75	52	18.56	517
			807.96	51	14.86	517
			1212.94	57	16.60	517
12425	1495.8	16.483	611.74	55	15.61	518
			620.67	52	18.56	518
			814.88	51	14.86	518
			1202.85	57	16.60	518
12450	1483.2	16.483	596.25	55	15.61	519
			603.34	52	18.56	519
			822.69	51	14.86	519
			1193.34	57	16.60	519

4400	5534.2	27.886	1328.74	28	28.77	197
			1763.00	31	27.08	197
			2333.41	27	28.60	197
			2495.19	29	27.83	197
4425	5521.6	27.886	1344.11	28	28.77	198
			1735.09	31	27.08	198
			2335.58	27	28.60	198
			2470.49	29	27.83	198
4450	5509	27.886	1359.88	28	28.77	199
			1707.19	31	27.08	199
			2338.07	27	28.60	199
			2445.86	29	27.83	199
4475	5496.5	27.886	1376.03	28	28.77	200
			1679.28	31	27.08	200
			2340.90	27	28.60	200
			2421.31	29	27.83	200
4500	5483.9	27.886	1392.57	28	28.77	201
			1651.38	31	27.08	201
			2344.06	27	28.60	201
			2396.82	29	27.83	201
4525	5471.3	27.886	1409.46	28	28.77	202
			1623.48	31	27.08	202
			2347.55	27	28.60	202
			2372.42	29	27.83	202
4550	5458.7	28.471	1426.70	28	28.77	203
			1595.59	31	27.08	203
			2348.10	29	27.83	203
			2351.37	27	28.60	203
4575	5446.1	28.471	1444.28	28	28.77	204
			1567.69	31	27.08	204
			2323.86	29	27.83	204
			2355.51	27	28.60	204
4600	5433.5	28.471	1462.18	28	28.77	205
			1539.80	31	27.08	205
			2299.70	29	27.83	205
			2359.98	27	28.60	205
4625	5421	28.471	1480.40	28	28.77	206
			1511.92	31	27.08	206
			2275.64	29	27.83	206
			2364.77	27	28.60	206
4650	5408.4	28.471	1484.04	31	27.08	207
			1498.92	28	28.77	207
			2251.66	29	27.83	207
			2369.89	27	28.60	207
4675	5395.8	28.471	1456.16	31	27.08	208
			1517.72	28	28.77	208
			2227.78	29	27.83	208
			2375.32	27	28.60	208
4700	5383.2	28.471	1428.29	31	27.08	209
			1536.81	28	28.77	209
			2203.99	29	27.83	209
			2381.07	27	28.60	209
4725	5370.6	28.471	1400.42	31	27.08	210
			1556.17	28	28.77	210
			2180.30	29	27.83	210
			2387.13	27	28.60	210
4750	5358.1	28.471	1372.56	31	27.08	211
			1575.78	28	28.77	211
			2156.72	29	27.83	211
			2393.50	27	28.60	211
4775	5345.5	28.471	1344.70	31	27.08	212
			1595.65	28	28.77	212
			2133.24	29	27.83	212
			2400.18	27	28.60	212
4800	5332.9	28.471	1316.84	31	27.08	213
			1615.75	28	28.77	213
			2109.87	29	27.83	213
			2407.17	27	28.60	213
4825	5320.3	28.471	1289.00	31	27.08	214
			1636.09	28	28.77	214
			2086.62	29	27.83	214
			2414.47	27	28.60	214
4850	5307.7	28.471	1261.16	31	27.08	215
			1656.65	28	28.77	215
			2063.48	29	27.83	215
			2422.06	27	28.60	215
4875	5295.2	28.471	1233.32	31	27.08	216
			1677.43	28	28.77	216
			2040.47	29	27.83	216
			2429.96	27	28.60	216
4900	5282.6	28.471	1205.49	31	27.08	217
			1698.41	28	28.77	217
			2017.58	29	27.83	217
			2438.15	27	28.60	217
4925	5270	28.471	1177.67	31	27.08	218
			1719.59	28	28.77	218
			1994.82	29	27.83	218
			2446.63	27	28.60	218
4950	5257.4	28.471	1149.86	31	27.08	219
			1740.97	28	28.77	219
			1972.19	29	27.83	219
			2455.40	27	28.60	219
4975	5244.8	28.471	1122.06	31	27.08	220
			1762.53	28	28.77	220
			1949.71	29	27.83	220
			2464.46	27	28.60	220
5000	5232.3	28.471	1094.27	31	27.08	221
			1784.26	28	28.77	221
			1927.37	29	27.83	221
			2473.80	27	28.60	221
5025	5219.7	28.471	1066.48	31	27.08	222
			1806.17	28	28.77	222
			1905.17	29	27.83	222
			2483.43	27	28.60	222
5050	5207.1	28.471	1038.71	31	27.08	223
			1828.25	28	28.77	223
			1883.14	29	27.83	223
			2493.33	27	28.60	223
5075	5194.5	28.471	1010.95	31	27.08	224
			1850.49	28	28.77	224
			1861.26	29	27.83	224
			2503.50	27	28.60	224
5100	5181.9	28.471	983.20	31	27.08	225

12475	1470.6	16.483	581.70	55	15.61	520
			586.83	52	18.56	520
			831.37	51	14.86	520
			1184.40	57	16.60	520
12500	1458.1	16.483	568.15	55	15.61	521
			571.22	52	18.56	521
			840.89	51	14.86	521
			1176.07	57	16.60	521
12525	1445.5	16.483	555.69	55	15.61	522
			556.59	52	18.56	522
			851.23	51	14.86	522
			1168.35	57	16.60	522
12550	1432.9	16.483	543.00	52	18.56	523
			544.37	55	15.61	523
			862.35	51	14.86	523
			1161.25	57	16.60	523
12575	1420.3	16.483	530.53	52	18.56	524
			534.29	55	15.61	524
			874.22	51	14.86	524
			1154.78	57	16.60	524
12600	1407.7	16.483	519.28	52	18.56	525
			525.51	55	15.61	525
			886.82	51	14.86	525
			1148.96	57	16.60	525
12625	1395.2	16.483	509.33	52	18.56	526
			518.09	55	15.61	526
			900.12	51	14.86	526
			1143.80	57	16.60	526
12650	1382.6	16.483	500.74	52	18.56	527
			512.09	55	15.61	527
			914.08	51	14.86	527
			1139.30	57	16.60	527
12675	1370	16.483	493.58	52	18.56	528
			507.57	55	15.61	528
			928.67	51	14.86	528
			1135.47	57	16.60	528
12700	1357.4	16.483	487.94	52	18.56	529
			504.56	55	15.61	529
			943.86	51	14.86	529
			1132.33	57	16.60	529
12725	1344.8	16.367	483.84	52	18.56	530
			503.09	55	15.61	530
			959.64	51	14.86	530
			1122.98	62	16.21	530
12750	1332.3	16.367	481.34	52	18.56	531
			503.18	55	15.61	531
			975.96	51	14.86	531
			1095.00	62	16.21	531
12775	1319.7	16.367	480.47	52	18.56	532
			504.82	55	15.61	532
			992.80	51	14.86	532
			1067.01	62	16.21	532
12800	1307.1	16.367	481.22	52	18.56	533
			508.01	55	15.61	533
			1010.13	51	14.86	533
			1039.03	62	16.21	533
12825	1294.5	15.787	483.59	52	18.56	534
			512.70	55	15.61	534
			1011.05	62	16.21	534
			1027.94	51	14.86	534
12850	1281.9	15.787	487.56	52	18.56	535
			518.86	55	15.61	535
			983.07	62	16.21	535
			1046.19	51	14.86	535
12875	1269.4	15.787	493.09	52	18.56	536
			526.44	55	15.61	536
			955.08	62	16.21	536
			1064.86	51	14.86	536
12900	1256.8	15.787	500.12	52	18.56	537
			535.37	55	15.61	537
			927.10	62	16.21	537
			1083.94	51	14.86	537
12925	1244.2	15.787	508.60	52	18.56	538
			545.60	55	15.61	538
			899.12	62	16.21	538
			1103.39	51	14.86	538
12950	1231.6	15.787	518.46	52	18.56	539
			557.05	55	15.61	539
			871.14	62	16.21	539
			1123.21	51	14.86	539
12975	1219	16.665	529.61	52	18.56	540
			569.64	55	15.61	540
			843.16	62	16.21	540
			1143.25	57	16.60	540
13000	1206.5	16.665	541.98	52	18.56	541
			583.30	55	15.61	541
			815.18	62	16.21	541
			1148.34	57	16.60	541
13025	1193.9	16.665	555.48	52	18.56	542
			597.97	55	15.61	542
			787.20	62	16.21	542
			1154.08	57	16.60	542
13050	1181.3	16.665	570.04	52	18.56	543
			613.56	55	15.61	543
			759.22	62	16.21	543
			1160.47	57	16.60	543
13075	1168.7	16.665	585.58	52	18.56	544
			630.00	55	15.61	544
			731.24	62	16.21	544
			1167.50	57	16.60	544
13100	1156.1	16.665	602.02	52	18.56	545
			647.24	55	15.61	545
			703.26	62	16.21	545
			1175.15	57	16.60	545
13125	1143.5	16.665	619.28	52	18.56	546
			665.22	55	15.61	546
			675.28	62	16.21	546
			1183.42	57	16.60	546
13150	1131	16.665	637.31	52	18.56	547
			647.30	62	16.21	547
			683.86	55	15.61	547
			1192.28	57	16.60	547
13175	1118.4	16.665	619.33	62	16.21	548

			1839.55	29	27.83	225
			1872.88	28	28.77	225
			2513.94	27	28.60	225
5125	5169.4	28.471	955.47	31	27.08	226
			1818.01	29	27.83	226
			1895.42	28	28.77	226
			2524.66	27	28.60	226
5150	5156.8	28.471	927.75	31	27.08	227
			1796.64	29	27.83	227
			1918.10	28	28.77	227
			2535.63	27	28.60	227
5175	5144.2	28.471	900.05	31	27.08	228
			1775.46	29	27.83	228
			1940.92	28	28.77	228
			2546.86	27	28.60	228
5200	5131.6	28.471	872.36	31	27.08	229
			1754.48	29	27.83	229
			1963.87	28	28.77	229
			2558.36	27	28.60	229
5225	5119	28.593	844.70	31	27.08	230
			1733.69	29	27.83	230
			1986.96	28	28.77	230
			2538.78	30	29.02	230
5250	5106.5	28.593	817.06	31	27.08	231
			1713.10	29	27.83	231
			2010.17	28	28.77	231
			2511.42	30	29.02	231
5275	5093.9	28.593	789.44	31	27.08	232
			1692.73	29	27.83	232
			2033.49	28	28.77	232
			2484.07	30	29.02	232
5300	5081.3	28.593	761.85	31	27.08	233
			1672.57	29	27.83	233
			2056.94	28	28.77	233
			2456.73	30	29.02	233
5325	5068.7	28.593	734.29	31	27.08	234
			1652.65	29	27.83	234
			2080.50	28	28.77	234
			2429.41	30	29.02	234
5350	5056.1	28.593	706.76	31	27.08	235
			1632.96	29	27.83	235
			2104.16	28	28.77	235
			2402.10	30	29.02	235
5375	5043.5	28.593	679.27	31	27.08	236
			1613.52	29	27.83	236
			2127.93	28	28.77	236
			2374.81	30	29.02	236
5400	5031	28.593	651.82	31	27.08	237
			1594.33	29	27.83	237
			2151.80	28	28.77	237
			2347.54	30	29.02	237
5425	5018.4	28.593	624.42	31	27.08	238
			1575.40	29	27.83	238
			2175.77	28	28.77	238
			2320.28	30	29.02	238
5450	5005.8	28.593	597.08	31	27.08	239
			1556.75	29	27.83	239
			2199.84	28	28.77	239
			2293.04	30	29.02	239
5475	4993.2	28.593	569.79	31	27.08	240
			1538.38	29	27.83	240
			2223.99	28	28.77	240
			2265.82	30	29.02	240
5500	4980.6	28.48	542.58	31	27.08	241
			1520.31	29	27.83	241
			2238.61	30	29.02	241
			2248.24	28	28.77	241
5525	4968.1	28.48	515.46	31	27.08	242
			1502.54	29	27.83	242
			2211.43	30	29.02	242
			2272.57	28	28.77	242
5550	4955.5	28.48	488.42	31	27.08	243
			1485.08	29	27.83	243
			2184.27	30	29.02	243
			2296.99	28	28.77	243
5575	4942.9	28.48	461.51	31	27.08	244
			1467.95	29	27.83	244
			2157.13	30	29.02	244
			2321.48	28	28.77	244
5600	4930.3	28.48	434.73	31	27.08	245
			1451.15	29	27.83	245
			2130.01	30	29.02	245
			2346.05	28	28.77	245
5625	4917.7	28.48	408.11	31	27.08	246
			1434.71	29	27.83	246
			2102.91	30	29.02	246
			2370.70	28	28.77	246
5650	4905.2	28.48	381.68	31	27.08	247
			1418.63	29	27.83	247
			2075.84	30	29.02	247
			2395.43	28	28.77	247
5675	4892.6	28.48	355.50	31	27.08	248
			1402.92	29	27.83	248
			2048.79	30	29.02	248
			2420.22	28	28.77	248
5700	4880	28.48	329.61	31	27.08	249
			1387.60	29	27.83	249
			2021.76	30	29.02	249
			2445.08	28	28.77	249
5725	4867.4	28.48	304.09	31	27.08	250
			1372.67	29	27.83	250
			1994.77	30	29.02	250
			2470.01	28	28.77	250
5750	4854.8	28.48	279.05	31	27.08	251
			1358.17	29	27.83	251
			1967.80	30	29.02	251
			2495.01	28	28.77	251
5775	4842.3	28.48	254.62	31	27.08	252
			1344.08	29	27.83	252
			1940.86	30	29.02	252
			2520.06	28	28.77	252
5800	4829.7	28.48	231.00	31	27.08	253
			1330.44	29	27.83	253

			656.04	52	18.56	548
			703.13	55	15.61	548
			1201.73	57	16.60	548
13200	1105.8	16.665	591.35	62	16.21	549
			675.41	52	18.56	549
			722.96	55	15.61	549
			1211.75	57	16.60	549
13225	1093.2	16.665	563.38	62	16.21	550
			695.36	52	18.56	550
			743.32	55	15.61	550
			1222.34	57	16.60	550
13250	1080.6	16.665	535.41	62	16.21	551
			715.85	52	18.56	551
			764.16	55	15.61	551
			1233.46	57	16.60	551
13275	1068.1	16.665	507.44	62	16.21	552
			736.84	52	18.56	552
			785.45	55	15.61	552
			1245.12	57	16.60	552
13300	1055.5	28.942	479.47	62	16.21	553
			758.28	52	18.56	553
			807.15	55	15.61	553
			1253.92	60	32.00	553
13325	1042.9	28.942	451.50	62	16.21	554
			780.13	52	18.56	554
			829.22	55	15.61	554
			1256.65	60	32.00	554
13350	1030.3	28.942	423.54	62	16.21	555
			802.37	52	18.56	555
			851.64	55	15.61	555
			1259.98	60	32.00	555
13375	1017.7	28.942	395.58	62	16.21	556
			824.95	52	18.56	556
			874.38	55	15.61	556
			1263.93	60	32.00	556
13400	1005.2	28.942	367.62	62	16.21	557
			847.86	52	18.56	557
			897.42	55	15.61	557
			1268.49	60	32.00	557
13425	992.58	28.942	339.67	62	16.21	558
			871.06	52	18.56	558
			920.73	55	15.61	558
			1273.64	60	32.00	558
13450	980	28.942	311.72	62	16.21	559
			894.54	52	18.56	559
			944.30	55	15.61	559
			1279.38	60	32.00	559
13475	967.42	28.942	283.79	62	16.21	560
			918.27	52	18.56	560
			968.10	55	15.61	560
			1285.71	60	32.00	560
13500	954.84	28.942	255.86	62	16.21	561
			942.23	52	18.56	561
			992.12	55	15.61	561
			1292.62	60	32.00	561
13525	942.26	28.942	227.95	62	16.21	562
			966.41	52	18.56	562
			1016.34	55	15.61	562
			1300.09	60	32.00	562
13550	929.68	28.942	200.06	62	16.21	563
			990.79	52	18.56	563
			1040.76	55	15.61	563
			1308.11	60	32.00	563
13575	917.1	28.942	172.20	62	16.21	564
			1015.36	52	18.56	564
			1065.34	55	15.61	564
			1316.68	60	32.00	564
13600	904.52	28.942	144.39	62	16.21	565
			1040.10	52	18.56	565
			1090.10	55	15.61	565
			1325.79	60	32.00	565
13625	891.94	28.942	116.67	62	16.21	566
			1065.00	52	18.56	566
			1115.00	55	15.61	566
			1335.42	60	32.00	566
13650	879.35	28.942	89.11	62	16.21	567
			1090.05	52	18.56	567
			1140.05	55	15.61	567
			1345.57	60	32.00	567
13675	866.77	28.942	61.94	62	16.21	568
			1115.24	52	18.56	568
			1165.23	55	15.61	568
			1356.22	60	32.00	568
13700	854.19	28.942	36.05	62	16.21	569
			1140.56	52	18.56	569
			1190.54	55	15.61	569
			1367.35	60	32.00	569
13725	841.81	28.942	18.11	62	16.21	570
			1166.00	52	18.56	570
			1215.96	55	15.61	570
			1378.97	60	32.00	570
13750	829.03	28.942	30.39	62	16.21	571
			1191.56	52	18.56	571
			1241.50	55	15.61	571
			1391.05	60	32.00	571
13775	816.45	25.276	55.54	62	16.21	572
			1217.22	52	18.56	572
			1267.14	55	15.61	572
			1396.94	59	29.00	572
13800	803.87	25.276	82.54	62	16.21	573
			1242.99	52	18.56	573
			1292.87	55	15.61	573
			1372.70	59	29.00	573
13825	791.29	25.276	110.04	62	16.21	574
			1268.85	52	18.56	574
			1318.70	55	15.61	574
			1348.62	59	29.00	574
13850	778.71	17.53	137.73	62	16.21	575
			1294.79	52	18.56	575
			1324.68	59	29.00	575
			1344.61	55	15.61	575
13875	766.13	17.53	165.52	62	16.21	576
			1300.91	59	29.00	576

			1913.95	30	29.02	253
			2545.18	28	28.77	253
5825	4817.1	28.48	208.48	31	27.08	254
			1317.25	29	27.83	254
			1887.07	30	29.02	254
			2570.36	28	28.77	254
5850	4804.5	31.135	187.40	31	27.08	255
			1304.53	29	27.83	255
			1860.22	30	29.02	255
			2584.52	47	31.89	255
5875	4791.9	31.135	188.37	31	27.08	256
			1292.28	29	27.83	256
			1833.41	30	29.02	256
			2572.11	47	31.89	256
5900	4779.4	31.135	152.13	31	27.08	257
			1280.54	29	27.83	257
			1806.63	30	29.02	257
			2559.95	47	31.89	257
5925	4766.8	31.135	139.67	31	27.08	258
			1269.30	29	27.83	258
			1779.89	30	29.02	258
			2548.03	47	31.89	258
5950	4754.2	31.135	132.05	31	27.08	259
			1258.58	29	27.83	259
			1753.19	30	29.02	259
			2536.37	47	31.89	259
5975	4741.6	25.837	130.12	31	27.08	260
			1248.40	29	27.83	260
			1726.53	30	29.02	260
			2513.72	35	25.06	260
6000	4729	25.837	134.14	31	27.08	261
			1238.77	29	27.83	261
			1699.91	30	29.02	261
			2488.09	35	25.06	261
6025	4716.5	25.837	143.60	31	27.08	262
			1229.70	29	27.83	262
			1673.34	30	29.02	262
			2462.52	35	25.06	262
6050	4703.9	25.837	157.54	31	27.08	263
			1221.20	29	27.83	263
			1646.81	30	29.02	263
			2437.01	35	25.06	263
6075	4691.3	25.837	174.87	31	27.08	264
			1213.29	29	27.83	264
			1620.34	30	29.02	264
			2411.54	35	25.06	264
6100	4678.7	25.837	194.70	31	27.08	265
			1205.98	29	27.83	265
			1593.91	30	29.02	265
			2386.14	35	25.06	265
6125	4666.1	25.837	216.34	31	27.08	266
			1199.27	29	27.83	266
			1567.54	30	29.02	266
			2360.79	35	25.06	266
6150	4653.5	25.837	239.30	31	27.08	267
			1193.19	29	27.83	267
			1541.23	30	29.02	267
			2335.50	35	25.06	267
6175	4641	25.837	263.23	31	27.08	268
			1187.73	29	27.83	268
			1514.98	30	29.02	268
			2310.28	35	25.06	268
6200	4628.4	25.837	287.90	31	27.08	269
			1182.91	29	27.83	269
			1488.78	30	29.02	269
			2285.12	35	25.06	269
6225	4615.8	25.837	313.12	31	27.08	270
			1178.74	29	27.83	270
			1462.66	30	29.02	270
			2260.03	35	25.06	270
6250	4603.2	25.837	338.78	31	27.08	271
			1175.22	29	27.83	271
			1438.61	30	29.02	271
			2235.00	35	25.06	271
6275	4590.6	25.837	364.78	31	27.08	272
			1172.35	29	27.83	272
			1410.63	30	29.02	272
			2210.05	35	25.06	272
6300	4578.1	25.837	391.06	31	27.08	273
			1170.15	29	27.83	273
			1384.73	30	29.02	273
			2185.17	35	25.06	273
6325	4565.5	25.837	417.56	31	27.08	274
			1168.61	29	27.83	274
			1358.91	30	29.02	274
			2160.36	35	25.06	274
6350	4552.9	25.837	444.24	31	27.08	275
			1167.75	29	27.83	275
			1333.18	30	29.02	275
			2135.64	35	25.06	275
6375	4540.3	25.837	471.07	31	27.08	276
			1167.55	29	27.83	276
			1307.54	30	29.02	276
			2110.99	35	25.06	276
6400	4527.7	25.837	498.03	31	27.08	277
			1168.02	29	27.83	277
			1282.00	30	29.02	277
			2086.43	35	25.06	277
6425	4515.2	25.837	525.10	31	27.08	278
			1169.17	29	27.83	278
			1256.56	30	29.02	278
			2061.96	35	25.06	278
6450	4502.6	25.837	552.26	31	27.08	279
			1170.98	29	27.83	279
			1231.23	30	29.02	279
			2037.58	35	25.06	279
6475	4490	25.837	579.50	31	27.08	280
			1173.46	29	27.83	280
			1206.03	30	29.02	280
			2013.29	35	25.06	280
6500	4477.4	25.837	606.80	31	27.08	281
			1176.59	29	27.83	281
			1180.94	30	29.02	281

			1320.82	52	18.56	576
			1370.61	55	15.61	576
13900	753.55	17.53	193.37	62	16.21	577
			1277.31	59	29.00	577
			1346.93	52	18.56	577
			1396.68	55	15.61	577
13925	740.97	17.53	221.25	62	16.21	578
			1253.89	59	29.00	578
			1373.11	52	18.56	578
			1422.83	55	15.61	578
13950	728.39	17.53	249.16	62	16.21	579
			1230.66	59	29.00	579
			1399.36	52	18.56	579
			1449.04	55	15.61	579
13975	715.81	17.53	277.08	62	16.21	580
			1207.63	59	29.00	580
			1425.68	52	18.56	580
			1475.32	55	15.61	580
14000	703.23	17.53	305.02	62	16.21	581
			1184.81	59	29.00	581
			1452.06	52	18.56	581
			1501.66	55	15.61	581
14025	690.65	17.53	332.96	62	16.21	582
			1162.23	59	29.00	582
			1478.50	52	18.56	582
			1528.06	55	15.61	582
14050	678.06	15.881	360.91	62	16.21	583
			1139.88	59	29.00	583
			1505.00	52	18.56	583
			1552.58	63	12.54	583
14075	665.48	18.385	388.87	62	16.21	584
			1117.78	59	29.00	584
			1525.00	63	12.54	584
			1531.55	52	18.56	584
14100	652.9	18.385	416.83	62	16.21	585
			1095.95	59	29.00	585
			1497.44	63	12.54	585
			1558.14	52	18.56	585
14125	640.32	18.385	444.79	62	16.21	586
			1074.41	59	29.00	586
			1469.90	63	12.54	586
			1584.79	52	18.56	586
14150	627.74	18.385	472.76	62	16.21	587
			1053.18	59	29.00	587
			1442.37	63	12.54	587
			1611.48	52	18.56	587
14175	615.16	18.385	500.72	62	16.21	588
			1032.26	59	29.00	588
			1414.86	63	12.54	588
			1638.22	52	18.56	588
14200	602.58	18.385	528.69	62	16.21	589
			1011.69	59	29.00	589
			1387.37	63	12.54	589
			1665.00	52	18.56	589
14225	590	18.385	556.67	62	16.21	590
			991.48	59	29.00	590
			1359.90	63	12.54	590
			1691.81	52	18.56	590
14250	577.42	29.785	584.64	62	16.21	591
			971.65	59	29.00	591
			1332.45	63	12.54	591
			1712.69	60	32.00	591
14275	564.84	29.785	612.61	62	16.21	592
			952.24	59	29.00	592
			1305.03	63	12.54	592
			1731.95	60	32.00	592
14300	552.26	29.785	640.59	62	16.21	593
			933.26	59	29.00	593
			1277.62	63	12.54	593
			1751.45	60	32.00	593
14325	539.68	29.785	668.57	62	16.21	594
			914.74	59	29.00	594
			1250.25	63	12.54	594
			1771.18	60	32.00	594
14350	527.1	24.874	696.54	62	16.21	595
			896.72	59	29.00	595
			1222.90	63	12.54	595
			1790.95	58	25.77	595
14375	514.52	24.874	724.52	62	16.21	596
			879.21	59	29.00	596
			1195.58	63	12.54	596
			1803.88	58	25.77	596
14400	501.94	22.85	752.50	62	16.21	597
			862.26	59	29.00	597
			1168.30	63	12.54	597
			1813.55	61	23.19	597
14425	489.35	22.85	780.48	62	16.21	598
			845.90	59	29.00	598
			1141.04	63	12.54	598
			1816.55	61	23.19	598
14450	476.77	22.85	808.46	62	16.21	599
			830.15	59	29.00	599
			1113.83	63	12.54	599
			1819.97	61	23.19	599
14475	464.19	22.85	815.07	59	29.00	600
			836.44	62	16.21	600
			1086.65	63	12.54	600
			1823.82	61	23.19	600
14500	451.61	22.85	800.68	59	29.00	601
			864.42	62	16.21	601
			1059.52	63	12.54	601
			1828.09	61	23.19	601
14525	439.03	22.85	787.02	59	29.00	602
			892.40	62	16.21	602
			1032.43	63	12.54	602
			1832.77	61	23.19	602
14550	426.45	22.85	774.13	59	29.00	603
			920.38	62	16.21	603
			1005.39	63	12.54	603
			1837.87	61	23.19	603
14575	413.87	22.85	762.05	59	29.00	604
			948.37	62	16.21	604
			978.40	63	12.54	604

			1989.10	35	25.06	281
6525	4464.8	25.837	634.17	31	27.08	282
			1155.99	30	29.02	282
			1180.39	29	27.83	282
			1965.01	35	25.06	282
6550	4452.3	25.837	661.58	31	27.08	283
			1131.19	30	29.02	283
			1184.83	29	27.83	283
			1941.02	35	25.06	283
6575	4439.7	25.837	689.05	31	27.08	284
			1106.53	30	29.02	284
			1189.91	29	27.83	284
			1917.14	35	25.06	284
6600	4427.1	25.837	716.55	31	27.08	285
			1082.04	30	29.02	285
			1195.63	29	27.83	285
			1893.38	35	25.06	285
6625	4414.5	25.837	744.09	31	27.08	286
			1057.72	30	29.02	286
			1201.97	29	27.83	286
			1869.73	35	25.06	286
6650	4401.9	25.837	771.66	31	27.08	287
			1033.58	30	29.02	287
			1208.93	29	27.83	287
			1846.20	35	25.06	287
6675	4389.4	25.837	799.26	31	27.08	288
			1009.65	30	29.02	288
			1216.49	29	27.83	288
			1822.80	35	25.06	288
6700	4376.8	25.837	826.89	31	27.08	289
			985.93	30	29.02	289
			1224.65	29	27.83	289
			1799.53	35	25.06	289
6725	4364.2	25.837	854.54	31	27.08	290
			962.43	30	29.02	290
			1233.38	29	27.83	290
			1776.40	35	25.06	290
6750	4351.6	25.837	882.21	31	27.08	291
			939.19	30	29.02	291
			1242.69	29	27.83	291
			1753.41	35	25.06	291
6775	4339	25.837	909.90	31	27.08	292
			916.21	30	29.02	292
			1252.55	29	27.83	292
			1730.56	35	25.06	292
6800	4326.5	25.837	893.51	30	29.02	293
			937.61	31	27.08	293
			1262.95	29	27.83	293
			1707.87	35	25.06	293
6825	4313.9	25.837	871.12	30	29.02	294
			965.34	31	27.08	294
			1273.89	29	27.83	294
			1685.34	35	25.06	294
6850	4301.3	25.837	849.07	30	29.02	295
			993.07	31	27.08	295
			1285.34	29	27.83	295
			1662.97	35	25.06	295
6875	4288.7	25.837	827.37	30	29.02	296
			1020.83	31	27.08	296
			1297.29	29	27.83	296
			1640.77	35	25.06	296
6900	4276.1	25.837	806.06	30	29.02	297
			1048.59	31	27.08	297
			1309.73	29	27.83	297
			1618.76	35	25.06	297
6925	4263.5	25.837	785.17	30	29.02	298
			1076.37	31	27.08	298
			1322.65	29	27.83	298
			1596.93	35	25.06	298
6950	4251	25.837	764.73	30	29.02	299
			1104.16	31	27.08	299
			1336.03	29	27.83	299
			1575.30	35	25.06	299
6975	4238.4	25.837	744.79	30	29.02	300
			1131.95	31	27.08	300
			1349.86	29	27.83	300
			1553.87	35	25.06	300
7000	4225.8	25.837	725.38	30	29.02	301
			1159.76	31	27.08	301
			1364.12	29	27.83	301
			1532.65	35	25.06	301
7025	4213.2	25.837	706.54	30	29.02	302
			1187.57	31	27.08	302
			1378.80	29	27.83	302
			1511.65	35	25.06	302
7050	4200.6	25.837	688.32	30	29.02	303
			1215.40	31	27.08	303
			1393.89	29	27.83	303
			1490.88	35	25.06	303
7075	4188.1	25.837	670.78	30	29.02	304
			1243.23	31	27.08	304
			1409.37	29	27.83	304
			1470.35	35	25.06	304
7100	4175.5	25.837	653.97	30	29.02	305
			1271.06	31	27.08	305
			1425.24	29	27.83	305
			1450.07	35	25.06	305
7125	4162.9	27.934	637.94	30	29.02	306
			1298.91	31	27.08	306
			1430.05	35	25.06	306
			1441.47	29	27.83	306
7150	4150.3	27.564	622.76	30	29.02	307
			1326.76	31	27.08	307
			1410.30	35	25.06	307
			1422.89	36	27.89	307
7175	4137.7	27.564	608.48	30	29.02	308
			1354.61	31	27.08	308
			1390.84	35	25.06	308
			1396.41	36	27.89	308
7200	4125.2	27.009	595.18	30	29.02	309
			1369.99	36	27.89	309
			1371.67	35	25.06	309
			1382.47	31	27.08	309

			1843.38	61	23.19	604
14600	401.29	22.85	750.82	59	29.00	605
			951.47	63	12.54	605
			976.35	62	16.21	605
			1849.30	61	23.19	605
14625	388.71	22.85	740.48	59	29.00	606
			924.61	63	12.54	606
			1004.33	62	16.21	606
			1855.62	61	23.19	606
14650	376.13	22.85	731.07	59	29.00	607
			897.81	63	12.54	607
			1032.31	62	16.21	607
			1862.34	61	23.19	607
14675	363.55	22.85	722.62	59	29.00	608
			871.09	63	12.54	608
			1060.30	62	16.21	608
			1869.45	61	23.19	608
14700	350.97	22.85	715.16	59	29.00	609
			844.45	63	12.54	609
			1088.28	62	16.21	609
			1876.95	61	23.19	609
14725	338.39	22.85	708.73	59	29.00	610
			817.90	63	12.54	610
			1116.26	62	16.21	610
			1884.84	61	23.19	610
14750	325.81	22.85	703.36	59	29.00	611
			791.45	63	12.54	611
			1144.25	62	16.21	611
			1893.12	61	23.19	611
14775	313.23	22.85	699.07	59	29.00	612
			765.10	63	12.54	612
			1172.23	62	16.21	612
			1901.76	61	23.19	612
14800	300.65	22.85	595.87	59	29.00	613
			738.88	63	12.54	613
			1200.21	62	16.21	613
			1910.78	61	23.19	613
14825	288.06	22.85	693.79	59	29.00	614
			712.80	63	12.54	614
			1228.20	62	16.21	614
			1920.16	61	23.19	614
14850	275.48	22.85	686.36	63	12.54	615
			692.84	59	29.00	615
			1256.18	62	16.21	615
			1929.91	61	23.19	615
14875	262.9	22.85	661.09	63	12.54	616
			693.02	59	29.00	616
			1284.17	62	16.21	616
			1940.01	61	23.19	616
14900	250.32	22.85	635.50	63	12.54	617
			694.33	59	29.00	617
			1312.15	62	16.21	617
			1950.45	61	23.19	617
14925	237.74	22.85	610.13	63	12.54	618
			696.75	59	29.00	618
			1340.14	62	16.21	618
			1961.25	61	23.19	618
14950	225.16	22.85	585.00	63	12.54	619
			700.29	59	29.00	619
			1368.12	62	16.21	619
			1972.38	61	23.19	619
14975	212.58	22.85	560.14	63	12.54	620
			704.93	59	29.00	620
			1396.11	62	16.21	620
			1983.84	61	23.19	620

7225	4112.6	29.378	582.92	30	29.02	310
			1343.63	36	27.89	310
			1352.80	35	25.06	310
			1388.16	32	30.40	310
7250	4100	29.378	571.77	30	29.02	311
			1317.34	36	27.89	311
			1334.26	35	25.06	311
			1360.19	32	30.40	311
7275	4087.4	29.378	561.80	30	29.02	312
			1291.12	36	27.89	312
			1316.05	35	25.06	312
			1332.22	32	30.40	312
7300	4074.8	29.378	553.06	30	29.02	313
			1264.98	36	27.89	313
			1298.19	35	25.06	313
			1304.25	32	30.40	313
7325	4062.3	26.083	545.62	30	29.02	314
			1238.92	36	27.89	314
			1276.28	32	30.40	314
			1280.89	35	25.06	314
7350	4049.7	26.083	539.53	30	29.02	315
			1212.94	36	27.89	315
			1248.31	32	30.40	315
			1263.57	35	25.06	315
7375	4037.1	26.083	534.83	30	29.02	316
			1187.05	36	27.89	316
			1220.35	32	30.40	316
			1246.84	35	25.06	316
7400	4024.5	26.083	531.57	30	29.02	317
			1161.27	36	27.89	317
			1192.38	32	30.40	317
			1230.52	35	25.06	317
7425	4011.9	26.083	529.78	30	29.02	318
			1135.58	36	27.89	318
			1164.41	32	30.40	318
			1214.63	35	25.06	318
7450	3999.4	26.083	529.45	30	29.02	319
			1110.01	36	27.89	319
			1136.45	32	30.40	319
			1199.18	35	25.06	319
7475	3986.8	26.083	530.61	30	29.02	320
			1084.56	36	27.89	320
			1108.49	32	30.40	320
			1184.19	35	25.06	320
7500	3974.2	26.083	533.23	30	29.02	321
			1059.23	36	27.89	321
			1080.52	32	30.40	321
			1169.68	35	25.06	321
7525	3961.6	26.083	537.30	30	29.02	322
			1034.04	36	27.89	322
			1052.56	32	30.40	322
			1155.66	35	25.06	322
7550	3949	26.083	542.79	30	29.02	323
			1009.00	36	27.89	323
			1024.60	32	30.40	323
			1142.16	35	25.06	323

Appendix C

MATLAB Files

See MATLAB files on the following pages.

```
% Thesis Project
%       Gaussian Simulation in 2-D
%       Using Ordinary Kriging
%       By Ashley Willcott
%↙
-------------------------------------------------------------------------↙
---
clear;
%
% file=input('What is the name of the input file? ','s');
% inputdata=load (file);
inputdata=load('FU5POR.txt');

% inputdata=load('krig.txt')
wellpath

maxdistance=0;          % This loop calculates the maximum distance↙
between any two points in the data loop.
for i=1:length(inputdata)  %  By definition the maximum lag should be↙
half the maximum distance
   for j=1:length(inputdata)
      distance(i,j)=dis(inputdata(i,1),inputdata(j,1),inputdata(i,2),↙
inputdata(j,2));
      maxdistance=max(max(distance));
  end
end
datavar=var(inputdata(:,3));

OK=0;
while OK==0
% lag=input('Choose the lag distance :'); %500
% tolerance=input('Choose the lag tolerance :'); %250
% atol=input('Choose the angular tolerance :'); %20

lag=1000;
tolerance=450;
atol=20;

angulartol=deg2rad(atol);
NoLag=round((maxdistance/2)/lag);
```

```
startangle=0;
% Ndir=2;
% inc=90;
Ndir=8;
inc=22.5;

covterm=0;

for var = 1:NoLag+1
    for var2=1:Ndir
        count(var2,var)=0;
        porsquaresum(var2,var)=0;
        sumdistance(var2,var)=0;
        h(var)=0;
    end
end

% This loop sets up the estimate for the variogram firstly to calculate the
% direction of maximum continuity
for i=1:length(inputdata)
   for j=1:length(inputdata)
      if distance(i,j)~0;
         angle=makepos1(inputdata(i,1),inputdata(j,1),inputdata(i,2),inputdata(j,2));
         for fill=0:NoLag
            if (distance(i,j) > fill*lag-tolerance) & (distance(i,j) <fill*lag+tolerance)
               for dir=1:Ndir
                  theta(dir)=deg2rad(startangle)+deg2rad(inc)*(dir-1);
                  if (angle >= theta(dir)-angulartol) & (angle <=theta(dir)+angulartol)
                     count(dir,fill+1)=count(dir,fill+1)+1;
                     porsquare=(inputdata(i,3)-inputdata(j,3))^2;
                     porsquaresum(dir,fill+1)=porsquaresum(dir,fill+1)+porsquare;
                     sumdistance(dir,fill+1)=sumdistance(dir,fill+1)+distance(i,j);
```

```
                    end
                end
            end
        end
    end
  end
end

xl=0:lag:(NoLag)*lag; % Array of lag distances

% This loop estimates the variogram from previous loop
for fill=1:NoLag+1
    for dir = 1:Ndir
        v(dir,fill)=1/(2*count(dir,fill))*porsquaresum(dir,fill);
        avgdis(dir,fill)=sumdistance(dir,fill)/count(dir,fill);
        direction(dir)=(dir-1)*inc;
        vminusvar(dir)=datavar-v(dir,fill);
        if vminusvar(dir) <0
            if count(dir,fill)>20
                continuity(dir,fill)=xl(fill);
            end
        end
    end
end

% Color strings are 'c', 'm', 'y', 'r', 'g', 'b', 'w', and 'k'.
% These correspond to cyan, magenta, yellow, red, green, blue, white,↙
and black.
% Line style strings are '-' for solid, '--' for dashed, ':' for↙
dotted, '-.' for dash-dot.
%  Omit the line style for no line.
%  The marker types are '+', 'o', '*', and 'x', and
%  the filled marker types are 's' for square, 'd' for diamond, '^' for↙
up triangle,
%          'v' for down triangle, '>' for right triangle, '<' for left↙
triangle,
%                      'p' for pentagram, 'h' for hexagram, and none↙
for no marker.
%
load test.mat
```

```
OK=1;
figure
plot(x1,datavar+x1*0); hold on
plot(x1,v(1,:),'s-')
plot(x1,v(2,:),'d-')
plot(x1,v(3,:),'v-')
plot(x1,v(4,:),'p-')
plot(x1,v(5,:),'h-')
plot(x1,v(6,:),'o-')
plot(x1,v(7,:),'x-')
plot(x1,v(8,:),'+-')%,x1,v(9,:));
xlabel('lag Distance (ft)')
ylabel('variogram')
legend('sample variance',num2str(direction(1)),num2str(direction(2)),↙
num2str(direction(3)),num2str(direction(4)),num2str(direction(5)),↙
num2str(direction(6)),num2str(direction(7)),num2str(direction(8)))%,↙
num2str(direction(9)))
title('Variogram Estimation, Choose the maximum direction of↙
Continuity')

figure
plot(x1,datavar+x1*0); hold on
plot(x1,v(1,:),'s-')
plot(x1,v(5,:),'v-')
xlabel('lag Distance (ft)')
ylabel('variogram')
legend('sample variance',num2str(direction(1)),num2str(direction(2)));
title('Variogram Estimation, Choose the maximum direction of↙
Continuity')
% fprintf('This plot had a lag distance of %i \n',lag)
% OK=input('is this plot OK? "1" if yes, "0" if no :');
% if OK==0
%     clear('v');
%     fprintf('please change paramters to tune the estimate \n\n')
% end

end

%This loop calculates the variogram model
for fill=1:NoLag+1
```

```
    v1(fill)=VsphN(10,30,10000,x1(fill));
    v2(fill)=VsphN(10,30,4000,x1(fill));
end

%fills data array
counter = 0;
for k=1:620         %  well path counter
    for i=1:68      %  Data counter
        counter=counter+1;
        data(counter,1)=dis(path(k,1),inputdata(i,1),path(k,2),↙
inputdata(i,2));
        data(counter,2)=i;
        data(counter,3)=k;
    end
end

mat=sortrows(data,[3,1]); % Sorts data array

% Takes top 4 entries at each point in the well path
j=0;
i=0;
counter = 0;
for k=1:620
    while counter < 4
        i=i+1;
        j=j+1;
        counter = counter + 1;
        newmat(j,1,k)=mat(i,1);
        newmat(j,2,k)=mat(i,2);
        newmat(j,3,k)=inputdata(mat(i,2),3);
    end
    newmat(j+1,1,k)=path(k,1);
    newmat(j+1,2,k)=path(k,2);
    newmat(j+1,3,k)=0;
    counter = 0;
    j=0;
    i=i+64;
end
%
Sill=40;
```

```
for k=1:620
    for i=1:4
        for j=1:4
            L1=inputdata(newmat(j,2,k),1)-inputdata(newmat(i,2,k),1);
            L2=inputdata(newmat(j,2,k),2)-inputdata(newmat(i,2,k),2);

            LD1=anisLD(4000,10000,L1,L2,deg2rad(90)); % theta is angle↙
of maximum continuity - min cont is assumed perpendicular

            V1=VsphN(10,Sill,1,LD1); % note for anisotropic variograms↙
a=1
            Cov0(i,k)=Sill-V1;
            Cov(i,j,k)=Sill-V1;

            if i==j
                Cov(i,j,k)=Sill;
            end

        end
    end
end

for k=1:620

    for z=1:4
        Cov(5,z,k)=1;
        Cov(z,5,k)=1;
    end

    Cov0(5,k)=1;
    Lam(:,k)=inv(Cov(:,:,k))*(Cov0(:,k));
    x(k,1)=dot(Lam(:,k),newmat(:,3,k))/100;
    Var(k)=Sill-dot(Lam(:,k),Cov0(:,k));

end

[mu,s,muci,sci] = normfit(x); % these variables calculate the normal↙
fit parameters for the random number generation in the risk assessment

figure
```

```
plot(x1,v(1,:),'s-');hold on
plot(x1,v1,'s:')
plot(x1,v(5,:),'v-')
plot(x1,v2,'v:')
xlabel('lag Distance (ft)')
ylabel('variogram')
legend('Estimate (east)', 'Model(east)', 'Estimate (north)','Model↙
(north)')
title('Model vs Estimation Comparison')
figure
plot(x1,v(1,:),x1,v(2,:));
xlabel('lag Distance (ft)')
ylabel('variogram')
legend(num2str(direction(1)),num2str(direction(2)))
title('Model vs Estimation Comparison')



savefile='test.mat';

save↙
(savefile,'x','mu','s','x1','datavar','v','direction','v1','v2','NoLag'↙
)
```

```
% Safety and Risk Term Project - type "pro" to run
%   For Safetly and Risk Engineering Term Project
%       Coded by: Ashley Willcott
%                 July 20 2004
%       Revised:  June 16 2005
%↙
-------------------------------------------------------------------------↙
--

clear;

load test.mat % This command loads the porosity matix (note that Risk.m↙
must be run first)

slope=fw(Swbar)/Swbar;  % Calculates slope from fractional flow↙
function

% Initalizing Reservoir Variables
L=8000*0.3048; % Length of the reservoir (m)
W=800*0.3048; % Width of the reservoir (m)
H=50;  % Height of the reservoir (m) 8.53
q=0.02894;  % Flux of the oil (m^3/s) 70; 2500 m^3/day
ut=q/(W*H);  % Total flux velocity (m/s)


% For risk analysis we need 50 sets of normally distributed porosity↙
data
%    Get parameters from Excel Descriptve statistics
%    Mean = 0.24,
%    Standard Deviation = 0.02

for numrisk=1:1
normpor=normrnd(mu,s,[620 500]);

for i=1:281
    production(i)=0;
    for j=1:500
        normprod(i,j)=0;
        difference(i,j)=0;
    end
```

```
end

%   This loop is for calculating original time to breakthrough for kriged
%   porosity
for i=1:620
    var(i,1)=x(i); % index 1 is porosity
    var(i,2)=3.0*10^(-10)*x(i)/(1-x(i))^2; % index 2 is Permeability
    var(i,4)=ut/x(i)*slope; % vf is velocity of the front
    var(i,3)=L/var(i,4)/(3.1536*10^7); % index 3 is Time to Breakthrough (years)
    ttbt=var(i,3);
    %var(i,4)=H*W*vf*ttbt*3.1536*10^7*6.28974/620; % index 4 is total production (barrels) for each layer % 8.53
end

%   This loop is calculating time to breakthrough for all other porosity data sets
for i=1:620
    for j=1:500
    perm(i,j)=3.0*10^(-10)*normpor(i,j)/(1-normpor(i,j))^2; % Permeability
    vf(i,j)=ut/normpor(i,j)*slope;                          % Velocity of the saturation front
    ttbt(i,j)=L/vf(i,j)/(3.1536*10^7);                      % Time to breakthrough
   q(i,j)= H*W*vf(i,j)*ttbt(i,j)*3.1536*10^7*6.28974/620;
    end
end

%   This is the calculation of all the production profiles
time = 0;
count = 0;

while time < 14.05
    count = count +1;
    for i=1:620

        if var(i,3) > time
            production(count)=production(count)+H*W*var(i,4)*var(i,1)
```

```
*6.28974/620*60*60*24;
            % note that 620 is number of segments
            % note that 6.28974 is barrels in 1 m^3
            % var(i,1) is porosity, var(i,4) is velocity of the front
            % this is to sum production in all shale layers
        end

        for j=1:500
            if ttbt(i,j) > time
                if count < 281
                normprod(count,j)=normprod(count,j)+H*W*vf(i,j)*normpor↙
(i,j)*6.28974/620*60*60*24; % in barrels of oil %q(i,j);%/10^6; % in↙
Millions of barrels of oil
                end
            end
        end

    end

    if count>1
        ttlgeoprod(count,1)=ttlprod(count-1,1)+production(count);
    else
        ttlgeoprod(count,1)=production(count);
    end

    for k=1:500
       if count>1
           ttlprod(count,k)=ttlprod(count-1,k)+normprod(count,k);
       else
           ttlprod(count,k)=normprod(count,k);
       end
    end

    t(count)=time;
    time = time + 0.05;

end

geoprodmax=max(ttlgeoprod);
```

```
for i=1:500
    norm100(i,1)=ttlprod(281,i);
end
totalsorted=sort(norm100);
% 95th percentile
alpha=round(0.95*size(norm100,1));

Risk(numrisk)=(totalsorted(alpha)-geoprodmax)*50*0.05/1000; %Risk↙
Factor
numrisk
end

% figure
% subplot(2,2,1); hist(x,50)
% xlabel('Bins')
% ylabel('Frequency')
% title('Porosity Histogram (geo)')
% axis([0 0.4 0 100])
%
% subplot(2,2,2); hist(normpor(:,1),50)
% xlabel('Bins')
% ylabel('Frequency')
% title('Porosity Histogram (norm)')
% axis([0 0.4 0 100])
%
% subplot(2,2,3); hist(normpor(:,50),50)
% xlabel('Bins')
% ylabel('Frequency')
% title('Porosity Histogram (norm)')
% axis([0 0.4 0 100])
%
% subplot(2,2,4); hist(normpor(:,100),50)
% xlabel('Bins')
% ylabel('Frequency')
% title('Porosity Histogram (norm)')
% axis([0 0.4 0 100])
%
% z=1:1:500;
% figure
% hist(Risk,50)
```

```
%
% figure
% scatter(z,Risk)
% xlabel('Realization Number')
% ylabel('Risk Factor')
% legend('Risk Factor')
% title('Risk Factor')

figure
subplot(2,2,1);plot(t,production)
xlabel('Time (years)')
ylabel('Vol Produced (US Barrels)')
legend('Production (Barrels)')
title('Production Profile (geo)')

subplot(2,2,2);plot(t,normprod(:,1));
xlabel('Time (years)')
ylabel('Vol Produced (US Barrels)')
legend('Production (Barrels)')
title('Production Profile (normal)')

subplot(2,2,3);plot(t,normprod(:,50));
xlabel('Time (years)')
ylabel('Vol Produced (US Barrels)')
legend('Production (Barrels)')
title('Production Profile (normal)')

subplot(2,2,4);plot(t,normprod(:,100));
xlabel('Time (years)')
ylabel('Vol Produced (US Barrels)')
legend('Production (Barrels)')
title('Production Profile (normal)')
```

```
% Simple Well path generator
xwell=-500:25:15500;
for iwell=1:620
    path(iwell,2)=-(78/155)*(xwell(iwell))+240200/31; % x coordinates
of well
    path(iwell,1)=xwell(iwell); % y coordinates of well
end
```

```
% Distance equation in 2-D
%↙
----------------------------------------------------------------------↙
---
function [dis]=dis(x1,x2,y1,y2)
dis=((x1-x2)^2+(y1-y2)^2)^(0.5);
```

```
% Length Calculation for Anisotropic Variogram
function [anisLD] = anisLD(a1,a2,L1,L2,theta);

Lu=L1*cos(theta)+L2*sin(theta);
Lv=-L1*sin(theta)+L2*cos(theta);

anisLD=sqrt((Lu/a1)^2+(Lv/a2)^2);
```

```
% Convert asin angle to be between 0-360 deg
%↙
----------------------------------------------------------------------↙
---
function [makepos]=makepos(x1,x2,y1,y2)
xy=dis(x1,x2,y1,y2);

ang=asin((y2-y1)/xy);
cosangle=(x2-x1)/xy;
sinangle=(y2-y1)/xy;

xbar=x2-x1;
ybar=y2-y1;
makepos=atan2(ybar,xbar);
```

```
% Combination Variogram (spherical with nugget)
function [VsphN] = VsphN(N,Co,a,x)
if x<a
    VsphN=N+Co*((3/2*(x/a))-1/2*((x/a)^3));
else
    VsphN=N+Co;
end
```

```
% Swbar
function [Swbar]=Swbar

flag = 1;
Sw=0;
slopeold=fw(0)/0.01;

while flag == 1
    Sw=Sw+0.001;
    slopenew=fw(Sw)/Sw;
    check=slopenew-slopeold;
    if check < 0
        flag = -1;
        Swbar=Sw;
    end
    slopeold=slopenew;

end
```

```
% Fractional flow function
function [fw]=fw(Sw)

muo=0.0003;
muw=0.01;
Krw=Sw^2;
Kro=(1-Sw)^2;
uw=Krw/muw;
uo=Kro/muo;
fw=uw/(uw+uo);
```

```
% This file chooses the sample points to remove from the Exhaustive
data
% set. It uses a MATLAB file created by MATLAB Central (Mathworks)
clear
data = load ('permxMLAB.txt');

x=1:1:1820;
y=90;

% remove y% of the data
N=fix((y/100)*1820);
index=myrandint(1,N,x,'noreplace');

for i=1:1820-N
    sample((i*3-2))=data(index(i),1);
    sample((i*3-1))=data(index(i),2);
    sample(i*3)=data(index(i),3);
    newdata(i,1)=data(index(i),1);
    newdata(i,2)=data(index(i),2);
    newdata(i,3)=data(index(i),3);
end

figure
scatter(data(:,1),data(:,2),10); hold on
scatter(newdata(:,1),newdata(:,2),35,'filled')

% GSLIB/MATLAB format
fid=fopen('Sample Population.txt','w');
fprintf(fid,'Regular Reservoir Sample Population \n 3 \n xcoord \n
ycoord \n permx \n');
fprintf(fid,'%12.2f %12.2f %12.6f \n',sample);
fclose(fid);
```

```
function ranInt = myrandint(outputRow,outputCol,outputRange,varargin)
% MYRANDINT(M,N,RANGE) is an M-by-N matrix with random integer entries
% drawn with replacement from elements of vector RANGE.  The elements in
% vector RANGE do not need to be contiguous or unique.  (Actually, they do
% not even need to be integers: The function works the exact same way with
% noninteger elements, but a warning is generated to alert the user that
% noninteger elements are being sampled.)
%
% To specify a contiguous integer range from Xlow to Xhi, use RANGE = [Xlow:Xhi].
%
% MYRANDINT(M,N,RANGE,'noreplace') is an M-by-N matrix with random integers
% drawn without replacement.
%
% This function is based around RAND and RANDPERM, and is intended as a
% modest imitation of Comm Toolbox's RANDINT.
% Note that this function was found on the Mathworks website


rand('state',15); % this is to keep the state constant for recalculation of the same random numbers at a later date

if isequal(size(outputRange),[1 2]) && ~isequal(outputRange(1),outputRange(2)-1),
    warning('To specify a range [low high] use [low:high].')
end
if ~isequal(round(outputRange),outputRange),
    warning('Specified RANGE contains noninteger values.')
end
if ~isequal(length(outputRange),length(outputRange(:))),
    error('Range must be a vector of integer values.')
end

numElements = outputRow*outputCol;
```

```
if isempty(varargin),

    ranInt = zeros(outputRow,outputCol);
    randIx = floor((length(outputRange))*rand(size(ranInt))) + 1;
    ranInt = outputRange(randIx);
    if ~isequal(size(randIx),size(ranInt)),
        ranInt = reshape(ranInt,size(randIx));
    end

elseif isequal(varargin{1},'noreplace'),

    if numElements > length(outputRange),
        error('Not enough elements in range to sample without↙
replacement.')
    else
        % Generate full range of integers
        XfullShuffle = outputRange(randperm(length(outputRange)));
        % Select the first bunch:
        ranInt = reshape(XfullShuffle(1:numElements),outputRow,↙
outputCol);
    end

else
    error('Valid argument is ''noreplace''.')
end
```

```
% This program aims to populate geostatistical realiztions with MWD
%
% This program was written by:
%   Ashley Willcott
%   Memorial University of Newfoundland
%   Masters Candidate
%
%↙
--------------------------------------------------------------------↙
--
clear;
% Initialization
% This block loads original data
data = load ('permxMLAB.txt');
sample = load ('Sample Population Mlab.txt');
well = load ('well bore.txt'); % paste the trajectory nodes here

NumNodes = length(well);    % this is the number of trajectory points
nearness = 60;              % this is the distance from the well bore to↙
the grid block for MWD
phase = 1;                  % this is the current phase of the drilling↙
process (note 1 is the minimum phase){Phase = stage}
sectionsize=650;            % this is the mD of each phase

% counters
q=1;                        % if you want to skip the loop set q not↙
equal 0
count=1;
segment=0;
old=0;
id=1;
countid=0;
%↙
--------------------------------------------------------------------↙
--

% This loop is a standalone loop to check against NetTool
while q==0 % this loop is a quick checking program to compare with↙
NetTool
    x=input ('x-coordinate from NetTool :');
```

```
    y=input ('y-coordinate from NetTool :');
    i=(x+25)/50;
    j=(y+25)/50;
    block=i+(j-1)*28;
    ans=data(block,3)/1000
    q=input ('q (0 to repeat) :');
end

% this loop discretizes the well path segments
for i=1:NumNodes-1
    deltax=well(i+1,1)-well(i,1);
    deltay=well(i+1,2)-well(i,2);
    N=10; % this is the number of segments in between trajectory points
    deltaxi=deltax/N;
    deltayi=deltay/N;
    for j=1:N+1
        xi(count)=well(i,1)+deltaxi*(j-1);
        yi(count)=well(i,2)+deltayi*(j-1);
        count=count+1;
    end
end

Nodes=length(xi); % this loop calculates running mD up to the end of a
given phase
for i=1:Nodes-1
    segment=segment+1;
    new=dis(xi(i),xi(i+1),yi(i),yi(i+1));
    mD(segment)=old+new;
    old=mD(segment);
    if mD(segment)/phase<sectionsize;
        phasemD(segment)=mD(segment);
    end
end

%This loop checks for grid blocks near the wellbore to input MWD
sizephase=length(phasemD);
for i=1:sizephase
    for j=1:length(data)
        if dis(xi(i),data(j,1),yi(i),data(j,2)) < nearness
            blockid(id)=j;
```

```
            id=id+1;
        end
    end
end

blockid=sort(blockid); % this loop records the block id for the nrear↙
well bore blocks
for i=1:length(blockid)-1
    if blockid(i+1)~= blockid(i)
        countid=countid+1;
        id(countid)=blockid(i);
    end
end

a=0;
for i=1:length(id)
    a=a+1;
    add(a)=data(id(i),1);
    a=a+1;
    add(a)=data(id(i),2);
    a=a+1;
    add(a)=data(id(i),3);
end

a=0;
for i=1:length(sample)
    a=a+1;
    newsample(a)=sample(i,1);
    a=a+1;
    newsample(a)=sample(i,2);
    a=a+1;
    newsample(a)=sample(i,3);
end

b=0;
count=a;
for i=count:length(add)+count-1
    a=a+1;
    b=b+1;
    newsample(a)=add(b);
```

```
end

% %↙
----------------------------------------------------------------------↙
---
% % FILE CREATION - *.txt files created in desire formats
% %
% GSLIB format
fid=fopen('newsampleGSLIB.txt','w');
fprintf(fid,'Regular Reservoir Base Case \n 3 \n xcoord \n ycoord \n↙
permx \n');
fprintf(fid,'%12.2f %12.2f %12.6f \n',newsample);
fclose(fid);

% MATLAB format
fid=fopen('newsample.txt','w');
fprintf(fid,'%12.2f %12.2f %12.6f \n',newsample);
fclose(fid);

% % This plots the locations of the MWD along with the sample↙
population
load ('newsample.txt');
figure
scatter(newsample(:,1),newsample(:,2)); hold on
plot(xi,yi); hold off
xlabel('X (m)')
ylabel('Y (m)')
title('Permeability Skeleton - Stage 1')
%
% figure
% scatter(sample(:,1),sample(:,2))
```

```
% This program aims to split realization files into sets of 8↙
realizations
% per file
%
% This program was written by:
%   Ashley Willcott
%   Memorial University of Newfoundland
%   Masters Candidate
%
%↙
-------------------------------------------------------------------------↙
--
clear;
% Initialization
% This block loads original data
data = load ('realization500stage5.dat');

NumReal = length(data)/1820;   % this is the number of realizations in↙
the file
NumSplit=8;              % this is the Number of realizations in each↙
split file

% counters
b=0;
c=0;
%↙
-------------------------------------------------------------------------↙
--

for j=1:round(NumReal/NumSplit)
    a=0;
    c=0;
    for i=1:NumSplit
        c=c+1;
        while a<c*1820*2
            a=a+1;
            b=b+1;
            if b<length(data)
            file(a,1,j)=data(b,1);
            a=a+1;
```

```
            file(a,l,j)=data(b,2);
            end
        end
    end
end

savefile='perm.mat';

save(savefile,'data')

% MATLAB format
fid=fopen('real10stage01.dat','w');
fprintf(fid,'%12.5f %12.5f \n',file(:,:,1));
fclose(fid);

fid=fopen('real10stage02.dat','w');
fprintf(fid,'%12.5f %12.5f \n',file(:,:,2));
fclose(fid);

fid=fopen('real10stage03.dat','w');
fprintf(fid,'%12.5f %12.5f \n',file(:,:,3));
fclose(fid);

fid=fopen('real10stage04.dat','w');
fprintf(fid,'%12.5f %12.5f \n',file(:,:,4));
fclose(fid);

fid=fopen('real10stage05.dat','w');
fprintf(fid,'%12.5f %12.5f \n',file(:,:,5));
fclose(fid);

fid=fopen('real10stage06.dat','w');
fprintf(fid,'%12.5f %12.5f \n',file(:,:,6));
fclose(fid);

fid=fopen('real10stage07.dat','w');
fprintf(fid,'%12.5f %12.5f \n',file(:,:,7));
fclose(fid);

fid=fopen('real10stage08.dat','w');
```

```
fprintf(fid,'%12.5f %12.5f \n',file(:,:,8));
fclose(fid);

fid=fopen('real10stage09.dat','w');
fprintf(fid,'%12.5f %12.5f \n',file(:,:,9));
fclose(fid);

fid=fopen('real10stage010.dat','w');
fprintf(fid,'%12.5f %12.5f \n',file(:,:,10));
fclose(fid);

fid=fopen('real10stage011.dat','w');
fprintf(fid,'%12.5f %12.5f \n',file(:,:,11));
fclose(fid);

fid=fopen('real10stage012.dat','w');
fprintf(fid,'%12.5f %12.5f \n',file(:,:,12));
fclose(fid);

fid=fopen('real10stage013.dat','w');
fprintf(fid,'%12.5f %12.5f \n',file(:,:,13));
fclose(fid);

fid=fopen('real10stage014.dat','w');
fprintf(fid,'%12.5f %12.5f \n',file(:,:,14));
fclose(fid);

fid=fopen('real10stage015.dat','w');
fprintf(fid,'%12.5f %12.5f \n',file(:,:,15));
fclose(fid);

fid=fopen('real10stage016.dat','w');
fprintf(fid,'%12.5f %12.5f \n',file(:,:,16));
fclose(fid);

fid=fopen('real10stage017.dat','w');
fprintf(fid,'%12.5f %12.5f \n',file(:,:,17));
fclose(fid);

fid=fopen('real10stage018.dat','w');
```

```
fprintf(fid,'%12.5f %12.5f \n',file(:,:,18));
fclose(fid);

fid=fopen('real10stage019.dat','w');
fprintf(fid,'%12.5f %12.5f \n',file(:,:,19));
fclose(fid);

fid=fopen('real10stage020.dat','w');
fprintf(fid,'%12.5f %12.5f \n',file(:,:,20));
fclose(fid);

fid=fopen('real10stage021.dat','w');
fprintf(fid,'%12.5f %12.5f \n',file(:,:,21));
fclose(fid);

fid=fopen('real10stage022.dat','w');
fprintf(fid,'%12.5f %12.5f \n',file(:,:,22));
fclose(fid);

fid=fopen('real10stage023.dat','w');
fprintf(fid,'%12.5f %12.5f \n',file(:,:,23));
fclose(fid);

fid=fopen('real10stage024.dat','w');
fprintf(fid,'%12.5f %12.5f \n',file(:,:,24));
fclose(fid);

fid=fopen('real10stage025.dat','w');
fprintf(fid,'%12.5f %12.5f \n',file(:,:,25));
fclose(fid);

fid=fopen('real10stage026.dat','w');
fprintf(fid,'%12.5f %12.5f \n',file(:,:,26));
fclose(fid);

fid=fopen('real10stage027.dat','w');
fprintf(fid,'%12.5f %12.5f \n',file(:,:,27));
fclose(fid);

fid=fopen('real10stage028.dat','w');
```

```
fprintf(fid,'%12.5f %12.5f \n',file(:,:,28));
fclose(fid);

fid=fopen('real10stage029.dat','w');
fprintf(fid,'%12.5f %12.5f \n',file(:,:,29));
fclose(fid);

fid=fopen('real10stage030.dat','w');
fprintf(fid,'%12.5f %12.5f \n',file(:,:,30));
fclose(fid);

fid=fopen('real10stage031.dat','w');
fprintf(fid,'%12.5f %12.5f \n',file(:,:,31));
fclose(fid);

fid=fopen('real10stage032.dat','w');
fprintf(fid,'%12.5f %12.5f \n',file(:,:,32));
fclose(fid);

fid=fopen('real10stage033.dat','w');
fprintf(fid,'%12.5f %12.5f \n',file(:,:,33));
fclose(fid);

fid=fopen('real10stage034.dat','w');
fprintf(fid,'%12.5f %12.5f \n',file(:,:,34));
fclose(fid);

fid=fopen('real10stage035.dat','w');
fprintf(fid,'%12.5f %12.5f \n',file(:,:,35));
fclose(fid);

fid=fopen('real10stage036.dat','w');
fprintf(fid,'%12.5f %12.5f \n',file(:,:,36));
fclose(fid);

fid=fopen('real10stage037.dat','w');
fprintf(fid,'%12.5f %12.5f \n',file(:,:,37));
fclose(fid);

fid=fopen('real10stage038.dat','w');
```

```
fprintf(fid,'%12.5f %12.5f \n',file(:,:,38));
fclose(fid);

fid=fopen('real10stage039.dat','w');
fprintf(fid,'%12.5f %12.5f \n',file(:,:,39));
fclose(fid);

fid=fopen('real10stage040.dat','w');
fprintf(fid,'%12.5f %12.5f \n',file(:,:,40));
fclose(fid);

fid=fopen('real10stage041.dat','w');
fprintf(fid,'%12.5f %12.5f \n',file(:,:,41));
fclose(fid);

fid=fopen('real10stage042.dat','w');
fprintf(fid,'%12.5f %12.5f \n',file(:,:,42));
fclose(fid);

fid=fopen('real10stage043.dat','w');
fprintf(fid,'%12.5f %12.5f \n',file(:,:,43));
fclose(fid);

fid=fopen('real10stage044.dat','w');
fprintf(fid,'%12.5f %12.5f \n',file(:,:,44));
fclose(fid);

fid=fopen('real10stage045.dat','w');
fprintf(fid,'%12.5f %12.5f \n',file(:,:,45));
fclose(fid);

fid=fopen('real10stage046.dat','w');
fprintf(fid,'%12.5f %12.5f \n',file(:,:,46));
fclose(fid);

fid=fopen('real10stage047.dat','w');
fprintf(fid,'%12.5f %12.5f \n',file(:,:,47));
fclose(fid);

fid=fopen('real10stage048.dat','w');
```

```
fprintf(fid,'%12.5f %12.5f \n',file(:,:,48));
fclose(fid);

fid=fopen('real10stage049.dat','w');
fprintf(fid,'%12.5f %12.5f \n',file(:,:,49));
fclose(fid);

fid=fopen('real10stage050.dat','w');
fprintf(fid,'%12.5f %12.5f \n',file(:,:,50));
fclose(fid);

fid=fopen('real10stage051.dat','w');
fprintf(fid,'%12.5f %12.5f \n',file(:,:,51));
fclose(fid);

fid=fopen('real10stage052.dat','w');
fprintf(fid,'%12.5f %12.5f \n',file(:,:,52));
fclose(fid);

fid=fopen('real10stage053.dat','w');
fprintf(fid,'%12.5f %12.5f \n',file(:,:,53));
fclose(fid);

fid=fopen('real10stage054.dat','w');
fprintf(fid,'%12.5f %12.5f \n',file(:,:,54));
fclose(fid);

fid=fopen('real10stage055.dat','w');
fprintf(fid,'%12.5f %12.5f \n',file(:,:,55));
fclose(fid);

fid=fopen('real10stage056.dat','w');
fprintf(fid,'%12.5f %12.5f \n',file(:,:,56));
fclose(fid);

fid=fopen('real10stage057.dat','w');
fprintf(fid,'%12.5f %12.5f \n',file(:,:,57));
fclose(fid);

fid=fopen('real10stage058.dat','w');
```

```
fprintf(fid,'%12.5f %12.5f \n',file(:,:,58));
fclose(fid);

fid=fopen('real10stage059.dat','w');
fprintf(fid,'%12.5f %12.5f \n',file(:,:,59));
fclose(fid);

fid=fopen('real10stage060.dat','w');
fprintf(fid,'%12.5f %12.5f \n',file(:,:,60));
fclose(fid);

fid=fopen('real10stage061.dat','w');
fprintf(fid,'%12.5f %12.5f \n',file(:,:,61));
fclose(fid);

fid=fopen('real10stage062.dat','w');
fprintf(fid,'%12.5f %12.5f \n',file(:,:,62));
fclose(fid);

fid=fopen('real10stage063.dat','w');
fprintf(fid,'%12.5f %12.5f \n',file(:,:,63));
fclose(fid);
```

Appendix D

Case Study 2 Plots and Data

See plots on the following pages

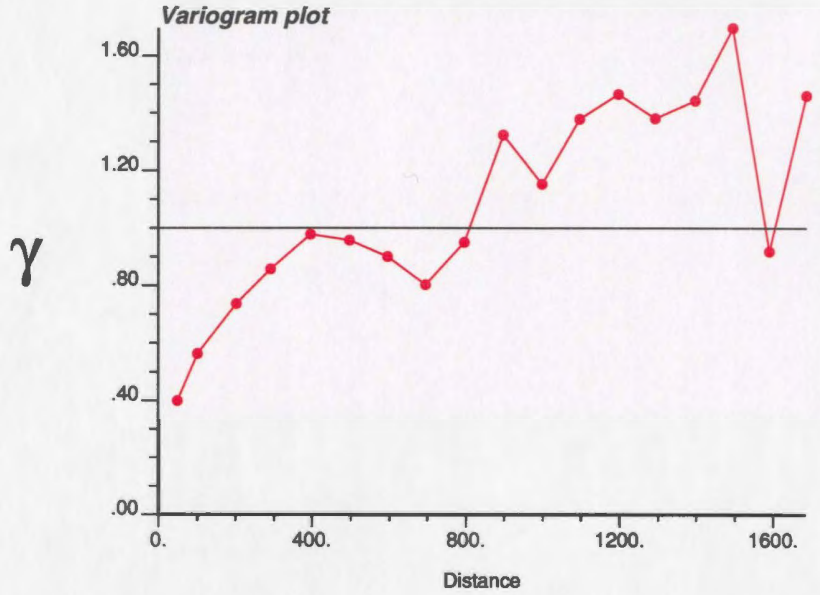

Figure 8.1: Sample Variogram Estimate - 0 Degrees

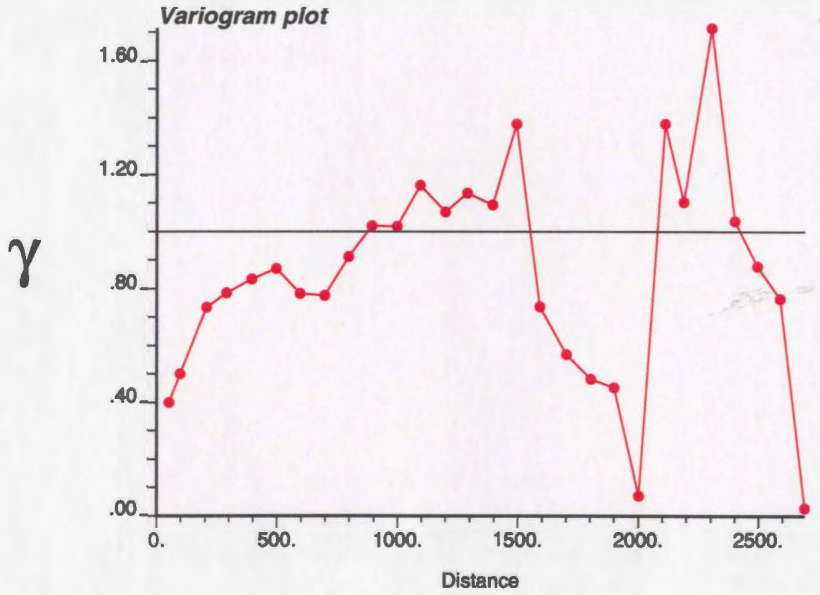

Figure 8.2: Sample Variogram Estimate - 22.5 Degrees

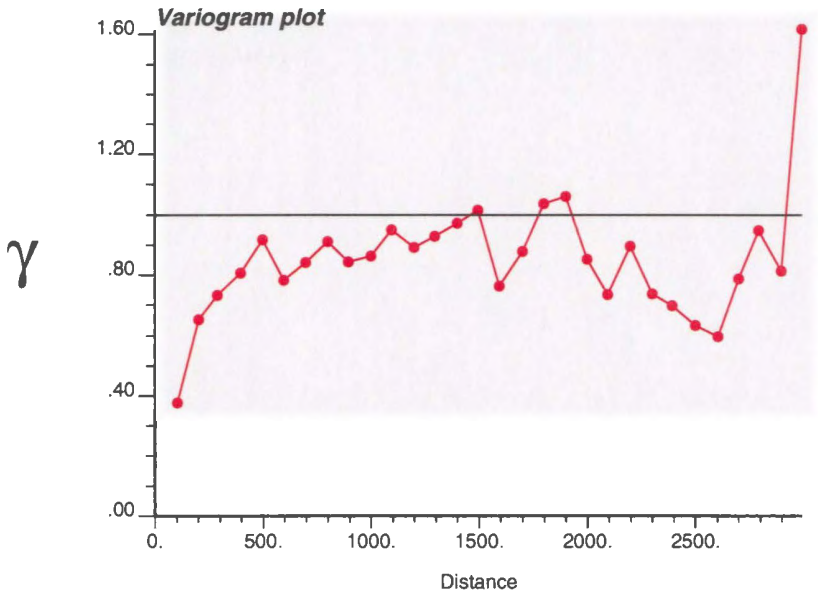

Figure 8.3: Sample Variogram Estimate - 45 Degrees

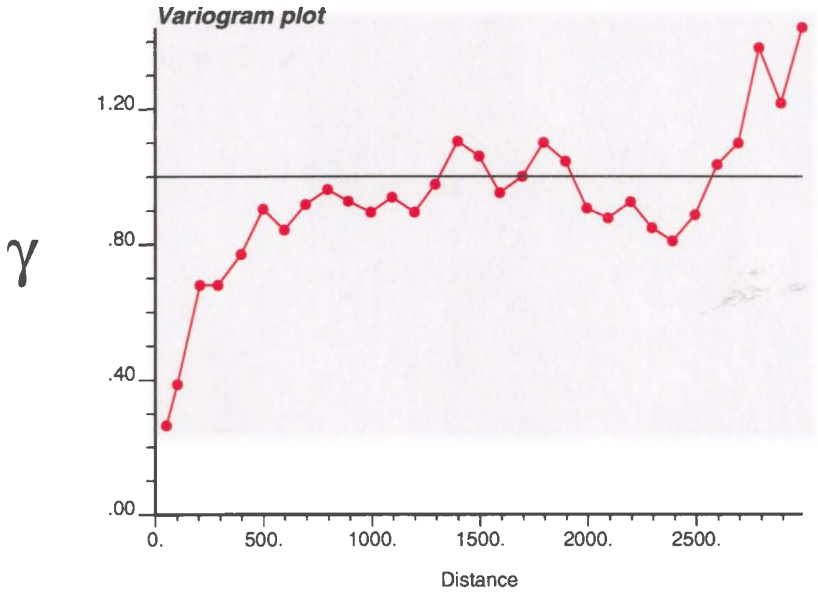

Figure 8.4: Sample Variogram Estimate - 67.5 Degrees

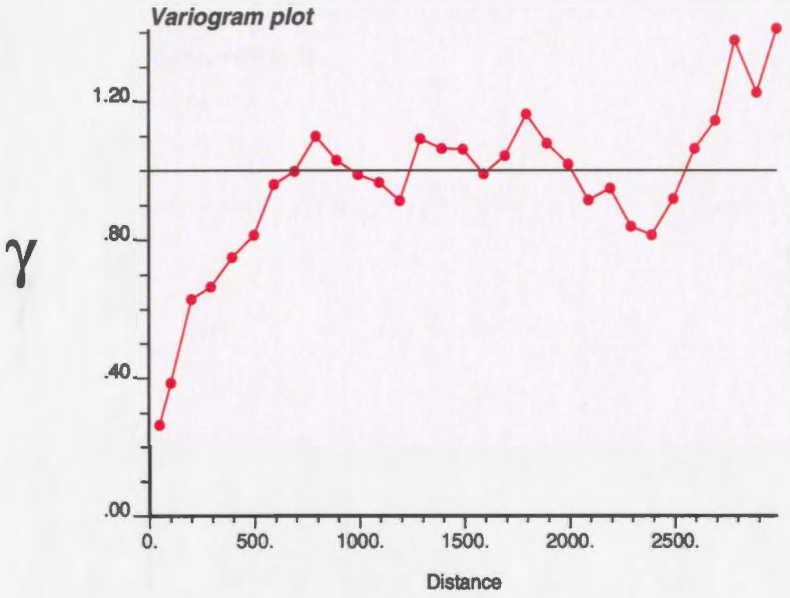

Figure 8.5: Sample Variogram Estimate - 90 Degrees

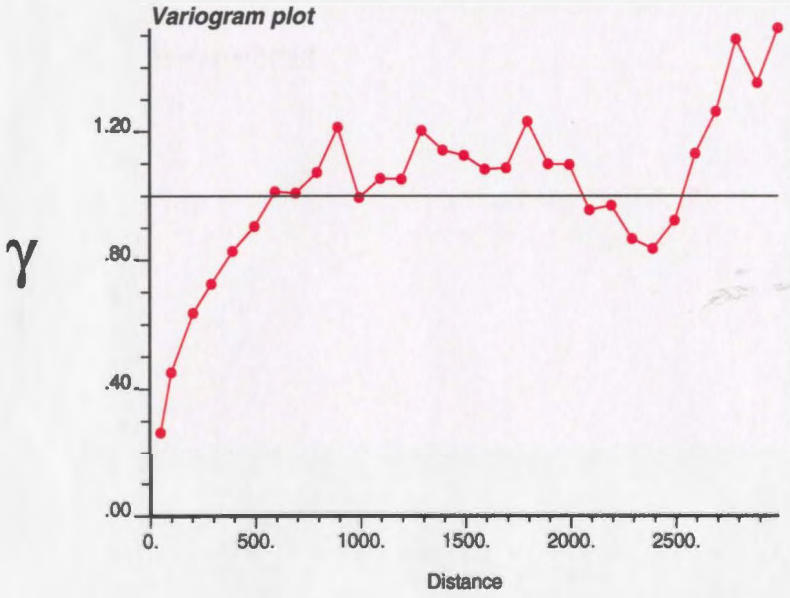

Figure 8.6: Sample Variogram Estimate - 112.5 Degrees

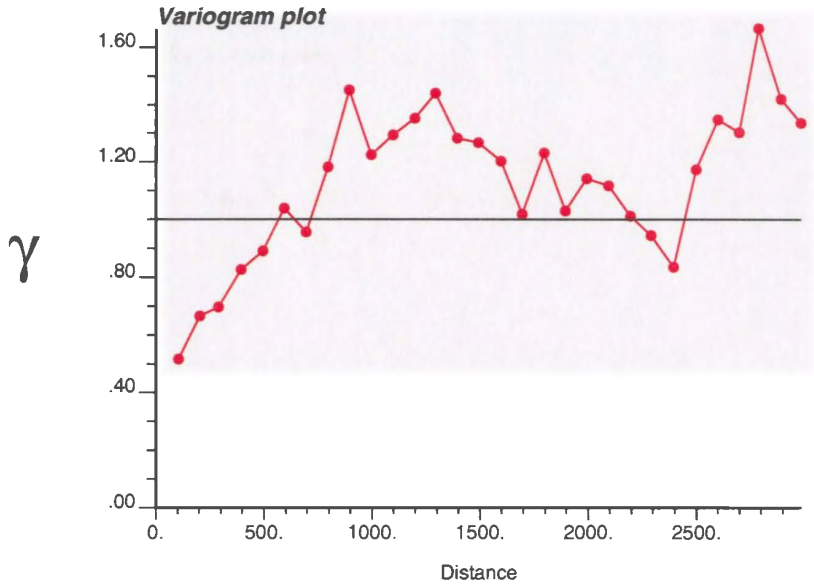

Figure 8.7: Sample Variogram Estimate - 135 Degrees

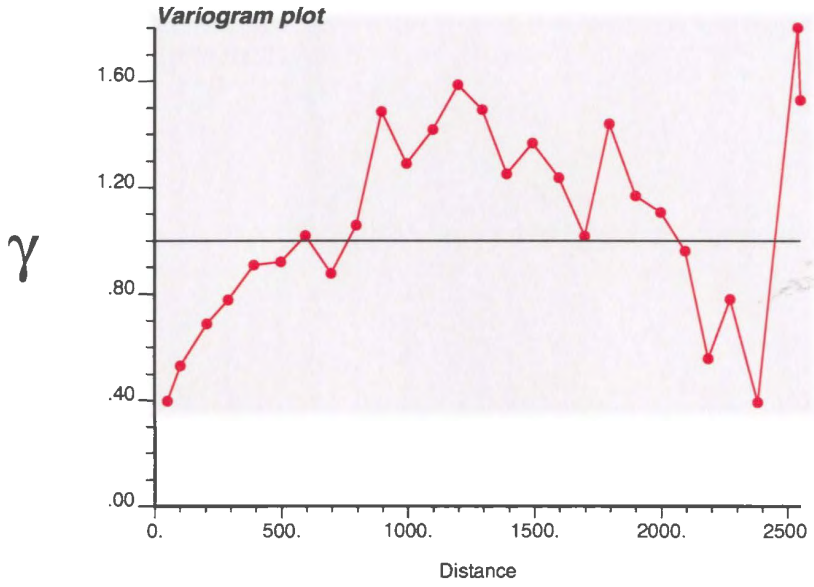

Figure 8.8: Sample Variogram Estimate - 157.5 Degrees

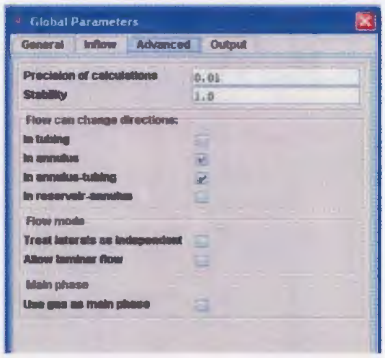

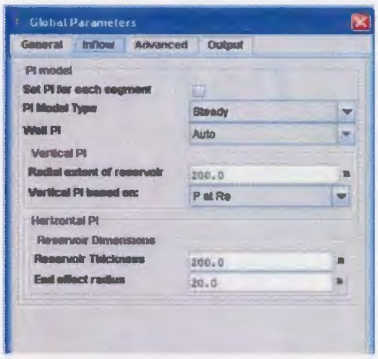

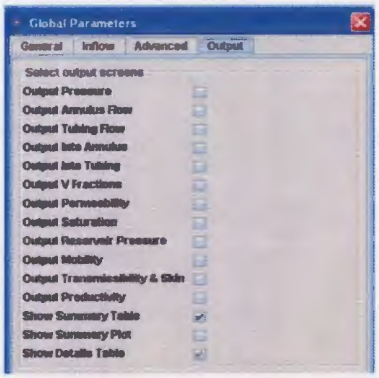

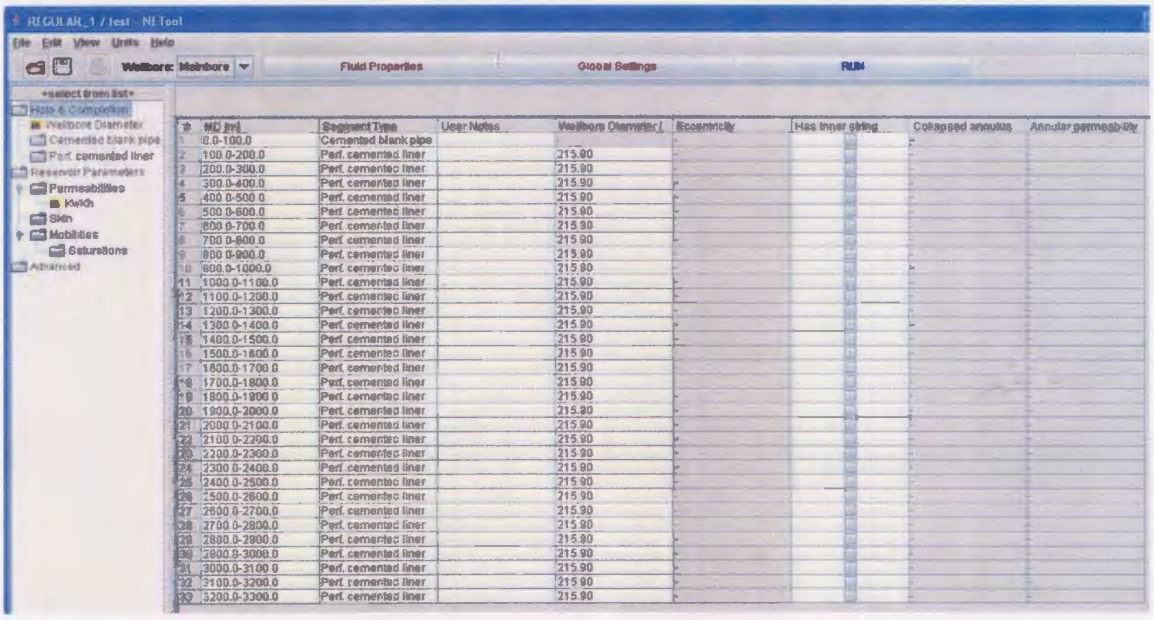

#	MD [m]	Segment Type	User Notes	Wellbore Diameter [	Eccentricity	Has inner string	Collapsed annulus	Annular permeability
1	0.0-100.0	Cemented blank pipe						
2	100.0-200.0	Perf. cemented liner		215.90				
3	200.0-300.0	Perf. cemented liner		215.90				
4	300.0-400.0	Perf. cemented liner		215.90				
5	400.0-500.0	Perf. cemented liner		215.90				
6	500.0-600.0	Perf. cemented liner		215.90				
7	600.0-700.0	Perf. cemented liner		215.90				
8	700.0-800.0	Perf. cemented liner		215.90				
9	800.0-900.0	Perf. cemented liner		215.90				
10	900.0-1000.0	Perf. cemented liner		215.90				
11	1000.0-1100.0	Perf. cemented liner		215.90				
12	1100.0-1200.0	Perf. cemented liner		215.90				
13	1200.0-1300.0	Perf. cemented liner		215.90				
14	1300.0-1400.0	Perf. cemented liner		215.90				
15	1400.0-1500.0	Perf. cemented liner		215.90				
16	1500.0-1600.0	Perf. cemented liner		215.90				
17	1600.0-1700.0	Perf. cemented liner		215.90				
18	1700.0-1800.0	Perf. cemented liner		215.90				
19	1800.0-1900.0	Perf. cemented liner		215.90				
20	1900.0-2000.0	Perf. cemented liner		215.90				
21	2000.0-2100.0	Perf. cemented liner		215.90				
22	2100.0-2200.0	Perf. cemented liner		215.90				
23	2200.0-2300.0	Perf. cemented liner		215.90				
24	2300.0-2400.0	Perf. cemented liner		215.90				
25	2400.0-2500.0	Perf. cemented liner		215.90				
26	2500.0-2600.0	Perf. cemented liner		215.90				
27	2600.0-2700.0	Perf. cemented liner		215.90				
28	2700.0-2800.0	Perf. cemented liner		215.90				
29	2800.0-2900.0	Perf. cemented liner		215.90				
30	2900.0-3000.0	Perf. cemented liner		215.90				
31	3000.0-3100.0	Perf. cemented liner		215.90				
32	3100.0-3200.0	Perf. cemented liner		215.90				
33	3200.0-3300.0	Perf. cemented liner		215.90				

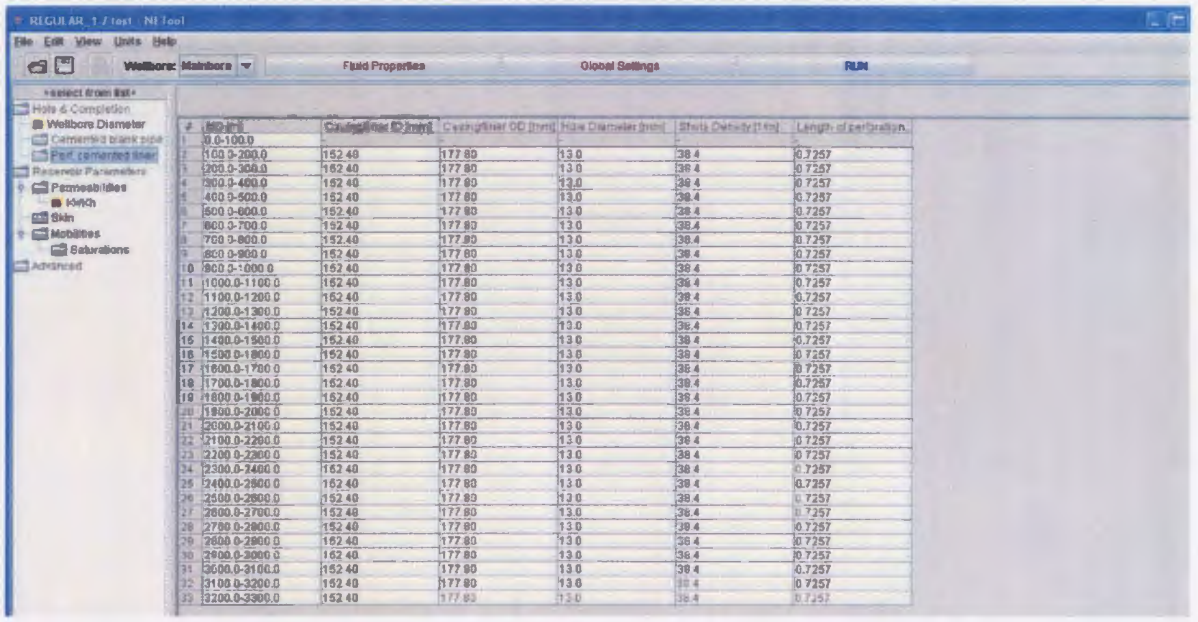

#	MD [m]	Casing/liner ID [mm]	Casing/liner OD [mm]	Hole Diameter [mm]	Shots Density [1/m]	Length of perforation
1	0.0-100.0					
2	100.0-200.0	152.40	177.80	13.0	38.4	0.7257
3	200.0-300.0	152.40	177.80	13.0	38.4	0.7257
4	300.0-400.0	152.40	177.80	13.0	38.4	0.7257
5	400.0-500.0	152.40	177.80	13.0	38.4	0.7257
6	500.0-600.0	152.40	177.80	13.0	38.4	0.7257
7	600.0-700.0	152.40	177.80	13.0	38.4	0.7257
8	700.0-800.0	152.40	177.80	13.0	38.4	0.7257
9	800.0-900.0	152.40	177.80	13.0	38.4	0.7257
10	900.0-1000.0	152.40	177.80	13.0	38.4	0.7257
11	1000.0-1100.0	152.40	177.80	13.0	38.4	0.7257
12	1100.0-1200.0	152.40	177.80	13.0	38.4	0.7257
13	1200.0-1300.0	152.40	177.80	13.0	38.4	0.7257
14	1300.0-1400.0	152.40	177.80	13.0	38.4	0.7257
15	1400.0-1500.0	152.40	177.80	13.0	38.4	0.7257
16	1500.0-1600.0	152.40	177.80	13.0	38.4	0.7257
17	1600.0-1700.0	152.40	177.80	13.0	38.4	0.7257
18	1700.0-1800.0	152.40	177.80	13.0	38.4	0.7257
19	1800.0-1900.0	152.40	177.80	13.0	38.4	0.7257
20	1900.0-2000.0	152.40	177.80	13.0	38.4	0.7257
21	2000.0-2100.0	152.40	177.80	13.0	38.4	0.7257
22	2100.0-2200.0	152.40	177.80	13.0	38.4	0.7257
23	2200.0-2300.0	152.40	177.80	13.0	38.4	0.7257
24	2300.0-2400.0	152.40	177.80	13.0	38.4	0.7257
25	2400.0-2500.0	152.40	177.80	13.0	38.4	0.7257
26	2500.0-2600.0	152.40	177.80	13.0	38.4	0.7257
27	2600.0-2700.0	152.40	177.80	13.0	38.4	0.7257
28	2700.0-2800.0	152.40	177.80	13.0	38.4	0.7257
29	2800.0-2900.0	152.40	177.80	13.0	38.4	0.7257
30	2900.0-3000.0	152.40	177.80	13.0	38.4	0.7257
31	3000.0-3100.0	152.40	177.80	13.0	38.4	0.7257
32	3100.0-3200.0	152.40	177.80	13.0	38.4	0.7257
33	3200.0-3300.0	152.40	177.80	13.0	38.4	0.7257

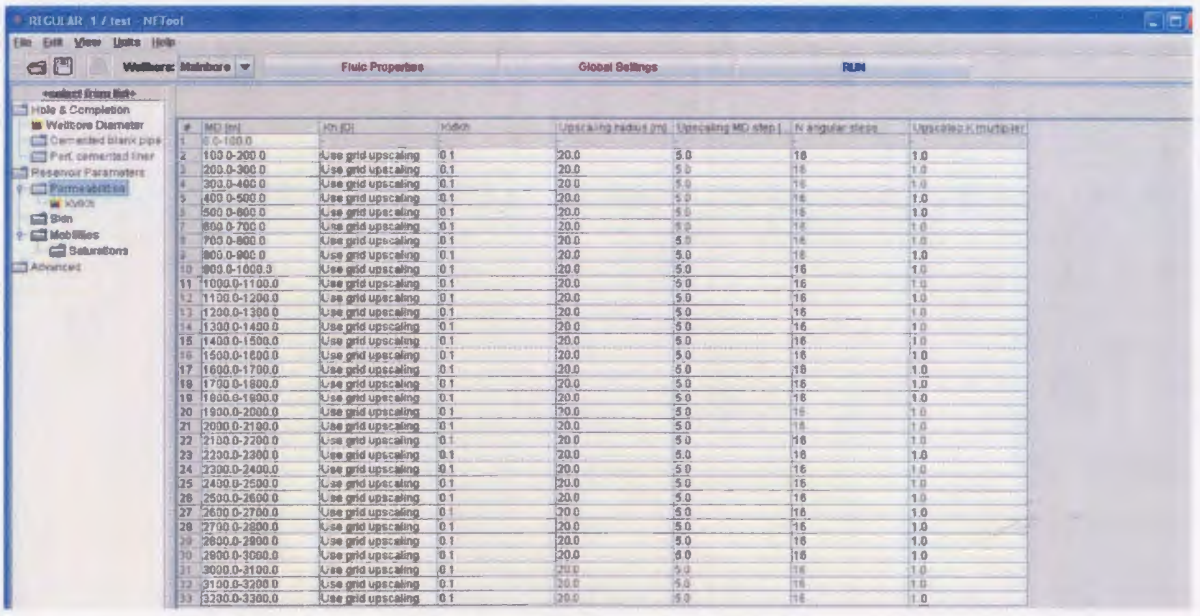

#	MD [m]	Kh [D]	Kv/Kh	Upscaling radius [m]	Upscaling MD step [	N angular steps	Upscaled K multiplier
1	0.0-100.0						
2	100.0-200.0	Use grid upscaling	0.1	20.0	5.0	16	1.0
3	200.0-300.0	Use grid upscaling	0.1	20.0	5.0	16	1.0
4	300.0-400.0	Use grid upscaling	0.1	20.0	5.0	16	1.0
5	400.0-500.0	Use grid upscaling	0.1	20.0	5.0	16	1.0
6	500.0-600.0	Use grid upscaling	0.1	20.0	5.0	16	1.0
7	600.0-700.0	Use grid upscaling	0.1	20.0	5.0	16	1.0
8	700.0-800.0	Use grid upscaling	0.1	20.0	5.0	16	1.0
9	800.0-900.0	Use grid upscaling	0.1	20.0	5.0	16	1.0
10	900.0-1000.0	Use grid upscaling	0.1	20.0	5.0	16	1.0
11	1000.0-1100.0	Use grid upscaling	0.1	20.0	5.0	16	1.0
12	1100.0-1200.0	Use grid upscaling	0.1	20.0	5.0	16	1.0
13	1200.0-1300.0	Use grid upscaling	0.1	20.0	5.0	16	1.0
14	1300.0-1400.0	Use grid upscaling	0.1	20.0	5.0	16	1.0
15	1400.0-1500.0	Use grid upscaling	0.1	20.0	5.0	16	1.0
16	1500.0-1600.0	Use grid upscaling	0.1	20.0	5.0	16	1.0
17	1600.0-1700.0	Use grid upscaling	0.1	20.0	5.0	16	1.0
18	1700.0-1800.0	Use grid upscaling	0.1	20.0	5.0	16	1.0
19	1800.0-1900.0	Use grid upscaling	0.1	20.0	5.0	16	1.0
20	1900.0-2000.0	Use grid upscaling	0.1	20.0	5.0	16	1.0
21	2000.0-2100.0	Use grid upscaling	0.1	20.0	5.0	16	1.0
22	2100.0-2200.0	Use grid upscaling	0.1	20.0	5.0	16	1.0
23	2200.0-2300.0	Use grid upscaling	0.1	20.0	5.0	16	1.0
24	2300.0-2400.0	Use grid upscaling	0.1	20.0	5.0	16	1.0
25	2400.0-2500.0	Use grid upscaling	0.1	20.0	5.0	16	1.0
26	2500.0-2600.0	Use grid upscaling	0.1	20.0	5.0	16	1.0
27	2600.0-2700.0	Use grid upscaling	0.1	20.0	5.0	16	1.0
28	2700.0-2800.0	Use grid upscaling	0.1	20.0	5.0	16	1.0
29	2800.0-2900.0	Use grid upscaling	0.1	20.0	5.0	16	1.0
30	2900.0-3000.0	Use grid upscaling	0.1	20.0	5.0	16	1.0
31	3000.0-3100.0	Use grid upscaling	0.1	20.0	5.0	16	1.0
32	3100.0-3200.0	Use grid upscaling	0.1	20.0	5.0	16	1.0
33	3200.0-3300.0	Use grid upscaling	0.1	20.0	5.0	16	1.0

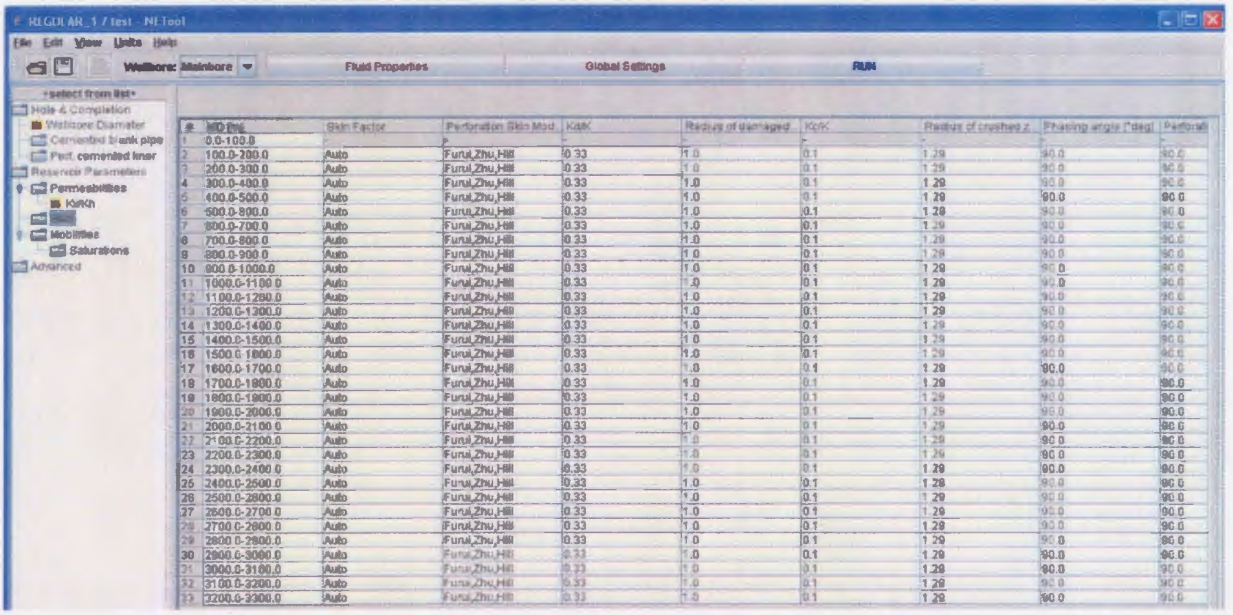

#	MD [m]	Skin Factor	Perforation Skin Mod.	Kz/K	Radius of damaged	Kd/K	Radius of crushed z	Phasing angle [deg]	Perforati
1	0.0-100.0	-	-	-	-	-	-	-	-
2	100.0-200.0	Auto	Furui_Zhu_Hill	0.33	1.0	0.1	1.29	90.0	90.0
3	200.0-300.0	Auto	Furui_Zhu_Hill	0.33	1.0	0.1	1.29	90.0	90.0
4	300.0-400.0	Auto	Furui_Zhu_Hill	0.33	1.0	0.1	1.29	90.0	90.0
5	400.0-500.0	Auto	Furui_Zhu_Hill	0.33	1.0	0.1	1.29	90.0	90.0
6	500.0-600.0	Auto	Furui_Zhu_Hill	0.33	1.0	0.1	1.29	90.0	90.0
7	600.0-700.0	Auto	Furui_Zhu_Hill	0.33	1.0	0.1	1.29	90.0	90.0
8	700.0-800.0	Auto	Furui_Zhu_Hill	0.33	1.0	0.1	1.29	90.0	90.0
9	800.0-900.0	Auto	Furui_Zhu_Hill	0.33	1.0	0.1	1.29	90.0	90.0
10	900.0-1000.0	Auto	Furui_Zhu_Hill	0.33	1.0	0.1	1.29	90.0	90.0
11	1000.0-1100.0	Auto	Furui_Zhu_Hill	0.33	1.0	0.1	1.29	90.0	90.0
12	1100.0-1200.0	Auto	Furui_Zhu_Hill	0.33	1.0	0.1	1.29	90.0	90.0
13	1200.0-1300.0	Auto	Furui_Zhu_Hill	0.33	1.0	0.1	1.29	90.0	90.0
14	1300.0-1400.0	Auto	Furui_Zhu_Hill	0.33	1.0	0.1	1.29	90.0	90.0
15	1400.0-1500.0	Auto	Furui_Zhu_Hill	0.33	1.0	0.1	1.29	90.0	90.0
16	1500.0-1600.0	Auto	Furui_Zhu_Hill	0.33	1.0	0.1	1.29	90.0	90.0
17	1600.0-1700.0	Auto	Furui_Zhu_Hill	0.33	1.0	0.1	1.29	90.0	90.0
18	1700.0-1800.0	Auto	Furui_Zhu_Hill	0.33	1.0	0.1	1.29	90.0	90.0
19	1800.0-1900.0	Auto	Furui_Zhu_Hill	0.33	1.0	0.1	1.29	90.0	90.0
20	1900.0-2000.0	Auto	Furui_Zhu_Hill	0.33	1.0	0.1	1.29	90.0	90.0
21	2000.0-2100.0	Auto	Furui_Zhu_Hill	0.33	1.0	0.1	1.29	90.0	90.0
22	2100.0-2200.0	Auto	Furui_Zhu_Hill	0.33	1.0	0.1	1.29	90.0	90.0
23	2200.0-2300.0	Auto	Furui_Zhu_Hill	0.33	1.0	0.1	1.29	90.0	90.0
24	2300.0-2400.0	Auto	Furui_Zhu_Hill	0.33	1.0	0.1	1.29	90.0	90.0
25	2400.0-2500.0	Auto	Furui_Zhu_Hill	0.33	1.0	0.1	1.29	90.0	90.0
26	2500.0-2600.0	Auto	Furui_Zhu_Hill	0.33	1.0	0.1	1.29	90.0	90.0
27	2600.0-2700.0	Auto	Furui_Zhu_Hill	0.33	1.0	0.1	1.29	90.0	90.0
28	2700.0-2800.0	Auto	Furui_Zhu_Hill	0.33	1.0	0.1	1.29	90.0	90.0
29	2800.0-2900.0	Auto	Furui_Zhu_Hill	0.33	1.0	0.1	1.29	90.0	90.0
30	2900.0-3000.0	Auto	Furui_Zhu_Hill	0.33	1.0	0.1	1.29	90.0	90.0
31	3000.0-3100.0	Auto	Furui_Zhu_Hill	0.33	1.0	0.1	1.29	90.0	90.0
32	3100.0-3200.0	Auto	Furui_Zhu_Hill	0.33	1.0	0.1	1.29	90.0	90.0
33	3200.0-3300.0	Auto	Furui_Zhu_Hill	0.33	1.0	0.1	1.29	90.0	90.0

Case Study 2 Data Summary
Total Production (100 nodes)
Base Case

Oil rate
8705.42

Oil rate						
Mean	**7508.65308**	**7996.53502**	**8138.9778**	**8173.3029**	**8272.6142**	**8377.9465**
STD	**441.3016076**	**286.298854**	**237.71587**	**213.302256**	**205.8006743**	**197.04078**
Realizations	**Stage 0**	**Stage 1**	**Stage 2**	**Stage 3**	**Stage 4**	**Stage 5**
1	7961.19	7709.16	8030.57	8067.51	8377.08	8348.31
2	7788.54	8034.47	7876.32	8166.37	7820.31	8800.73
3	7083.24	8676.85	8291.96	8124.59	8143.6	8131.92
4	7912.51	8215.49	7872.02	8070.06	8141.67	8229.65
5	7418.69	7893.03	8016.8	8322.77	8236.8	8296.19
6	7331.71	8030.41	7846.38	8355.34	8417.38	8166.77
7	7787.07	7991.61	8387.03	8019.89	7871.11	8359.83
8	7679.76	7569.9	8063.98	8341.54	8038.62	8039.96
9	7220.05	8274.8	7870.91	8180.75	8194.35	8112.72
10	6941.77	8109.13	7638.14	7800.46	8185.14	8300.45
11	7662.89	8041.24	8457.92	8168.88	8075.73	8610.22
12	8442.84	8588.46	8344.97	8185.4	8505.99	8341.79
13	7016	7546.54	7770.2	7966.38	8347.31	8671.1
14	7319.86	7576.1	8196.6	8459.41	8329.84	8391.05
15	6996.29	8178.54	8232.4	8251.47	8186.07	8376.08
16	8075.25	8138.9	8093.49	8412.22	7988.53	8333.6
17	7720.06	7866.58	7978.84	8261.71	8167.79	8507.32
18	7255.39	7281.84	7741	8262.32	8280.36	8398.55
19	7530.68	8051.63	7841.74	8488.31	8274.97	8405.3
20	7012.12	8213.85	8255.61	8339.31	8524.25	8523.34
21	6845.48	8128.71	7748.3	8161.18	8066.38	8257.58
22	7652.68	8128.71	8432.69	8103.24	8841.36	8309.48
23	7654.18	7468.69	7988.67	7929.09	7952.8	8496.2
24	7610.59	8132.8	8083.6	8198.4	8396.26	8077.72
25	7680.83	8805.23	8735.79	8208.04	8218.93	8196.18
26	6847.66	7801.74	7766.14	8284.64	8445.84	8186.43
27	7381.96	7675.64	8135.34	8214.72	7724.35	8086.39
28	6871.99	8356.53	8544.01	8505.32	8038.7	8402.66
29	7549.65	8267.42	8182.65	8470.05	8326.3	8581.45
30	7901.05	7922.3	8161.48	8252.28	8572.76	8465.95
31	7517.78	7840.14	7915.82	8073.49	8247.29	8264.61
32	7665.46	8371.86	8315.27	8016.06	8505.75	8294.11
33	7831.35	7788.16	7613.79	8085.67	8332.95	8360.5
34	7363.7	8292.59	8207.12	8589.79	8446.79	8550.09
35	8241.96	8433.78	7819.28	8538.16	8349.18	8614.09
36	7175.01	7812.91	8219.83	7899.07	8202.97	8310.07
37	8378.37	7778.39	7918.93	8125.7	8420.71	8391.19
38	7411.98	7607.56	8014.77	7886.51	8485.52	8561.14
39	7843.1	7566.47	8073.17	8492.4	8584.08	8671.18
40	7921.54	7792.76	8517.36	8108.72	8121.7	8365.57
41	7496.66	7674.14	8250.29	8396.38	8570.06	8277.58
42	7464.61	8201.13	8269.18	8110.46	7927.33	8030.74
43	8164.77	7803.97	8404.55	7878.25	8378.87	8064.7
44	7391.46	7656.6	8263.24	8039.47	8120.05	8530.65
45	7702.09	7669.08	8170.02	8270.7	8237.19	8736.45
46	7362.29	7531.31	8339.59	8000.21	7915.87	8501.53
47	7071.41	7976.96	7956.49	8014.08	8615.58	8447.32
48	6689.51	7391.2	8482.66	8220.95	8395.74	8396.67
49	7259.88	8139.62	7843.46	8393.05	8341.78	8474.87
50	7078.74	8016.51	8267.51	8278.65	8369.16	8262.18

51	8314.8	7945	7948.67	8271.94	8186.45	8364.26
52	7126.65	7962.61	8006.19	7799.9	8219.55	8354.18
53	7071.29	7625.99	8213.92	8105.35	8243.21	8623.17
54	7283.26	8075.85	8341.88	8780.69	8261.52	8690.65
55	7487.8	7942.92	7709.36	8176.55	8369.29	8624.51
56	6811.72	8305.46	8116.58	8319.34	8337.46	8539.14
57	7117.45	8322.9	8141.88	8431.19	8201.98	8547.94
58	7027.26	7888.01	8122.22	8276.84	8528.43	8501.02
59	7309.44	8208	7676.3	8323.89	8044.88	8449.3
60	7286.68	8269.07	7820.14	8137.14	8343	8376.54
61	7489.67	7982.32	8355.58	8338.78	8699.03	8527.79
62	8105.26	8151.24	8336.54	8286.53	8483.73	8410.89
63	7105.97	8028.12	8184.58	8270.19	8021.48	8289.28
64	8229.95	7981.05	8409.95	8082.72	8543.9	8270.15
65	7290.78	7785.19	7960.85	8193.06	7870.58	8808.81
66	7109.78	7553.3	8372.44	8125.51	8181.3	8311.04
67	6721.8	7985.08	8170.22	8064.3	8216.25	8472.76
68	7375.19	7551.24	7952.22	8183.33	8301.01	7994.83
69	7629.74	7692.16	8049.16	8425.94	8116.53	8275.63
70	7495.72	7708.68	8438.04	8226.51	8371.55	8048.42
71	7971.6	8208.41	8249.46	8089.39	8674.34	8212.77
72	7082.98	8285.94	8093.36	7972.74	8171.87	8700.89
73	7551.96	7824.37	8310.49	8350.75	8157.38	8074.56
74	7050.97	8590.76	8025.69	7868.3	8173.61	8222.55
75	7510.68	8320.55	8122.29	8542.12	8029.23	8465.6
76	7250.7	7529.64	7997.1	8345.95	8685.34	8827.86
77	7962.56	8221.35	8162	7720.4	8044.83	8371.76
78	7422.56	7964.16	8179.77	7790.43	8481.15	8180.73
79	7398.12	8053.89	8578.86	8220.57	8027.74	8557.73
80	7886.95	7728.49	7942.2	8224.83	8288.13	8417.03
81	7946.66	8117.17	8179.8	8364.06	8124.43	8274.32
82	7768.36	7846.3	8315.95	8434.99	8279.81	8623.01
83	6841.88	8580.63	8098.24	8379.67	8350.97	8391.03
84	7491.82	8521.85	7803.16	8188.45	8327.09	8487.03
85	8008.13	8235.56	8370.42	8431.89	8391.12	8547.3
86	8444.56	7884.07	8050.2	7913.45	8291.41	8505.86
87	6837.26	7993.09	7918.03	8294.78	8450.1	8368.72
88	7625.53	7545.75	8079.8	8161.03	8380.72	8352.06
89	6974.66	7939.42	8018.12	8110.53	8192.67	8258.14
90	6873.43	7687.24	8044.39	8009.79	8086.16	8266.71
91	7963.99	7864.01	7820.27	8061.45	8303.61	8253.04
92	7527.44	8247.5	8103.96	8300.99	8369.77	8005.94
93	7889.94	8098.11	8231.46	7820.11	8109.29	8411.18
94	7368.16	8697.93	7935.6	8017.57	8275.36	8585.79
95	7353.56	7774.43	7523.89	8450.63	8137.15	8641.44
96	7272	7863.17	7804.17	7915.39	8510.24	8544.51
97	7455.68	8350.12	8058.15	8490.42	8106.41	8517.74
98	7615.02	8075.01	8093.39	8196.7	8345.15	8101.09
99	7177.29	8100.95	7744.66	8287.06	8165.55	8403.61
100	8022.61	8161.26	8550.71	8242.96	8208.16	8492.93
101	8456.45	8043.73	7947.58	8412.57	8484.3	8043.03
102	7924.66	8142.92	8020.14	8514.44	8477.96	8318.61
103	7501.45	8391	8313.5	8127.17	8360.03	8715.9
104	7879.34	8332.63	8192.73	8373.52	8581.56	8673.45
105	7688.52	7987.78	8319.97	8325.27	8286.61	8320.04
106	7669.2	7995.61	8125.38	8368.45	7969.66	8267.08
107	7719.3	7925.55	8207.56	8219.51	8647.93	8570.53
108	7732.56	7812.34	8514.66	8501.91	8309.99	8555.03
109	7137.71	8083.5	8257.92	8237.65	8465.18	8457.25
110	7535.8	7851.6	8427.16	7967.06	8206.74	8066.98
111	6862.5	8122.91	7764.91	7826.46	8266.86	8560.11

112	6709.83	8136.4	7478.52	8129.05	8089.82	8172.47
113	7912.97	8086.31	7984.49	8221.71	8024.46	7994.62
114	7422.6	7773.43	8497.27	8541.45	8293.01	8643.23
115	7389.4	8255.55	7482.77	8354.36	7935.66	8010.55
116	7463.89	8025.33	8165.88	8019.07	8253.66	8508.47
117	7702.2	8111.03	8332.92	7928.49	8450.51	8478.63
118	6602.12	8036.47	8361.43	8333.75	8609.29	8493.89
119	7022.36	7861.69	8072.97	8130.22	8212.19	8366.52
120	7697.19	7853.01	8336.78	8418.8	8397.08	8138.93
121	8167.84	7945.94	8093.61	8214.65	8561.36	8417.48
122	7488.13	8196.91	7781.19	8006.07	8359.65	8295.32
123	6711.33	8368.48	8275.23	8478.32	8261.89	8185
124	7607.79	7593.57	8520.04	7955.34	8046.72	8473.75
125	7277.01	7934.58	7937.54	8196.33	8046.72	8439.02
126	6826.54	7820.13	8093.35	8435.31	8535.8	8213.82
127	7457	8145.53	7887.32	8020.57	8207.07	8418.72
128	7464.57	7853.4	7982.59	8293.34	8172.47	8148.47
129	8016.35	7792.33	7950.03	8063.87	8596.54	8392.09
130	8055.11	8431.49	8722.85	8256.52	8135.05	8359.95
131	6915.61	7730.58	8134.39	8238.88	7959.07	8311.05
132	7074.72	8086.33	8199.61	7992.12	8242.28	8376.91
133	7347.58	7842.57	8370.85	7920.49	8196.5	8587.64
134	7389.66	7986.81	7868.09	7959.81	8389.57	8387.27
135	7923.36	8285.66	7999.14	7945.53	8282.31	8461
136	7265.42	8211.6	8420.68	8322.28	8172.03	8280.23
137	6676.99	7989.92	7938.28	8123.84	8370.94	8206.25
138	7127.55	7996.59	7839.95	8231.78	8004.57	8370.67
139	7646.55	7550.36	8214.79	8651.97	7990.07	8418.23
140	6842.17	8367.01	8016.2	8562.1	8062.86	8233.23
141	7826.02	8139.53	8194.99	8229.28	8551.79	8549.42
142	7383.26	8375.47	8164.65	8322.75	8522.84	8479.43
143	7538.3	8204.91	8424.45	7813.52	8478.72	8102.8
144	7315.76	7315.75	8503.87	8138.46	8117.15	8324.69
145	6929.22	8085.28	8124.55	7835.06	8333.46	8301.18
146	7168.59	8163.2	7961.93	7800.95	8421.54	8229.77
147	6983.5	7850.44	7795.88	8049.81	8216.8	8312.2
148	7764.53	8123.3	7960.81	8273.38	8373.74	8408.81
149	7776.85	7610.26	8381.56	8408.06	7900.9	8430.92
150	7338.44	8126.1	8213.85	8180.55	8509.18	8133.08
151	7554.17	7270.88	8225.58	8527.81	8014.71	8431.87
152	7070.53	7707.45	8082.23	8246.56	8486.9	8481.07
153	7856.1	7791.43	8174.11	8118.98	8402.28	8564.62
154	7932.61	7784.52	8320.35	8041.14	8336.42	8509.19
155	6963.06	7992.93	8302.32	8171.92	8186.69	8758.5
156	7525.57	8267.21	7873.48	7961.64	8374.47	8475.17
157	7818.55	8131.01	8180.56	8083.53	8072.7	8444.24
158	6948.28	7763.1	7865.47	7913.49	8461.68	8607.41
159	7014	8263.34	8351.71	7785.49	8303.98	8458.53
160	7149.76	8034.29	8158.52	8353.58	8118.51	8597.08
161	6893.49	8390.02	8172.07	8286.74	8239.41	8518.36
162	8109.45	8183.96	7967.55	8310.18	7964.46	8413.12
163	8309.7	8109.54	8332.47	8251.71	7779.41	8414.47
164	7366.6	8359.46	7810.84	8035.22	8020.11	8491.83
165	7394.47	7811.4	8049.78	8047.99	8249.03	8630.35
166	7694.22	7830.68	8213.94	8485.24	8493.15	8375.64
167	7675.13	7917.4	7946.69	8040.2	8283.7	8463.57
168	7358.56	8246.34	8029.81	7936.99	8368.67	8523.07
169	7590.75	8486.53	7816.1	8010.64	8097.56	8513.71
170	7680.66	8308.79	8425.56	8203.28	8633.94	8552.77
171	7843.02	7774.39	8376.19	8138.08	7948.31	8643.04
172	7346.42	7763.35	8066.28	7802.07	8425.68	8286.17

173	7528.49	7946.43	8004.74	7735.14	8009.86	8454.59
174	6698.42	7759.2	8552.67	7815.31	8322.29	8438.99
175	7577.78	7823.59	8009.07	8089.03	8038.36	8508.3
176	7564.99	7790.77	8243.15	7826.59	8289.5	8571.48
177	7189.99	8132.66	7565.39	8253.15	8273.4	8170.87
178	6395.41	8484.4	8469.25	8146.79	8483.66	8302.9
179	7109.75	8009.96	8129.39	8247.61	8114.4	8620.2
180	8326.66	8071.01	7785.08	8051.26	8288.4	8236.57
181	7430.17	7732.83	7678.53	8393.81	8271.92	8358.93
182	7614.74	7732.83	8046.7	8085.87	8367.62	8501.94
183	7747.88	8478.64	7641	8286.87	8015.36	8303.61
184	6908.51	8208.39	8129.73	8406.28	8383.34	8854.35
185	8070.76	7978.74	8005.16	8080.1	8287.68	8370.37
186	6867.82	7840.4	8172.43	8222.54	8364.14	8600.88
187	7987.5	7975.08	8097.66	8212.34	8445.04	8490.46
188	7899.31	7613.11	7984.28	8063.6	8391.3	8095.11
189	7248.25	7918.77	8037.97	8020.26	8308.69	8585.16
190	7641.86	7286.1	7925.62	7932.15	8109.18	8210.04
191	8037.15	8525.26	8247.56	8201.87	8263.94	8294.62
192	7771.24	7818.93	7932.82	8642.48	8427.24	8472.7
193	7566.28	8395.2	8162.16	8199.91	8717.26	8511.47
194	7171.5	7811.58	8144.81	7952.58	8564.97	8347.02
195	7098.54	8100.72	8732.39	8152.77	8292.81	8512.43
196	7954.61	7713.29	7961.85	8320.39	8735.02	7942.35
197	7560.67	7692.53	8454.14	7680.65	8052.59	8145.15
198	6960.38	8322.6	8430.87	7733.93	7959.88	8182.1
199	6709.64	7678.53	8196.5	7647.08	8357.26	8363.38
200	7640.92	7630.15	8379.54	8278.64	8089.8	8438.15
201	7773.7	7739.12	8269.89	8648.22	8273.91	8163.67
202	7152.55	7964.91	7903.33	8503.02	8370.01	8385.5
203	7093.14	8703.22	7833.25	8393.08	8332.34	8123.1
204	7367.65	8378.22	7823.08	8223.34	8307.96	8618.39
205	7722.53	8251.93	8217.69	8334.83	8232.83	8070.03
206	8120.6	7606.06	8657.86	7993.64	8347.19	8693.68
207	7258.18	7606.06	8449.66	8354.61	8399.33	8465.4
208	7259.88	8239.27	8246.37	7986.14	8150.89	8130.96
209	8083.61	7821.77	8055.73	8579.72	8571.4	8569.17
210	7514.28	7887.36	8080.76	8229.77	8173.98	8376.19
211	7836.39	8351.52	8305.95	8383.29	8221.66	8383.41
212	7286.37	7918.04	8242.28	8547.01	8257.25	8601.32
213	8058.89	8077.54	8455.12	8363.56	8513.03	8163.03
214	7873.85	7946.58	8061.25	8340.75	8199.22	8043.5
215	7778.11	8033.22	7879.85	8477.95	8191.67	8340
216	7651.21	7662.85	8017.88	7843.44	8003.07	8027.73
217	7531.35	7797.54	8694.14	8108.13	8506.49	8270.18
218	6658.38	8150.55	8331.89	8116.63	7955.45	8623.77
219	7632.13	7701.48	8137.21	8058.25	8306.01	8361.81
220	8324.5	8202.66	8567.35	7926.4	8148.5	8139.2
221	7166.32	8025.16	7995.95	8265.36	8226.11	8602.23
222	7860.21	8040.89	8491.59	7905.75	8235.59	8367.56
223	8324.73	7759.18	7913.32	8242.74	8254.02	8432.1
224	7753.51	8363.94	8063.09	8364.63	8171.64	8621.25
225	7047.24	8419.58	8181.32	8282.54	8410.02	8835.91
226	8006.7	7791.17	7975.1	8316.29	8255.49	8162.52
227	6906.11	8043.4	8323.94	8261.26	8301.96	8233.85
228	7508.67	8039.54	7693.26	7725.38	8223.96	8412.35
229	6791.84	8548.3	7821.43	7770.52	8018.99	8134.07
230	7759.68	7999.49	8411.15	7970.84	8563.06	8444.98
231	7144.06	8195.72	8103.64	8091.96	8344.38	8336.72
232	8039.79	8090.44	8250.91	8149.47	8277.2	8419.72
233	7757.32	7577.45	8095.11	7852.22	7997.5	8509.7

234	7443.69	8155.83	7994.73	8244.6	8328.38	8282.57
235	7057.74	8322.48	8319.49	8143.71	8090.34	8538.71
236	7077.47	8259.74	7756.09	8461.87	8075.67	7924.79
237	8039.01	8002.58	7958.67	7989.78	8122.08	8433.03
238	7567.74	7950.94	8457.33	8012.86	8387.89	8347.22
239	7560.8	7960.05	7918	8559.25	8300.06	8063.56
240	7763.16	8620.39	8165.95	7889.05	8562.13	8130.77
241	6827.84	7891.83	8360.48	8023.05	8340	8117.14
242	8139.87	7788.94	8360.41	8440.8	8368.2	8301.99
243	7907.89	7806.28	7793.71	8246.14	7892.93	8725.85
244	6608.21	7999.52	8147.75	8149.66	7955.14	8398.83
245	7815.2	8090.39	7914.21	8085.19	8511.97	8496.09
246	7844.34	8289.98	8025.95	8240.16	7862.57	8738.56
247	8115	8626	8187.96	8130.59	8565.62	8518.15
248	8142.31	8030.22	8314.17	8357.31	8410.67	8373.16
249	7975.48	8366.65	8075.61	8239.74	8250.97	8774.77
250	8199.39	7884.68	8222.82	7746.05	8343.2	8379.87
251	7110.66	8075.98	8251.08	8119.78	7897.22	8433.13
252	7647.98	8088.95	8437.98	8324.77	8287.3	8266.81
253	7746.16	8360.35	7958.58	7955.59	8149.91	8300.84
254	6939.42	8122.22	8343.62	8125.01	8473.88	8215.52
255	6865.85	7998.75	7976.65	8244.23	8527.33	8504.1
256	7542.59	7474.13	8341.24	8420.83	7944.64	8437.3
257	8123.58	8323.22	8558.37	8003.66	8321.81	8353.24
258	7638.06	8286.42	7785.4	8394.82	8080.5	8419.8
259	7424.21	8360.02	8106.63	7945.63	8794.59	8157.77
260	7493.83	7593.44	8379.38	8512.09	7952.15	8559.13
261	6577.33	8159.34	8443.59	8204.93	8386.85	8289.85
262	7643.08	7919.72	8067.56	8010.47	8249.86	8136.62
263	7653.75	8182.12	8110.1	8358.71	8068.37	8329.51
264	7302.76	7877.83	7950.75	8329.31	8273.68	8592.02
265	7513.75	8343.48	7807.42	8171.96	7982.6	8573.88
266	7428.4	7923.1	8135.79	8313.68	8367.19	8178.94
267	7769.34	7668.79	7985.86	7865.44	8325.21	8248.76
268	7638.67	7932.62	8020.76	7959.32	8653.88	7996.86
269	8050.43	8420.78	7881.17	7926.34	8525.92	8196.54
270	7249.59	7872.33	8312.04	8158.58	8756.29	8341.19
271	7023.21	7652.4	7888.59	7813.25	8017.13	8579
272	7025.15	8231.64	8403.79	8355.37	8385.68	8548.77
273	7725.92	7685.22	8278.55	7761.98	8409.7	8861.42
274	8094.35	7276.15	8019.15	8610.18	7975.25	8412.19
275	8066.75	8321.41	8219.17	8010.03	8513.26	8150.1
276	7779.33	7622.1	8417.19	8834.32	8207.52	8688.95
277	7388.32	8325.31	8275.48	7913.52	8375.15	8044.6
278	7538.06	7993.6	8096.84	8106.81	8298.35	8462.6
279	7900.22	7853.5	8148.87	8057.5	8336.21	8475.81
280	6271.82	8398.42	7995.7	8388.04	8188.23	8412.64
281	7482.51	7914.3	7837.28	7828.2	8457.49	8577.87
282	7492.81	7880.32	8341.87	8296.04	7890.22	8482.2
283	7975.79	7507.81	8494.47	7990.28	7607.74	8049.34
284	6709.57	7808.68	7775.51	8327.3	7993.09	8499.99
285	7683.27	7590.73	8183.81	8449.85	8575.11	8429.09
286	6963.24	8403.81	8154.01	8239.09	8459.04	8201.65
287	7956.14	7721.18	7846.57	8193.3	8515.61	8389.13
288	7503.14	7809.55	8267.36	7906.08	8005.54	8331.33
289	6784.96	7803.77	8125.68	8343.14	8059.26	8402.94
290	7363.18	7995.67	7878.19	7738.12	8035.91	8268.03
291	8277.4	8365.2	8084.28	8394.07	8186.25	8307.41
292	8211.81	8409.47	8267.79	8251.11	8252.67	8488.37
293	8075.7	8187.42	8199.99	8180.84	8318.34	8471.52
294	7037.09	8368.94	8471.9	8543.09	8395.17	8254.78

295	7401.32	8509.55	8225.34	8152.19	8377.55	8251.64
296	6777.54	8354.18	8042.49	8406.49	7972.93	8035.92
297	8227.85	8222.85	8352.56	8375.53	8345.59	8567.1
298	7339.71	7928.88	8233.83	8112.69	8238.94	8551.32
299	7418.99	7886.68	8250.53	7980.76	8449.81	8570.69
300	7509.78	7372.17	8118.06	8448.22	8013.7	8289.63
301	7228.35	8038.88	8202.5	7939.06	8262.05	8859.29
302	7754.4	7926.2	7905.3	8197.89	8216.02	8460.68
303	6334.3	7685.25	7978.18	7989.98	8546.03	8664.27
304	8195.27	8413.52	8134.37	8289.9	8063.69	8359.45
305	7136.79	7899.36	8251.78	8017.53	8253.66	8437.45
306	7505.07	8189.52	7354.82	8139.12	8029.06	8667.47
307	7847.97	8540.19	8583.34	8214.95	8192.71	8587.59
308	7216.22	8098.05	8387.39	8373.49	8501.23	8260.01
309	7926.96	7758.43	8332.47	8321.06	8288.97	8357.85
310	6854.26	7872.21	8162.71	8134.2	8518.87	8112.48
311	7147.69	8568.17	8365.35	8429.4	8506.71	8076.8
312	7200.13	7950.39	8048.11	8214.81	8151.78	8396.88
313	8028.08	7907.07	8234.67	7896.61	8432.37	8123.62
314	7712.33	8129.37	8313.12	8338.86	8226.63	8399.83
315	7580.41	7842.59	8224.15	8545.14	8418.25	8537.16
316	7758.26	7924.8	8174.37	7996.47	8002.48	8338.6
317	7298.1	8159.45	8073.99	8133.42	7801.35	8345.65
318	8671.3	7498.13	8512.34	8106.73	8418.92	8005.3
319	6689.1	7972.93	7855.91	7926.95	8296.48	8343.96
320	7934.99	7622.54	8014.95	7757.78	8457.27	8127.29
321	7408.5	7658.86	8244.28	8257.63	8184.17	8350.88
322	7244.93	8224.25	7935.74	8036.1	8792.45	8360.01
323	7131.57	7709.61	8101.62	8139.49	8196.71	8464.67
324	7479.64	7767.92	8133.69	8009.3	8417.74	8667.77
325	7633.76	8098.33	7943.22	8130.08	8374.11	8396.86
326	7840.46	8260.84	8095.75	8197.39	8225.54	8507.47
327	7185.43	8140.17	7967.49	7958.45	8053.37	8818.59
328	8316.57	8574.79	8494.96	7719.34	8019.75	8402.22
329	7179.31	8345.56	8433.45	8361.29	8075.89	8368.79
330	7877.37	7391.96	8140.72	7638.68	8155.93	8323.42
331	8010.6	8398.87	7911.9	8143.77	8210.86	8425.81
332	7609.85	7724.24	8708.1	7786.8	8209.66	8321.26
333	8025.7	7962.07	8235.39	8497.68	8317.28	8439.39
334	7610.66	7802.8	8176.26	8122.45	8241.07	8478.87
335	5740.61	7681.16	8265.45	7702.27	8023.13	8041.67
336	7686.23	7953.09	8225.69	7822.32	7941.08	8651.96
337	8126.76	7820.84	8300.71	8299.72	8358.16	8228.61
338	7808.12	8186.14	8081.55	8313.78	8440.55	7888.91
339	7774.31	7935.82	8136.19	7719.41	8324.03	8154.8
340	7707.08	7727	8281.93	8318.42	8286.24	7909.55
341	7662.12	8252.07	8481.5	8244.95	8093.92	8447.51
342	7339.27	7219.98	8177.14	7975.09	8010.89	8062.04
343	8111.18	8185.84	7889.75	8456.04	8182.06	8306.76
344	7299.82	7827.07	8403.27	8166.97	8232.35	8270.71
345	7183.7	8142.56	8013.19	8544.93	8604.25	8071.93
346	8056.38	7902.7	8217.6	8604.08	8378.95	7930.11
347	7026.2	7930.99	8418.75	8250.4	8754.7	8271.44
348	7711.42	7799.36	8490.42	8432.42	8169.97	8068.79
349	7680.67	7495.53	7743.79	8242.45	8433.14	8473.98
350	8055.08	7396.45	8447	7919.22	7913.38	8566.07
351	6968.78	8204.12	7916.95	8257.85	8164.28	8189.19
352	7404.39	7328.59	8365.82	8083.66	8227.19	8370.74
353	7988.94	8158.77	8356.16	8008.87	8291.14	8322.24
354	6922.01	8141.95	8157.27	8442	8197.63	8542.21
355	7514.92	8089.96	7891.7	8066.39	8189.97	8268.79

356	7961.82	8212.29	8234.99	7982.78	7926.6	8518.25
357	8044.67	7923.71	8194.05	7888.15	7885.48	8075.04
358	7767.75	8090.17	7970.85	8093.9	8823.98	7887.59
359	7149.07	8086.44	8608.18	8078.55	8093.85	8480.52
360	7173.41	7698.74	8646.31	8203.46	8067.44	8252.71
361	7068.08	8455.31	8094.66	8096.32	8429.57	8549.83
362	8126.95	7613.57	7923.65	8297.56	8315.04	8205.86
363	6997.43	7493.93	7757.5	8044.35	8621.12	8447.22
364	7945.5	8010.62	8421.3	8241.8	8404.44	8602.24
365	7576.53	8308.82	7923.85	8065.75	8075.77	8256.8
366	6902.27	8311.2	8277.46	7978.76	8359.87	8061.19
367	7898.22	7859.01	7869.05	8353.04	8163.06	8764.13
368	7371.58	7951.98	8368.08	8209.03	8440.56	8323.56
369	7110.65	7501.66	7893.44	7705.07	8027.59	8375.27
370	8249	8160.12	8014.48	8281.95	8650.08	8584.37
371	8209.76	7970.2	7935.69	8395.02	8296.74	8407.71
372	6754.34	8133.75	8476.28	8113.19	8207.09	8191.69
373	8124.16	7699.46	8327.62	8176.56	8113.17	8132.63
374	7439	7861.27	7866.23	8376.72	8217.21	8637.01
375	7388.23	7874.4	8108.57	8539.63	8290.58	8166.39
376	7653.66	8034.47	7695.14	8253.38	8411.33	8473.27
377	8219.81	7897.27	7934.76	8233.52	8281.31	8431.66
378	7720.76	7720.15	7885.99	8097.87	8452.23	8611.42
379	8256.66	7861.9	7743.44	8184.77	8638.45	8549.03
380	7635.4	7877.48	7940.14	8609.3	8182.95	8346.49
381	7785.86	8265.88	8178.83	8110.43	8267.94	8561.99
382	8206.04	8038.9	7783.08	8164.52	8316.05	8119.33
383	7097.04	8379.19	8137.41	8373.29	8416.7	8279
384	7005.91	7962.15	8137.41	8555.31	8379.05	8451.45
385	7316.49	7817.73	8609.58	8142.89	8003.29	8739.52
386	7571.39	7805.79	8228.59	7792.62	8082.05	8407.24
387	7957.56	7871.73	8050.31	8273.54	8135.36	8380.4
388	8145.33	7934.8	8219.78	8383.24	7994.08	8417.02
389	7279.06	7827.22	7971.64	8382.9	8537.4	8398.68
390	7066.62	8052.43	7741.66	8260.1	8545.43	8465.34
391	7963.59	8063.31	8365.18	8271.65	8040.61	8523.23
392	7186.42	8230.1	7883.62	7909.41	8068.41	8607.72
393	7079.19	8034.54	8102.2	7790.19	8044.98	8693.34
394	7358.02	8162.12	7996.08	8088.9	8579.43	8523.98
395	7878.97	7765.16	8008.57	8324.1	8300.24	8424.18
396	8145.39	7634.6	8098.92	7955.71	8265.13	8691.02
397	7041.03	7693.68	8040.64	8147.01	8159.5	8505.28
398	7227.92	7733.09	8091.58	8360.93	8474.79	8614.27
399	7700.16	7688.5	8191.87	8158.12	8511.17	8093.87
400	6862.57	7482.1	8185.67	7968.63	8121.81	8251.51
401	6814.72	7628.74	8606.29	7955.7	8055.88	8141.16
402	7781.36	8171.09	7863	8289.36	8694.7	8449.42
403	7956.51	7779.2	8375.94	8067.22	8514.84	8459.15
404	7773.66	8200.12	8129.85	8205.73	8463.73	8566.78
405	7341.33	8174.92	7936.82	8310.66	8189.53	8272.65
406	7455.05	8158.58	8059.69	8341.57	8193.02	8409.54
407	7414.42	7966.64	7759.33	8234.64	8172.65	7999.5
408	8124.58	8208.02	8423.13	8367.7	8529.12	8400.87
409	7657.95	7564.38	8327.32	8012.05	8093.95	8617.52
410	7895.49	8303.34	8454.07	8135.5	8670.28	8697.37
411	7644.65	7852.33	7991.4	8493.02	8140.87	8326.34
412	7296.04	8466.17	7907.87	8024.86	8548	8441.77
413	7374.21	8388.42	7939.23	7957.2	8382.48	8046.52
414	7707.29	7750.38	8182.26	8171.89	8435.06	8149.6
415	7643.6	8603.32	8125.8	8562.32	8354.05	7868.71
416	6909.61	8267.91	8000.45	8035.09	8403.92	8245.16

417	7183.35	7699.76	8173.99	8200.52	8294.61	8216
418	8148.7	8206.87	8513.79	8253.69	8395.99	8386.46
419	6864.32	7805.45	7953.27	8130.44	7993.05	8110.22
420	7596.5	7854.24	8105.73	8259.16	8654.77	8736.48
421	8223.1	7899.56	7775.81	7977.18	8014.86	8361.41
422	6925.14	8254.09	7719.83	8494.47	8003.79	8151.97
423	8502.85	8253.7	7822.76	8517.33	8295.83	8653.33
424	7595.16	8031.45	8197.4	8510.36	8203.95	8287.81
425	7428.31	8386.59	7966.73	8255.48	8130.82	8381.83
426	7275.82	8450.59	8232.18	8107.95	8527.6	8508.55
427	7390.59	8154.15	8482.68	8026.8	8334.31	8438.9
428	7477.8	8462.65	8066.53	8144.15	8108.87	8416.68
429	7586.84	7932.46	8009.96	8087.8	8602.99	8454.35
430	7823.75	8172.86	7620.15	7824.15	8765.56	8428.5
431	7560.35	8533.68	7785.36	8332.76	7971.44	8669.02
432	6879.71	7449.5	8376.87	8223.31	8610.82	8551.89
433	8000.24	7766.18	8382.03	8172.62	8369.61	8047.25
434	7719.94	8338.28	7850.75	8325.39	8531.16	8281.38
435	7856.05	8673.6	8421.74	8205.17	8424.03	8491.08
436	7711.77	8204.54	7770.17	8313.12	8265.69	8292.31
437	6953.94	7850.84	8328.15	8035.21	8355.03	8357.03
438	7757.46	7856.04	8431.62	8225.35	7934.67	8480.48
439	7742.97	7695.07	8223.14	8127.38	8479.92	8164.43
440	7687.84	8056.35	8190.85	8142.94	8291.77	8247.9
441	7870.67	7798.69	8611.85	8293.39	8681.66	8416.38
442	7649.26	7908.79	8621.86	7916.32	8166.67	8399.1
443	8254.45	7793.33	8394.99	8253.82	8439.49	8434.87
444	7846.93	7640.37	7772.49	8285.21	8431.6	8282.47
445	7580.13	8062.07	8058.53	8186.99	7980.63	8109.54
446	7410.43	7864.06	8122.65	8577.33	8509.19	8672.86
447	7339	7654.04	8082.84	8427.06	8057.73	8618.91
448	6877.72	8429.98	7541.69	8130.2	8196.83	8291.81
449	7991.72	8015.33	8108.84	8174.21	8129.75	8316.8
450	7709.98	8204.02	8526.58	7892.07	8397.23	8270.48
451	7269.28	7478.22	8190.24	8300.69	8101.55	8344.39
452	7586.4	8108.14	8470.75	7823.98	8250.23	8389.75
453	7217.26	7979.17	7983.72	8108.81	8231.28	8678.65
454	7488.85	7852.78	8289.73	8263.54	7952.04	8252.44
455	7171.59	8148.4	8283.62	8264.33	8175.47	8569.73
456	6630.85	7950.1	8136.41	8171.38	7959.56	8220.75
457	8183.74	8191.84	8100.2	8355.5	7920.76	8606.64
458	6919.49	7684.74	8205.18	8046.97	8304.52	8066.82
459	8185.55	7904.56	8304.11	7989.96	8299.03	8296.96
460	7997.05	7889.46	8318.39	7809.84	8148.19	8480.04
461	7398.15	8324.3	7990.53	8359.38	8200.37	7975.17
462	8059.17	7639.66	8498.19	8019.63	8291.64	8663.59
463	7098.17	8088.53	8250.71	8289.56	8198.95	8191.91
464	7306.28	8398.04	8376.96	8502.5	8514.47	8344.48
465	7183.04	8162.72	8202.2	8627.68	8303.24	8435.81
466	6674.5	7823.47	7880.44	8275.01	8259.39	8392.52
467	7022.31	8380.87	8355.11	7927.92	8114.1	8782.74
468	7128.04	7790.4	8326.65	7854.68	8502.36	8510.18
469	7269.44	8152.34	8298.68	8408.76	8227.91	8124.44
470	7601.46	7854.34	8279.9	7856.63	7916.6	8007.99
471	7151.75	7476.17	8193	8209.47	7877.28	8213.84
472	7440.95	7814.63	8295.15	8039.48	8376.89	8098.81
473	7428.08	8344.03	8148.24	8056.46	8307.29	8219.97
474	7214.54	7767.62	7927.7	8161.45	8405.63	8427.66
475	7689.04	8177.53	8116.28	7984.74	8402.44	8192.57
476	8382.22	8134.44	8078.79	7918.23	8294.21	8132.65
477	7594.31	8173.24	7862.1	8288.53	7797.89	8109.89

478	7218.76	7574.17	8432.52	8001.86	8586.54	7999.1
479	7931.45	7875.54	8243.1	8151.46	8404.88	8538.49
480	7628.41	7892.22	8432.29	8307.27	8172.35	8331.45
481	7455.78	7782.6	8498.31	7929.49	8495.99	8351.33
482	8004.4	8138.92	8210.26	8399.86	8004.73	8720.22
483	8332.65	7903.83	8260.38	7807.29	8524.93	8454.99
484	7362.31	8150.85	8199.26	7755.02	8137.82	8287.17
485	7479.83	7922.91	7865.42	8078.68	8388.4	8438.38
486	7745.72	8090.86	8118.21	8124.38	8066.21	8595.93
487	7534.2	7914.7	8368.9	8039.18	8257.17	8316.62
488	7255.31	7681.55	8118.55	8128.91	8291.65	8221.1
489	6904.87	7957.53	8141.75	8041.76	8264.81	8788.03
490	7655.16	7764.67	8120.84	8013.7	8361.23	8343.29
491	6991.12	8055.81	8109	8094.52	8617.7	7872.63
492	7823.55	7632.15	8247.91	8169.22	8142.83	8143.01
493	7362.79	7537.03	8071.26	8456.11	8188.23	8506.46
494	7922.97	8106.62	8602.43	8011.81	8334.29	8020.42
495	7208.32	8006.08	8312.6	8487.8	8400.43	8398.48
496	6873.24	8222.39	8520.94	8038.19	8190.88	8374.24
497	6998.13	8514.99	7989.56	7921.84	8176.05	8469.13
498	6792.03	8538.6	7874.42	8162.61	8181.13	8545.13
499	8421.7	8008.63	8316.93	8115.76	8444.02	8640.22
500	7633.45	7699.67	8624.68	8325.88	8299.15	8669.66